Cosmology

Julien Larena

Département de physique

Université de Montpellier

September 2024-February 2025

Par l'espace, l'univers me comprend et m'engloutit comme un point; par la pensée, je le comprends.

Pascal, Pensées, fragment 104.

Forewords

These notes are intended for a one semester course in Theoretical Cosmology. The focus is on understanding the formation of large scale structure and which physics can be probed with large galaxy surveys. Unfortunately, there is not enough time in one semester to cover the entire, rich topic of modern cosmology. In particular, there is only a very partial treatment of the Boltzmann equation in cosmology, and the Cosmic Microwave Background is only touched upon in order to provide the essential information: for example, polarisation is not treated at all; Big-Bang nucleosynthesis cannot be treated in details and is only described crudely. We concentrate mostly on the Universe after matter-radiation equality and the formation of structure. Inflation is introduced to explain how to resolve problems in the standard model, and a quick presentation of the general mechanism and origin of structures is provided in the simplest of inflationary context (single field inflation). Most chapters end with exercises that you are strongly encouraged to study in details. Calculations and reasoning that are omitted or done in the text of the notes are also, implicitly, left to the reader and you are required to redo them by yourselves, even if they were done in part or in full during the classes.

Some references to books and lecture notes you may find useful:

- *Primordial cosmology*, by P. Peter and J.-P. Uzan [16];
- *Physical foundation of cosmology*, by V. Mukhanov [13];
- *Physical cosmology*, by J. Peebles [14];

- *Principles of physical cosmology*,by J. Peebles [15];
- *Cosmology*, by D. Baumann [4].

Notations and conventions

- Lorentzian metrics in 4 dimensions will be written in the $(-,+,+,+)$ signature. Physically, this means that positive spacetime intervals, $\mathrm{d}s^2$ will be spacelike and proper times will be $\mathrm{d}\tau^2 = -\mathrm{d}s^2$.
- 4-vectors will be denoted with boldface letters, capital or not, e.g.: $\boldsymbol{u}$, $\boldsymbol{X}$ etc. The same convention will apply to linear maps such as tensor fields but not to (scalar) functions.
- 3-vectors, i.e. the spatial part of 4-vectors will be denoted with an arrow, e.g.: $\vec{v}$ or $\vec{V}$.
- Symmetrisation and antisymmetrisation of tensor indices are conventionally denoted:

$$A_{(\mu\nu)} = \frac{1}{2}\left[A_{\mu\nu} + A_{\nu\mu}\right]$$
$$A_{[\mu\nu]} = \frac{1}{2}\left[A_{\mu\nu} - A_{\nu\mu}\right] \ .$$

  If anything 'gets in the way'. then we use the notation $(\mu|$ and $|\nu)$, e.g.:

$$A_{(\mu|\rho|\nu)} = \frac{1}{2}\left[A_{\mu\rho\nu} + A_{\nu\rho\nu}\right] \ ,$$

  i.e. the symmetrisation only affects the first and last indices, by-passing the second one.
- The notes are written in units with the speed of light equal to unity: $c = 1$. In some instances, we put the appropriate powers of c back into important formulæ. When dealing with the early Universe, we also use natural units in which $\hbar = h/2\pi = 1$ and $k_B = 1$. Students are encouraged to do that systematically using dimensional analysis. This is a very good exercise.

We list some useful numerical values that one may find useful when working on the content of these notes. Some of these values are approximate and the values adopted here will suffice to obtain results that are precise enough for our purposes.

1. *Fundamental Constants*:
   - Speed of light: $c = 299\,792\,458\, m \cdot s^{-1} \simeq 3 \times 10^8\ \mathrm{m} \cdot \mathrm{s}^{-1}$
   - Planck constant: $h = 6.62607015 \times 10^{-34} \mathrm{J} \cdot \mathrm{s}$
   - Boltzmann constant: $k_B = 1.380649 \times 10^{-23}\ \mathrm{J} \cdot \mathrm{K}^{-1}$
   - Newton constant: $G \simeq 6.67 \times 10^{-11}\ \mathrm{N} \cdot \mathrm{m}^2 \cdot \mathrm{kg}^{-2}$.
   - Planck Mass: $M_{\mathrm{Pl}} = \sqrt{\frac{\hbar c}{G}} \simeq 1.67 \times 10^{-27}\ \mathrm{kg} \simeq 1.22 \times 10^{19} \mathrm{GeV}/c^2$
   - Radiation density constant: $a_S = \frac{\pi^2 k_B^4}{15\hbar^3 c^2} \simeq 7.5657 \times 10^{-16} \mathrm{J} \cdot \mathrm{m}^{-3} \cdot \mathrm{K}^{-4}$
2. *Conversion factors*:
   - $1\,\mathrm{eV} \simeq 1.6 \times 10^{-19}\,\mathrm{J}$
   - $1\,\mathrm{s} \simeq 1,5 \times 10^{24}\,\mathrm{GeV}^{-1}\hbar/c$
   - $1\,\mathrm{m} \simeq 5.1 \times 10^{15}\,\mathrm{GeV}^{-1}\hbar$
   - $1\,\mathrm{kg} \simeq 5.5 \times 10^{26}\,\mathrm{GeV}\hbar/c^2$
   - $1\,\mathrm{K} \simeq 8.6 \times 10^{-14}\,\mathrm{GeV}^{-1}/k_B$
   - $1\,\mathrm{AU} \simeq 1.5 \times 10^{11}\,\mathrm{m}$
   - $1\,\mathrm{pc} \simeq 3 \times 10^{16}\,\mathrm{m}$
   - $1\,\mathrm{yr} \simeq 3.16 \times 10^{7}\,\mathrm{s}$
   - $1\,\mathrm{sterad} = 1\,\mathrm{rad}^2 = \left(\frac{180}{\pi}\right)^2\,\mathrm{deg}^2$
3. *Sun's characteristics*:
   - $M_\odot \simeq 2 \times 10^{30}\,\mathrm{kg}$
   - $R_\odot \simeq 7 \times 10^{8}\,\mathrm{m}$

Contents

1

Introduction: The scope of cosmology

Contents

1.1 What is cosmology, and what is it not?

What is the world made of? What is its shape? Did it have a beginning or always existed? Does it have boundaries or not? What is its size? What is its fate? Where are we in it?
All these questions have helped shape human cultures. They are questions about the Universe and our place inside it. They are at the heart of Cosmology: they are central to any attempt, mythical, mystical, religious, metaphysical etc., at finding our place in existence. However with the advent of modern science in the 17^{th} century, some of these questions have started to receive scientific, rather than metaphysical or mythical answers, they have be incorporated into the scientific discourse. Of course, to this day, some of those questions have remained outside the purview of science, such as, e.g. the notion of origin of the Universe. The story these notes aim to tell is about the ones who can, partially or in full, receive scientific answers, within the context of current physical theories. This means answers that are revocable, subject to the tribunal of observations, experiments and theoretical arguments. This means that the model presented here is only temporary and constantly being tested and revised, at least in its minute details.
For all those scientific questions, we can use the word cosmology, dropping the capital letter.[1]
Before we start diving into physical cosmology, it is worth reflecting on the origin and meaning of the word cosmology. 'Cosmos' is a Greek word ('$\kappa\acute{o}\sigma\mu o\varsigma$') that originally means order, good order, but also jewellery or (physical) ornament. This makes for an a priori surprising relation that we still encounter today in the proximity of words such as cosmology and cosmetics. This probably comes from an analogy drawn between the bright stars 'embellishing' the night sky and jewellery such as pearl necklaces etc., also used to embellish the earthly body.
The Universe is full of these wondrous embellishments and I hope this course will help illuminate some of those: behind the sometimes dry and tedious calculations, one must try never to forget the magnificent and awful realities that we are trying to describe.

In this short introduction, we will list a few basic observational facts about our Universe. Primarily this will be useful to set the characteristic scales that will be studied in the notes. In addition, the two main facts we will encounter, i.e. the recession of distant galaxies and the statistical isotropy of the distribution of matter around us, will be the basic starting points for the construction of a model

[1] Thanks are due to J.-P. Uzan for having introduced this use in his book 'Big-bang, Comprendre l'univers depuis ici et maintenant', Flammarion 2018.

of the Universe that will be explored in the rest of these notes.

1.2 The Observed Universe: basic facts

Admittedly, modern cosmology started with the discovery by Slipher, Hubble and others at the beginning of the XX^{th} century, that the distant nebulæ of old times were in fact distant galaxies, in all points similar to our own[2]. Very quickly, these first physical cosmologists measured the velocities of these galaxies using the redshift experienced by spectroscopic lines in the light they emit. This led to the discovery of the universal recession of distant galaxies: seen from our point of view, distant galaxies appear to be moving away from us, with a velocity proportional to their distance to us. This is **Hubble-Lemaître's law**; see Fig. 1.1:

$$v = H_0 d\,, \tag{1.1}$$

where H_0 is known as the **Hubble constant**. Its modern value is currently the topic of a controversy but it is in the range:

$$H_0 = 65 - 75 \text{km/s/Mpc}. \tag{1.2}$$

It means that an object located at a distance from us of 1 Mpc, moves away from us with a velocity of 65 to 75 km/s. This law tells us that the Universe is expanding around us: it is a dynamical, evolving object for which we can try and uncover a history. Writing this history is the task of cosmology.

As you can see, a new unit has appeared here: the parsec, symbol pc. It is a very useful and common unit in cosmology. It is defined as the distance at which an "object" that measures 1 AU subtends an angle on the sky of 1 arcsecond:

$$1 \text{ pc} = \frac{648000}{\pi} \text{ AU} \simeq 3.1 \times 10^{13} \text{ m} \simeq 3.26 \text{ light-years}. \tag{1.3}$$

The star nearest to the Sun, Proxima Centauri, is at 1.3 pc from here. The disk of the Milky Way is some 30 kpc wide, and the Sun is located approximately 8 kpc from the centre of the Milky Way.

[2]Kant contemplated such an idea with his island Universes, presented in one of his first book: "Universal Natural History and Theory of the Heavens", published in 1755; this was the first attempt to apply Newton's theory of gravitation to the building of a cosmology.

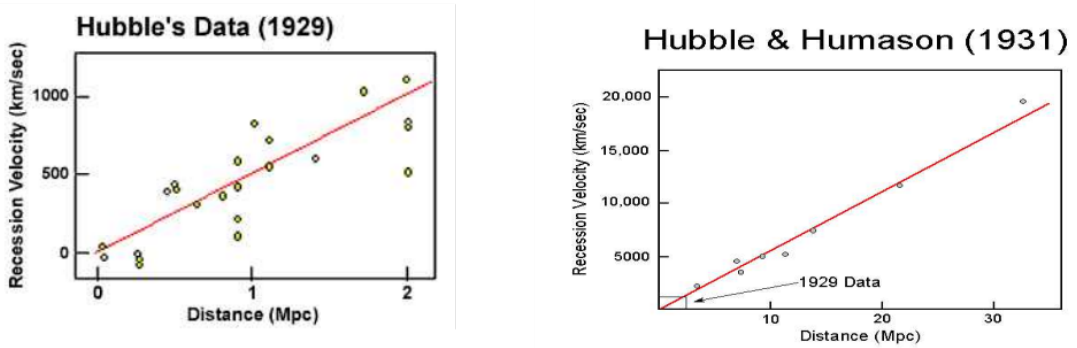

(https://starchild.gsfc.nasa.gov/docs/StarChild/questions/redshift.html)

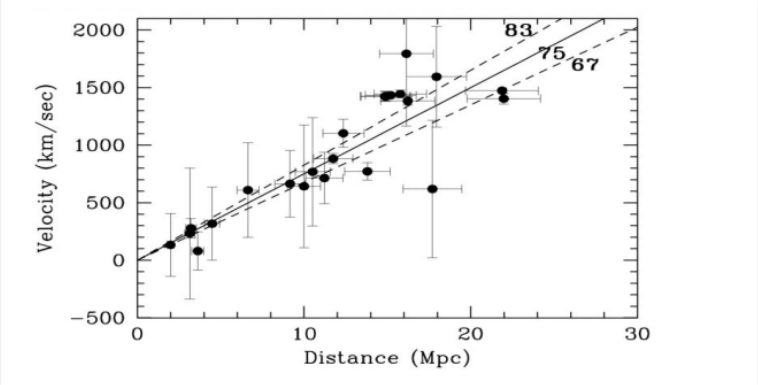

(Freedman et al (2001), ApJ 553, 47)

Figure 1.1: The Hubble law, then and now. Recent measurements from [11].

The nearest galaxy is Andromeda, and it is about 780 kpc from us. Going further away, the nearest large cluster of galaxy, the Virgo cluster is about 17 Mpc from here. It has a typical size of 1 Mpc. Large scale structures such as filaments and walls along which galaxies align in the Universe can be several Gpc across, and the visible Universe has a radius of approximately 50 Gpc. These notes are concerned with the dynamics of the Universe and structures found in it on scales typically larger than 1 Mpc, all the way up to the size of the visible Universe. This means that the physics we will describe has to span approximately 4 orders of magnitude in physical size today.
What happens when we look on the largest of these scales, that is if we are only concerned with describing the Universe smoothed on scales of a few hundreds of Mpc? The Universe appears extremely regular, when looked at on such large enough scales. This is visible in surveys of galaxies, which simply count the number of distant objects; see Fig. 1.2. But this is even more stricking when looking as far back as possible, and measuring the background relic radiation known as the Cosmic Microwave Background (CMB), the remnant of an epoch known as decoupling, when photons decoupled from matter and became free to propagate in the Universe, creating a thermal bath which today consists of approximately 400 to 500 photons per cubic cm^3 all over the Universe; see Fig. 1.2. This background radiation corresponds to a black body radiation of temperature $T_0 \simeq 2.725$ K, which is extraordinarily isotropic around us: fluctuations in this temperature do not exceed 1 part in 100 000. Therefore the Universe is **statistically isotropic around us**. Observed on large enough scales, it is isotropic, and on top of this isotropic background, one can detect small fluctuations on small scales which average out when smoothed appropriately.

So here is our task: building a cosmological model that can describe a Universe smooth on large scales, but full of structures on small scales. Let us start our journey.

1.3 Problems

Pb. 1.1 Estimate the angular size, as seen by an observer on Earth, of the galaxy Andromeda and of the cluster of galaxies Virgo.

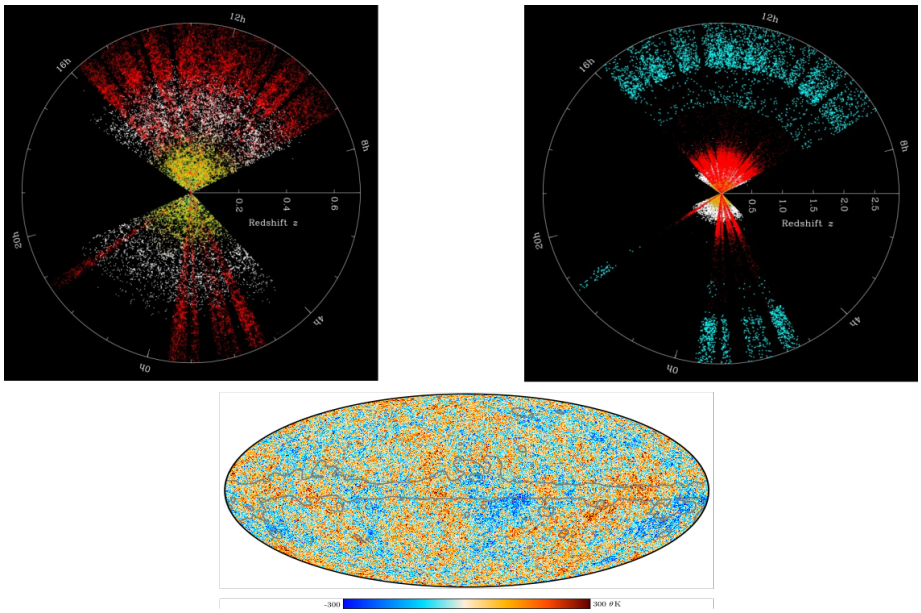

Figure 1.2: Top left: Combination of SDSS normal galaxies (yellow dots), SDSS Luminous Red Galaxies (white dots) and BOSS LUminous Red Galaxies (red dots). Each point is a galaxy. On such diagrams, we are located at the centre and the distance to this centre denotes the redshift, which is linked to the distance to us; see later: the farther an object, the larger its redshift. Top Right: Same as top left, but with BOSS quasars added (blue dots), probing a much deeper Universe. Credit: M. Blanton/SDSS. Bottom: Temperature anisotropies in the Cosmic Microwave Background measured by PLANCK.

2

The homogeneous and isotropic Universe

Contents

2.1 The Friedmann-Lemaître-Robertson-Walker Universe

2.1.1 Large-scale geometry of the Universe

As emphasised in the previous section, on large enough scales, the Universe appears remarkably isotropic around us: the temperature of the cosmic microwave background radiation does not vary by more that one part in 100000 over the whole sky, and the distribution of galaxies in the late Universe is also very isotropic when smoothed on sufficiently large scales. This fact will be of great use to simplify the description of our Universe on large scales. Indeed, the prospect of solving the equations of General Relativity without any hypothesis on the symmetries of the solution is absolutely daunting (6 independent, coupled, non-linear partial differential equations!), so any guidance towards simplifying assumptions is very welcome indeed. Let us thus assume the following:

Observed isotropy

On average, our Universe is statistically isotropic around us.

Unfortunately, we do not have any direct access to what the Universe could look like to distant observers, located in other galaxies and to move forward, we have to assume the Copernican principle that is not directly based on as simple observational facts as isotropy[1]:

The Copernican principle

We are typical cosmological observers; i.e. we do not occupy a special spatial location in our Universe.

This means that whatever properties of our Universe we observe, on average, any other observer should observe the same properties. In particular, since we have assumed average isotropy around us, the Universe must appear isotropic, on average, to any other typical observer. This is known as the cosmological principle and as we are going to see, taken as a strong statement, it determines the geometry of our Universe unambiguously.

Let us, for now, simplify our description a bit further and drop the "average" qualification from these statements. That is, let us assume that the Universe is perfectly isotropic for any typical observer. Let us populate our spacetime with a family of such typical observers, each with its own worldline

[1] However, one can now try and test this principle; see, e.g. [8] for a review.

thus defining a field of timelike vectors u that are the 4-velocities of these observers. This preferred set of observers is really important and is also known as the set of fundamental observers. Let us call t the proper time measured by these observers along their worldlines. Their flow in spacetime defines a preferred foliation of spacetime into hypersurfaces Σ_t orthogonal to the field u at every point, such that the metric tensor takes the form:

$$\boldsymbol{g} = -\boldsymbol{u} \otimes \boldsymbol{u} + \boldsymbol{\gamma}(t) \ , \tag{2.1}$$

where $\boldsymbol{\gamma}(t)$ is the induced metric on the spatial slice Σ_t at fixed proper time t. According to the cosmological principle, the hypersurfaces Σ_t ought to be isotropic around each of their points. This means that any quantity defined on Σ_t is spherically symmetric around each point. But this implies that the hypersurfaces Σ_t are also homogeneous, i.e. that each quantity defined on them is invariant by translation as well. Thus the Copernican principle, combined with isotropy around fundamental observers implies that the hypersurfaces Σ_t are invariant under rotations and translations, i.e. maximally symmetric; see appendix B of the notes of General Relativity (M1) for details about such 3 dimensional hypersurfaces. Combining all this, on large enough scales, the geometry of the Universe is well-approximated by the *Friedmann-Lemaître-Robertson Walker* metric (hereafter FLRW metric):

The Friedmann-Lemaître-Robertson Walker (FLRW) metric

$$\boldsymbol{g} = -\mathrm{d}t \otimes \mathrm{d}t + a^2(t)\left[\frac{1}{1-Kr^2}\mathrm{d}r \otimes \mathrm{d}r + r^2\left(\mathrm{d}\theta \otimes \mathrm{d}\theta + \sin^2\theta\,\mathrm{d}\phi \otimes \mathrm{d}\phi\right)\right] \tag{2.2}$$

$$\mathrm{d}s^2 = -\mathrm{d}t^2 + a^2(t)\left[\frac{\mathrm{d}r^2}{1-Kr^2} + r^2\left(\mathrm{d}\theta^2 + \sin^2\theta\,\mathrm{d}\phi^2\right)\right] \ , \tag{2.3}$$

where:

1. t is the *proper time measured by fundamental observers* (those seeing an isotropic and homogeneous Universe);
2. r is the *coordinate radial distance*;
3. $\mathrm{d}\Omega^2 = \mathrm{d}\theta^2 + \sin^2\theta\,\mathrm{d}\phi^2$ is the round metric on the 2-sphere S^2, also called the "celestial sphere" (sky) of fundamental observers;

4. $a(t)$is the *scale factor*;

5. $K \in \mathbb{R}$ is the *scalar curvature of space*.

The non-zero connection coefficients of the FLRW metric in (t, r, θ, ϕ) coordinates are:

Connection coefficients of the FLRW metric in (t, r, θ, ϕ) coordinates

$$\Gamma^0{}_{ij} = \frac{\dot{a}}{a} g_{ij} \; ; \; \Gamma^1{}_{01} = \Gamma^1{}_{10} = \frac{\dot{a}}{a} \tag{2.4}$$

$$\Gamma^1{}_{11} = \frac{Kr}{1 - Kr^2} \; ; \; \Gamma^1{}_{22} = -r(1 - Kr^2) \; ; \; \Gamma^2{}_{33} = -r(1 - Kr^2) \sin^2\theta \tag{2.5}$$

$$\Gamma^2{}_{02} = \Gamma^2{}_{20} = \frac{\dot{a}}{a} \; ; \; \Gamma^2{}_{12} = \Gamma^2{}_{21} = \frac{1}{r} \; ; \; \Gamma^2{}_{33} = -\sin\theta\cos\theta \tag{2.6}$$

$$\Gamma^3{}_{03} = \Gamma^3{}_{30} = \frac{\dot{a}}{a} \; ; \; \Gamma^3{}_{13} = \Gamma^3{}_{31} = \frac{1}{r} \; ; \; \Gamma^3{}_{23} = \Gamma^3{}_{32} = \frac{\cos\theta}{\sin\theta} \; . \tag{2.7}$$

Here and afterwards, a dot will denote a derivative with respect to the time coordinate t.

2.1.2 Kinematics

We can now explore the basic geometric properties of the FLRW metric. t is the proper time measured by fundamental observers along their worldlines defined by $\mathrm{d}r = \mathrm{d}\theta = \mathrm{d}\phi = 0$. It is often called the *cosmic time*. The 4-velocity of fundamental observers is then simply, in those coordinates:

$$u^\mu = \delta^\mu_0 . \tag{2.8}$$

In the following, we will denote by γ_{ij} the components of the metric of conformal space:

$$\gamma_{ij} = \frac{1}{\sqrt{1 - Kr^2}} \delta^r_i \delta^r_j + r^2 \delta^\theta_i \delta^\theta_j + r^2 \sin^2\theta \delta^\phi_i \delta^\phi_j \; . \tag{2.9}$$

Now, consider two fundamental observers, spatially separated ($\mathrm{d}t = 0$), and located at r and $r + \Delta r$, $\phi = \phi_0$ and $\theta = \theta_0$, with $\Delta r \ll 1$. Then, the physical distance between these observers is given by:

$$\Delta d_{\mathrm{phys}}(r, t) = a(t) \frac{\Delta r}{\sqrt{1 - Kr^2}} \; . \tag{2.10}$$

The number K represents the curvature of the spacelike hypersurfaces at constant t and we can already see that for physical reasons, r has a finite range in the case $K > 0$. Although this coordinate

system, (t, r, θ, ϕ) is natural from a physical point of view, one can introduce a new set of coordinates that proves much more useful from a mathematical and physical point of view. First, let us introduce the *conformal time* η, such that:

$$\mathrm{d}\eta = \frac{\mathrm{d}t}{a(t)} \,, \tag{2.11}$$

or in integral form:

$$\eta - \eta_0 = \int_{t_0}^{t} \frac{\mathrm{d}t'}{a(t')} \,. \tag{2.12}$$

This time coordinate allows one to "factor out" the scale factor and rewrite the line element:

$$\mathrm{d}s^2 = a^2(\eta) \left[-\mathrm{d}\eta^2 + \frac{\mathrm{d}r^2}{1 - Kr^2} + r^2 \left(\mathrm{d}\theta^2 + \sin^2\theta \, \mathrm{d}\phi^2 \right) \right] \,, \tag{2.13}$$

where, as usual, we have used the physicist's abuse of notation and set $a(\eta) \equiv a\left(t(\eta)\right)$, with $t(\eta)$ obtained by inverting the relation $\eta(t)$ coming from Eq. (2.12). Next, we introduce a radial coordinate χ adapted to the type of spatial curvature K, such that:

$$\mathrm{d}\chi = \frac{\mathrm{d}r}{\sqrt{1 - Kr^2}} \,, \tag{2.14}$$

or equivalently, setting $\chi = 0$ for $r = 0$:

$$\chi = \int_0^r \frac{\mathrm{d}r'}{\sqrt{1 - Kr'^2}} \,. \tag{2.15}$$

As a matter of fact, the integration in this case is quite easy to perform, and one gets:

$$r(\chi) \equiv S_K(\chi) = \begin{cases} \frac{1}{\sqrt{K}} \sin\left(\sqrt{K}\chi\right) & \text{for } K > 0 \\ \chi & \text{for } K = 0 \\ \frac{1}{\sqrt{-K}} \sinh\left(\sqrt{-K}\chi\right) & \text{for } K < 0 \end{cases} \,. \tag{2.16}$$

Note that this makes apparent what the admissible range of the radial coordinate is:

- For $K > 0$, as $r \in \left[0, 1/\sqrt{K}\right]$, $\chi \in [0, \pi]$;
- For $K \leq 0$, as $r \in [0, +\infty)$, $\chi \in [0, +\infty)$.

Then, the line element finally reads:

$$\mathrm{d}s^2 = a^2(\eta) \left[-\mathrm{d}\eta^2 + \mathrm{d}\chi^2 + S_K^2(\chi) \left(\mathrm{d}\theta^2 + \sin^2\theta \, \mathrm{d}\phi^2 \right) \right] \,. \tag{2.17}$$

This form is both remarkable and convenient for various reasons.

- Spatial hypersurfaces of constant η are, up to a conformal factor $a^2(\eta)$ the simplest constant curvature 3-dimensional manifolds. For $K = 0$, we recover the standard Euclidean "flat" space with its flat metric in spherical coordinates, $\mathbb{E}^3$. For $K > 0$, this is simply the round metric on a 3-sphere $\mathbb{S}^3$ of radius $1/\sqrt{K}$. And, finally, for $K < 0$, this is the standard metric on hyperbolic space $\mathbb{H}^3$. Note that this form also makes it clear that the radius of a 2-sphere at coordinate distance χ from the origin is given by $S_K(\chi)$ in the sense that the physical area of such a 2-sphere (at $\mathrm{d}\eta = \mathrm{d}\chi = 0$) is exactly $4\pi S_K^2(\chi)$.
- Radial light rays ($\mathrm{d}s^2 = \mathrm{d}\theta = \mathrm{d}\phi = 0$) are straight lines at $\pm\pi/4$ angles: $\chi - \chi_0 = \pm\,(\eta - \eta_0)$.

In these coordinates, the non-zero connection coefficients are: (symmetry in lower indices is implicit)

Connection coefficients of the FLRW metric in $(\eta, \chi, \theta, \phi)$ coordinates

$$\Gamma^0{}_{00} = \frac{a'}{a}\ ;\ \Gamma^0{}_{11} = \frac{a'}{a}\ ;\ \Gamma^0{}_{22} = \frac{a'}{a}S_K^2\ ;\ \Gamma^0{}_{33} = \sin^2\theta\,\Gamma^0{}_{22} \tag{2.18}$$

$$\Gamma^1{}_{01} = \frac{a'}{a}\ ;\ \Gamma^1{}_{22} = -S_K\frac{\mathrm{d}S_K}{\mathrm{d}\chi}\ ;\ \Gamma^1{}_{33} = \sin^2\theta\,\Gamma^1{}_{22} \tag{2.19}$$

$$\Gamma^2{}_{02} = \frac{a'}{a}\ ;\ \Gamma^2{}_{12} = \frac{1}{S_K}\frac{\mathrm{d}S_K}{\mathrm{d}\chi}\ ;\ \Gamma^2{}_{33} = -\sin\theta\cos\theta \tag{2.20}$$

$$\Gamma^3{}_{03} = \frac{a'}{a}\ ;\ \Gamma^3{}_{13} = \frac{1}{S_K}\frac{\mathrm{d}S_K}{\mathrm{d}\chi}\ ;\ \Gamma^3{}_{23} = \frac{\cos\theta}{\sin\theta}\ . \tag{2.21}$$

Here and from now on, a prime will denote a derivative with respect to conformal time, η. Fundamental observers have 4-velocity $\boldsymbol{u} = \frac{\partial}{\partial t}$ with components $(1,0,0,0)_{(t,r,\theta,\phi)}$, thus, in this new coordinate system, $u^\mu = \left(\frac{1}{a}, 0, 0, 0\right) = \frac{1}{a}\delta^\mu_0$. If we consider two such fundamental observers located in space at $\vec{x}_1$ and $\vec{x}_2$, their physical separation at time t is given by:

$$\vec{r}_{12} = a(t)\,(\vec{x}_1 - \vec{x}_2)\ . \tag{2.22}$$

The position vectors $\vec{x}_1$ and $\vec{x}_2$ are constant in time by definition of fundamental observers.Thus:

$$\frac{\mathrm{d}}{\mathrm{d}t}\vec{r}_{12} = \dot{a}\,(\vec{x}_1 - \vec{x}_2) = \frac{\dot{a}}{a}\vec{r}_{12}. \tag{2.23}$$

The function:

$$H(t) \equiv \frac{\dot{a}}{a} \tag{2.24}$$

is called the *Hubble rate* and Eq. (2.23) is the *Hubble-Lemaître's law*. Written at present time, $t = t_0 \sim 13.7$ Gyr, it gives the historical Hubble-Lemaître's law, and reads:

$$\vec{v} = H_0 \vec{r}\,, \tag{2.25}$$

with $H_0 = H(t_0)$ the *Hubble constant*. It expresses the fact that cosmological objects like galaxies move with respect to each other with a velocity that is greater the farther they are from each other. In an expanding Universe, $H_0 > 0$ and the velocity is a recession velocity: distant galaxies move away from each other.

Finally, let us focus on the trajectories and properties of light rays in the FLRW Universe. In the geometric optics limit (i.e. when the wavelength of the light considered is small with respect to the typical curvature radius of spacetime), valid in the cosmological context, the propagation of electromagnetic waves is well-approximated by the properties of light rays, i.e. null curves with tangent vector field $\boldsymbol{k}$ with components $k^\mu = \frac{\mathrm{d}x^\mu}{\mathrm{d}\lambda}$ satisfying:

$$\begin{cases} \boldsymbol{g}(\boldsymbol{k}, \boldsymbol{k}) = k_\mu k^\mu = 0 & (2.26) \\ \nabla_{\boldsymbol{k}} \boldsymbol{k} = k^\nu \nabla_\nu k^\mu = 0\,. & (2.27) \end{cases}$$

Here, λ is an affine parameter along the light ray considered. Let $h_{\mu\nu} = g_{\mu\nu} + u_\mu u_\nu$ be the components of the *projection tensor* $\boldsymbol{h} = \boldsymbol{g} + \boldsymbol{u} \otimes \boldsymbol{u}$ which projects orthogonally on hypersurfaces of constant t (or equivalently constant η). Then, in cosmic time coordinates:

$$h_{\mu\nu} = g_{\mu\nu} + \delta_{\mu 0}\delta_{\nu 0}\,, \tag{2.28}$$

so that $h_{0\mu} = 0$. Then, let $E = -k^\mu u_\mu$ and $p^\mu = h^\mu{}_\nu k^\nu$. For a future directed light ray, E is the energy of the light ray (for a past directed light ray it is minus the energy) as measured in the rest-frame of the fundamental observer, and p^μ/E are the components of the instantaneous direction of propagation of the light ray in the same rest frame; it is everywhere orthogonal to the 4-velocity of the observers: $p^\mu u_\mu = 0$. p^μ are simply the components of the 3-momentum of the photons. Then, we can write uniquely:

$$k^\mu = E u^\mu + p^\mu\,. \tag{2.29}$$

Using $\boldsymbol{g}(\boldsymbol{k}, \boldsymbol{k}) = 0$, we get:

$$-E^2 + a^2 \gamma_{ij} p^i p^j = 0. \tag{2.30}$$

Then, projecting the null geodesic equation along $\boldsymbol{u}$:

$$u_\nu \left(k^\mu \nabla_\mu k^\nu\right) = 0 \,, \tag{2.31}$$

we get:

$$E\dot{E} + a^2 H \gamma_{ij} p^i p^j = 0 \,. \tag{2.32}$$

Hence, using Eq. (2.30), we obtain:

$$\frac{\dot{E}}{E} = -H = -\frac{\dot{a}}{a} \,, \tag{2.33}$$

which is trivial to integrate, to get:

$$E = \frac{C_0}{a} \,, \; C_0 \in \mathbb{R} \,. \tag{2.34}$$

For a light ray with frequency ν, the energy of a photon is given by $E = h\nu$, so that the frequency of light is affected by cosmic expansion along the trajectory of photons, according to:

$$\nu(t) = \frac{a\left(t_e\right)}{a(t)} \nu\left(t_e\right) \,, \tag{2.35}$$

where t_e is the time at which the photons have been emitted by their source located at $(t_e, \chi_e, \theta_e, \phi_e)$. If a fundamental observer located at the centre of the coordinate system ($\chi = 0$) receives this light today, at $t = t_0$, the redshift z is defined by:

$$z \equiv \frac{\lambda\left(t_0\right) - \lambda\left(t_e\right)}{\lambda\left(t_e\right)} \,, \tag{2.36}$$

and in the FLRW context:

$$\boxed{1 + z = \frac{a\left(t_0\right)}{a\left(t_e\right)}} \,. \tag{2.37}$$

The name redshift is justified by the fact that, in an expanding universe, $a\left(t_0\right) > a\left(t_e\right)$, so that $\lambda\left(t_0\right) > \lambda\left(t_e\right)$: the wavelength of the light has been moved to higher values, towards the redder part of the spectrum. In a purely expanding FLRW Universe, there is a one-to-one and onto relationship between times of emission and redshifts at observation, so that one can interchangeably use either t or $z(t) = a\left(t_0\right)/a\left(t\right) - 1$ to characterise past events. We will use this freedom extensively in what follows. Moreover, note that scale factor and coordinate radial distance are only defined simultaneously up to an overall scaling. This means that by setting the units for radial distances appropriately at time $t = t_0$ ("today"), one can always set $a_0 = a\left(t_0\right) = 1$. From now on, we will

fix units this way. We will also, by convention, agree that a subscript 0 attached to any function corresponds to the value of that function at the value of the proper time today, t_0, or equivalently at the present value of the conformal time η_0 (or equivalently at $z = 0$).

2.1.3 Distances

The coordinate distances given by the radial coordinates r and χ, such as the one used to derive the Hubble-Lemaître's law are not measurable quantities in General Relativity, as they are calculated purely by the spacelike separation of two events in spacetime. Physically meaningful distances ought to be related to observable quantities involving causal processes; in cosmology such physically relevant distances are obtained by determining distances measured down the past lightcone of an observer, because almost every piece of information we get about the distant Universe is obtained via electromagnetic observations. We will define two relevant distances, related respectively to the luminosity of sources and to their angular size. But before we define these physical distances, it is convenient to introduce one coordinate distance that is important in deriving them: the comoving radial distance.

Comoving radial distance

Consider a fundamental observer located at $\chi = 0$, receiving at $\eta = \eta_0$ light that was emitted by a distant source at a time t corresponding to a redshift z. By an appropriate choice of our coordinate system, we can ensure that the light ray propagates radially, with $\mathrm{d}\theta = \mathrm{d}\phi = 0$. Then, along the light ray propagating from the source to the observer, we have $\mathrm{d}s^2 = 0$, i.e.:

$$\mathrm{d}\chi = -\frac{\mathrm{d}t}{a(t)} = -\frac{\mathrm{d}a}{a^2 H} \,. \tag{2.38}$$

The minus sign ensures that the ray propagates forward in time from the source at $\chi > 0$ to the observer at $\chi = 0$. Using a as a "time" variable instead of t is safe as long as they are related in a monotonous way, which is true in an expanding Universe (see dynamics below). Then, using $1 + z = 1/a$, we get:

$$\mathrm{d}\chi = \frac{\mathrm{d}z}{H(z)} \,. \tag{2.39}$$

The *comoving radial distance* between the source and the observer is then simply the change in χ along the light ray between source and observer (see Fig. 2.1), and it is obtained by integrating the

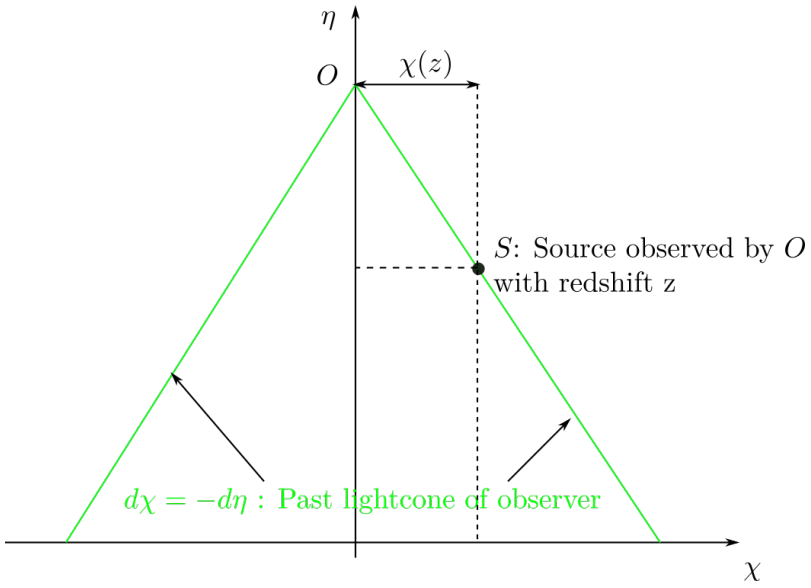

Figure 2.1: Definition of the comoving radial distance.

previous differential relation:

$$\chi(z) \equiv \int_0^z \frac{\mathrm{d}z'}{H(z')} \,. \tag{2.40}$$

It is not an observable. It can be used to defined another unobservable, but important distance: the *comoving angular distance*. Consider the comoving 2-sphere at $\mathrm{d}\eta = \mathrm{d}\chi = 0$ at $\chi = \chi(z)$, then, its round metric gives the line element (it is comoving so we ignore the scale factor):

$$\mathrm{d}s^2_{com} = S^2_K(\chi(z)) \left(\mathrm{d}\theta^2 + \sin^2\theta\, \mathrm{d}\phi^2\right) \,. \tag{2.41}$$

A small source located on that sphere and observed at the centre under a small solid angle $\mathrm{d}\Omega^2_{obs}$ subtends a small transverse area portion of the sphere $\mathrm{d}S^{source}_{com}$ such that:

$$\mathrm{d}S^{source}_{com} = S^2_K(\chi(z))\mathrm{d}\Omega^2_{obs} \,; \tag{2.42}$$

see Fig. 2.2 for a detail of the geometry.

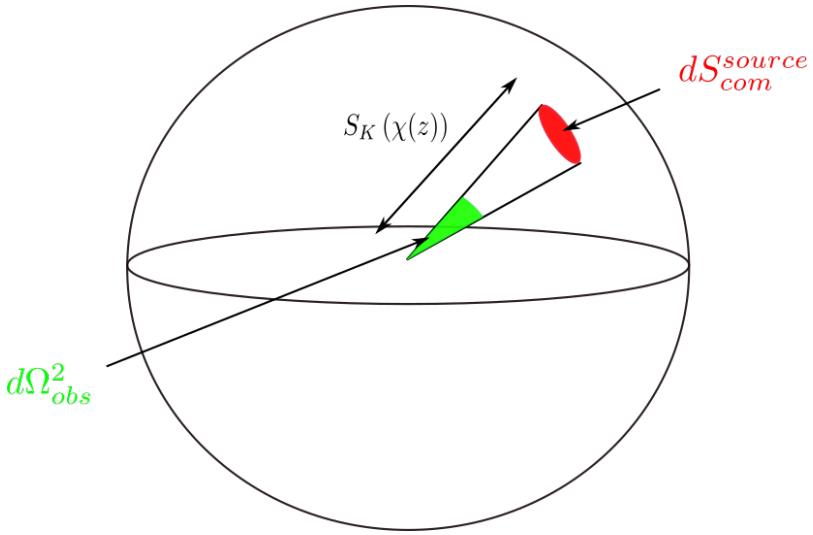

Figure 2.2: Definition of the comoving angular distance.

The *comoving angular distance* between the source at redshift z and the observer is then defined as the ratio:

$$R_{ang}^2(z) \equiv \frac{\mathrm{d}S_{com}^{source}}{\mathrm{d}\Omega_{obs}^2}. \tag{2.43}$$

Thus:

$$\boxed{R_{ang}(z) = S_K\left(\chi(z)\right)\ .} \tag{2.44}$$

The effect of curvature on this comoving angular distance is summarised on Fig. 2.3. The green curves represent light rays coming from the boundary of the small distant object and reaching the observer at the point of convergence. An object of the same size, located at the same coordinate distance $\chi(z)$ will have a different observed angular size in spaces of different curvature. The black dotted lines represent the opening angle observed in each case. We see that because $\sin(u)/u < 1$ and $\sinh u/u > 1$, the observed angle will be larger in the $K > 0$ case and smaller in the $K < 0$ case, compared to the $K = 0$ case.

Angular diameter distance

The comoving angular distance is not directly observable because it depends on the comoving (coordinate) size of the source which is not observable. However, by relating this comoving size to the

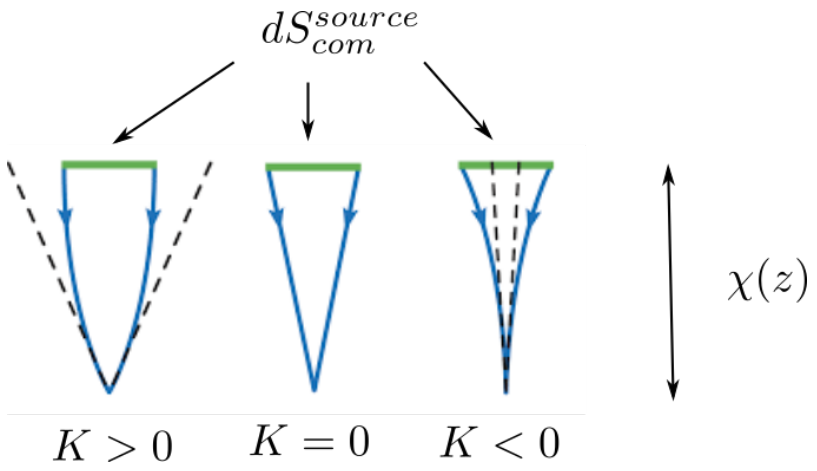

Figure 2.3: Effect of spatial curvature on the angular size of distant objects.

actual, physical transverse size of the source:

$$\mathrm{d}S_{phys}^{source} = a^2 \mathrm{d}S_{com}^{source} \ , \tag{2.45}$$

one can obtain an observable distance: the *angular diameter distance* $D_A(z)$ of an object located at redshift z with respect to the observer, defined as:

$$D_A^2 \equiv \frac{\mathrm{d}S_{phys}^{source}}{\mathrm{d}\Omega_{obs}^2} \ . \tag{2.46}$$

This is measurable in principle. Indeed, if the observer can measure the apparent angular size of the source on their sky and if they have an independent knowledge of the absolute physical size of the source (from theoretical modelling), they can deduce the angular diameter distance. This is why measurements of the angular diameter distance require the knowledge of *standard rulers*, i.e. object whose physical size is stable over time and known to great accuracy. We see that the angular diameter distance to a source located at redshift z is thus:

$$D_A(z) = aR_{ang}(z) = \frac{1}{1+z} S_K\left(\chi(z)\right) \ . \tag{2.47}$$

Luminosity distance

The other distance that turns out to be useful in cosmology makes use of another class of objects called *standard candles*. These are objects whose absolute luminosity is assumed well known and

stable from independent theoretical models. So assume that an observer at $\chi = 0$ and $t = t_0$ observes such a source located at a comoving radial distance $\chi(z)$ with absolute luminosity L_{source}. Assuming that the source radiates isotropically, the observed flux, Φ_{obs} will correspond to the isotropic flux through a sphere of radius $D_L(z)$:

$$\Phi_{obs} = \frac{L_{source}}{4\pi D_L^2} \ . \tag{2.48}$$

This D_L is the *luminosity distance* between the source and the observer. By definition, the luminosity is the power of the source, i.e. the rate of change of energy by units of time:

$$L_{source} = \frac{\Delta E_{emit}}{\Delta t_{emit}} = \frac{\Delta E(z)}{\Delta t(z)} \ . \tag{2.49}$$

Because of the redshift experienced by light between emission and observation, the change of energy observed is given by:

$$\Delta E_{obs} = \frac{\Delta E_{emit}}{1+z} \ . \tag{2.50}$$

Moreover, For two light rays emitted from the source in an interval of conformal time $\Delta\eta_{emit}$ and arriving at the observer in an interval $\Delta\eta_0$, we have: $\Delta\eta_0 = \Delta\eta_{emit}$ (light rays are straight lines in $\eta - \chi$ coordinates). Thus, going to proper time:

$$\Delta t_0 = \frac{1}{a}\Delta t_{emit} = (1+z)\Delta t_{emit} \ . \tag{2.51}$$

Therefore, the observed luminosity is given by:

$$L_{obs} = \frac{\Delta E_{obs}}{\Delta t_0} = \frac{1}{(1+z)^2}\frac{\Delta E_{emit}}{\Delta t_{emit}} = \frac{1}{(1+z)^2} L_{source} \ . \tag{2.52}$$

On the other hand, the observed flux is the ratio of the total observed luminosity at the time of observation by the surface area over which this luminosity is distributed, S^{phys}. This surface area is the physical area today of the sphere centred on the source of comoving radius $R_{ang}(z) = S_K(\chi(z))$:

$$S^{phys} = a_0^2 S^{com} = 4\pi S_K^2(\chi(z)) \ . \tag{2.53}$$

Thus:

$$\Phi_{obs} = \frac{L_{source}}{(1+z)^2 \times 4\pi S_K^2(\chi(z))} \ . \tag{2.54}$$

Equating the two expressions for the observed flux, we get:

$$\boxed{D_L(z) = (1+z) S_K\left(\chi(z)\right) \ .} \tag{2.55}$$

Note that the angular and luminosity distances are related by the *distance-duality relation*:

$$D_L(z) = (1+z)^2 D_A(z) \ . \tag{2.56}$$

This relation is actually true in any spacetime, in any metric theory of gravity, as long as the number of photons is conserved during the propagation of light between source and observer.
In a flat FLRW universe, these distances take the simple integral expressions:

Angular and luminosoty distances in flat FLRW

$$D_A(z) = \frac{1}{1+z}\int_0^z \frac{dz'}{H(z')} \tag{2.57}$$

$$D_L(z) = (1+z)\int_0^z \frac{dz'}{H(z')}. \tag{2.58}$$

These various notions of distance are all equally valid and their use depends on the physical system we want to evaluate the distance to. Fig 2.4 shows the radial comoving distance $\chi(z)$, the angular distance $D_A(z)$ and the luminosity distance $D_L(z)$ as functions of redshift for the nominal cosmology we introduce below; see Eqs. (2.143)-(2.148). Clearly, although they match for small redshifts (left panel), they differ significantly as soon as we probe further back into the past (right panel). In particular, the angular diameter distance exhibits a non-monotonous behaviour which means that after some redshift, objects that are further into the past appear smaller and smaller! Finally, note that we need knowledge of the dynamics on the FLRW Universe between the source and the observer, through the Hubble rate $H(z)$ to determine the behaviour of these distances. This dynamics is what we will focus on next.

2.1.4 Dynamics

To determine the dynamics of the FLRW Universe, one needs to write the Einstein Field Equations:

$$R_{\mu\nu} - \frac{1}{2}Rg_{\mu\nu} + \Lambda g_{\mu\nu} = 8\pi G T_{\mu\nu} \ , \tag{2.59}$$

for the FLRW metric and the appropriate energy-momentum content. For the left-hand side of those equations, we have, in proper time:

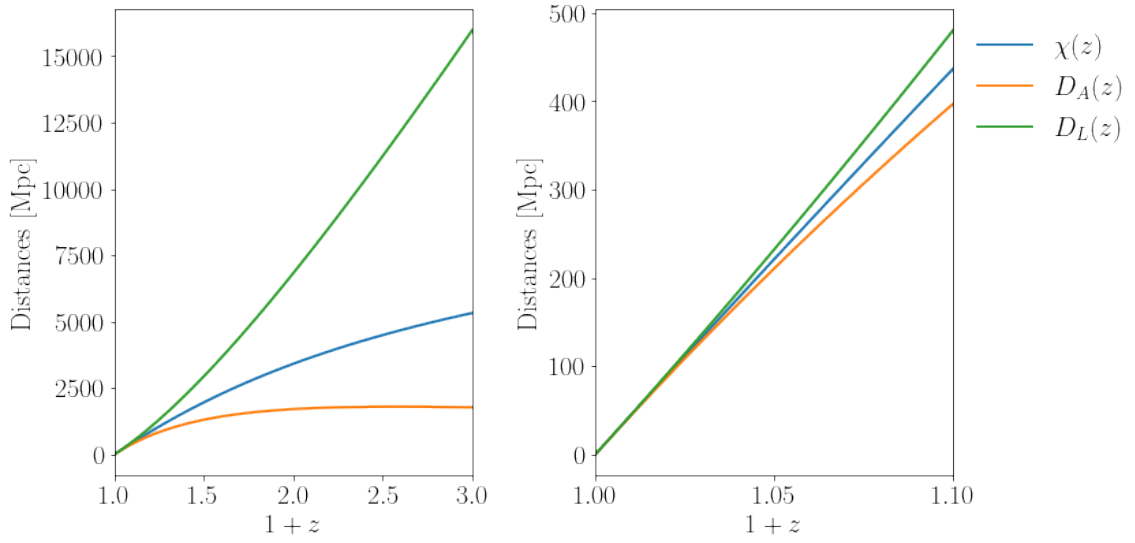

Figure 2.4: Radial comoving distance $\chi(z)$, angular distance $D_A(z)$ and luminosity distance $D_L(z)$ as functions of redshift for the nominal cosmology of Eqs. (2.143)-(2.148).

Ricci tensor for the FRLRW metric in (t, r, θ, ϕ) coordinates

$$\begin{cases} R_{00} = -3\dfrac{\ddot{a}}{a} & (2.60) \\ R_{ij} = a^2\left(2H^2 + \dfrac{\ddot{a}}{a} + 2\dfrac{K}{a^2}\right)\gamma_{ij} & (2.61) \\ R = 6\left(H^2 + \dfrac{\ddot{a}}{a} + \dfrac{K}{a^2}\right) . & (2.62) \end{cases}$$

Energy-momentum content

But what of $T_{\mu\nu}$? In principle, we should include all possible particles and fields present in the Universe, photons, electrons, protons, all atoms once they have formed, neutrinos, exotic sources like Dark Matter and Dark Energy (see below) etc. Usually, these are treated as independent, non-interacting fluids, with energy densities $\rho_i(t)$ and pressure $p_i(t)$. By symmetry, they ought to be comoving and their common 4-velocity sets the 4-velocity field of fundamental observers. Then

one can show easily that these fluids ought to be perfect (no heat flux or anisotropic pressure), thus having energy-momentum tensors:

$$T^{(i)}_{\mu\nu} = (\rho_i + p_i)\, u_\mu u_\nu + p_i g_{\mu\nu} \ , \tag{2.63}$$

which separately obey a conservation equation (non-interacting):

$$\nabla_\mu T^{(i)\mu}{}_\nu = 0 \ . \tag{2.64}$$

Then, for each fluid, we can define an equation of state:

$$w_i = \frac{p_i}{\rho_i} \ , \tag{2.65}$$

and Eq. (2.64) leads to:

$$\dot{\rho}_i + 3\,(1 + w_i)\, H\rho_i = 0 \ , \tag{2.66}$$

for each individual fluid. The total energy-momentum content is then an effective fluid with effective, total density, pressure and equation of state:

$$\begin{cases} \rho = \sum_i \rho_i & (2.67) \\ p = \sum_i p_i & (2.68) \\ w = \dfrac{p}{\rho} \ , & (2.69) \end{cases}$$

modelled by the *total energy-momentum tensor*, with components in (t, r, θ, ϕ) coordinates:

$$T_{\mu\nu} = (\rho + p)\, \delta_{\mu 0}\delta_{\nu 0} + p g_{\mu\nu} \ . \tag{2.70}$$

The conservation of this total energy-momentum tensor then leads to:

$$\dot{\rho} + 3\,(1 + w)\, H\rho = 0 \ . \tag{2.71}$$

Usually, in cosmology, the various standard fluids are separated into two main classes:

Non-relativistic fluids: These are fluids whose internal velocity dispersion is small. Individual particles of the fluid move slowly compared with the speed of light. For these fluids, the pressure $p_i \sim 0$, so that $w_i \sim 0$. Standard baryonic and leptonic matter fall into this category for most of the history of the Universe. So do neutrinos in the very late-time Universe. Cold Dark Matter is also non-relativistic throughout the history of the Universe. These non-relativistic fluids are often called dust or simply matter when the context is clear.

Relativistic fluids: These are fluids with internal particle velocities close to the speed of light. In that case, $p_i \simeq \frac{1}{3}\rho_i$ so that $w_i = 1/3$. Photons are such particles. So are neutrinos in the early Universe.

We will return to a more refined description of these components in chapter 3. But it is common to consider more exotic fluids. For example, taking the cosmological constant from the LHS to the RHS of the Einstein field equations, one can formally rewrite its effect as that of a perfect fluid with $p_\Lambda = -\rho_\Lambda$, thus $w_\Lambda = -1$. Perfect fluids with a constant equation of state are called barotropic. So dust and relativistic fluids are barotropic fluids; so is the cosmological constant if it is interpreted as a fluid. They are widely used in cosmology as they provide gvery good approximations to the actual content of the Universe.
Solving Eq. (2.66) for non-relativistic and relativistic fluids we see that:

$$\rho_{NR}(a) = \rho_{NR,0}a^{-3} \tag{2.72}$$

$$\rho_R(a) = \rho_{R,0}a^{-4}\,. \tag{2.73}$$

Therefore, in an expanding universe, dust is diluted by a factor proportional to the volume increase; this simply means that the number of particles (thus the total energy) in a given physical volume remains constant while the volume increases. Relativistic matter on the other hand receives an extra dilution in $1/a$; this comes from the redshift of the energy of individual photons in the fluid. It is common to write a subscript m for non-relativistic matter, and r for relativistic matter, which is what we will do from now on. For the cosmological constant, we get:

$$\rho_\Lambda = \text{cst} = \frac{\Lambda}{8\pi G}\,. \tag{2.74}$$

Dynamical equations

We are now ready to write the equations governing the dynamics of the FLRW Universe with a total matter content given by ρ and p. Combining the Ricci tensor and its trace from Eqs. (2.60)-(2.62) and the total energy-momemtum tensor, Eq. (2.70) within the Einstein field equations, we get:

FLRW dynamics in cosmic time

$$H^2 = \left(\frac{\dot{a}}{a}\right)^2 = \frac{8\pi G}{3}\rho - \frac{K}{a^2} + \frac{\Lambda}{3} \quad \text{(Friedmann Eq.)} \tag{2.75}$$

$$\frac{\ddot{a}}{a} = -\frac{4\pi G}{3}(\rho + 3p) + \frac{\Lambda}{3} \quad \text{(Raychaudhury Eq.)} \tag{2.76}$$

$$\dot{\rho} = -3H(\rho + p) \quad \text{(Continuity Eq.)}. \tag{2.77}$$

Note that these three equations are not independent (show it), so we only truly have two independent equations for three unknown functions. Thus, we need to assume an equation of state $p(\rho)$ to be able to solve this system. In conformal time, using the connection coefficients from Eqs. (2.18)-(2.21) and introducing the *conformal Hubble rate*:

$$\mathcal{H} = \frac{a'}{a} = aH\,, \tag{2.78}$$

we obtain the following dynamical equations:

FLRW dynamics in conformal time

$$\mathcal{H}^2 = \left(\frac{a'}{a}\right)^2 = \frac{8\pi G}{3}\rho a^2 - K + \frac{\Lambda}{3}a^2 \quad \text{(Friedmann Eq.)} \tag{2.79}$$

$$\mathcal{H}' = -\frac{4\pi G}{3}(\rho + 3p)\,a^2 + \frac{\Lambda}{3}a^2 \quad \text{(Raychaudhury Eq.)} \tag{2.80}$$

$$\rho' = -3\mathcal{H}(\rho + p) \quad \text{(Continuity Eq.)}. \tag{2.81}$$

Let us assume first, for simplicity, that the total fluid is barotropic, i.e. with a constant equation of state w: $p = w\rho$. Then the continuity equation can be easily solved:

$$\rho(a) = \rho_0 a^{-3(1+w)}\,. \tag{2.82}$$

In that case, assuming $K = \Lambda = 0$ and $w \neq 1$, we can solve the Friedmann equation and retain only the expanding solution:

$$a(t) = \left(\frac{t}{t_0}\right)^{\frac{2}{3(1+w)}} \quad \text{and} \quad a(\eta) = \left(\frac{\eta}{\eta_0}\right)^{\frac{2}{1+3w}}\,, \tag{2.83}$$

and also:

$$H(t) = \frac{2}{3(1+w)t} \text{ or } \mathcal{H}(\eta) = \frac{2}{(1+3w)\eta} \ . \tag{2.84}$$

One notes that:

$$\begin{cases} a \propto t^{2/3} \propto \eta^2 \text{ for a non-relativistic fluid} & (2.85) \\ a \propto t^{1/2} \propto \eta \text{ for a relativistic fluid.} & (2.86) \end{cases}$$

Also, for a cosmological constant $\Lambda \neq 0$ only:

$$a(t) = \exp\left[\sqrt{\frac{\Lambda}{3}}\,(t - t_0)\right] \ . \tag{2.87}$$

These scalings wil be very important throughout.

Let us now introduce dimensionless density parameters:

$$\Omega_i(z) \equiv \frac{8\pi G\rho_i(z)}{3H^2(z)} \tag{2.88}$$

$$\Omega(z) \equiv \frac{8\pi G\rho(z)}{3H^2(z)} = \sum_i \Omega_i(z) \text{ (Total energy content)} \tag{2.89}$$

$$\Omega_\Lambda(z) = \frac{8\pi G\rho_\Lambda}{3H^2(z)} \tag{2.90}$$

$$\Omega_K(z) = -\frac{K}{a^2(z)H^2(z)}. \tag{2.91}$$

Then the Friedmann equation becomes simply a balancing equation valid at all time/reshift:

$$\Omega + \Omega_\Lambda + \Omega_K = 1 \ . \tag{2.92}$$

In particular, today:

$$\sum_i \Omega_{i,0} + \Omega_{\Lambda,0} + \Omega_{K,0} = 1 \ . \tag{2.93}$$

For each barotropic fluid of constant equation of state w_i:

$$\Omega_i(z) = \Omega_{i,0}\left(\frac{H_0}{H(z)}\right)^2 (1+z)^{3(1+w_i)} \ . \tag{2.94}$$

Thus, we can introduce the dimensionless expansion rate:

$$E(z) \equiv \frac{H}{H_0} \ , \tag{2.95}$$

so that:

$$E^2(z) = \sum_i \Omega_{i,0}(1+z)^{3(1+w_i)} + \Omega_{K,0}(1+z)^2 + \Omega_{\Lambda,0} \ . \tag{2.96}$$

Cosmological eras

Finally, let us assume that the Universe is filled with a non-relativistic fluid and a relativistic one, as well as a cosmological constant. For simplicity, let us set $K = 0$. We can introduce the critical density of the Universe:

$$\rho_{c,0} = \frac{3H_0^2}{8\pi G} \,, \tag{2.97}$$

so that we have:

$$\rho_m = \Omega_{m,0}\rho_{c,0}a^{-3} = \Omega_{m,0}\rho_{c,0}(1+z)^3 \tag{2.98}$$

$$\rho_r = \Omega_{r,0}\rho_{c,0}a^{-4} = \Omega_{r,0}\rho_{c,0}(1+z)^4 \tag{2.99}$$

$$\rho_\Lambda = \Omega_{\Lambda,0}\rho_{c,0} \,. \tag{2.100}$$

Thus, as illustrated on Fig. 2.5, we see that in an expanding Universe, for generic choices of the parameters today, the Universe goes through three distinct phases:

1. $\rho(a) \sim a^{-4}$ as $a \to 0$. This is a *Radiation Dominated Era* (RDE): when the energy content and the dynamics of the Universe are dominated by the relativistic fluid;

2. At some point, the non-relativistic fluid starts to dominate the energy content and $\rho \sim a^{-3}$. This is a *Matter Dominated Era* (MDE);

3. Finally, provided one waits for long enough, since all energy densities decay except the one coming from the cosmological constant, a final epoch starts when the expansion of the Universe is governed by the cosmological constant. This is the *Dark Energy Dominated Era* (ΛDE). In the asymptotic future, when all the fluids have been infinitely diluted, the Universe is in a steady state called the de Sitter Universe.

The transition between the RDE and MDE occurs at *matter-radiation equality*, at a redshift (exercise):

$$1 + z_{\rm eq} = \frac{\Omega_{m,0}}{\Omega_{r,0}} \simeq 3\,200 \,, \tag{2.101}$$

where we used the nominal cosmology parameters of Eqs (2.143)-(2.148) for the numerical estimate. These three phases in the history of an expanding Universe will be key to our analysis of the growth of large-scale structure. A last piece of information we will need about the background is the only

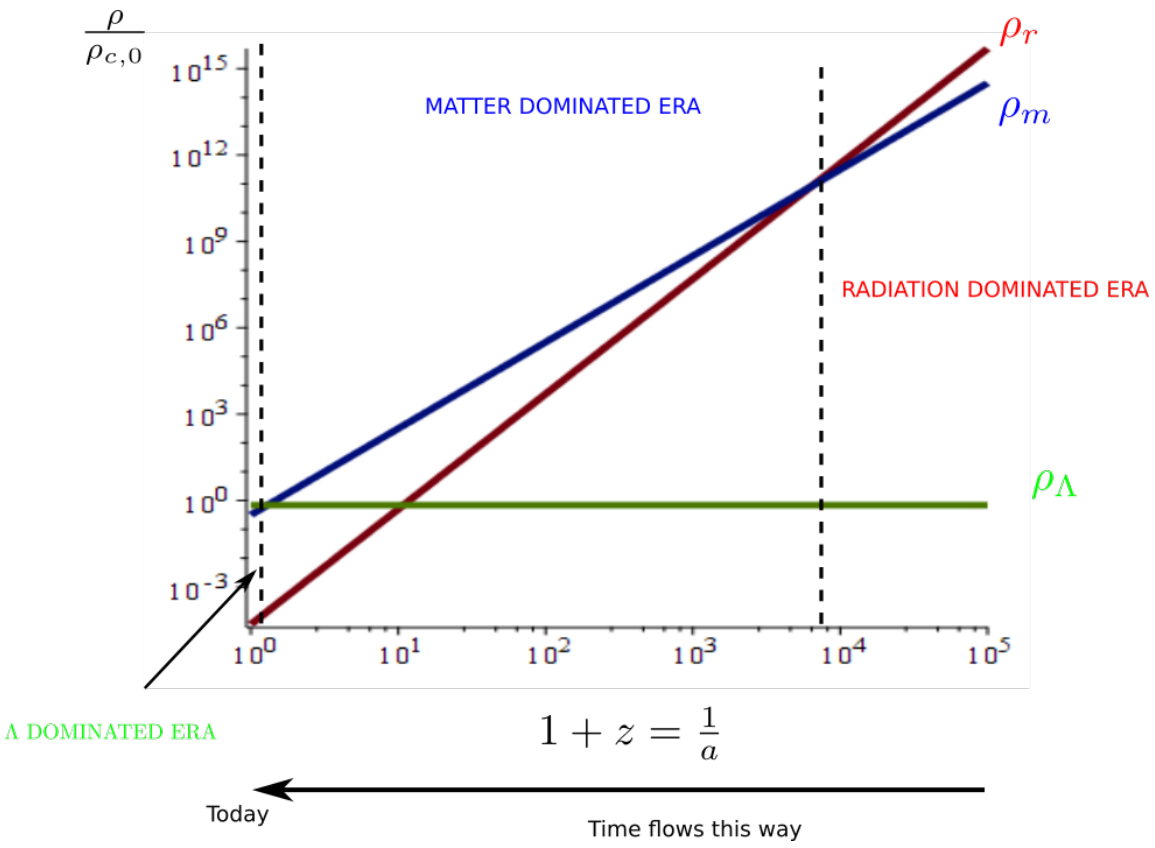

Figure 2.5: Log-log plot of the densities in a cosmology with $\Omega_{m,0} = 0.317$, $\Omega_\Lambda = 0.683$ and $\Omega_{r,0} = 2.10^{-5}$. The densities are expressed in units of the critical density. Typical values for the critical density are of the order $\rho_c \simeq 1.10^{-27}$ kg.m^{-3}.

characteristic scale that enters this extremely symmetric model: the Hubble radius. The *physical Hubble radius* is the (time-dependent) length:

$$R_H = cH^{-1} \ . \tag{2.102}$$

So we see that this scale grows during a MDE and a RDE as: $R_H(t) \propto t$ and is constant during a ΛDE. Actually, it will be more natural to consider the *conformal Hubble scale*:

$$R_{\mathcal{H}} = c\mathcal{H}^{-1}. \tag{2.103}$$

During a RDE, it goes like $R_{\mathcal{H}} = c\eta$, and during a MDE: $R_{\mathcal{H}} = c\eta/2$. On the other hand, it decreases in a ΛDE: $R_{\mathcal{H}} = R_{\mathcal{H},i}\eta_i/\eta$. We will see that this behaviour is important in the formation of structure.

2.2 The hot Big-Bang model

2.2.1 Why hot?

From the behaviour of the FLRW scale factor in presence of relativistic and non-relativistic matter fluids, we deduced that an expanding Universe, i.e. a Universe that was smaller with denser fluids in the past, ought to have undergone a transition between two phases: its early history is characterised by a Radiation Dominated Era, followed by a Matter Dominated Era. The relativistic fluid that dominates the dynamics during the Radiation Dominated Era has a density:

$$\rho_r \propto a^{-4} \propto (1+z)^4 \ . \tag{2.104}$$

Assuming that this fluid is in thermodynamical equilibrium at temperature T and zero chemical potential (for simplicity), the energy density in terms of the distribution function, $f\,(p,T)$, of the particles in the fluid is given by:

$$\rho = \int f\,(p,T)\,E(p)\mathrm{d}^3p \ . \tag{2.105}$$

Thus, for relativistic particles with $T \gg m$, whether particles are fermions or bosons[2]:

$$\rho \propto T^4 \ . \tag{2.106}$$

[2]The exact relation reads:

$$\rho(T) = a_S T^4 \ ,$$

where $a_S = 7.5657 \times 10^{-16}\mathrm{J}\cdot\mathrm{m}^{-3}\cdot\mathrm{K}^{-4}$ is the *radiation density constant*.

The expanding Universe was hotter in the past (when it was also denser). This is why one talks of a *Hot Big-Bang* model.

2.2.2 Thermal history

Thus, the temperature of the relativistic fluid (mostly photons) in the past is given, in terms of redshift by:

$$T(z) = T_0(1+z) \ , \tag{2.107}$$

where $T_0 \simeq 2.725$ K is the temperature of the CMB today. Strictly speaking, this is the common temperature of all matter species in the Universe only as long as all forms of matter remain in thermal equilibrium. For example, baryons only remain coupled with photons until recombination and decoupling, after which their temperature starts to deviate from the one of photons. However, it is common to call the temperature of the CMB the 'temperature of the Universe' and to use it as a clock to describe the thermal history of the Universe. Note that during the Radiation Dominated era[3]:

$$H(T) \propto \sqrt{\rho(T)} \propto T^2 \ . \tag{2.108}$$

Thus the typical timescale of expansion of the Universe evolves as:

$$\tau_H = H^{-1} \propto T^{-2} \ . \tag{2.109}$$

Let us consider an interaction between particles with rate Γ (units of inverse time). As long as $\Gamma \gg H$, the interaction remains efficient, the particles involved in the interaction have enough time to interact before being separated by the cosmic expansion, and they remain in thermal equilibrium. However, as soon as $\Gamma < H$, the interactions freeze and the various particles involved start evolving independently: they decouple. Considering that the content of our Universe is well-described by the standard model of particle physics, this leads to an elegant thermal history of the Universe[4]:

[3]Exactly, we have:

$$H(T) = \sqrt{\frac{8\pi G}{3}\rho_r(T)} = \sqrt{\frac{8\pi}{3M_{\rm Pl}^2}a_S T^4} = \sqrt{\frac{8\pi^3}{45}}\frac{T^2}{M_{\rm Pl}} \simeq 2\frac{T^2}{M_{\rm Pl}} \ ,$$

where we used natural units.

[4]We used that $T_0 = 2.275$ K $\simeq 2 \cdot 10^{-4}$ eV and that $T(z) = T_0(1+z)$ to determine the redshifts from the temperatures. The time t is the cosmic time, conventionally set to 0 at the Big-Bang, i.e. the time at which the model becomes singular.

1. $T > 100$ GeV; $z > 10^{15}$; $t < 20$ ps: Quantum Gravity; Inflation; Baryogenesis. This very early period is not described adequately by the standard model of particle physics and its details remain the topic of conjectures and speculations. For reasons to be explored later, it seems to include a phase of accelerated expansion of the Universe called inflation, or something that would produce similar signatures on the later Universe. It also needs to include a mechanism responsible for the asymmetry between matter and anti-matter that we observe today.

2. $T = 100$ GeV; $z = 10^{15}$; $t = 20$ ps: Electroweak phase transition. The electromagnetic and weak interactions separate via the Higgs mechanism, and particles acquire their masses.

3. $T = 150$ MeV; $z = 10^{12}$; $t = 20\,\mu$s: QCD phase transition. Above that temperature, quarks are asymptotically free, i.e. they are only subjected to the weak interaction. But below that temperature, the strong interaction kicks in and quarks and gluons form bound states: baryons (three quarks) and mesons (pairs quark-antiquark).

4. $T = 1$ MeV; $z = 6 \cdot 10^9$; $t = 1$ s: neutrinos decoupling. Weak interactions are no longer fast enough to maintain neutrinos in thermal equilibrium with the rest of matter. They decouple and form an hypothetical cosmic neutrino background that should permeate the whole Universe today (but has not yet been observed) with its own temperature.

5. $T = 500$ keV; $z = 2 \cdot 10^9$; $t = 6$ s: electron-positron annihilation. Electrons and positrons cannot be maintained in thermal equilibrium with photons and annihilate, releasing energies in the photon fluid (reason why the CMB has a different temperature than the cosmic neutrino background). A small asymmetry between matter and anti-matter is necessary to keep some electrons around after this phase.

6. $T = 100$ keV; $z = 4 \cdot 10^8$; $t = 3$ min: Big Bang Nucleosynthesis (BBN). Some protons and neutrons escape the thermal equilibrium and bound to form atomic nuclei via a complex network of nuclear reactions. Only the light elements are formed in any significant quantity: deuterium, helium, lithium and beryllium. The amount of each element formed during this primordial phase can be calculated very accurately in the standard model and the agreement

As will become apparent when we introduce inflation, this reference time is actually quite arbitrary in standard cosmology, as the Big-Bang singularity disappears from the physical Universe and potentially even completely.

of these predictions with observations constitutes one of the most robust pillar of the Hot Big-Bang model.

7. $T = 0.75$ eV; $z = 3400$; $t = 60$ kyr: Matter-Radiation Equality. The energy densities of relativistic and non-relativistic matter coincide.

8. $T = 0.26 - 0.33$ eV; $z = 1100 - 1400$; $t = 260 - 380$ kyr: Recombination. Electrons and baryons (mostly protons and helium nuclei) combine to form atoms (neutral hydrogen, helium atoms) via e.g. $e^- + p \rightarrow H + \gamma$ once the converse reaction is energetically disfavoured. Matter becomes neutral and the mean-free path of photons increases rapidly. This leads to:

9. $T = 0.23 - 0.28$ eV; $z = 1000 - 1200$; $t = 380$ kyr: Photon decoupling also called simply decoupling. Before recombination, photons and electrons are tightly coupled via Thomson scattering: $e^- + \gamma \rightarrow e^- + \gamma$. However, when atoms start to form and matter becomes neutral, free electrons become scarce and Thomson scattering becomes inefficient. Therefore, the photons mean free path increases rapidly and they decouple from the rest of matter, forming a thermal bath of radiation that free streams and permeates the Universe: this is the Cosmic Microwave Background. In parallel, ordinary matter is now free from the influence of the radiation fluid and can start falling in the gravitational wells of Dark Matter that have already started to form under their own gravitational pull: structures start to form in the Universe.

10. $T = 2.6 - 7$ meV; $z = 11 - 30$; $t = 100 - 400$ Myr: Reionisation. The formation of the first stars lead to bursts of energetic radiation which gradually re-ionise the neutral hydrogen formed during recombination.

11. $T = 0.33$ meV; $z = 0.4$; $t = 9$ Gyr: Dark Energy-Matter equality. The cosmological constant starts to dominate the dynamics of the Universe. See below.

12. $T = 0.24$ meV; $z = 0$; $t = 13.8$ Gyr: Today.

Chapter 3 offers a more detailed account of some of these processes.

2.3 The dark sector

In addition to the matter-energy content provided by the standard model of particle physics, the standard model of cosmology needs to introduce at least two new sources of the gravitational field

to account for the behaviour of the Universe and objects inside it. Because these new sources are, to date, only felt through their gravitational interaction, and do not seem to interact significantly via electromagnetic interactions, they are called dark.

2.3.1 Dark Matter

The first dark component that one needs to introduce is an additional fluid of non-relativistic particles known as Dark Matter. The nature of Dark Matter has not yet been determined and this is a true puzzle for fundamental physics. However, as we will see, it is clear that at cosmological/extragalactic scales, something peculiar happens that needs to be explained. The standard lore is to assume the presence of Dark Matter and to hope that its constituents will be identified at some point, be they fundamental particles, condensates of fundamental particles, or even small black holes formed in the primordial phases of the history of the Universe and remaining to this day. Alternatives consider that gravity and/or inertia itself is modified to account for the unexpected phenomena. Although these are puzzling and interesting possibilities, we will not explore them in this introductory course.

The first evidence for Dark Matter comes from the observations of distant spiral galaxies. The visible part of a spiral galaxy forms a thin disc of radius $R_d \sim$ a few kpc, with stars orbiting in quasi-circular orbits. Newtonian mechanics applied to the motion of these stars leads to a profile of velocity as a function of the distance to the centre of the galaxy r given by:

$$\frac{v^2(r)}{r} = \frac{GM\,(<r)}{r^2}\,, \tag{2.110}$$

where $M\,(<r)$ is the total mass contained within a shell of radius r. Thus, at distances $r \geq R_d$ beyond the size of the disc, if all the mass of the galaxy is contained into stars (and interstellar gas), $M\,(<r) \to M$ reaches a constant value, and the velocity profile should scale like:

$$v(r) \propto \frac{1}{\sqrt{r}}\,. \tag{2.111}$$

But observations do not support such a decrease. Instead, the velocity profile reaches a constant value $v_\infty \neq 0$ as r becomes large. This is illustrated for a specific galaxy on Fig. 2.6.

Such a profile requires the presence of additional matter beyond the observable disc of the galaxy, with a distribution of mass going as:

$$M(r) \propto r \text{ for } r \geq R_d\,, \tag{2.112}$$

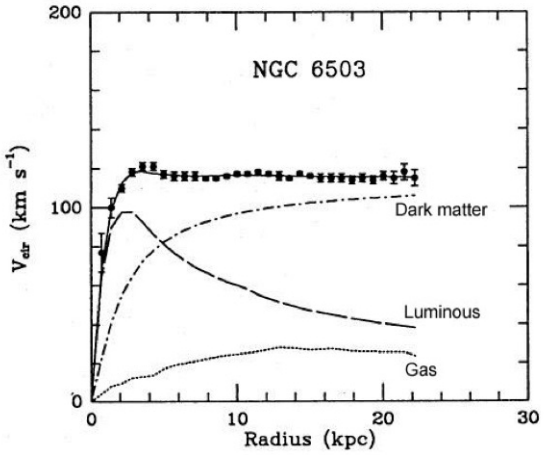

Figure 2.6: Rotation Velocity in the galaxy NGC6503, together with the respective contributions from diffuse gas, stars (labelled luminous), and the Dark Matter halo necessary to account for the observed profile. From [5].

which, for a spherically distributed halo, corresponds to an additional density of matter $\rho(r) \sim 1/r^2$. This is Dark Matter on galactic scales. The presence of such halos has also been confirmed by gravitational lensing of distant light by galaxies and clusters of galaxies. Finally, let us mention that Dark Matter is also needed on cosmological scales:

- BBN gives us a precise measurement of the ratio of baryonic matter to radiation in the Universe and the amount of radiation can be inferred from observation of the CMB. These facts in combination lead to a small energy density of baryons, too small to constitute the entire energy budget in non-relativistic particles.

- We will see that during the Matter Dominated era, small-scale matter overdensities grow like the scale factor: $\delta \propto a \propto 1/(1+z)$. However, baryons can only start to grow structure after they decouple from photons This means that, if the non-relativistic fluid only consisted of baryons, an overdensity of size 1 today should have been of size $\sim 10^{-3}$ at decoupling. This is 2 orders of magnitude larger than the overdensities in the photon-baryon plasma at decoupling inferred from the observations of the CMB. Thus structures have had to start forming earlier, in a fluid that did not feel the pressure waves of the plasma: a weakly interacting Dark Matter

component does just that.

2.3.2 Late-time Universe: Λ

Dark Matter is thus required to explain the formation and behaviour of structure in the Universe. On the largest scales and latest times, on the other hand, another problem arises. Let us introduce the *deceleration parameter*:

$$q_0 = -\frac{\ddot{a}}{aH^2}_{|t=t_0} \ . \tag{2.113}$$

Note that, neglecting radiation in the late Universe:

$$q_0 = \frac{1}{2}\Omega_{m,0} - \Omega_{\Lambda,0} \ . \tag{2.114}$$

We can then Taylor expand all quantities around the present time, e.g., at the relevant, dominant orders:

$$a(t) \simeq 1 + H_0 (t - t_0) - \frac{1}{2} q_0 H_0^2 (t - t_0)^2 \tag{2.115}$$

$$z(t) \simeq -H_0 (t - t_0) \tag{2.116}$$

$$E(z) \simeq 1 + (1 + q_0) z \ . \tag{2.117}$$

Thus, the luminosity distance of a distant object at small redshift behaves like:

$$D_L(z) \simeq H_0^{-1} \left(z + \frac{1 - q_0}{2} z^2 \right) \ . \tag{2.118}$$

It is possible to calibrate the luminosity curves of Type 1a Supernovæ and use them as standard candles, i.e. as distant objects whose intrinsic luminosity can be determined. Then, one can measure their apparent luminosity on Earth and determine their luminosity distance. By measuring their redshift, one can thus determine a distance-redshift relation $D_L(z)$ and constrain cosmology. Actually, the quantity that is usually being reported in the distance modulus:

$$\mu(z) - M = -2.5 \log \left[\frac{\phi(z)}{\phi\,(10\ \mathrm{pc})} \right] \ , \tag{2.119}$$

where $\phi(z)$ is the flux of a source located at redshift z and $\phi\,(10\ \mathrm{pc})$ the one of a source at 10 pc. The factor -2.5 is arbitrary and was chosen to match the definition of magnitude given by Hipparcos

for stars. $\mu(z)$ is the apparent, measured, magnitude of the object, and M its absolute magnitude defined with respect to the magnitude of the Sun:

$$M = -2.5 \log \left(\frac{L}{3.8 \times 10^{26}\ \mathrm{W}} \right) + 4.75\ . \tag{2.120}$$

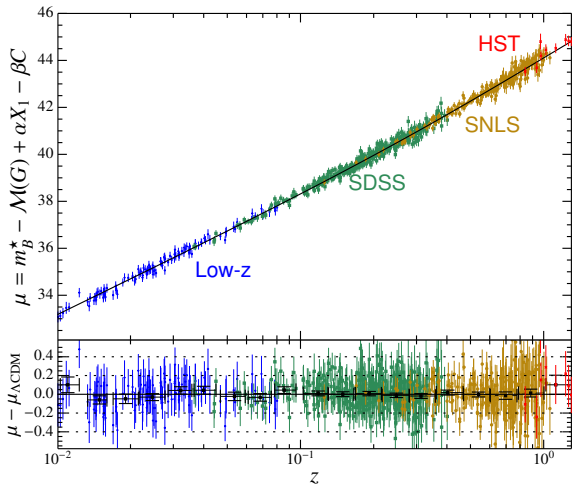

Figure 2.7: Distance modulus of distant Supernovæ 1a and residuals with respect to a flat FLRW Universe with Cold Dark Matter and $K = 0$. From [6].

Such observations have been performed with greater and greater accuracy since 1998, and consistently report $q_0 < 0$, i.e. a relation whose second derivative at the origin is larger than H_0^{-1}. But this is only possible if $\Omega_{\Lambda,0} \neq 0$, in other words, if $\Lambda \neq 0$. Moreover, it means that the expansion of the Universe is currently accelerating: $\ddot{a} > 0$, a phenomenon that cannot emerge from any standard source of the gravitational field. Thus, if one were to assume $\Lambda = 0$, one would have to introduce some non-standard, exotic matter source (or modify gravity) to ensure $\ddot{a} > 0$; this is what is dubbed Dark Energy. So far, there is no evidence favouring an exotic Dark Energy over a simple cosmological constant so in what follows we will limit our discussion to this simple scenario. Fig. 2.7 summarises measurements of the distance-redshift relation from various recent projects. Note that cosmological evidence for the presence of a cosmological constant are now numerous and we do not only rely on these $m(z)$ diagrams.

2.4 Limits of the model: Inflation

The hot Big-Bang model we just described has been extraordinarily successful at explaining a wide range of observations, as well as at predicting some quantities that were measured later. By any measure, it is a very successful scientific model. However, it suffers from a few shortcomings that have to do with its initial state. The initial singularity is clearly a problem, but we are going to see that it is not just a mathematical one. Rather, it comes with some physical implications that are quite puzzling and need to be overcome. This will be the role played by a phase in the history of the Universe taking place before the radiation dominated epoch and known as cosmic inflation. Let us stress immediately that although the principles of inflation and its overall phenomenology are very useful in solving the problems of the hot Big-Bang model, inflation as a model does not enjoy the same status as the rest of the cosmological model. In particular, it is not as well tested and constrained as the hot Big-Bang phase. There are essentially four problems with the standard Big-Bang model:

- The causality problem. In the hot Big-Bang, regions of spacetime that appear extremely similar to us did not have enough time to interact with each other. But then, why are they so similar?

- The flatness problem. In the standard, ΛCDM model, the Universe appears to be close to spatially flat today. In the Hot Big-Bang model, that means it must have started extremely flat at the Big-Bang. How can it be?

- The relic problem. At high energies, close to the initial singularity, phase transitions should have produced topological defects with very high densities. Why don't we see them around us?

- The origin of structures problem. How are the seeds for structure formation generated?

Inflation will somehow solve all these problems at once. In this section, we will highlight the problems of the standard model listed above and sketch how inflation solves the first three of them, that is, the ones which have to do with the background expansion history, rather than with structures. A somewhat more detailed treatment of inflation can be found in Chapter 8, in particular as far as the origin of structures is concerned (which will not be treated it).

2.4.1 The causality problem

Let us consider an observer O ('Us') today (at $\eta = \eta_0$), observing the Cosmic Microwave background emitted at η_{dec}. The situation is summarised on Fig. 2.8 in an (η, χ) diagram. The surface of last scattering for O[5] appears as a sphere of radius given by the comoving radial distance $\chi(z_{dec}) = \int_0^{z_{dec}} dz'/H(z')$. Thus, the diameter represented on the diagram is given by:

$$d_{tot,dec} = 2\int_0^{z_{dec}} \mathrm{d}z'/H(z') \simeq 2 \times 1.93 H_0^{-1} \,, \tag{2.121}$$

where we used standard values for the cosmological parameters and we neglected the effect of the cosmological constant on the expansion history (the argument is not affected by this approximation). Let us now consider events at $\eta = \eta_{dec}$ located on or inside the past lightcone of O. The regions of space at the initial time (at the Big-Bang), $\eta = 0$, which have had time to influence these events at η_{dec} are balls at $\eta = 0$ with (comoving) diameters:

$$d_i = 2\int_{z_{dec}}^{+\infty} \frac{\mathrm{d}z'}{H(z')} \simeq 2 \times 4 \cdot 10^{-2} H_0^{-1} \,. \tag{2.122}$$

On the other hand, the intersection of the past lightcone of O with the initial space slice at $\eta = 0$, which gives the set of all the points that actually influenced the events on or inside the last scattering surface seen by O, delimits a ball of (comoving) diameter:

$$d_{tot,i} = 2\int_0^{+\infty} \frac{\mathrm{d}z'}{H(z')} \simeq 2 \times 1.98 H_0^{-1} \,. \tag{2.123}$$

Therefore, the number of disconnected regions at the Big-Bang, each able to influence a different point on or inside the last scattering surface is roughly given by:

$$N \simeq \left(\frac{d_{tot,i}}{d_i}\right)^3 \simeq 10^5 \,. \tag{2.124}$$

The corresponding points at η_{dec} have not had time to interact in any causal way but if we live in an almost FLRW Universe, they ought to have almost the same temperature, as seen in the CMB temperature anisotropies which are of the order of 10^{-5}. Unless the initial conditions at $\eta = 0$ were set extremely precisely (fine-tuned) to ensure this coincidence at η_{dec}, this is not possible.

[5] This is the surface obtained as the section of the space at time t_{dec} at which photons decouple from baryonic matter by the past lightcone of the observer O. Strictly speaking, decoupling is not instantaneous, and last-scattering for an observer is not quite a surface, but this does not modify the argument and we will ignore this subtlety.

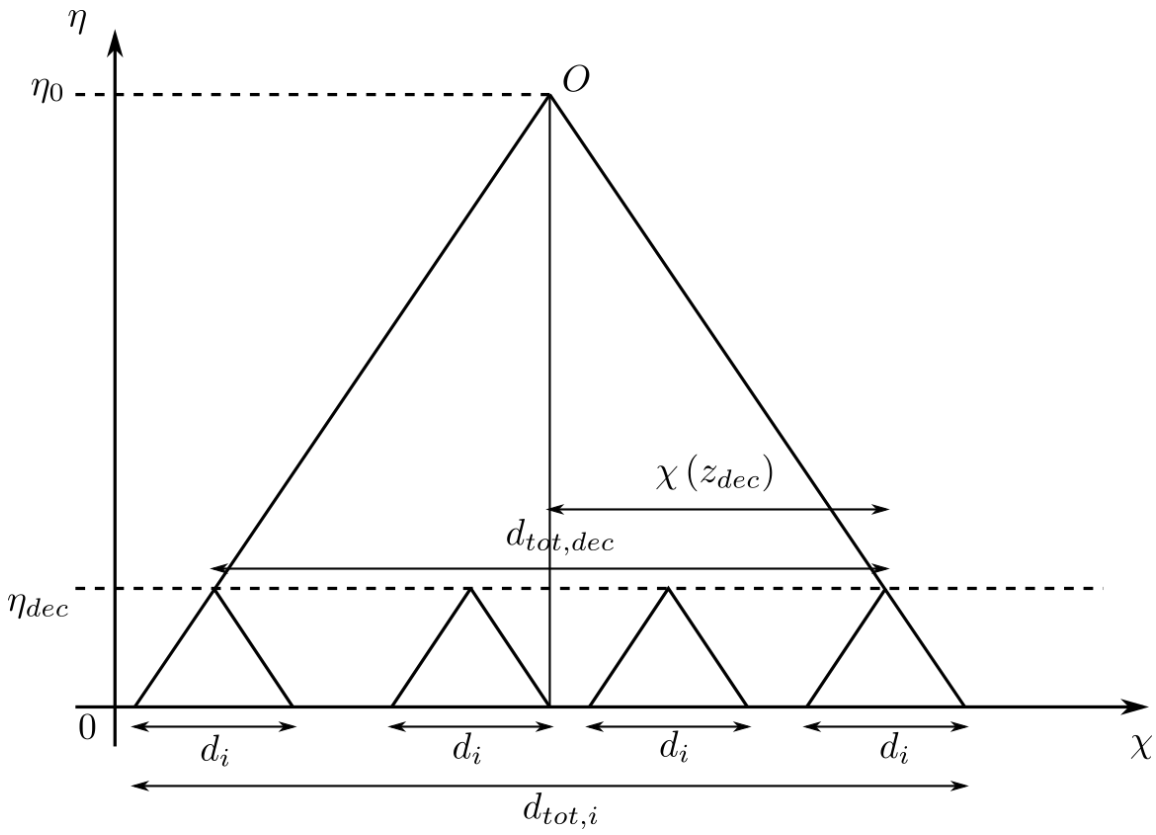

Figure 2.8: Spacetime diagram to illustrate the causality problem

One might be worried that this argument depends on the Copernican principle, since we talk about events located inside our past lightcone at last scattering, so events that we do not observe. We can turn things around and examine what happens on the last scattering surface only. Consider now an event located at $\eta = 0$. The intersection of the inside of its future lightcone with the hypersurface at last scattering will be a ball of proper diameter:

$$D_i = \frac{1}{1+z_{dec}} d_i \simeq 2 \times 4 \times 10^{-5} H_0^{-1} \ . \tag{2.125}$$

If it intersects the last scattering surface, it does so on a patch with typical size D_i. On the other hand, the distance form 0 to the last scattering surface is given by:

$$D = \frac{1}{1+z_{dec}} d_{tot,dec} \simeq 2 \times 10^{-3} H_0^{-1} \ . \tag{2.126}$$

This means that the angular size, as seen from 0, of a patch of the last scattering surface that has been influenced by an event at the Big-Bang is given by:

$$\Delta\theta \simeq \frac{D_i}{D} \simeq 2 \times 10^{-2} \sim 1^o \ . \tag{2.127}$$

The number of such disconnected patches on the CMB sky is roughly given by the ratio of the solid angles:

$$N' \simeq \frac{\Delta\theta^2}{4\pi} \simeq 10^4 \ . \tag{2.128}$$

All these patches have not had time to thermalise by causal contact and yet, they exhibits remarkably similar properties on the sky observed by 0. How is this possible?

2.4.2 The flatness problem

In a hot Big-Bang scenario, still neglecting the effects of Λ for simplicity, we can write the evolution of the curvature parameter as:

$$\Omega_K(z) = \frac{\Omega_{K,0}}{\Omega_{m,0}(1+z) + \Omega_{r,0}(1+z)^2} \ . \tag{2.129}$$

The problem is that this function is decreasing: since we observe a small curvature parameter today, typically $\left|\Omega_{K,0}\right| < 10^{-2}$, the effect of curvature needs to have been even smaller in the past. In the early Universe, close to the Big-Bang:

$$\Omega_K(z) \sim \frac{\Omega_{K,0}}{\Omega_{r,0}} (1+z)^{-2} \text{ when } z \to +\infty \ . \tag{2.130}$$

Thus, using $\Omega_{r,0} \sim 10^{-5}$:

$$\left|\Omega_{K,i}\right| < 10^3 \, (1 + z_i)^{-2} \ . \tag{2.131}$$

At BBN, this bound is of order 10^{-7} and it reaches 10^{-61} at the Planck time. Therefore, the Universe needs to start in an extremely flat configuration in order to get a very flat Universe today. Of course, this is only a problem if one considers that this is an unnatural initial state; in absence of a measure giving us the likelihood of a given curvature, this is impossible to assess. Therefore, this problem with the hot Big-Bang is of a different nature than the causality problem. Whereas the latter is really linked to a physical difficulty, the former is only a problem as far as "taste" for "natural" initial conditions is concerned.

2.4.3 The relic problem

As we have seen, as the Universe cools down, some phase transitions occur when fundamental symmetries are broken. If Grand Unified scenarii are correct, when the Grand Unification theory breaks down, at the very early stages of the Radiation Dominated epoch, some topological defects such as monopoles are created. These carry a very large amount of energy density that, if present, would completely dominate the expansion of the Universe and change the expansion history that we know. So, why are these topological defects not around and dominating the expansion of the Universe?

2.4.4 Origin of structure

Finally, as we mentioned before, we need to find a way to generate density fluctuations in the early Universe that are large enough to give rise to the structures we observe via gravitational infall. Moreover, because of the behaviour of the Hubble radius, we know that, in a Universe with only a matter dominated and a radiation dominated eras, all physical scales on which we observe fluctuations in the matter distribution today will eventually exit the Hubble radius if we trace them backward in time far enough. This means that these fluctuations cannot have been generated causally in the Hot Big-Bang model (because the Hubble radius fixes approximately the scale below which causal processes are efficient in the Universe; see below). How is this possible?

2.4.5 The idea of inflation

Let us get back to the comoving distance between a point at an initial time t_i for the expansion of the Universe and a point at time = t further in the future:

$$\chi(t) = \int_{t_i}^{t} \frac{\mathrm{d}t'}{a\,(t')} = \int_{\ln a_i}^{\ln a} \mathcal{H}^{-1}\,(a')\,\mathrm{d}\ln a' \,, \tag{2.132}$$

where we have written $a_i = a(t_i)$. Note that here, since we want to replace the Big-Bang by something else, we do not yet assume that $a_i = 0$. For a perfect fluid with w = cst, the comoving Hubble scale $\mathcal{H}^{-1} = (aH)^{-1}$ behaves as:

$$\mathcal{H}^{-1} = (aH)^{-1} \propto a^{(1+3w)/2} \,. \tag{2.133}$$

Thus, for standard matter, with $1 + 3w > 0$, this scale increases with the expansion of the Universe. But this means that the integral in Eq. (2.132) is dominated by its upper limit and receives a vanishing contribution from the early times. Indeed, performing the integral (and using the fact that we are tracing lightrays, so that $\mathrm{d}\chi = -\mathrm{d}\eta$), we get:

$$\chi(a) = \eta - \eta_i \propto a^{(1+3w)/2} - a_i^{(1+3w)/2} \,, \tag{2.134}$$

with $\eta_i \propto a_i^{(1+3w)/2}$. Note that $\chi(a)$ is always finite and that $\eta_i \to 0$ when $a_i \to 0$, i.e. in case of a Big-Bang singularity. But what happens if, at early times, i.e. before the radiation dominated era, there is an era with $1 + 3w < 0$? In that case, we have that:

$$\frac{\mathrm{d}}{\mathrm{d}t}\mathcal{H}^{-1} \propto \frac{1+3w}{2} a^{(3w-1)/2}\mathcal{H} < 0 \,. \tag{2.135}$$

Therefore, the comoving Hubble scale $\mathcal{H}^{-1}$ now decreases as a increases. But this means that, in that case, the integral in Eq. (2.132) is dominated by its lower bound, and that the Big-bang sigularity gets pushed to negative values of the conformal time:

$$\eta_i \propto \frac{2}{1+3w} a_i^{(1+3w)/2} \to -\infty \text{ when } a_i \to 0 \,. \tag{2.136}$$

In principle, by choosing this early phase to be arbitrarily long, one can push the Big-Bang singularity arbitrarily far into the past, thus asymptotically ridding the cosmological model of the Big-Bang singularity. This means one has "much more conformal time available" between the singularity

and decoupling, allowing for regions to interact causally. The comoving distance between the Big-Bang and decoupling can now be made arbitrarily large. This early phase during which $\mathcal{H}^{-1}$ is a decreasing function of time is known as inflation, since:

$$\frac{\mathrm{d}}{\mathrm{d}t}\mathcal{H}^{-1} = -\frac{\ddot{a}}{\dot{a}^2} < 0 \Rightarrow \ddot{a} > 0 \,, \tag{2.137}$$

meaning that the expansion is actually accelerating. The behaviour of causally connected regions in a Universe with an early inflationary phase is presented in Fig. 2.9, to be contrasted with what we saw in a standard Big-Bang model. Fig. 2.10 also presents the behaviour of the comoving Hubble scale and of physical scales in such a Universe. Note that during inflation, scales that were initially sub-Hubble are expelled for the comoving Hubble scale and only re-enter later, during the standard hot Big-Bang phase, either when radiation or matter dominate the expansion. That will explain why structures that are sub-Hubble today but were super-Hubble in the past actually formed causally: they were actually sub-Hubble in an even more distant past, during inflation. How much inflation do we need to solve the causality problem? At the very least, we need the comoving distance to decoupling to fit into the comoving Hubble radius at the beginning of inflation. This will ensure that all the points in our CMB sky today will have been in causal contact at some point during inflation, before separating out later. Note that $\chi\left(z_{dec}\right) \simeq 2H_0^{-1}$ so that, up to an irrelevant factor of 2, we can impose that the Hubble radius today fits entirely in the comoving Hubble radius at the beginning of inflation. Our condition corresponds to (keeping $a_0 = 1$ for symmetry in the expressions):

$$\left(a_0 H_0\right)^{-1} < \left(a_I H_I\right)^{-1} \,. \tag{2.138}$$

Now, neglecting the matter dominated and Λ dominated phases (which lower the comoving Hubble radius compared to keeping only radiation, so our bound is stronger here), we get:

$$\frac{a_0 H_0}{a_E H_E} \simeq \frac{a_0}{a_E}\left(\frac{a_E}{a_0}\right)^2 = \frac{a_E}{a_0} = \frac{T_0}{T_E} \,. \tag{2.139}$$

Assuming that the end of inflation is around the Grand Unified Theory scale (which ensures that the monopoles get diluted by inflation and thus also solves the relic problem), so that $T_E \sim 10^{15} - 10^{16}$ GeV, we find that:

$$\left(a_I H_I\right)^{-1} > 10^{28}\left(a_E H_E\right)^{-1} \,, \tag{2.140}$$

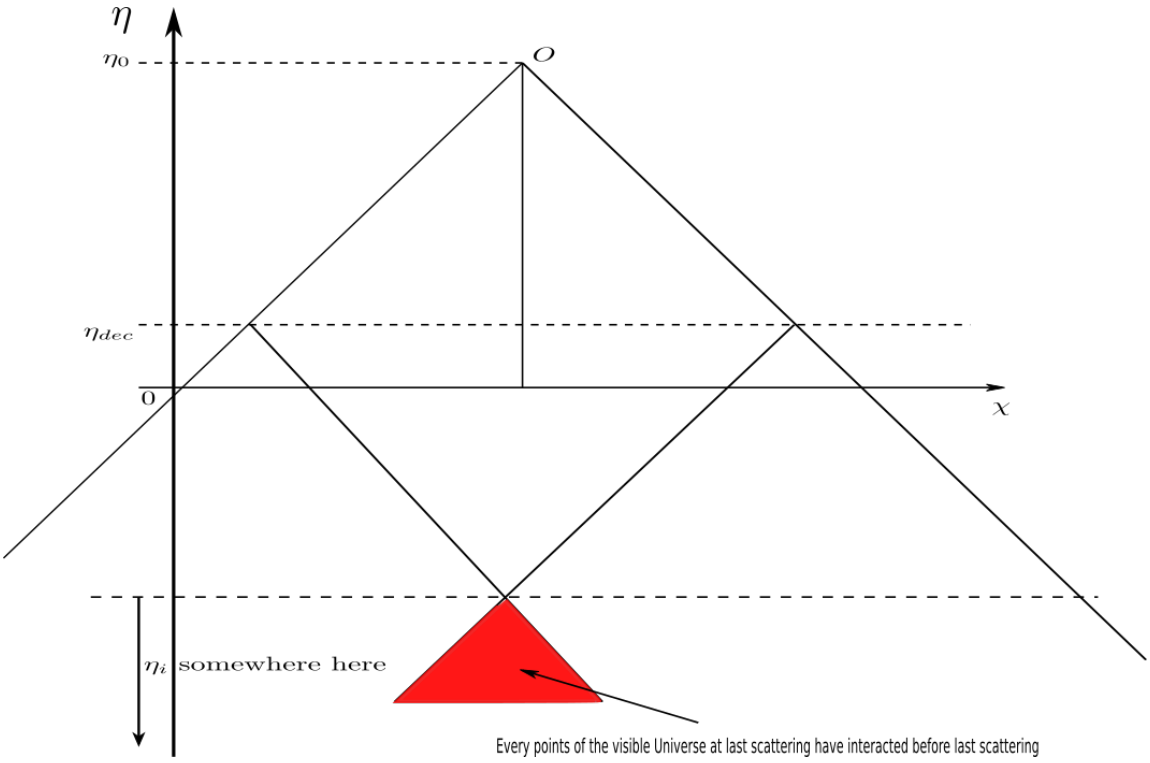

Figure 2.9: How the causality problem is resolved by an early phase of inflation. In the red region, two antipodal points on the last scattering surface which would have been totally causally disconnect in the standard Big-Bang scenario, can now have interacted in their past, thus thermalising by physical process and sharing a nearly equal temperature, as observed. The choice of η_i must be made such that at least antipodal points have interacted; this ensures that other points on the last scattering surface will also have had time to interact.

thus, the comoving Hubble radius must shrink by 28 orders of magnitude during inflation. For an almost constant Hubble rate, this implies that the number of e-folds must be:

$$N \equiv \ln\left(\frac{a_E}{a_I}\right) > 64 \ . \tag{2.141}$$

Note that in terms of physical distance, this corresponds to a physical Hubble radius H^{-1} increasing dramatically. Such a huge amount of inflation, in addition to solving the causality problem and the monopole problem (because the volume increases so much that the density of monopoles, if they exist, decreases dramatically), also addresses the flatness problem. This is because during inflation, the parameter $\Omega_K(a)$ actually decreases dramatically. Hence any curvature present at the beginning of inflation would have been wiped out by a factor 10^{-56}:

$$\frac{\Omega_K\left(a_E\right)}{\Omega_K\left(a_I\right)} = \left(\frac{a_I H_I}{a_E H_E}\right)^2 < \left(10^{-28}\right)^2 = 10^{-56} \ . \tag{2.142}$$

The physical volume of the Universe increases so much during inflation that the curvature becomes very small.

2.5 A concordance model

The FLRW Universe with $\Lambda \neq 0$, some Cold Dark Matter, and flat spatial sections ($K = 0$) is called the *concordance model of cosmology*. In addition to the parameters of the standard model of particle physics (that are considered determined and fixed in the concordance model), it contains a certain number of free parameters that need to be determined by observations or principles. The 6 cosmological parameters that are left free and to be determined in the concordance model are usually:

1. the physical baryon density: $\Omega_{b,0}h^2$, where $h = H_0/(100\ \text{km/s/Mpc})$;
2. the physical CDM density: $\Omega_{c,0}h^2 = \left(\Omega_{m,0} - \Omega_{b,0}\right)h^2$;
3. the age of the Universe: t_0;
4. the optical depth of reionisation τ;
5. the scalar spectral index n_s (a parameter of inflation; see below);

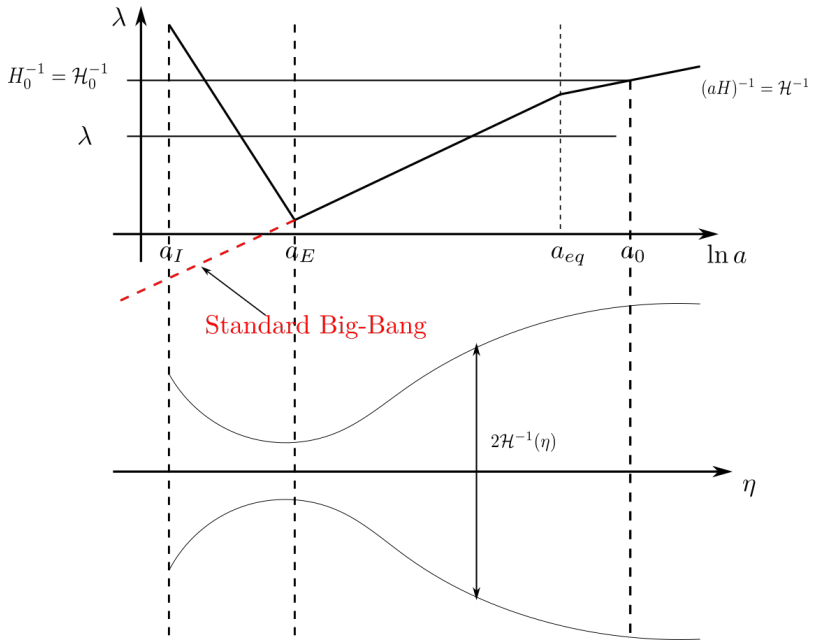

Figure 2.10: Upper part: Behaviour of comoving scales in an inflationary Universe. Inflation starts at a_I and ends at a_E, after which the standard hot Big-Bang expansion starts: rafiation dominated era followed by a matter dominated era (the effects of the cosmological constants are ignored for illustrative purposes here). Comoving scales $\lambda < a_I H_I$ start sub-Hubble and are expelled from the Hubble sphere during inflation. They only re-enter the Hubble radius during the Hot Big-Bang phase. Lower part: Qualitative behaviour of a section of the comoving Hubble sphere. The transition between inflation and the radiation dominated phase is called reheating and is yet poorly understood.

6. the amplitude of initial curvature perturbations Δ^2_ζ (a parameter of inflation; see below).

The cosmological parameters that are fixed by default in the concordance model are:

1. the curvature parameter: $K = 0$;
2. the tensor to scalar ratio: $r = 0$ (a parameter of inflation; see below);
3. the running of the spectral index: $\frac{dn_s}{d\ln k} = 0$;
4. the sum of the masses of neutrinos: $\sum m_\nu = 0.06$ eV/c^2;
5. the effective number of relativistic degrees of freedom: $N_{eff} = 3.046$.

All other parameters can be determined by calculations. Today, due to the not so small number of these parameters, and to intrinsic degeneracies between them in observables, the most precise determination of these parameters, or any different combination of those and extra parameters that one may want to leave free, comes from combining constraints that can be inferred from different observations, e.g., CMB anisotropies, supernovæ 1a, Baryon Acoustic Oscillations, Weak lensing shear surveys, BBN, galaxy number counts etc. This is why the model is called concordant: it provides the minimal, "simplest" model that can account for most (if not all) of the current observations available on our Universe. Over the last decade, as observations became more and more precise, some tensions started to appear in this concordance model. Careful scrutiny and more and more precise observations have not led to any resolution of these tensions but it remains unclear whether or not such issues can be attributed to new physics, beyond the minimal ΛCDM model, to systematic biases due to our inability to accurately model non-linear physics on multiple scales to fit the model to observations, or to observational errors. As a matter of fact, there is not a single model that can currently account for all these tensions at once at still pass with success all the other tests that ΛCDM passed. Therefore, for pedagogical purposes, we can concentrate on this model. Deviations from it are small and, although they might prove very important from a conceptual level, they will most likely not alter the big picture significantly. The interested students will find an extensive review of these recent issues in [3].

We will use the following nominal values for background cosmological parameters, unless otherwise stated:

Nominal background parameters

$$\Omega_{K,0} = 0 \tag{2.143}$$
$$\Omega_{m,0} = 0.32 \tag{2.144}$$
$$\Omega_{b,0} = 0.05 \tag{2.145}$$
$$\Omega_{\Lambda,0} = 0.68 \tag{2.146}$$
$$\Omega_{r,0} = 10^{-4} \tag{2.147}$$
$$H_0 = 67 \text{ km/s/Mpc.} \tag{2.148}$$

2.6 Problems

Pb. 2.1 For a constant equation of state $w \neq -1$, show that

$$a \propto t^{2/3(1+w)} \propto \eta^{2/(1+3w)} , \tag{2.149}$$

and find the similar result for the special case $w = -1$.

Pb. 2.2 Find, in terms of the density parameters today:

- the redshifts of the radiation-to-matter and matter-to-cosmological constant transitions;
- the Hubble radius and comoving Hubble radius at these transitions.

Pb. 2.3 Using the nominal value for Ω_m and Ω_b estimate the number of hydrogen atoms per m^3 in the Universe, as well as the total mass of non-relativistic matter inside a volume of 1 Gpc^3. Use this to estimate how many galaxies of mass $10^{11} M_\odot$ one expects.

Pb. 2.4 Find the surface area and volume of the Hubble sphere (Sphere of radius the Hubble radius) centred on a typical observer in an FLRW Universe.

Pb. 2.5 Write a Python code to plot the comoving radial distance $\chi(z)$ (in units of Mpc) as a function of redshift in the nominal cosmology. Plot:

- $(z, \chi(z))$ for $0 \leq z \leq 10$;

- $(\log(1+z), \chi(z))$ for $0 \leq z \leq 1090 = z_{dec}$.

Determine the comoving radius of the decoupling sphere $\chi\left(z_{dec}\right)$.

Pb. 2.6 Show that, in standard cosmology:

- $d_A(z) \sim z^{-1}$ and $d_L(z) \sim z$ when $z \longrightarrow +\infty$;
- $d_A(z)$ always has a maximum and at this maximum: $d_A = H^{-1}$;
- $d_L(z)$ never has a maximum;
- $d_A(z)$ has a point of inflection.

Pb. 2.7 Show that in a ΛCDM model at late times (neglecting radiation):

$$\frac{\mathrm{d}\Omega_m}{\mathrm{d}\ln a} = -3(1-\Omega_m)\Omega_m \ . \tag{2.150}$$

Solve this equation numerically and represent the solution.

Pb. 2.8 In the radiation dominated era, show that the scale factor behaves as:

$$a(t) = \left(2H_0\sqrt{\Omega_{r0}}t\right)^{1/2} \ . \tag{2.151}$$

Deduce $H(t)$, $\rho_r(t)$ and $z(t)$ and sketch the results. Use these results to estimate the age of the Universe and its temperature at $z = 10^9$ and $z = 10^4$ (Use appropriate units for the age, and quote the temperature in kelvin and electronvolts).

Pb. 2.9 The lookback time $\Delta t(z) = t_0 - t(z)$ of an emitter with redshift z is defined as the difference in cosmic time between the present and the time at which the light signal was emitted.

- Show that:
$$\Delta t(z) = t_0 - t(z) = \int_0^z \frac{\mathrm{d}z'}{(1+z')\,H\,(z')} \ . \tag{2.152}$$
- Plot the lookback time in units of Gyr as a function of $0 \leq z \leq 1100$.
- Determine the lookback time at $z = 1$ and $z = z_{dec}$.

Pb. 2.10 Consider a late time ΛCDM model (neglecting radiation).

- Show that:
$$a(t) = \left(\frac{\Omega_{m,0}}{\Omega_{\Lambda,0}}\right)^{1/3} \sinh^{2/3}\left[\frac{3H_0\sqrt{\Omega_{\Lambda,0}}}{2}t\right] \ . \tag{2.153}$$

- Determine the age of the Universe in terms of H_0 and $\Omega_{m,0}$. Estimate its value in Gyr,
- Show that:
$$\frac{\ddot{a}}{aH^2} = -\frac{1}{2}\left(\Omega_m - 2\Omega_\Lambda\right) \ . \tag{2.154}$$
and find the condition for acceleration.
- Find the redshift z_{acc} at which acceleration starts in terms of $\Omega_{m,0}$.
- Compare z_{acc} with the redshift at which the energy densities of matter and cosmological constant are equal.
- At which cosmic time does acceleration starts?

Pb. 2.11 Consider the Universe filled with matter and radiation during its early times, when one can neglect Λ.

- Show that:
$$H_0 t = \frac{2}{3\sqrt{\Omega_{m,0}}}\left[\left(a + a_{eq}\right)^{1/2}\left(a - 2a_{eq}\right) + 2a_{eq}^{3/2}\right] \ , \tag{2.155}$$
where $a_{eq} = \frac{\Omega_{r,0}}{\Omega_{m,0}}$ is the scale factor at matter-radiation equality.
- Determine the age of the Universe at $z = z_{eq}$ and at $z = z_{dec}$.

Pb. 2.12 Consider a matter-only Universe ($\Omega_{m,0} = 1$).

- Show that:
$$d_A(z) = 2H_0^{-1}\left[\frac{1}{1+z} - \frac{1}{(1+z)^{3/2}}\right] \ . \tag{2.156}$$
- Derive the redshift at which d_A is maximum and find this maximum value.
- Find the point of inflection of $d_A(z)$.
- Sketch $d_A(z)$ with all the key features.
- Sketch the angular size, $\theta_H(z)$ of the Hubble scale $H^{-1}(z)$, showing all the key features.
- Skecth the angular size $\theta_{BAO}(z)$ of the BAO scale $R_{BAO}(z) = (150\ \text{Mpc})/(1+z)$.

Pb. 2.13 Redo the previous question numerically in the nominal cosmology.

Pb. 2.14 Suppose that we observe the same galaxy at two different proper times t_0 and $t_0 + \delta t_0$. Show that, the change in its redshift is given by:

$$\frac{\delta z}{\delta t_0} = H_0 \left[(1+z) - E(z) \right] \ . \tag{2.157}$$

This is called the redshift drift. What is the expression of this redshift drift at small redshift?

3 Thermal history of the Universe

Contents

In chapter 2, we studied the properties and the dynamics of the FLRW model that describes the Universe on large scales. We saw that its expansion history could be roughly divided into three phases: a radiation dominated phase, a matter dominated one and then a Λ dominated epoch. As we explore the Universe further into the past, we encounter a distribution of matter that is denser, hotter and host to more and more energetic physical processes. The Universe is also more homogeneous and in the first few minutes of its history, many of its properties are fully captured by the FLRW model. As will will see in the next chapters, this is less and less the case as structure start to grow. In this chapter, we are going to explore in more details some of the important phases listed briefly in subsection 2.2.2.

3.1 Thermodynamics in an expanding Universe

During the radiation dominated phase, the state of matter is completely different to what we are accustomed, being dominated by a plasma of relativistic particles. This section explains how to write the thermodynamical properties of this plasma in an expanding Universe.

3.1.1 Thermodynamics quantities

Let us consider a particle with position $\vec{x}$ and associated momenta $\vec{p}$. These are the *physical* positions and momenta, not the comoving ones, but for ease of notations, we remove the subscript in this chapter only. In quantum mechanics, in a given volume of momentum space V, one only finds a discrete spectrum of momentum eigenstates, with a density of state given by $L^3/h^3 = V/h^3$. Thus, the density of states in phase space is given by $1/h^3$. If the particle has g internal degrees of freedom (e.g. spin), then the density of states becomes g/h^3. From now on, we will work in natural units, for which the reduced Planck constant $\hbar = h/2\pi = 1$. For a gas of particles, the distribution of particles according to momentum eigenstates is given by the distribution function in phase space $f(\vec{x}, \vec{p}, t)$. Homogeneity implies that we should drop the $\vec{x}$-dependence, and because of the monotonous expansion, we can replace t by the temperature of the gas T (via the Hubble parameter). Finally, isotropy implies that the distribution function can only depend on the momentum via its norm, $\|\vec{p}\| = p$. Therefore, the density of particles in phase space is given by the product of the density of states for each particle by the density of particle in phase space. The number of particles

in a given volume element is thus:

$$\mathrm{d}n(p,T) = \frac{g}{(2\pi)^3} f(p,T)\mathrm{d}V \ . \tag{3.1}$$

Therefore, the *number density* is given by:

$$n(T) = \frac{g}{(2\pi)^3} \int \mathrm{d}^3\vec{p}\, f(p,T) \ . \tag{3.2}$$

The fact that f only depends on the norm p encourages one to use spherical coordinates in momentum space to perform this integral, so that:

$$\mathrm{d}^3\vec{p} = p^2 \mathrm{d}p \sin\theta \mathrm{d}\theta \mathrm{d}\phi \ , \tag{3.3}$$

and one can perform the angular integrals at no cost to get:

$$n(T) = \frac{g}{2\pi^2} \int_0^{+\infty} \mathrm{d}p\, p^2 f(p,T) \ . \tag{3.4}$$

Since we have that:

$$p^2 = E^2 - m^2 \ , \tag{3.5}$$

where m is the mass of the particles in the gas and E their energy, we can write this in a form that will be more convenient for us:

$$\boxed{n(T) = \frac{g}{2\pi^2} \int_m^{+\infty} E\sqrt{E^2 - m^2} f(E,T)\mathrm{d}E \ ,} \tag{3.6}$$

where we used the same name for the distribution function expressed in terms of energy and momentum in a slight (but usual) abuse of notations. The *energy density* in the gas can be evaluated similarly by integrating $E(p)f(p,T)$ over momentum space to get:

$$\boxed{\rho(T) = \frac{g}{2\pi^2} \int_m^{+\infty} E^2\sqrt{E^2 - m^2} f(E,T)\mathrm{d}E \ .} \tag{3.7}$$

The case of pressure is more subtle. Consider a small, oriented, area element in real space, $\mathrm{d}A$ with normal vector $\vec{n}$. All the particles hitting on this surface between a time t and a time $t + \mathrm{d}t$ with a velocity $\|\vec{v}\|$ were, at $t = 0$ in a small spherical shell of radius $\|\vec{v}\|\mathrm{d}t$ at a distance $R = \|\vec{v}\|t$ of the

surface element. The number of particles with energy E in a volume element $\mathrm{d}V = R^2\|\vec{v}\|\mathrm{d}t\mathrm{d}\Omega$ (where $\mathrm{d}\Omega$ is the solid angle element) is given by:

$$\mathrm{d}N(E,t,\|v\|,\theta,\phi) = \frac{g}{2\pi^2}f(E)\mathrm{d}V = \frac{g}{2\pi^2}f(E)R^2\|\vec{v}\|\mathrm{d}t\mathrm{d}\Omega\ . \tag{3.8}$$

However, not all particles in the volume $\mathrm{d}V$ hit the surface element $\mathrm{d}A$. Since the velocity distribution is isotropic, the number of particles hitting the surface element is thus:

$$\mathrm{d}N_A(E,t,\|v\|,\theta,\phi) = \frac{\mathrm{d}A\vec{n}\cdot\vec{v}}{4\pi R^2}\mathrm{d}N(E,t,\|v\|,\theta,\phi)\ . \tag{3.9}$$

If we assume that the collisions with the surface are elastic, then each collision transfers a momentum $2\,|\vec{p}\cdot\vec{n}|$ to the surface, so that the pressure caused by particles with velocity $\|\vec{v}\|$ is:

$$\mathrm{d}P(E,t,\|\vec{v}\|,\theta,\phi) = \int\frac{2\,|\vec{p}\cdot\vec{n}|}{\mathrm{d}A\mathrm{d}t}\mathrm{d}N_A\ . \tag{3.10}$$

Using that $E\|\vec{v}\| = \|\vec{p}\|$ and integrating over $\vec{v}\cdot n < 0$, i.e. only over particles moving towards the surface element, we get:

$$\mathrm{d}P(E,T) = \frac{g}{(2\pi)^3}\frac{p^2}{3E}f(E,T)\ , \tag{3.11}$$

so that, integrating once more over E and doing the angular integrals, the *pressure* in the gas is given by:

$$P(E,T) = \frac{g}{6\pi^2}\int_m^{+\infty}\left(E^2-m^2\right)^{3/2}f(E,T)\mathrm{d}E\ . \tag{3.12}$$

Note that in this chapter, in order not to confuse pressure with momenta, we use a capital letter P for the pressure, while we use a normal size p in the rest of these notes, as is usual in cosmology.

3.1.2 Equilibrium thermodynamics

Distribution function

In kinetic equilibrium, when particles of a gas exchange energy and momentum efficiently, the distribution function of particles is either a Fermi-Dirac one, for fermions, or a Bose-Einstein one for bosons:

$$f(E,T) = \frac{1}{\mathrm{e}^{(E-\mu(T))/T}\pm 1}\ , \tag{3.13}$$

where the + sign is for fermions and the − sign for bosons. $\mu(T)$ is the chemical potential, which encodes possible changes in the total number of particles in the gas. At low temperatures $T \ll E - \mu$, both distributions reduce to a Maxwell-Boltzmann form:

$$f(E,T) \simeq \mathrm{e}^{-(E-\mu(T))/T} \ . \tag{3.14}$$

As the Universe expands, both T and $\mu(T)$ ought to change in the appropriate way to ensure that conservation equations for ρ and n are satisfied. The number density, energy density, and pressure then takes very interesting forms in certain limits. Setting $x = m/T$ and $y = \mu/T$, we can define the integral:

$$I^{\pm}_{(m,n)}(x,y) = \int_x^{+\infty} \frac{u^m \left(u^2 - x^2\right)^{n/2}}{\mathrm{e}^{u-y} \pm 1} \mathrm{d}u \ . \tag{3.15}$$

Then:

$$\begin{cases} n(T) = \dfrac{g}{2\pi^2} T^3 I^{\pm}_{(1,1)} & (3.16) \\ \rho(T) = \dfrac{g}{2\pi^2} T^4 I^{\pm}_{(2,1)} & (3.17) \\ P(T) = \dfrac{g}{6\pi^2} T^4 I^{\pm}_{(0,3)} \ . & (3.18) \end{cases}$$

We can then distinguish between relativistic and non-relativistic particles.

- *Relativistic particles*: In that case, $T \gg m$.
  - *Bosons*:

    There are two cases.
    - If $T \gg \mu$, then:

$$\begin{cases} n(T) = \dfrac{g\zeta(3)}{\pi^2} T^3 & (3.19) \\ \rho(T) = \dfrac{\pi^2 g}{30} T^4 & (3.20) \\ P(T) = \dfrac{1}{3}\rho(T) \ . & (3.21) \end{cases}$$

    - If $\mu < -T$, then:

$$\begin{cases} n(T) = \dfrac{g}{\pi^2} \mathrm{e}^{\mu/T} T^3 & (3.22) \\ \rho(T) = \dfrac{3g}{\pi^2} \mathrm{e}^{\mu/T} T^4 & (3.23) \\ P(T) = \dfrac{1}{3}\rho(T) \ . & (3.24) \end{cases}$$

· *Fermions*:

There are three cases.

◇ If $T \gg \mu$, then:

$$\begin{cases} n(T) = \dfrac{3g\zeta(3)}{4\pi^2} T^3 & (3.25) \\ \rho(T) = \dfrac{7\pi^2 g}{240} T^4 & (3.26) \\ P(T) = \dfrac{1}{3}\rho(T)\ . & (3.27) \end{cases}$$

◇ If $\mu \gg T \gg m$, then:

$$\begin{cases} n(T) = \dfrac{g\mu^3}{6\pi^2} & (3.28) \\ \rho(T) = \dfrac{g\mu^3}{8\pi^2} & (3.29) \\ P(T) = \dfrac{1}{3}\rho(T)\ . & (3.30) \end{cases}$$

◇ If $\mu < -T$, then:

$$\begin{cases} n(T) = \dfrac{g}{\pi^2} \mathrm{e}^{\mu/T} T^3 & (3.31) \\ \rho(T) = \dfrac{3g}{\pi^2} \mathrm{e}^{\mu/T} T^4 & (3.32) \\ P(T) = \dfrac{1}{3}\rho(T)\ . & (3.33) \end{cases}$$

- *Non relativistic particles*: In that case, $T \ll m$ and we have only one case, *valid for both fermions and bosons*:

$$\begin{cases} n(T) = g \left(\dfrac{mT}{2\pi}\right)^3 \mathrm{e}^{(\mu-m)/T} & (3.34) \\ \rho(T) = \left(m + \dfrac{3}{2}T\right) n(T) & (3.35) \\ P(T) = n(T)T \ll \rho(T)\ . & (3.36) \end{cases}$$

Here, we have introduces the Riemann ζ function:

$$\zeta(s) = \frac{1}{\Gamma(s)} \int_0^{+\infty} \frac{u^{s-1}}{\mathrm{e}^s - 1} \mathrm{d}s\ , \tag{3.37}$$

where $\Gamma(s)$ is the Gamma function. We have:

$$\zeta(3) \simeq 1.202\ . \tag{3.38}$$

Note that we recover that:

- $P = \frac{1}{3}\rho$ for relativistic fluids;
- $P \ll \rho$ for non-relativistic fluids.

Chemical potential

If a species of particles is in *chemical equilibrium*, then its chemical potential is related to the chemical potential of all the species it interacts with. For example, if a species 1 has some interactions with 3 other species, say 2, 3 and 4, via the reaction:

$$1 + 2 \leftrightarrow 3 + 4 \ , \tag{3.39}$$

then the chemical potentials obey:

$$\mu_1 + \mu_2 = \mu_3 + \mu_4 \ , \tag{3.40}$$

with obvious notations. This translates the fact that the rates of reaction are the same in both directions. Since photons are involved in inelastic scatterings such as Bremsstrahlung, $e^- + p \leftrightarrow e^- + p + \gamma$, we have at chemical equilibrium:

$$\mu_{e^-} + \mu_p = \mu_{e^-} + \mu_p + \mu_\gamma \ , \tag{3.41}$$

which implies that *photons have zero chemical potential*:

$$\mu_\gamma = 0 \ . \tag{3.42}$$

Therefore, any particle X that is maintained in chemical equilibrium with its antiparticle via particle-antiparticle annihilation:

$$X + \bar{X} \leftrightarrow \gamma + \gamma \ , \tag{3.43}$$

must satisfy:

$$\mu_X + \mu_{\bar{X}} = 0 \ . \tag{3.44}$$

This implies that, for relativistic species, as soon as $\mu_A \neq 0$, we have an asymmetry between particles and antiparticles:

$$n_X - n_{\bar{X}} \simeq \frac{g_X T^3}{6\pi^2} \left[\pi^2 + \left(\frac{\mu_X}{T} \right)^2 \right] \frac{\mu_X}{T} \ , \tag{3.45}$$

whereas, as soon as the temperature drops to $T \ll m_X$ and the particles become non-relativistic:

$$n_X - n_{\bar{X}} \simeq 2g_X \left(\frac{m_X T}{2\Pi}\right)^{3/2} \mathrm{e}^{-m_X/T} \sinh\left(\frac{\mu_X}{T}\right) , \tag{3.46}$$

and the asymmetry is exponentially suppressed. This can be attributed to pair annihilations. This is what happens to electrons and positrons.

We speak of *thermal equilibrium* between species if they are in kinetic and chemical equilibria. These species then share a common temperature T, which, in cosmology, is usually identified with the temperature of photons and called the 'temperature of the Universe'. This is the one we use as a proxy for time evolution in the thermal history.

In standard cosmology, all species have very small chemical potentials which can thus be neglected.

3.1.3 Effective number of relativistic species

The total energy density of radiation at temperature T (cosmic time t such that $T = T(t)$, where T is the temperature of the gas of photons) is the sum of the energy densities of all relativistic species:

$$\rho_r(T) = \sum_i \rho_i(T) = \frac{\pi^2}{30} g_*(T) T^4 , \tag{3.47}$$

where $g_*(T)$ is the *effective number of relativistic degrees of freedom* at temperature T. This receives contribution from relativistic bosons and fermions alike, but we must distinguish between those that are in thermal equilibrium with photons, and those that are not:

$$g_*(T) = g_*^{\mathrm{th}}(T) + g_*^{\mathrm{dec}}(T) . \tag{3.48}$$

Relativistic species in thermal equilibrium with photons contribute to g_*^{th} and we get[1]:

$$g_*^{\mathrm{th}}(T) = \sum_{i=\mathrm{boson}} g_i + \frac{7}{8} \sum_{i=\mathrm{fermion}} g_i . \tag{3.49}$$

When the temperature drops below the mass m_i of a given species, this species becomes non-relativistic and its contribution is removed from the sum in Eq. (3.49). Thus, if there were only thermalised species, the effective number of relativistic degrees of freedom would look like a series of constant steps, with drops at each temperature $T = m_i$ for masses of particles in the standard model. This is pretty close to the actual plot of $g_*(T)$ presented on Fig. 3.1.

[1] We always have $\mu \ll T$.

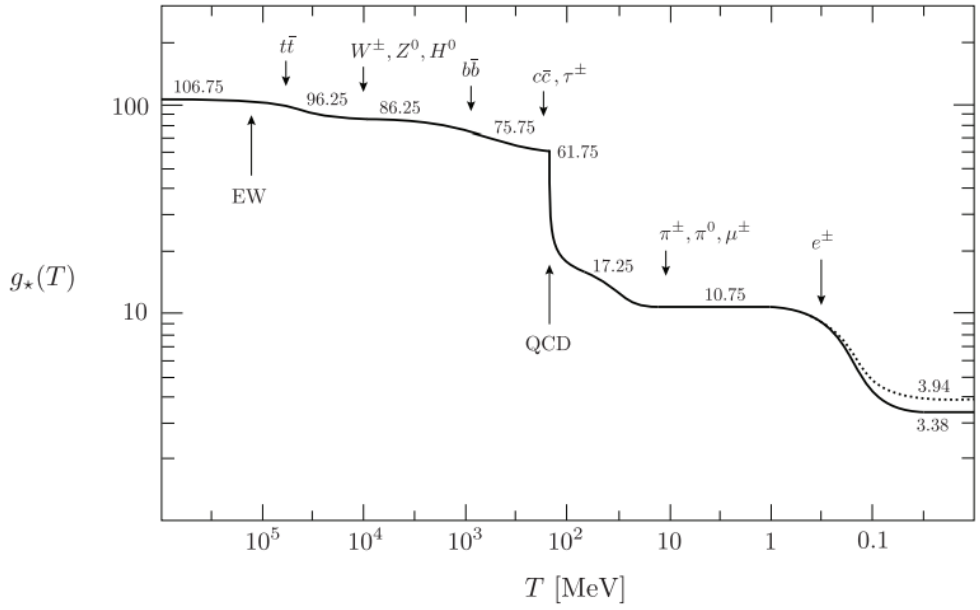

Figure 3.1: Effective number of relativistic degrees of freedom as a function of the temperature. The dotted line represents this effective number in the expression for entropy; see subsection 3.1.4. Figure from [4].

For the relativistic particles that are not in thermal equilibrium with photons we have to suppose a priori that they have temperatures $T_i \neq T \gg m_i$. Then, we say that they have decoupled from the thermal bath and they contribute to $g_*^{\rm dec}(T)$:

$$g_*^{\rm dec}(T) = \sum_{i=\text{boson}} g_i \left(\frac{T_i}{T}\right)^4 + \frac{7}{8} \sum_{i=\text{fermion}} g_i \left(\frac{T_i}{T}\right)^4 . \tag{3.50}$$

Again, if a particle becomes non-relativistic after having decoupled from photons, it must be dropped from this sum. Table 3.1 presents all the particles of the standard model with their mass, spin etc., counting carefully degrees of freedom. Bosons are in blue and fermions in red. We have 90 fermionic degrees of freedom and 20 bosonic ones.

Clearly, for $T \geq 100$ MeV, all the particles are relativistic. Besides, at the beginning, all those particles are in thermal equilibrium. This is because they are interacting via weak interactions, for

Type	Name	Mass	Internal dof	g
Quarks	$t, \bar{t}$	174 GeV	S=1/2; 3 colours	$2 \times 2 \times 3 = 12$
	$b, \bar{b}$	4.2 GeV	S=1/2; 3 colours	$2 \times 2 \times 3 = 12$
	$c, \bar{c}$	1.25 GeV	S=1/2; 3colours	$2 \times 2 \times 3 = 12$
	$s, \bar{s}$	95 MeV	S=1/2; 3colours	$2 \times 2 \times 3 = 12$
	$d, \bar{d}$	3-7 MeV	S=1/2; 3colours	$2 \times 2 \times 3 = 12$
	$u, \bar{u}$	1.5-3 MeV	S=1/2; 3colours	$2 \times 2 \times 3 = 12$
Gluons	8	0	S=1	$2 \times 8 = 16$
Leptons	$\tau^{\pm}$	1.7 GeV	S=1/2	$2 \times 2 = 4$
	$\mu^{\pm}$	105 MeV	S=1/2	$2 \times 2 = 4$
	$e^{\pm}$	511 keV	S=1/2	$2 \times 2 = 4$
	$\nu_{\tau}, \bar{\nu}_{\tau}$	<18 MeV	S=1/2	2
	$\nu_{\mu}, \bar{\nu}_{\mu}$	<190 keV	S=1/2	2
	$\nu_{e}, \bar{\nu}_{e}$	<2 eV	S=1/2	2
EW gauge bosons	W^{+}	80 GeV	S=1	3
	W^{-}	80 GeV	S=1	3
	Z^{0}	91 GeV	S=1	3
	γ	0	S=1	2
Higgs boson	H^{0}	>114 GeV	S=0	1

Table 3.1: Particles of the standard model and their properties.

which one can estimate that:

$$\frac{\Gamma}{H} \sim \frac{10^{16}\ \text{GeV}}{T} > 1\ . \tag{3.51}$$

Above 30 GeV, we thus have:

$$g_*(T) = 28 + \frac{7}{8} \times 90 = 106.75\ . \tag{3.52}$$

Then, they start decoupling. First, the top quarks, which are the most massive, annihilate with their antiparticles when $T \sim 30$ GeV. Thus g_* drops to:

$$g_*(T) = 28 + \frac{7}{8} \times 78 = 96.25\ . \tag{3.53}$$

Then, it is the turn of the Higgs and the gauge bosons, followed by the bottom quarks, the charm quarks and the τ lepton each annihilating with their antiparticles. Each time, the effective number of relativistic degrees of freedom drop. Around 150 MeV, 40 fermionic and 10 bosonic degrees of freedom have decoupled and we are thus left with:

$$g_*(T) = 18 + \frac{7}{8} \times 50 = 61.75\ . \tag{3.54}$$

Then, at $T \sim 150$ MeV, before the strange quarks had time to annihilate, matter undergoes the QCD phase transition during which quarks combine to produce baryons and mesons. All of those baryons and mesons, except the pions are non-relativistic and drop from g_*. Thus, after the QCD phase transition, the only relativistic species in equilibrium with the thermal bath are pions, electrons, muons, neutrinos and photons themselves. There are three kind of pions, each with spin 0, so they count for $g_* = 3 \times 1 = 3$; the photons count for 2; electrons, muons and each family of neutrinos have 2 internal spin states, therefore, in total:

$$g_* = 2 + 3 + \frac{7}{8} \times (4 + 4 + 6) = 17.25\ . \tag{3.55}$$

Note that we have not taken into account any decoupled contribution to g_* since all decoupled species are non-relativistic at this point. Next, electrons and positrons annihilate, but here, something important happens to neutrinos, so we must postpone our discussion until later.

3.1.4 Entropy

Using Eqs. (3.16)-(3.18), we can show that for particles in equilibrium:

$$\frac{\mathrm{d}P}{\mathrm{d}T} = \frac{\rho + P}{T} + nT\frac{\mathrm{d}}{\mathrm{d}T}\left(\frac{\mu}{T}\right)\ . \tag{3.56}$$

Thus, using the continuity equation:

$$\dot{\rho} + 3H(\rho + P) = 0 \,, \tag{3.57}$$

which we can rewrite:

$$\mathrm{d}\left(\rho a^3\right) = -P\mathrm{d}(a^3) \,, \tag{3.58}$$

we see that the quantity:

$$s = \frac{\rho + P - n\mu}{T} \,, \tag{3.59}$$

obeys the conservation law:

$$\mathrm{d}\left(sa^3\right) = -\left(\frac{\mu}{T}\right)\mathrm{d}\left(na^3\right) \,. \tag{3.60}$$

Thus, the quantity sa^3 is *conserved* provided matter is neither created nor destroyed or that chemical potentials can be neglected. Hence, in standard cosmology, we can write:

$$sa^3 = \text{ constant} \,. \tag{3.61}$$

Rewriting Eq. (3.59) with $\mu = 0$, and differentiating, we get:

$$T\mathrm{d}\left(sa^3\right) = \mathrm{d}\left(\rho a^3\right) + P\mathrm{d}\left(a^3\right) \,, \tag{3.62}$$

which is exactly:

$$T\mathrm{d}S = \mathrm{d}U + p\mathrm{d}V \,, \tag{3.63}$$

so that:

$$S = sa^3 \tag{3.64}$$

is the *entropy* of the Universe. To a very good approximation, it is conserved during the Hot Big-Bang phase. The quantity s is thus the *entropy density*. It is obtained by summing over all species:

$$s = \sum_i \frac{\rho_i + P_i}{T_i} \,. \tag{3.65}$$

Note that non-relativistic species' contributions go like:

$$\frac{\rho_i + P_i}{T_i} \propto T_i^2 \mathrm{e}^{-m_i/T_i} \,, \tag{3.66}$$

so they are exponentially suppressed and can be neglected. The entropy density is thus dominated by relativistic species and we find that:

$$s = \frac{2\pi^2}{45} q_*(T) T^3 \ , \tag{3.67}$$

where we have defined the *effective number of degrees of freedom in entropy*:

$$q_*(T) = g_*^{\rm th}(T) + q_*^{\rm dec}(T) \ , \tag{3.68}$$

with the contribution of decoupled species differing from their contributions in g_*, because of the T^3 dependence in s:

$$q_*^{\rm dec}(T) = \sum_{i=\text{boson}} g_i \left(\frac{T_i}{T}\right)^3 + \frac{7}{8} \sum_{i=\text{fermion}} g_i \left(\frac{T_i}{T}\right)^3 \ . \tag{3.69}$$

In the standard model, q_* and g_* are equal until neutrinos decouple from the thermal bath, which happens around 1 s; see Fig. 3.1. We can use the conservation of entropy to obtain two important results:

- Since $s \propto a^{-3}$, the total number of particles of a given species in a comoving volume, i.e. the comoving number density is *defined* via[2]:

  $$N_i = \frac{n_i}{s} \ . \tag{3.70}$$

  If particles are not destroyed nor created, then N_i is constant.

- Using Eq. (3.67), we see that:

  $$q_*(T) T^3 a^3 = \text{ constant} \ . \tag{3.71}$$

  Since, away from particle mass thresholds, when species become non-relativistic, the effective number of degrees of freedom remain almost constant (save the evolution of decouples species), we have:

  $$\boxed{T \propto a^{-1}} \ . \tag{3.72}$$

[2]The comoving momentum is $p_{\rm com} = a^{-1} p$, in the definition of the number density:

$$n_i(T) = a^{-3} N_i(T) \ .$$

Plugging that in the Friedmann equations, we get:

$$H \sim \frac{T^2}{M_{\rm Pl}} \,. \tag{3.73}$$

Therefore, $T \propto t^{-1/2}$, and we can write:

$$\frac{T}{1\ \text{MeV}} \simeq 1.5 g_*^{-1/4} \left(\frac{1\ \text{sec}}{t}\right)^{1/2} \,, \tag{3.74}$$

which shows that the Universe's temperature was approximately 1 MeV 1 second after the Big-Bang. The factor $q_*(T)$ in Eq. (3.71) accounts for the fact that when a species becomes non-relativistic, its entropy is transferred to the remaining relativistic species, resulting in a temperature that decreases slightly slower that $1/a$.

3.1.5 Neutrino decoupling; Electron-positron annihilation and the Cosmic Neutrino Background

Neutrino decoupling

Neutrinos couple to the thermal bath via weak interactions with leptons, e.g.:

$$\nu_e + \bar{\nu}_e \leftrightarrow e^+ + e^- \tag{3.75}$$

$$e^- + \bar{\nu}_e \leftrightarrow e^- + \bar{\nu}_e \,. \tag{3.76}$$

The interaction rates of such reactions are $\Gamma \sim G_F^2 T^5$, where G_F is the Fermi coupling constant. Therefore:

$$\frac{\Gamma}{H} \sim \left(\frac{T}{1\ \text{MeV}}\right)^3 \,. \tag{3.77}$$

Hence, we expect neutrinos to decouple from the thermal bath around 1 MeV. A more careful estimate provides 0.8 MeV. Once they've decoupled, neutrinos are in free-fall and follow geodesics while retaining their relativistic Fermi-Dirac statistics (even after they have become non-relativistic, because their masses are so small). Since the physical 3-momentum of a particle scales as $p \propto a^{-1}$, we can write the number density of neutrinos as:

$$n_\nu = \frac{g_\nu}{2\pi^2} \int_0^{+\infty} \mathrm{d}p \frac{p^2}{\mathrm{e}^{E(p)/T_\nu} + 1} \tag{3.78}$$

$$= \frac{g_\nu a^{-3}}{2\pi^2} \int_0^{+\infty} \mathrm{d}q \frac{q^2}{\mathrm{e}^{q/aT_\nu} + 1} \,, \tag{3.79}$$

where we introduced the time independent variable $q = ap$, and we neglected the mass of the neutrinos to write $E \simeq p$. After decoupling, the number of neutrinos must be conserved, which requires $n_\nu \propto a^{-3}$. But this is consistent with Eq. (3.79) only if:

$$T_\nu \propto a^{-1} \, . \tag{3.80}$$

Since $T = T_\gamma \propto a^{-1}$ as long as particles do not annihilate, we expect particle annihilations to modify the relationship between the neutrinos and photon temperatures.

Electron-positron annihilation

The most important annihilation from this point of view is the one between electrons and positrons, which happens shortly after neutrinos decoupled from the thermal bath. Indeed, this happens when T becomes smaller than $m_e \simeq 0.5$ MeV. Then, the reactions:

$$e^+ + e^- \leftrightarrow \gamma + \gamma \, , \tag{3.81}$$

become unbalanced:

$$e^+ + e^- \rightarrow \gamma + \gamma \, , \tag{3.82}$$

and the entropy of electrons and positrons is transferred to photons, but not the neutrinos, which have already decoupled from photons. Thus, the photon gas is heated relative to the neutrino gas. Before annihilation, but after neutrinos decoupling, we have, all other things being equal:

$$q_*^{\rm th} = 2 \text{ (bosons=photons; 2 spin states)} + \frac{7}{8} \times 4 \text{ (fermions=electrons+positrons; 2 spin states each)} = \frac{11}{2} \, , \tag{3.83}$$

while after annihilations, since the fermions have disappeared:

$$q_*^{\rm th} = 2 \text{ (bosons=photons; 2 spin states)} \, . \tag{3.84}$$

Since the entropy of the thermal bath is conserved and the decoupled part is not affected here, we can write:

$$a^3 q_*^{\rm th} T^3_{|\rm before} = a^3 q_*^{\rm th} T^3_{|\rm after} \, ; \tag{3.85}$$

so that the photons (thermal bath) temperature becomes:

$$T_{|\rm after} = \left(\frac{11}{4} \right)^{1/3} T_{|\rm before} \, . \tag{3.86}$$

On the other hand, the neutrinos temperature after annihilation hasn't changed and is still equal to the thermal bath's temperature before annihilation (remember that they scale the same way, in $1/a$ when species do not decouple). Therefore, after the electron-positron annihilation, the thermal bath is slightly hotter than the neutrino one:

$$T = \left(\frac{11}{4}\right)^{1/3} T_\nu \ . \tag{3.87}$$

Since neutrinos are still relativistic, the effective numbers of relativistic species after electron-positron annihilation becomes, for $T \ll m_e$:

$$g_* = 2 + \frac{7}{8} \times 2 \times N_{\rm eff} \left(\frac{4}{11}\right)^{4/3} \tag{3.88}$$

$$q_* = 2 + \frac{7}{8} \times 2 \times N_{\rm eff} \left(\frac{4}{11}\right) \ , \tag{3.89}$$

where we introduced the *effective number of neutrino species*, $N_{\rm eff}$. For instantaneous decoupling of neutrinos, we have $N_{\rm eff} = 3$. However, neutrino decoupling is not really instantaneous and some neutrinos were not decoupled when electron-positron annihilation took place. Therefore, some of the entropy and energy released by annihilations did find its way into the neutrino bath. Taking this into account, we get $N_{\rm eff} = 3.046$, so that, at $T \ll m_e$:

$$g_* = 3.36 \tag{3.90}$$

$$q_* = 3.94 \ . \tag{3.91}$$

Since Eq. (3.87) remains valid until today, the temperature of neutrinos in our local Universe is slightly lower than the one for the CMB: $T_{\nu,0} = 1.95$ K. This sea of neutrinos in the Cosmic Neutrino Background, which remains unobserved to this day.

3.1.6 Decoupling in general

What we learned from neutrinos can easily be generalised. When a species decouples from the thermal bath because its interactions with other particles of the bath are no longer efficient enough to maintain it in thermal equilibrium, it subsequently evolves independently from the rest of the Universe (except for the gravitational interaction, of course). If decoupling occurs at time t_D, then the distribution function of the decoupled species at time t_D is:

$$f_i\left(p, t_D\right) = \frac{1}{\mathrm{e}^{E(p)/T_i(t_D)} \pm 1} \ . \tag{3.92}$$

After decoupling, particles propagate freely and the functional form of the distribution is conserved. However, the 3-momentum scales as $p(t) = p\left(t_D\right) a\left(t_D\right)/a(t)$, so that, at any time $t > t_D$, we must have:

$$\forall t > t_D,\ f_i\left(p,t\right) = f_i\left(p\left(t_D\right),t_D\right) = f_i\left(\frac{a(t)}{a\left(t_D\right)}p,t_D\right) . \tag{3.93}$$

If the particles were relativistic at decoupling, then we can write $E = p$ and the condition (3.93) implies:

$$\forall t > t_D,\ \mathrm{e}^{p/T_i(t_D)} \pm 1 = \mathrm{e}^{a(t)p/(a(t_D)T_i(t_D))} . \tag{3.94}$$

Therefore:

$$\forall t > t_D,\ \frac{T_i(t)}{T_i\left(t_D\right)} = \frac{a\left(t_D\right)}{a(t)} = \frac{1+z}{1+z_D}\ \text{(Relativistic species at decoupling).} \tag{3.95}$$

However, if the particles were non-relativistic at decoupling, we would have:

$$E = \sqrt{m^2+p^2} \simeq m + \frac{p^2}{2m} , \tag{3.96}$$

and the distribution function would read for $t \geq t_D$:

$$f_i(p,t) \simeq \mathrm{e}^{-m/T}\mathrm{e}^{-p^2/2mT} . \tag{3.97}$$

so that condition (3.93) would give:

$$\forall t > t_D,\ \exp\left[-\frac{m}{T_i(t)} - \frac{p^2}{2mT_i(t)}\right] = \exp\left[-\frac{m}{T_i(t_D)} - \frac{a^2(t)p^2}{2ma^2\left(t_D\right)T_i\left(t_D\right)}\right] . \tag{3.98}$$

Clearly, this cannot be satisfied. However, if we introduce an effective chemical potential after decoupling, $\mu(t)$, we can modify the condition to read:

$$\forall t > t_D,\ \exp\left[-\frac{m-\mu}{T_i(t)} - \frac{p^2}{2mT_i(t)}\right] = \exp\left[-\frac{m}{T_i(t_D)} - \frac{a^2(t)p^2}{2ma^2\left(t_D\right)T_i\left(t_D\right)}\right] . \tag{3.99}$$

Thus, we have to scale the temperature as:

$$\forall t > t_D,\ \frac{T_i(t)}{T_i\left(t_D\right)} = \left[\frac{a\left(t_D\right)}{a(t)}\right]^2 = \left[\frac{1+z}{1+z_D}\right]^2\ \text{(Non-relativistic species at decoupling).} \tag{3.100}$$

And we have a chemical potential

$$\forall t > t_D,\ \mu(t) = m\left[1 - \frac{T_i(t)}{T_i\left(t_D\right)}\right] = m\left[1 - \left(\frac{a\left(t_D\right)}{a(t)}\right)^2\right] \quad \text{(Non-relativistic species at decoupling).} \tag{3.101}$$

3.2 Out-of-equilibrium

If all species always remained at equilibrium in the thermal bath, the Universe would be extremely boring. As we have seen above, we can say a few things about decoupled species by using equilibrium thermodynamics. But there are details we want to probe further. In particular, we wish to describe the decoupling itself. In this section, we want to try and understand what happens to a decoupled species all at once: how does it get out of equilibrium, and what becomes of its cosmological abundance afterwards? We will focus on three examples of out-of-equilibrium dynamics: Dark Matter relics, recombination and BBN.

3.2.1 Boltzmann equation

The evolution of the distribution function of a species i is governed at all times by the *Boltzmann equation*:

$$p^\mu \frac{\partial f_i}{\partial x^\mu} - \Gamma^\mu{}_{\nu\rho} p^\nu p^\rho \frac{\partial f_i}{\partial p^\mu} = C_i\left[f_i\right] \ , \tag{3.102}$$

where $C_i\left[f_i\right]$ is the collision term, that describes the interactions of species i with other species. In a homogeneous and isotropic Universe, The Boltzmann equation becomes simply:

$$E\frac{\partial f_i}{\partial t} - Hp^2\frac{\partial f_i}{\partial E} = C_i\left[f_i\right] \ . \tag{3.103}$$

Using the definition of the particles number density, Eq. (3.6), and integrating with respect to the 3-momentum, we get:

$$\dot{n}_i + 3Hn_i = C_i \ , \tag{3.104}$$

where:

$$C_i = \frac{g_i}{(2\pi)^3}\int \frac{C_i\left[f_i(\vec{p},t)\right]}{E_i}\mathrm{d}^3\vec{p} \ . \tag{3.105}$$

The hard part is always to model the collision term. To treat the examples we have in mind here, it will be sufficient to concentrate on interactions that lead to reaction of the form:

$$1 + 2 \leftrightarrow 3 + 4 \, . \tag{3.106}$$

Let us suppose that we are focussing on the abundance of particles of species 1, so we are looking for an equation for n_1. Rewriting:

$$\dot{n}_1 + 3\mathcal{H}n_1 = \frac{1}{a^3}\frac{\mathrm{d}\left(n_1 a^3\right)}{\mathrm{d}t} \, , \tag{3.107}$$

we see that the collision term gives us the rate of change, per volume, of the total number of particles of species 1 in that volume. It ought to be the difference between the rate of production of such particles and their rate of annihilation:

$$\frac{1}{a^3}\frac{\mathrm{d}\left(n_1 a^3\right)}{\mathrm{d}t} = \text{Production} - \text{Annihilation} \, . \tag{3.108}$$

It is reasonable to expect the rate of production to be proportional to n_3 and n_4 while the rate of annihilation should be proportional to n_1 and n_2. Thus, we can write:

$$\frac{1}{a^3}\frac{\mathrm{d}\left(n_1 a^3\right)}{\mathrm{d}t} = \alpha n_3 n_4 - \beta n_1 n_2 \, , \tag{3.109}$$

with α and β some positive coefficients. $\beta = \langle \sigma v \rangle$ is often called the *thermally averaged cross section* as it is related to the cross section calculated in quantum field theory (brackets here mean averaging over v). In chemical equilibrium, the number of particles 1 should not change so that:

$$\alpha = \left(\frac{n_1 n_2}{n_3 n_4}\right)_{\mathrm{eq}} \beta \, , \tag{3.110}$$

where in the brackets, the number densities ought to be evaluated at equilibrium using the results of subsection 3.1.2. Therefore, we arrive at:

$$\boxed{\frac{1}{a^3}\frac{\mathrm{d}\left(n_1 a^3\right)}{\mathrm{d}t} = -\beta\left[n_1 n_2 - \left(\frac{n_1 n_2}{n_3 n_4}\right)_{\mathrm{eq}} n_3 n_4\right] \, .} \tag{3.111}$$

If we introduce the number of particles in a comoving volume, $N_i = n_i / s_i$, this equation becomes:

$$\frac{\mathrm{d}\ln N_1}{\mathrm{d}\ln a} = -\frac{\Gamma_1}{H}\left[1 - \left(\frac{N_1 N_2}{N_3 N_4}\right)_{\mathrm{eq}} \frac{N_3 N_4}{N_1 N_2}\right] \, , \tag{3.112}$$

with $\Gamma_1 = n_2\beta = n_2 \langle\sigma v\rangle$ the rate of interaction encountered before. If $\Gamma_1 + \gg H$, then the system evolves towards its equilibrium. Indeed, if initially, $N_1 \gg N_{1,\mathrm{eq}}$, while all the other species are close to their equilibrium configurations, then the RHS of Eq. (3.112) is negative, which means that particles of species 1 are rapidly destroyed and N_1 quickly converges towards $N_{1\mathrm{eq}}$. On the other hand, if we start with $N_1 \ll N_{1,\mathrm{eq}}$, while all the other species are close to their equilibrium configurations, the RHS is positive and particles of species 1 are rapidly produced to reach the equilibrium.

However, when $\Gamma_1 < H$, the RHS is suppressed and N_1 settles at a constant value, leaving some relic abundance of particles 1 in the Universe. Let us illustrate that on three examples.

3.2.2 Dark Matter relics

This example is not as well established as the next two, as it relies on an unconfirmed model for Dark Matter. Although they have not been found at the LHC, and their existence is becoming less and less evident, weakly interacting massive particles (WIMP) are a good pedagogical candidate for Dark Matter. Let us assume that a heavy Dark Matter particle X and its antiparticle $\bar{X}$, of mass m_X annihilate to produce two nearly massless particles q and $\bar{q}$. We will assume that these light particles are coupled to the thermal bath, for example, because they carry an electric charge. Thanks to this hypothesis, we can write that, at all times:

$$n_q = n_{q,\mathrm{eq}} \text{ and } n_{\bar{q}} = n_{\bar{q},\mathrm{eq}} \ . \tag{3.113}$$

Finally, we assume, for simplicity, that there is no initial asymmetry between X and $\bar{X}$ so that $n_{\bar{X}} = n_X$. Hence, the total number of WIMPs X in a comoving volume, N_X obeys:

$$\frac{\mathrm{d}N_X}{\mathrm{d}t} = -s \langle\sigma v\rangle \left[N_X^2 - N_{X,\mathrm{eq}}^2\right] \ . \tag{3.114}$$

Since the interesting part of the dynamics is centred around $T = m_X$, let us switch to the variable:

$$x = \frac{m_X}{T} \ , \tag{3.115}$$

such that:

$$\frac{\mathrm{d}x}{\mathrm{d}t} = -\frac{1}{T}\frac{\mathrm{d}T}{\mathrm{d}t}x \simeq Hx \ , \tag{3.116}$$

where we assumed that $T \propto a^{-1}$ (the effective number of relativistic degrees of freedom is not expected to vary during the process). During the radiation dominated epoch, that we are interested

in:

$$\frac{H(x)}{H(1)} = \frac{1}{x^2} \,, \tag{3.117}$$

and therefore, Eq. (3.114) takes the form of a Riccati equation:

$$\frac{\mathrm{d}N_X}{\mathrm{d}x} = -\frac{\lambda}{x^2}\left[N_X^2 - \left(N_{X,\mathrm{eq}}^2\right)\right] \,. \tag{3.118}$$

The factor:

$$\lambda = \frac{2\pi^2 q_* \left(m_X\right) m_X^3 \left\langle\sigma v\right\rangle}{45H\left(m_X\right)} \,, \tag{3.119}$$

can be regarded as a constant. Let us assume that the particle X is so massive that the decoupling happens when it is already non-relativistic. In that case, using the previous results:

$$N_{X,\mathrm{eq}}(T) = \frac{45 g_X}{2\pi^4 q_*} x^{3/2} \mathrm{e}^{-x} \,, \tag{3.120}$$

and we can integrate Eq. (3.118) numerically. The results are presented on Fig. 3.2 for two values of λ. Clearly, N_X follows its equilibrium value at $x \ll 1$, but it deviates as T passes through m_X, to freeze-out to a constant, relic, value $N_{X,\infty} \gg N_{X\mathrm{eq}}(T)$ as $T \gg m_X$. The solution starts deviating from the equilibrium value around $T \sim m_X/10$, at a value of $x_t \sim 10$. To estimate the relic abundance, we neglect $N_{X,\mathrm{eq}}$ is the evolution equation, to write:

$$\frac{\mathrm{d}N_X}{\mathrm{d}x} = -\frac{\lambda}{x^2} N_X^2 \quad \text{for } x \gg 1 \,. \tag{3.121}$$

This can be integrated from x_t to infinity, to give:

$$\frac{1}{N_{X,\infty}} - \frac{1}{N_X\left(x_t\right)} = \frac{\lambda}{x_f} \,. \tag{3.122}$$

Since $N_X\left(x_t\right) \gg N_{X,\infty}$, we obtain:

$$\boxed{N_{X,\infty} \simeq \frac{x_t}{\lambda} \,.} \tag{3.123}$$

We see on Fig. 3.2 that multiplying λ by 100 drops $N_{X,\infty}$ by approximately two orders of magnitude, so our estimate is not bad and we can indeed fix x_t independently of λ, in a first approximation. Since, after freeze-out, the total number of particles is conserved, we can write:

$$N_{X,0} = N_{X,\infty} \,, \tag{3.124}$$

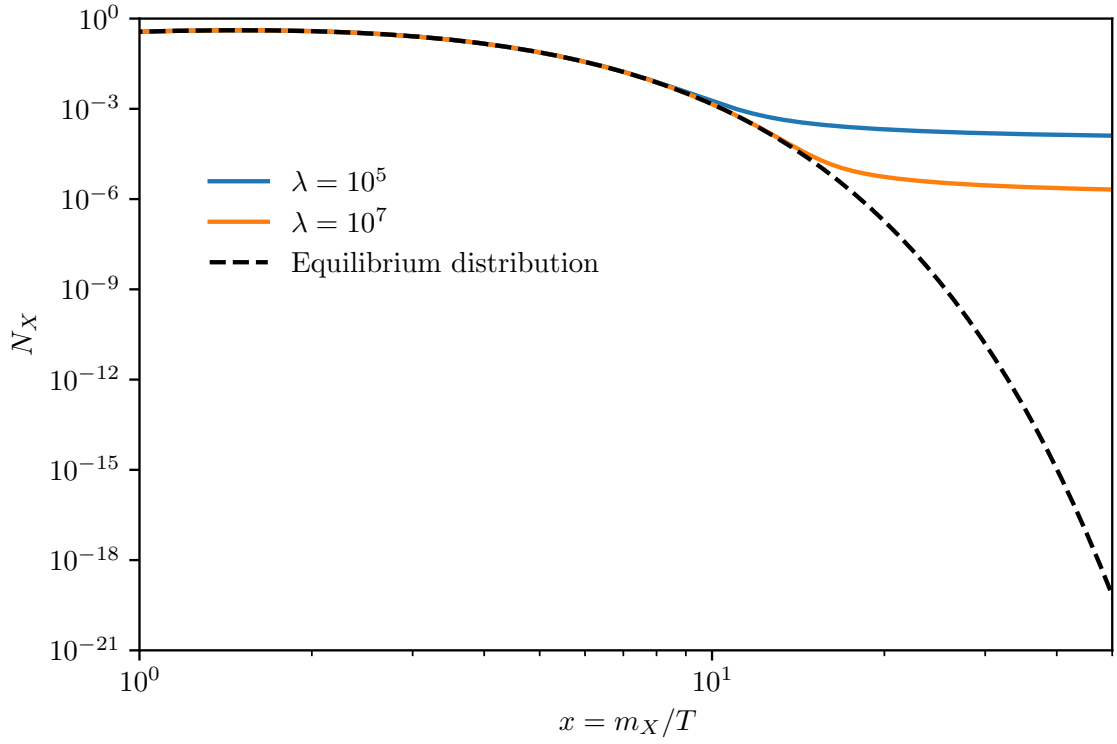

Figure 3.2: The abundance of Dark Matter relic X as a function of temperature as the temperature drops below the mass of the particle.

so that the density of relic today is:

$$\Omega_X = \frac{8\pi G \rho_{X,0}}{3H_0^2} \tag{3.125}$$

$$= \frac{m_X n_{X,0}}{3M_{\rm Pl}^2 H_0^2} \tag{3.126}$$

$$= \frac{m_X N_{X,0} s_0}{3M_{\rm Pl}^2 H_0^2} \tag{3.127}$$

$$= \frac{m_X N_{X,\infty} s_0}{3M_{\rm Pl}^2 H_0^2} \tag{3.128}$$

$$= \frac{\pi}{9} \frac{x_t}{\langle \sigma v \rangle} \frac{q_* (T_0)}{q_* (m_X)} \left(\frac{g_* (m_X)}{10} \right)^{1/2} \frac{T_0^3}{M_{\rm Pl}^3 H_0^2} \, . \tag{3.129}$$

With measured values for H_0 and T_0, and writing $q_* (T_0) = 3.91$ and $q_* (m_X) = g_* (m_X)$, we get:

$$\Omega_X h^2 \sim 0.1 \left(\frac{x_t}{10} \right) \left(\frac{100}{g_* (m_X)} \right)^{1/2} \frac{10^{-12} \text{ GeV}^{-2}}{\langle \sigma v \rangle} \, . \tag{3.130}$$

For WIMPs of a mass $m_X \sim 100$ GeV, when $g_* \sim 100$, we obtain the required value for:

$$\langle \sigma v \rangle \sim 10^{-12} \text{ GeV}^{-2} \, . \tag{3.131}$$

You can check that for such a species, that decoupled while already non-relativistic (at $T \sim m_X/10$), the temperature of the relic in the late Universe is indeed very very small. Indeed, we have today:

$$T_X (t_0) = T_X (t_D) \left[\frac{1+z}{1+z_D} \right]^2 \tag{3.132}$$

$$= T_{X,D} \left(\frac{T_0}{T_D} \right)^2 \tag{3.133}$$

$$= T_{X,D} \left(\frac{T_0}{T_{X,D}} \right)^2 \tag{3.134}$$

$$= \frac{T_0^2}{T_{X,D}} = 10 \frac{T_0^2}{m_X} ; , \tag{3.135}$$

where we used that, at decoupling, $T_D = T_{X,D}$. Therefore:

$$T_{X,0} \simeq 4 \times 10^{-18} \text{ eV} \ll T_0 \simeq 2 \times 10^{-4} \text{ eV} ; , \tag{3.136}$$

if we use $m_X = 10$ GeV.

3.2.3 Big-Bang Nucleosynthesis

When the Universe has cooled down to temperatures of the order of 100 MeV, its dynamics is dominated by the relativistic species that remains in thermal equilibrium: electrons, positrons, neutrinos and photons. Neutrons and protons, as well as the mesons that formed at the QCD phase transition are non-relativistic at this stage and are just spectators as far as the energy budget is concerned. All these particles are still maintained in thermal equilibrium by weak interactions:

$$\nu_e + n \leftrightarrow p + e^- \nu,\ e^+ + n \leftrightarrow p + \bar{\nu}_e\ ,\ n \leftrightarrow p + e^- + \bar{\nu}_e\ , \tag{3.137}$$

as well as:

$$e^+ + e^- \leftrightarrow \gamma + \gamma\ . \tag{3.138}$$

When this equilibrium stops, nuclear reactions can be activated and the first, light, chemical elements are created. This is Big-Bang (or primordial) nucleosynthesis. In these notes, we will try and understand the very basic first step of this extremely complicated process, namely, the formation of helium.

Equilibrium abundances

At temperatures above 1 MeV, all nuclei with atomic number A are in equilibrium. Since they are non relativistic, their number densities are:

$$n_A(T) = g_A \left(\frac{m_A T}{2\pi}\right)^{3/2} \mathrm{e}^{-(m_A - \mu_A)/T}\ . \tag{3.139}$$

As long as reactions remain efficient, chemical equilibrium is achieved and the chemical potentials are fixed. For a nucleus with A nucleons and Z protons:

$$\mu_A = Z\mu_p + (A - Z)\mu_n\ , \tag{3.140}$$

where μ_p is the chemical potential of protons, and μ_n that of neutrons. If we neglect the mass difference $Q = m_n - m_p \simeq 1.293$ MeV in the power law pre-factor[3], we get the number densities of protons and neutrons:

$$\begin{cases} n_p = 2\left(\dfrac{m_N T}{2\pi}\right)^{3/2} \mathrm{e}^{-(m_p - \mu_p)/T} & (3.141) \\ n_n = 2\left(\dfrac{m_N T}{2\pi}\right)^{3/2} \mathrm{e}^{-(m_n - \mu_n)/T}\ , & (3.142) \end{cases}$$

[3] But not in the exponential, where it makes a huge impact!

with $m_N = \left(m_n + m_p\right)/2$. Note that for any nucleon, we have:

$$\begin{aligned} \mathrm{e}^{-(m_A-\mu_A)/T} =& \mathrm{e}^{\mu_A/T}\mathrm{e}^{-m_A/T} && (3.143)\\ =& \mathrm{e}^{(-Z\mu_p-(A-Z)\mu_n)/T}\mathrm{e}^{-m_A/T} && (3.144)\\ =& \left[\mathrm{e}^{\mu_p/T}\right]^Z \left[\mathrm{e}^{\mu_n}/T\right]^{A-Z} \mathrm{e}^{-m_A/T} && (3.145)\\ =& 2^{-A} n_p^Z n_n^{A-Z} \left(\frac{2\pi}{m_N T}\right)^{3A/2} \mathrm{e}^{B_A/T} , && (3.146) \end{aligned}$$

where we have defined the nucleus binding energy:

$$B_A = Z m_p + (A-Z) m_n - m_A . \tag{3.147}$$

We also define the *mass fraction* of the nucleus with atomic number A as the ratio of the mass of the nucleus over the total mass of nucleons:

$$X_A = \frac{A n_A m_N}{m_N n_b} = \frac{A n_A}{n_b} , \tag{3.148}$$

where:

$$n_b = n_n + n_p + \sum_A A n_A , \tag{3.149}$$

is the total *number density of baryons*. This is usually expressed in terms of the *baryon-to-photon ratio*:

$$\eta = \frac{n_b}{n_\gamma} . \tag{3.150}$$

The photon number density is given by the standard result $n_\gamma = 2\zeta(3)T^3/\pi^2$, and we get:

$$\boxed{X_A = g_A A^{5/2} \left[\zeta(3)\pi^{-1/2} 2^{(3A-5)/(2A-2)}\right]^{A-1} \eta^{A-1} X_p^Z X_n^{A-Z} \mathrm{e}^{B_A/T} .} \tag{3.151}$$

Note that if entropy is low, $\eta \sim 1$ and X_A is controlled by the value of $\mathrm{e}^{B_A/T}$ and the nucleus with (A, Z) is stable as soon as $T \sim B_A$. However, in a high-entropy Universe as ours, where $\eta \ll 1$, the nucleus is stable only when $\mathrm{e}^{B_A/T} \sim \eta^{1-A} \gg 1$ as soon as $A > 1$, so that the abundance of the nucleus only starts increasing for $T \sim B_A/((1-A)\ln\eta) < B_A$: *the formation of the heavy nuclei is delayed*.

During this early equilibrium phase, the abundances of neutrons and protons are controlled by the reactions (3.137), so that we have:

$$\mu_n + \mu_\nu = \mu_p + \mu_e \ . \tag{3.152}$$

Thus, using Eqs. (3.141)-(3.142), we get the *neutron-to-proton ratio*:

$$\boxed{\left(\frac{n}{p}\right)_{\rm eq} = \left(\frac{n_n}{n_p}\right)_{\rm eq} = {\rm e}^{-Q/T}} \tag{3.153}$$

where we have neglected the chemical potentials of the electrons and neutrinos. Besides, we have seen that in a high entropy Universe, at those temperatures, $X_A \ll 1$, so that $n_b = n_n + n_p$. Thus, the abundance of free neutrons is:

$$X_{n,{\rm eq}} = \frac{n}{n+p} = \left[1 + {\rm e}^{Q/T}\right]^{-1} \ . \tag{3.154}$$

Therefore, for $T \gg Q \simeq 1.293$ MeV, $X_{n,{\rm eq}} = X_{p,{\rm eq}} = 1/2$ and $X_A \simeq 0$ for $A > 1$.

Freeze-out of weak interactions

The reaction rate of the reaction $p + e^- \leftrightarrow \nu_e + n$ that keeps neutrons and protons in equilibrium is given by:

$$\Gamma = \frac{7\pi}{60}\left(1 + 3g_*^2\right) G_F^2 T^5 \ , \tag{3.155}$$

so that, using $g_* = 10.75$, we get:

$$\frac{\Gamma}{H} \simeq \left(\frac{T}{0.8\ {\rm MeV}}\right)^3 \ . \tag{3.156}$$

Therefore, the weak interactions freeze out at:

$$T_f \simeq 0.8\ {\rm MeV} \ , \tag{3.157}$$

around the time $t_f \simeq 1.15$ s. To determine the neutron abundance at freeze-out, one would need to study the Boltzmann equation for that species. As it turns out, one can show that neutrons follows their equilibrium distribution all the way to freeze-out, so that we can evaluate:

$$X_n\left(T_f\right) \simeq X_{n,{\rm eq}}\left(T_f\right) = \left[1 + {\rm e}^{1.293/08}\right]^{-1} \simeq 0.165 \simeq \frac{1}{6} \ . \tag{3.158}$$

This leads to:

$$\left(\frac{n}{p}\right)_f \simeq 0.198 \simeq \frac{1}{5} \,. \tag{3.159}$$

After freeze-out, this fraction would remain constant if free neutrons were stable. But at temperatures below 0.2 MeV ($t \geq 100$ s) neutrons decay via β-decay, with a decay-time such $\tau_n \simeq 887$ s, become important, and the neutron abundance needs to be corrected:

$$X_n(t) = X_n\left(T_f\right) \mathrm{e}^{-t/\tau_n} = \frac{1}{6}\mathrm{e}^{-t/\tau_n} \,. \tag{3.160}$$

Light elements abundances

Light nucleons will start forming by a series of nuclear reactions once free neutrons are available. However, no element can form until deuterium starts forming, as densities are too low to allow for any reactions involving more than two-body interactions. The first reaction of importance is thus:

$$n + p \leftrightarrow D + \gamma \,. \tag{3.161}$$

Deuterium forms directly from free neutrons and protons so as long as these are in sufficient supply, the deuterium abundance follows its equilibrium value. Using $\mu_n + \mu_p = \mu_D$, Eq. (3.139) for $A = D$ and $g_D = 3$, and Eqs (3.141)-(3.142), we get:

$$\left(\frac{n_D}{n_p n_n}\right)_{\mathrm{eq}} = \frac{3}{4}\left(\frac{4\pi}{m_N T}\right)^{3/2} \mathrm{e}^{B_D/T} \,, \tag{3.162}$$

with $B_D \simeq 2.22$ MeV. Therefore:

$$\left(\frac{X_D}{X_n X_p}\right) = 2\left(\frac{n_D}{n_p} n_n\right)_{\mathrm{eq}} \quad n_b = 2\eta n_\gamma \left(\frac{n_D}{n_p} n_n\right)_{\mathrm{eq}} \,, \tag{3.163}$$

which leads to:

$$\left(\frac{X_D}{X_n X_p}\right) = \frac{24\zeta(3)}{\sqrt{\pi}}\left(\frac{T}{m_N}\right)^{3/2} \mathrm{e}^{B_D/T} \,. \tag{3.164}$$

Since $\eta \simeq 5 \times 10^{-10} \ll 1$, the formation of deuterium is thus delayed until:

$$T_{\mathrm{nuc}} \simeq 0.06 \text{ MeV}. \tag{3.165}$$

This corresponds to a time $t_{\rm nuc} \simeq 330\,{\rm s} \simeq 5.5\,{\rm min}$. At that time, the abundance of neutrons has fallen to:

$$X_{n,{\rm nuc}} \simeq \frac{1}{8}\,. \tag{3.166}$$

The binding energy of helium is larger than that of deuterium, which means that as soon as it can form, helium formation will be strongly favoured. This is clear on Fig. 3.3,which shows the evolution of the abundances over time. Helium is produced almost immediately after deuterium and at $t = t_{\rm nuc}$, almost all of the remaining neutrons are captured into helium nucleii. Since each helium nucleus

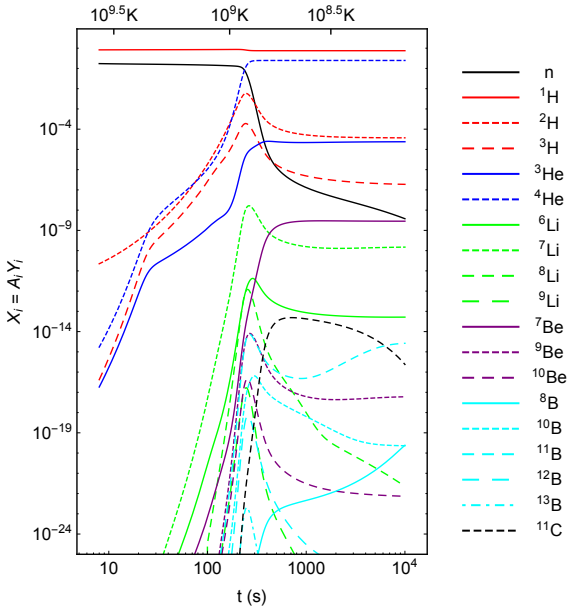

Figure 3.3: Evolution of the various nuclear species during BBN. This is the result of a numerical integration using PRIMAT. Figure from [17].

contains 2 neutrons, we get: $n_{\rm He} = \frac{1}{2} n_n\,(t_{\rm nuc})$:

$$\frac{n_{\rm He}}{n_p} \simeq \frac{X_n\,(t_{\rm nuc})\,/2}{1 - X_n\,(t_{\rm nuc})} \simeq \frac{1}{16}\,. \tag{3.167}$$

In terms of mass fraction:

$$X_{\rm He} = \frac{4 n_{\rm He}}{n_p}\,, \tag{3.168}$$

so that:

$$X_{\rm He} \simeq \frac{1}{4}\,, \tag{3.169}$$

which is in agreement with recent measurements of η by CMB experiments; see Fig. 3.4. All

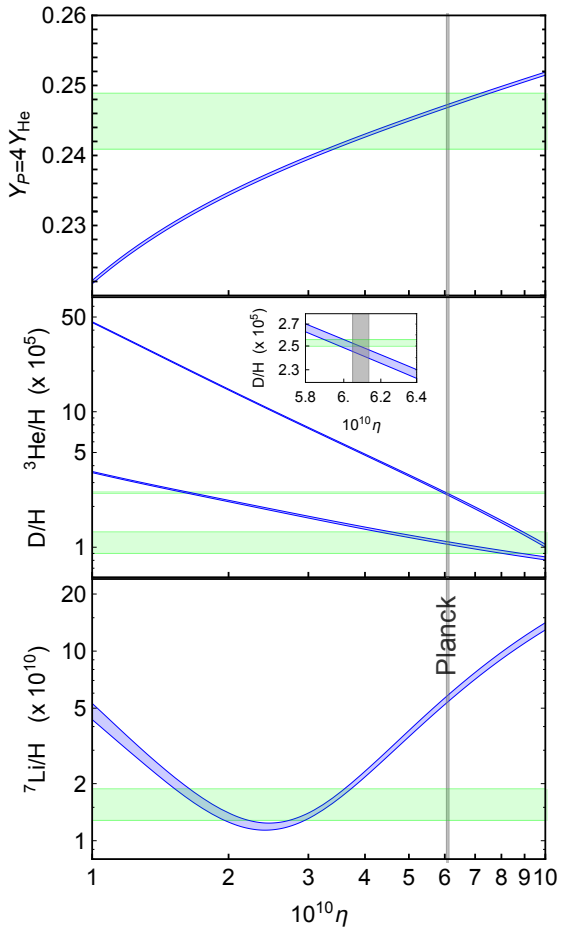

Figure 3.4: Constraints on primordial abundances of light elements. Figure from [17].

other elements are produced in trace amounts. To predict their abundances, one ought to solve the full system of coupled non-linear Boltzmann equations governing the complex network of nuclear

reactions involved. Observations then constrain the baryon to photon ratio to be:

$$\eta \simeq 5 \times 10^{-10} \ . \tag{3.170}$$

3.2.4 Recombination and decoupling

As we have seen, after BBN, the Universe is essentially made of photons, neutrinos, electrons and protons (and a bit of helium). While the temperature of the thermal bath remains large compared to the ionisation energy of hydrogen, matter remains ionised and photons couple to electrons via Compton scattering, while electrons and protons couple via Coulomb scattering. As soon as the temperature becomes low enough, electrons and nuclei combine to form neutral atoms (essentially hydrogen plus a bit of helium). This is *recombination*. In the process, the density of free electrons fall sharply and the mean free path of photons increase rapidly to become larger than the Hubble scale. This is the *decoupling* of photons from matter[4], making the Universe transparent. These photons are the Cosmic Microwave Background (CMB). Let us see how this process unfolds. This treatment is very crude but gives the main ideas and good orders of magnitude.
The photoionisation reaction:

$$p + e^- \leftrightarrow H + \gamma \ , \tag{3.171}$$

is responsible for keeping the equilibrium between electrons and photons. As long as equilibrium is maintained, the abundances of each species (they are all non-relativistic after electron-positron annihilation) follow:

$$n_{i,\mathrm{eq}} = g_i \left(\frac{m_i T}{2\pi}\right)^{3/2} \mathrm{e}^{-(m_i-\mu_i)/T} \quad \text{for} \ \ i = e,\ p,\ \mathrm{H} \ . \tag{3.172}$$

Since at chemical equilibrium we have $\mu_p + \mu_e = \mu_H$, we can remove the dependence on chemical potentials by considering:

$$\left(\frac{n_\mathrm{H}}{n_e n_p}\right)_\mathrm{eq} = \frac{g_H}{g_e g_p}\left(\frac{2\pi m_\mathrm{H}}{m_e m_p T}\right)^{3/2} \mathrm{e}^{B_\mathrm{H}/T} \tag{3.173}$$

$$\simeq \left(\frac{2\pi}{m_e T}\right)^{3/2} \mathrm{e}^{B_\mathrm{H}/T} \ , \tag{3.174}$$

[4]Note that, if we were to follow our convention so far, it is really matter that decoupled from the thermal bath in which only photons remain.

where we used $m_H \simeq m_p$ in the prefactor, but not in the exponential, where the difference is important. Indeed, The binding energy of hydrogen is:

$$B_{\rm H} = m_p + m_e - m_H = 13.6 \text{ eV}. \tag{3.175}$$

Since the Universe is neutral, we have $n_e = n_p$ and, at equilibrium:

$$\left(\frac{n_{\rm H}}{n_e^2}\right)_{\rm eq} = \left(\frac{2\pi}{m_e T}\right)^{3/2} {\rm e}^{B_{\rm H}/T} \ . \tag{3.176}$$

The fraction of free electrons, i.e. those note yet recombined into atoms, is given by:

$$X_e(T) = \frac{n_e(T)}{n_b(T)} \simeq \frac{n_e}{n_p + n_{\rm H}} = \frac{n_e}{n_e + {\rm n}_H} \ , \tag{3.177}$$

where we have neglected the impact of every other nucleus except protons (including helium), to write $n_b \simeq n_p + n_{\rm H}$. Then, clearly:

$$\frac{X_e^2}{1 - X_e} = \frac{n_e^2}{n_{\rm H} n_b} \ . \tag{3.178}$$

Evaluating this at equilibrium and using $n_b = \eta n_\gamma = 2\zeta(3)\eta T^3/\pi^2$, we arrive at the:

Saha equation

$$\left(\frac{1 - X_e}{X_e^2}\right)_{\rm eq} = \frac{2\zeta(3)}{\pi^2}\eta \left(\frac{2\pi T}{m_e}\right)^{3/2} {\rm e}^{B_H/T} \ . \tag{3.179}$$

First, notice that at $T = B_H = 13.6$ eV, we have:

$$\left(\frac{1 - X_e}{X_e^2}\right)_{\rm eq} (B_{\rm H}) \simeq 10^{-17} \ . \tag{3.180}$$

Clearly, once again the high entropy implies $X_e \sim 1$ way after the temperature has reached the binding energy. If we define recombination as the moment at which only 10% of electrons remain free, then we find:

$$T_{\rm rec} \simeq 0.3 \text{ eV} \simeq 3\,600 \text{ K} \ . \tag{3.181}$$

This definition is quite arbitrary, but so his our approximation. However, if we decrease X_e past that point, we will see that it decreases sharply with temperature, so that past $X_e = 0.1$, the temperatures

only vary by a few 10 percents. Using $T_{\rm rec} = T_0\,(1 + z_{\rm rec})$ with the measured value $T_0 = 2.73$ K, we get the *redshift of recombination*:

$$\boxed{z_{\rm rec} \simeq 1\,320\ .} \tag{3.182}$$

Since we are in the matter dominated phase, this converts into a cosmic time:

$$t_{\rm rec} \simeq 290\,000\ {\rm yrs}\ . \tag{3.183}$$

The coupling of electrons to photons is mostly due to Compton scattering:

$$e^- + \gamma \leftrightarrow e^- + \gamma\ . \tag{3.184}$$

The rate of this reaction is given by:

$$\Gamma = n_e \sigma_T\ , \tag{3.185}$$

where $\sigma_T \simeq 2 \times 10^{-3}\ {\rm MeV}^{-2}$ is the Thomson cross-section. Since the density of free electrons fall sharply during recombination, so does this reaction rate. Photons and electrons then decouple roughly when:

$$n_e\,(T_{\rm dec})\,\sigma_T = H\,(T_{\rm dec})\ . \tag{3.186}$$

Note that we are now in the matter dominated phase:

$$H^2\,(T_{\rm dec}) = \Omega_{m,0} H_0^2\,(1 + z_{\rm dec})^3 = \Omega_{m,0} H_0^2 T_0^3 T_{\rm dec}^{-3}\ . \tag{3.187}$$

Moreover:

$$n_e\,(T_{\rm dec})\,\sigma_T = n_b X_e\,(T_{\rm dec})\,\sigma_T = \frac{2\zeta(3)\sigma_T}{\pi^2}\eta X_e\,(T_{\rm dec})\,T_{\rm dec}^3\ . \tag{3.188}$$

Thus:

$$X_e\,(T_{\rm dec})\,T_{\rm dec}^{3/2} = \frac{\pi^2 H_0 \sqrt{\Omega_{m,0}}}{2\zeta(3)\eta\sigma_T T_0^{3/2}}\ . \tag{3.189}$$

Using the Saha equation to determine $X_e\,(T_{\rm dec})$, this gives:

$$T_{\rm dec} \simeq 0.27\ {\rm eV}\ , \tag{3.190}$$

which converts into the redshift:

$$\boxed{z_{\rm dec} \simeq 1\,100\ ,} \tag{3.191}$$

and a cosmic time:

$$t_{\rm dec} \simeq 380\,000 \text{ yrs} \,. \tag{3.192}$$

Notice that between recombination and decoupling, the ionisation fraction decreases significantly, from $X_e\,(T_{\rm red}) \simeq 0.1$ to $X_e\,(T_{\rm dec}) \simeq 0.01$. After decoupling, photons propagate freely in space-time: they are in free fall and follow lightlike geodesics. The Saha equation assumes that electrons keep their equilibrium distribution throughout the process. Although a full numerical study of the Boltzmann equation shows that this is a good approximation at recombination, this is not so good at decoupling, when the actual distribution has started to deviate significantly from it equilibrium configuration. On the other hand, we have done many other approximations, so we do not need to be overly rigorous here. Finally, let us mention that the ionisation fraction does not tend to 0 and that, after recombination and decoupling, we are left with some free electrons, to the tune of X_e equal to a few 10^{-4}, exactly like we were left with some relic dark matter and relic neutrons.

3.3 Problems

Pb. 3.1 The temperature of the Cosmic Microwave background today is $T_0 \simeq 2.73$ K. Show that the number density and energy density of photons today are thus:

$$\begin{cases} n_{\gamma,0} \simeq 410 \text{ cm}^{-3} & (3.193) \\ \rho_{\gamma,0} \simeq 4.6 \times 10^{-34} \text{g cm}^{-3} \,. & (3.194) \end{cases}$$

Deduce that $\Omega_\gamma h^2 \simeq 2.5 \times 10^{-5}$.

Pb. 3.2 Since the Universe is neutral, the number density of protons n_p must be equal to $n_{e^+} - n_{e^-}$. Using the BBN constraints:

$$\eta = \frac{n_b}{n_\gamma} \simeq 5 \times 10^{-10} \,, \tag{3.195}$$

show that the chemical potentials of electrons and positrons are very small and can be neglected.

Pb. 3.3 Discuss what would happen to the production of helium during BBN if:

(a) the baryons density today was larger than currently estimated;

(b) Newton's constant was larger at BBN than estimated today;

(c) the neutron-proton mass difference was a bit larger than currently accepted.

4 Cosmological perturbation theory

Contents

4.1 A simple model: Newtonian perturbation theory

4.1.1 Phenomenology

At the very early stages of the history of the Universe, something akin to an inflationary phase creates small fluctuations in energy density and curvature, around an otherwise homogeneous and isotropic background. However, gravitation is attractive and we thus expect initially small overdensities to become denser over time, while small initial underdensities will become more and more depleted of matter and form relatively emptier regions of the Universe. This is more or less what happens in the real Universe. Cold Dark Matter, because it is only subjected to its own gravity and the gravitational pull of other fields, forms structure first. The infall of baryonic matter into structure is delayed by radiation drag due to the coupling of charged matter with photons via Compton scattering in the early Universe. After decoupling, photons free stream and baryonic matter is free to fall into Cold Dark Matter potential wells which have already formed. At that stage, the cosmic web begins to take shape. This, in essence, is the story we want to tell in this chapter and the next one.
In an FLRW context, the preferred coordinate system comoving with fundamental observers, $\vec{x}$, forms a grid subjected to the Hubble expansion, and CDM particles cluster by moving with respect to this Hubble flow with some peculiar velocity field. Indeed, the physical position of a particle is:

$$\vec{r}(t) = a(t)\vec{x} \ . \tag{4.1}$$

Thus the physical velocity of that particle reads:

$$\frac{d}{dt}\vec{r}(t) = \vec{v}_{\rm phys} = H\vec{r} + a(t)\frac{d}{dt}\vec{x}(t) \ . \tag{4.2}$$

The first term is the Hubble flow, while the second one is the peculiar velocity of the particle; see Fig. 4.1.

4.1.2 Newtonian perturbations

Before moving to general relativistic perturbation theory, it is worth exploring in some details the Newtonian case, although the Newtonian Universe is ill-defined, mainly for two (not independent) reasons:

1. it helps build a solid intuition of what happens on small enough scales, where relativistic effects can be neglected;

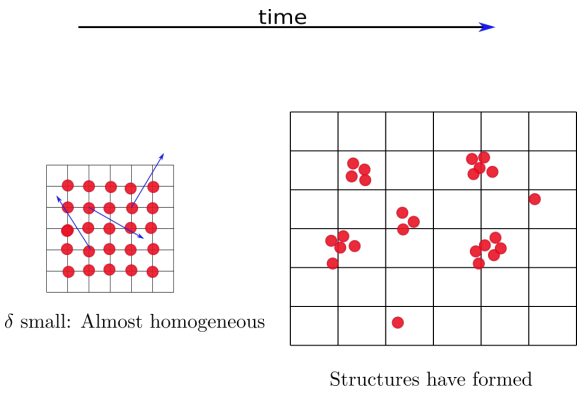

Figure 4.1: Generic idea of structure formation in an FLRW universe. The expansion of the fixed grid is combined with peculiar motion of matter. The matter distribution starts nearly homogeneous with some distribution of peculiar velocities (blue arrows) and evolved towards more clustering via gravitational pull.

2. it actually makes an accurate prediction for the rate of growth of structure in a Universe dominated by non-relativistic matter.

Case of a static Universe

The adiabatic, inviscid (zero viscosity) flow of a fluid with energy density $\rho\left(t,\vec{r}\right)$ and pressure $p\left(t,\vec{r}\right)$ subjected to a gravitational potential $\Phi\left(t,\vec{r}\right)$ in Newtonian mechanics is characterised by the following couple of partial differential equations:

$$\partial_t \rho + \vec{\nabla}\cdot\left(\rho\vec{v}\right) = 0 \text{ (Continuity Equation)} \tag{4.3}$$

$$\partial_t \vec{v} + \left(\vec{v}\cdot\vec{\nabla}\right)\vec{v} = -\frac{1}{\rho}\vec{\nabla}p - \vec{\nabla}\Phi \text{ (Euler Equation) .} \tag{4.4}$$

The continuity equation is an expression of the conservation of energy in the system, while the Euler equation is the form taken by the Navier-Stokes equation for an adiabatic, inviscid fluid flow. Keeping in mind that in cosmology we have a homogeneous and isotropic background upon which small perturbations develop, we are interested in what happens to small fluctuations in the energy density of the fluid around a homogeneous solution to the continuity and Euler equations. Thus, we

look for solutions in the form:

$$\rho\left(t,\vec{r}\right) = \bar{\rho}(t) + \delta\rho\left(t,\vec{r}\right) \tag{4.5}$$

$$\vec{v}\left(t,\vec{r}\right) = \vec{\bar{v}}(t) + \delta\vec{v}\left(t,\vec{r}\right) \ . \tag{4.6}$$

The homogeneous pressure does not enter the equations, and its fluctuations δp are related to the energy density fluctuations by the **adiabatic sound speed** of the fluid, c_s:

$$\delta p = c_s^2 \delta\rho \ . \tag{4.7}$$

Moreover, the gravitational field obeys the Poisson equation:

$$\Delta\Phi = 4\pi G\rho \ . \tag{4.8}$$

It is easy to see that the only regular solution to this equation for an homogeneous energy density $\bar{\rho}$ is a pure function of time. Indeed, by symmetry, such a solution $\bar{\Phi}$ ought to be a pure function of r at most. But then, the Poisson equation reads:

$$\frac{1}{r^2}\frac{\partial}{\partial r}\left[r^2\frac{\partial}{\partial r}\bar{\Phi}\right] = 4\pi G\bar{\rho}(t) \ , \tag{4.9}$$

whose solution reads:

$$\bar{\Phi}(t,r) = \frac{2\pi G\bar{\rho}(t)}{3}r^2 + \frac{F(t)}{r} + G(t) \ , \tag{4.10}$$

for some functions $F(t)$ and $G(t)$. Requiring regularity of the potential at $r = 0$ (this point cannot be distinguished from any other point by the assumption of homogeneity), we get $F(t) = 0$ and the only solution is a pure function of time, which drops from Euler's equation and can thus be discarded: we can set $G(t) = 0$. However, we see that we have a term left that is infinite in the limit $r \to +\infty$. This means that the actual background value of the potential is ill-defined in Newtonian mechanics, for a homogeneous Universe. This alone indicates that there is a problem talking about a cosmology in Newtonian physics, since the notion of an infinite, homogeneous Universe does not make sense... In any case, this shows that for the purpose of structure formation, it is enough to consider that, up to a (possibly infinite) shift the gravitational potential is sourced by the fluctuations in the energy density and is an order 1 quantity:

$$\Delta\Phi = 4\pi G\delta\rho \ . \tag{4.11}$$

Next, expanding the continuity and Euler equations at first order in the fluctuations, and separating the homogeneous part and the perturbed part, we get, for the homogeneous solution:

$$\bar{\rho}(t) = \text{cst} \tag{4.12}$$

$$\vec{\bar{v}}(t) = \vec{0} \text{ (really a constant, but must vanish by symmetry).} \tag{4.13}$$

With a little algebra, this then leads to an equation for the fluctuations:

Newtonian Evolution of density fluctuations

$$\frac{\partial^2}{\partial t^2}\delta\rho - c_s^2 \Delta\delta\rho = 4\pi G\bar{\rho}\delta\rho \ . \tag{4.14}$$

The term on the RHS is due to the presence of gravitation (as can be seen from the $4\pi G$ factor in front of it). In absence of gravitation, this corresponds to a wave equation for the free sound waves in the fluid, and the gravitational field introduces some forcing term. As usual, decomposing the wave solution into Fourier modes allows one to determine the dispersion relation in the medium. Let:

$$\delta\rho\,(t,\vec{r}) = \int \widehat{\delta\rho}\left(\omega,\vec{k}\right) e^{i\left(\omega t - \vec{k}\cdot\vec{r}\right)} d\omega d^3\vec{k} \ . \tag{4.15}$$

Then, Eq. (4.14) leads to a modified dispersion relation:

Jean's instability

$$\omega^2\,(k) = c_s^2 k_J^2 \left[\left(\frac{k}{k_J}\right)^2 - 1\right] \ , \tag{4.16}$$

where we introduced the *Jean's wavevector*:

$$k_J \equiv \sqrt{\frac{4\pi G\bar{\rho}}{c_s^2}} \ . \tag{4.17}$$

To see what this means, it is useful to go back to real space and introduce wavelengths associated with the Fourier modes, $\lambda = 2\pi/k$ and the *Jean's length* which characterises the onset of gravitational effects in the fluid:

$$\lambda_J \equiv c_s\sqrt{\frac{\pi}{G\bar{\rho}}} \ . \tag{4.18}$$

Then, the dispersion relation (4.16) becomes:

$$\omega^2 = \frac{4\pi^2 c_s^2}{\lambda_J^2}\left[\left(\frac{\lambda_J}{\lambda}\right)^2 - 1\right] . \tag{4.19}$$

We see that the various modes in the perturbation $\delta\rho$ will behave differently depending on the scale involved, as gravitation and sound waves compete:

- For $\lambda > \lambda_J$ ($k < k_J$), i.e. on scales larger than the Jean's length, $\omega^2 < 0$, thus leading to a mode that will grow exponentially with $e^{|\omega|t}$; on those scales, the typical time for sound waves to propagate, $t_{\text{sound}} \sim \lambda/c_s$ is larger than the characteristic time of gravitational collapse, $t_{\text{grav}} \sim 1/\sqrt{G\bar{\rho}}$, and the gravitational pull wins over the pressure term. This leads to a gravitational instability and to the formation of a structure.

- For $\lambda < \lambda_J$ ($k > k_J$), i.e. on scales smaller than the Jean's length, $\omega^2 > 0$ and the mode oscillates. In that case, we obtain pressure supported oscillations in the fluid density, as $t_{\text{sound}} < t_{\text{grav}}$.

Thus, in a medium with a nonzero sound speed, perturbations will only grow on large enough scales, where pressure gradients are not large enough to counter the effect of gravity and to support oscillations. The transition scale, i.e. the Jean's length depends on the average energy density on the fluid, which in the static case is a constant.

Case of an expanding Universe

The general picture presented previously in the static case extends to a Newtonian expanding Universe. However, the expansion here cannot be obtained dynamically, as will be the case in the relativistic context. Rather, it has to be introduced by hand, by following the phenomenological picture presented above. In order to do that, we rewrite the continuity and Euler equations, highlighting that they are valid in physical coordinates $\vec{r}$:

$$\partial_t \rho + \vec{\nabla}_{\vec{r}} \cdot (\rho \vec{v}) = 0 \text{ (Continuity Equation)} \tag{4.20}$$

$$\partial_t \vec{v} + \left(\vec{v} \cdot \vec{\nabla}_{\vec{r}}\right)\vec{v} = -\frac{1}{\rho}\vec{\nabla}_{\vec{r}} p - \vec{\nabla}_{\vec{r}}\Phi \text{ (Euler Equation).} \tag{4.21}$$

We also rewrite the Poisson equation similarly:

$$\Delta_{\vec{r}}\Phi = 4\pi G\bar{\rho}\delta\rho. \tag{4.22}$$

Then, we introduce comoving coordinates $\vec{x}$ related to the physical ones by: $\vec{r}(t) = a(t)\vec{x}$. Note that the physical coordinates now depend on time explicitly because of the overall expansion of the grid. Hence, infinitesimal particles of fluid have a peculiar velocity with respect to a fiducial coordinate grid determined by the comoving coordinates $\vec{x}$:

$$\vec{u} = a(t)\frac{d\vec{x}}{dt} \,, \tag{4.23}$$

so that their physical velocity can be separated (arbitrarily somehow) into a Hubble flow and a peculiar flow:

$$\vec{v} = H\vec{r} + \vec{u} \,, \tag{4.24}$$

where:

$$H = \frac{1}{a}\frac{da}{dt} \tag{4.25}$$

is the Hubble rate. Then, one can further see that:

$$\vec{\nabla}_{\vec{r}} = \frac{1}{a}\vec{\nabla}_{\vec{x}} \tag{4.26}$$

$$\partial_t \rho\left(t, \vec{r}(t)\right) = \partial_t \rho\left(t, \vec{x}\right) - H\vec{x}\cdot\vec{\nabla}_{\vec{x}}\rho\left(t, \vec{x}\right) \,. \tag{4.27}$$

Hence, substituting in the continuity and Euler equations, one gets their counterparts expressed with respect to the comoving grid:

$$\partial_t \rho + 3H\rho + \frac{1}{a}\vec{\nabla}_{\vec{x}}\left(\rho\vec{u}\right) = 0 \tag{4.28}$$

$$\partial_t \vec{u} + H\vec{u} + \frac{1}{a}\left(\vec{u}\cdot\vec{\nabla}_{\vec{x}}\right)\vec{u} = -\frac{1}{a\rho}\vec{\nabla}_{\vec{x}}p - \frac{1}{a}\vec{\nabla}_{\vec{x}}\Phi \,. \tag{4.29}$$

Once one has decomposed quantities into a homogeneous solutions and fluctuations, as in the static case, it is convenient to introduce the *density contrast* $\delta\left(t, \vec{x}\right) = \delta\rho\left(t, \vec{x}\right)/\bar{\rho}(t)$, such that:

$$\rho\left(t, \vec{x}\right) = \bar{\rho}(t)\left(1 + \delta\left(t, \vec{x}\right)\right) \,. \tag{4.30}$$

Then, using a dot for time derivatives, we get:

$$\dot{\delta} + \frac{1}{a}\vec{\nabla}_{\vec{x}}\cdot\left[(1+\delta)\vec{u}\right] = 0 \,. \tag{4.31}$$

And, after some cumbersome albeit straightforward manipulations, using $\delta p = c_s^2\delta\rho$:

$$\ddot{\delta} + 2H\dot{\delta} - \frac{1}{a^2}\Delta_{\vec{x}}\delta = \frac{1}{a^2}\vec{\nabla}_{\vec{x}}\cdot\left[(1+\delta)\vec{\nabla}_{\vec{x}}\Phi\right] + \frac{1}{a^2}\partial_i\partial_j\left[(1+\delta)u^i u^j\right] \,. \tag{4.32}$$

Once again, the gravitational potential is determined by the Poisson equation:

$$\Delta_{\vec{x}}\Phi = 4\pi G\bar{\rho}a^2\delta \ . \tag{4.33}$$

This system of equation is non-linear and in principle allows one to follow the solution to arbitrary values of δ and $|\vec{u}| \ll 1$. In what follows we will concentrate on the first order, linear terms and expand these equations, neglecting any terms quadratic in δ or the velocity (or product of both). Then, Eq. (4.32) becomes simply:

Newtonian evolution of perturbations in expanding Universe

$$\ddot{\delta} + 2H\dot{\delta} - \frac{c_s^2}{a^2}\Delta_{\vec{x}}\delta = 4\pi G\bar{\rho}\delta \ . \tag{4.34}$$

This looks very similar to Eq. (4.14) with some sort of 'time dependent' speed of sound c_s/a, and the additional presence of a drag term $2H\dot{\delta}$ which expresses the fact that the expansion of the Universe ($H > 0$) opposes the collapse of structures. If we neglect this expansion drag, the analysis performed above can be almost exactly replicated, and one finds the dispersion relation:

$$\omega^2 = c_s^2\left[k^2 - k_J^2(t)\right] \ . \tag{4.35}$$

with a time-dependent Jean's length:

$$k_J(t) = \sqrt{\frac{4\pi G\bar{\rho}(t)a^2(t)}{c_s^2}} \ . \tag{4.36}$$

Thus the analysis performed in the static case still applies, but now individual, fixed, wavelengths (modes) can change from a sound-wave dominated regime to a gravitationally dominated one (and vice-versa) as the Universe expands: length scales that start too small to collapse can be led to collapse at a later stage. But this all depends on the behaviour of $\bar{\rho}(t)a^2(t)$. Small scale fluctuations that are initially oscillating will start growing by gravitational pull at a later time if $\bar{\rho}a^2$ is a decreasing function of time. For $\bar{\rho} \propto a^n$, this means if $n < -2$, which is the case for a Universe dominated by relativistic or non-relativistic fluids, as we have seen.

4.2 Relativistic perturbation theory

The Newtonian perturbation theory we presented above is a very good description of structure formation on small scales in the late-time Universe. However, if one wants to arrive at a consistent description of structure on all scales and of their evolution from the early Universe to today, one needs to develop a fully relativistic model of structure formation. This is what we will attempt in the rest of this chapter. We will start by a description of the generic concept of perturbations of a spacetime. That will lead us to the notion of a gauge[1]. However, after presenting this generic framework, unlike what is done in many modern textbooks, we will specify a convenient gauge to perform all our calculations, instead of trying to do everything in a gauge-invariant way. This means that the reader who is not too fluent in General Relativity can skip most of the next subsection without much loss. In the next chapter, we will come back briefly to the gauge issue to define physically relevant quantities and describe structures in the late-time Universe, but we will try to keep the discussion accessible without prerequisite from the next subsection.

4.2.1 Perturbing a spacetime

It is usual in physics to try and approach complex systems lacking any apparent symmetry by trying to describe them as only slightly non-symmetrical, and related to a highly symmetrical, well-known, physical system by a small perturbations. For example, as a first approximation, the surface of the Earth is well-approximated by a sphere, and departures from sphericity such as ellipticity due to rotation, mountains and valleys etc. can be described as small hierarchical perturbations around a perfectly spherical, idealised Earth. The spherical Earth model is what we will call a background geometry, while the corrections to sphericity will be called perturbations of the geometry. The advantage of such a description is that a sphere is a highly symmetrical object, thus quantities and dynamics can be easily calculated exactly on it (equations are easier to solve on a sphere that on a general "bumpy" surface). Then corrections to these quantities and dynamics due to the non-sphericity can be calculated order by order in importance of the perturbers on various relevant scales.
Now, there is an ambiguity here due to the very symmetric nature of a sphere. I can label points on the sphere by their latitude and longitude but of course, these are completely arbitrary in the sense that latitudes depend on identifying poles, while longitudes depend on selecting a reference merid-

[1]Be careful: this is a related, but distinct concept from the usual "gauge" of field theory.

ian. Thus, given a mountain on Earth considered as a small perturbation on the shape of the surface, locating it at a given latitude and longitude is completely arbitrary. This means that whatever impact the mountain has on physical quantities cannot depend on the point of the idealised spherical model at which we have anchored it: the symmetries of the "background" model introduce some indetermination in the perturbed model, and this indetermination has to be removed (physicists say "gauged" out) once physical quantities are constructed. In essence this is the gauge problem in General Relativity. Let us see how it works in details.

We start with a highly-symmetrical background spacetime $(\bar{M}, \bar{\boldsymbol{g}})$, where $\bar{M}$ is a differentiable manifold and $\bar{\boldsymbol{g}}$ a Lorentzian metric on M which is a known, exact solution of the Einstein Field equations. $\bar{\boldsymbol{g}}$ is usually highly symmetrical, e.g. Minkowski, Schwarzschild, Friedmann-Lemaître-Robertson-Walker etc. We consider a second differentiable manifold M, which is diffeomorphic to $\bar{M}$ so they could be treated as the same manifold, up to identifying points in M and points in $\bar{M}$. Let us pick such an identification by selecting a specific diffeomorphism $\phi : \bar{M} \to M$. This choice is arbitrary, and this will be important in what follows. Next, we pick a Lorentzian metric $\boldsymbol{g}$ on M. We would like to make precise the following statement:

The manifold $(M, \boldsymbol{g})$ is close to the manifold $\left(\bar{M}, \bar{\boldsymbol{g}}\right)$.

Let $p \in \bar{M}$ and a local chart $(U, \bar{\varphi})$ around p such that $\varphi(p) = \bar{x}$. Let (V, φ) be a local chart of M containing $\varphi(U)$, such that $\varphi(\phi(p)) = x$. In order to compare the metric $\boldsymbol{g}$ to the metric $\bar{\boldsymbol{g}}$, we are going to pullback $\boldsymbol{g}$ onto $\bar{M}$, using our selected diffeomorphism ϕ. A pictorial representation of the set-up can be found in figure 4.2. Given:

$$\boldsymbol{g} = g_{\alpha\beta} \mathrm{d}x^{\alpha} \otimes \mathrm{d}x^{\beta} , \tag{4.37}$$

we get the pullback metric on $\bar{M}$, $\boldsymbol{\phi}^{*}\boldsymbol{g}$ defined, for any two vector fields $\bar{\boldsymbol{X}}$ and $\bar{\boldsymbol{Y}}$ on $\bar{M}$, by:

$$\left(\boldsymbol{\phi}^{*}\boldsymbol{g}\right)\left(\bar{\boldsymbol{X}}, \bar{\boldsymbol{Y}}\right) \equiv \boldsymbol{g}\left(\boldsymbol{\phi}_{*}\bar{\boldsymbol{X}}, \boldsymbol{\phi}_{*}\bar{\boldsymbol{Y}}\right) , \tag{4.38}$$

where $\boldsymbol{\phi}_{*}\bar{\boldsymbol{X}}$ and $\boldsymbol{\phi}_{*}\bar{\boldsymbol{Y}}$ are the pushforward of $\bar{\boldsymbol{X}}$ and $\bar{\boldsymbol{Y}}$ onto M; see appendix A. Then, the symmetric, rank 2 tensor $\boldsymbol{\phi}^{*}\boldsymbol{g}$ is well-defined on $\bar{M}$ and defines a new metric tensor on the background, which can thus be compared to the background metric $\bar{\boldsymbol{g}}$ pointwise. We define the difference between the two metrics as:

$$\boldsymbol{h} = \boldsymbol{\phi}^{*}\boldsymbol{g} - \bar{\boldsymbol{g}} \tag{4.39}$$

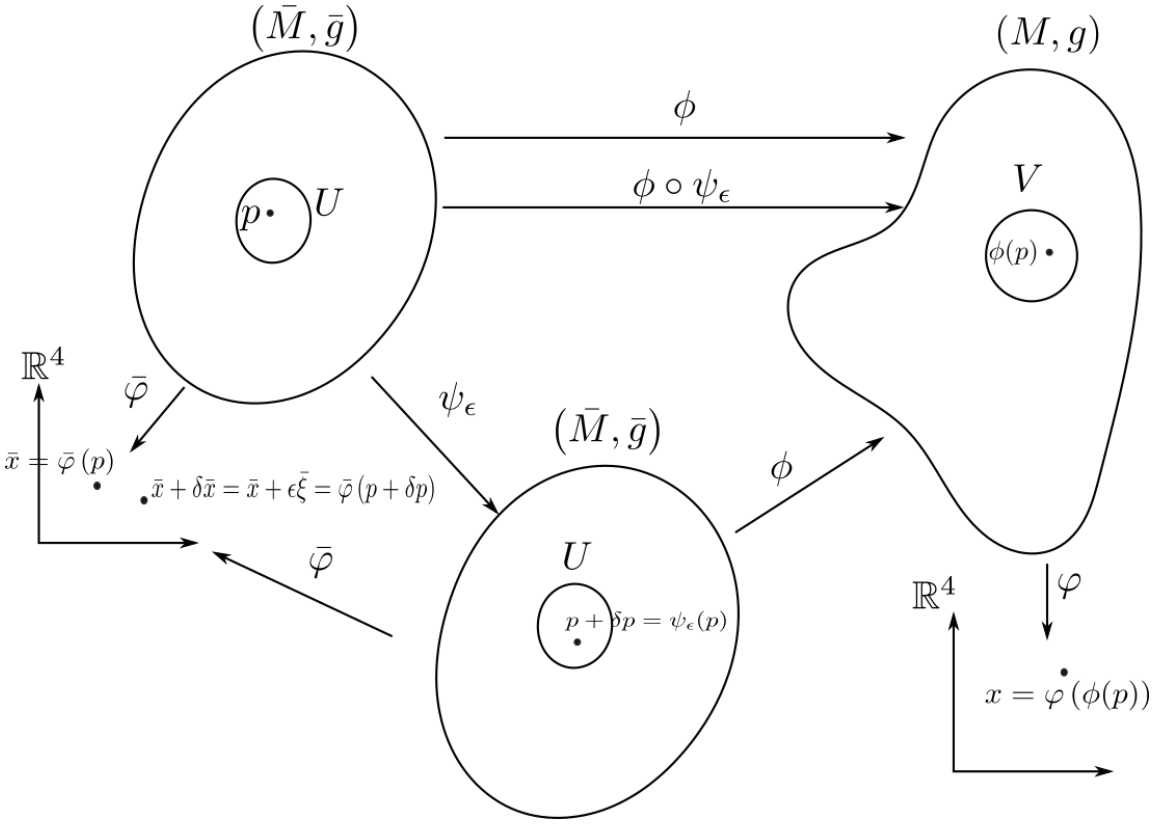

Figure 4.2: Sets and maps necessary to set-up the gauge transformations.

as a symmetric rank-two tensor on the background $\bar{M}$, such that:

$$h_{\mu\nu}(\bar{x})\,\mathrm{d}\bar{x}^{\mu}\otimes\mathrm{d}\bar{x}^{\nu}=\left[(\phi^{*}g)_{\mu\nu}(\bar{x})-\bar{g}_{\mu\nu}(\bar{x})\right]\mathrm{d}\bar{x}^{\mu}\otimes\mathrm{d}\bar{x}^{\nu}\ . \tag{4.40}$$

We will say that $(M,\boldsymbol{g})$ is close to $(\bar{M},\bar{\boldsymbol{g}})$, or is a perturbed spacetime with respect to the background $(\bar{M},\bar{\boldsymbol{g}})$ if and only if we can find one diffeomorphism ϕ between $\bar{M}$ and M such that the components of $\boldsymbol{h}$ are small (compared to 1). In that case, $\boldsymbol{h}$ is called a perturbation to the background metric $\bar{\boldsymbol{g}}$. Note that there is no reason whatsoever for the components $\left|h_{\mu\nu}\right|$ to be small for an arbitrary diffeomorphism ϕ. Nevertheless, if we assume that there is such a ϕ that leads to a small difference tensor $\boldsymbol{h}$, then there is an infinite number of diffeomorphisms between $\bar{M}$ and M which keep the metrics $\boldsymbol{g}$ and $\bar{\boldsymbol{g}}$ close. Indeed, consider an arbitrary vector field on $\bar{M}$:

$$\bar{\boldsymbol{\xi}}=\bar{\xi}^{\mu}\frac{\partial}{\partial\bar{x}^{\mu}}\ . \tag{4.41}$$

Let $\epsilon\in\mathbb{R}$, small. Then we can define a one-parameter family of diffeomorphisms $\psi_{\epsilon}:\bar{M}\to\bar{M}$ by displacing points of $\bar{M}$ along the flow of $\bar{\boldsymbol{\xi}}$ by an amount ϵ:

$$\forall\bar{x}=\bar{\varphi}(p)\in\bar{\varphi}(U),\ \bar{y}^{\mu}=[\bar{\varphi}(p+\delta p)]^{\mu}=\bar{x}^{\mu}+\delta\bar{x}^{\mu}=\bar{x}^{\mu}+\epsilon\bar{\xi}^{\mu}\ . \tag{4.42}$$

Then, by construction, $\phi\circ\psi_{\epsilon}$ will also be a diffeomorphism between $\bar{M}$ and M, for $|\epsilon|\ll 1$. Thus we can pick up any one of those to define our metric perturbation $\boldsymbol{h}$, so that we are left with a family of perturbations, indexed by a choice of the vector field $\bar{\boldsymbol{\xi}}$:

$$\begin{aligned}\boldsymbol{h}^{(\epsilon)} &\equiv (\boldsymbol{\phi}\circ\boldsymbol{\psi}_{\epsilon})^{*}\boldsymbol{g}-\bar{\boldsymbol{g}} &(4.43)\\ &= \left(\boldsymbol{\psi}_{\epsilon}^{*}\left(\boldsymbol{\phi}^{*}\boldsymbol{g}\right)\right)-\bar{\boldsymbol{g}}\ . &(4.44)\end{aligned}$$

How are members of this family of perturbations related to each other?
We can notice that:

$$\begin{aligned}\boldsymbol{h}^{(\epsilon)} &= \psi_{\epsilon}^{*}(\boldsymbol{h}+\bar{\boldsymbol{g}})-\bar{\boldsymbol{g}} &(4.45)\\ &= \boldsymbol{\psi}_{\epsilon}^{*}\boldsymbol{h}+\boldsymbol{\psi}_{\epsilon}^{*}\bar{\boldsymbol{g}}-\bar{\boldsymbol{g}}\ \text{(linearity of pullback)} &(4.46)\\ &= \boldsymbol{h}+\boldsymbol{\psi}_{\epsilon}^{*}\bar{\boldsymbol{g}}-\bar{\boldsymbol{g}}\ \ \left(\boldsymbol{\psi}_{\epsilon}^{*}\boldsymbol{h}=\boldsymbol{h}\ \text{at leading order since}\ \epsilon,\ \|\boldsymbol{h}\|\ll 1\right) &(4.47)\\ &= \boldsymbol{h}+\epsilon\frac{\boldsymbol{\psi}_{\epsilon}^{*}\bar{\boldsymbol{g}}-\bar{\boldsymbol{g}}}{\epsilon}\ . &(4.48)\end{aligned}$$

Note that we see the Lie derivative of $\bar{\boldsymbol{g}}$ along $\bar{\boldsymbol{\xi}}$ appear. Indeed, by definition:

$$\mathcal{L}_{\bar{\xi}}\bar{\boldsymbol{g}}=\lim_{\epsilon\to 0}\frac{\boldsymbol{\psi}_{\epsilon}^{*}\bar{\boldsymbol{g}}-\bar{\boldsymbol{g}}}{\epsilon}\ . \tag{4.49}$$

Let us calculate this term. For the ease of notation, let us define:

$$\boldsymbol{G}_{\boldsymbol{\epsilon}} = \boldsymbol{\psi}_{\boldsymbol{\epsilon}}^{*}\bar{\boldsymbol{g}} \ . \tag{4.50}$$

Then, by definition for two arbitrary vector fields $\bar{X}$ and $\bar{Y}$ on $\bar{M}$:

$$\boldsymbol{G}_{\boldsymbol{\epsilon}|p}\left(\bar{\boldsymbol{X}},\bar{\boldsymbol{Y}}\right) \equiv \bar{\boldsymbol{g}}_{|p+\delta p}\left(\boldsymbol{\psi}_{\boldsymbol{\epsilon},*}\bar{\boldsymbol{X}},\boldsymbol{\psi}_{\boldsymbol{\epsilon},*}\bar{\boldsymbol{Y}}\right) \ . \tag{4.51}$$

Then, we also have:

$$\begin{aligned}
\left[\boldsymbol{\psi}_{\boldsymbol{\epsilon},*}\bar{\boldsymbol{X}}\right]^{\mu} &= \frac{\partial\left(\bar{x}^{\mu}+\epsilon\bar{\xi}^{\mu}\right)}{\partial\bar{x}^{\nu}}\bar{X}^{\nu} && (4.52)\\
&= \left(\delta^{\mu}_{\nu}+\epsilon\frac{\partial\bar{\xi}^{\mu}}{\partial\bar{x}^{\nu}}\right)\bar{X}^{\nu} && (4.53)\\
&= \bar{X}^{\mu}+\epsilon\bar{X}^{\nu}\frac{\partial\bar{\xi}^{\mu}}{\partial\bar{x}^{\nu}} \ . && (4.54)
\end{aligned}$$

In particular:

$$\left[\psi_{\epsilon,*}\frac{\partial}{\partial\bar{x}^{\mu}}\right]^{\alpha} = \delta^{\alpha}_{\mu}+\epsilon\frac{\partial\bar{\xi}^{\alpha}}{\partial\bar{x}^{\mu}} \ . \tag{4.55}$$

Finally:

$$\begin{aligned}
\left(G_{\epsilon}\right)_{\mu\nu} &\equiv \boldsymbol{G}_{\boldsymbol{\epsilon}}\left(\frac{\partial}{\partial\bar{x}^{\mu}},\frac{\partial}{\partial\bar{x}^{\nu}}\right) && (4.56)\\
&= \bar{\boldsymbol{g}}(p+\delta p)\left[\psi_{\epsilon,*}\frac{\partial}{\partial\bar{x}^{\mu}},\psi_{\epsilon,*}\frac{\partial}{\partial\bar{x}^{\nu}}\right] && (4.57)\\
&= \bar{g}_{\alpha\beta}\left(\bar{x}^{\sigma}+\epsilon\bar{\xi}^{\sigma}\right)\left[\delta^{\alpha}_{\mu}+\epsilon\frac{\partial\bar{\xi}^{\alpha}}{\partial\bar{x}^{\mu}}\right]\left[\delta^{\beta}_{\nu}+\epsilon\frac{\partial\bar{\xi}^{\beta}}{\partial\bar{x}^{\nu}}\right] && (4.58)\\
&= \left(\bar{g}_{\alpha\beta}\left(\bar{x}^{\sigma}+\epsilon\bar{\xi}^{\sigma}\frac{\partial\bar{g}_{\alpha\beta}}{\partial\bar{x}^{\sigma}}\right)\right)\left(\delta^{\alpha}_{\mu}\delta^{\beta}_{\nu}+\epsilon\delta^{\beta}_{\nu}\frac{\partial\bar{\xi}^{\alpha}}{\partial\bar{x}^{\mu}}+\epsilon\delta^{\alpha}_{\mu}\frac{\partial\bar{\xi}^{\beta}}{\partial\bar{x}^{\nu}}\right) && (4.59)\\
&= \bar{g}_{\mu\nu}\left(\bar{x}\right)+\epsilon\left[\xi^{\sigma}\frac{\partial\bar{g}_{\mu\nu}}{\partial\bar{x}^{\sigma}}+\bar{g}_{\alpha\nu}\frac{\partial\bar{\xi}^{\alpha}}{\partial\bar{x}^{\mu}}+\bar{g}_{\mu\alpha}\frac{\partial\bar{\xi}^{\alpha}}{\partial\bar{x}^{\nu}}\right] && (4.60)\\
&= \bar{g}_{\mu\nu}\left(\bar{x}\right)+2\nabla_{(\mu}\bar{\xi}_{\nu)} \ . && (4.61)
\end{aligned}$$

Thus, we see that under a gauge transformation generated by the vector field $\boldsymbol{\xi}$, the perturbation to the background metric transforms as:

$$\boxed{h^{(\epsilon)}_{\mu\nu} = h_{\mu\nu}+2\epsilon\nabla_{(\mu}\bar{\xi}_{\nu)} \ .} \tag{4.62}$$

Note that this change at order ϵ vanishes if $\bar{\boldsymbol{\xi}}$ is a Killing vector field of the background metric $\bar{\boldsymbol{g}}$; see appendix A. Such changes in the components of the metric perturbation under an infinitesimal diffeomorphism of $\bar{M}$ along a vector field that is not a Killing vector field of $\bar{\boldsymbol{g}}$ are called gauge transformations for the perturbation. Every two metric perturbations related to each other by a gauge transformation (4.62) for an appropriate choice of field $\bar{\boldsymbol{\xi}}$ represent the same physical configuration, since physical properties cannot depend on the arbitrary choice of $\bar{\boldsymbol{\xi}}$. Therefore, one usually performs perturbative calculations in a specific gauge, i.e. choosing a specific form of the perturbation $\boldsymbol{h}$, but in the end, one must make sure to relate everything that has been calculated to observables from which gauge degrees of freedom have been removed.
Finally, note that we have chosen to present gauge transformations from an active viewpoint, i.e. by shifting points of $\bar{M}$ around while keeping the local charts fixed. One could arrive at the same gauge transformations (4.62) by adopting a passive viewpoint and changing the local charts along the flow of $\bar{\boldsymbol{\xi}}$ while keeping the points fixed, via: $\bar{x}^\mu \mapsto \bar{x}^\mu - \epsilon\bar{\xi}^\mu$. This is left as an exercise to the reader.

4.2.2 Perturbed FLRW spacetimes

Let us now go back to cosmology. We assume that we have a well-defined FLRW background, $\bar{\boldsymbol{g}}$, and we wish to study small fluctuations around it, representing local inhomogeneities. For simplicity, and because this is the case we will study in the next chapters, we assume thatthe background FLRW model is flat. The arguments presented here are not affected by this assumption. Local inhomogeneities can be described by a perturbation as exposed in the previous subsection. For convenience, and to stick with common practice, we actually define our perturbations in the conformal time representation, and we write $\boldsymbol{h}$ for the conformal perturbations in Cartesian coordinates:

$$\begin{aligned} \mathrm{d}s^2 &= a^2(\eta)\left(\bar{g}_{\mu\nu} + h_{\mu\nu}\right)\mathrm{d}x^\mu \mathrm{d}x^\nu && (4.63)\\ &= a^2(\eta)\left[(-1+h_{00})\,\mathrm{d}\eta^2 + 2h_{0i}\mathrm{d}\eta\mathrm{d}x^i + \left(\delta_{ij} + h_{ij}\mathrm{d}x^i\mathrm{d}x^j\right)\right]\,. && (4.64)\end{aligned}$$

By symmetry, $h_{\mu\nu}$ consists of 10 independent components, h_{00} (1), h_{0i} (3) and h_{ij} (6). However, we know that the Einstein equations only determine 6 independent functional degrees of freedom, so what is going on? Well, we have our gauge freedom, which is equivalent to choosing a vector field $\boldsymbol{\xi}$, i.e. four independent functions (the components of $\boldsymbol{\xi}$). Once this is done, we can use this vector field to fix four of the ten functions characterising the perturbation $h_{\mu\nu}$. This is called fixing a gauge.

There are many particular choices of gauges that turn out to be more or less convenient in various situations. Before we discuss the gauge that we will choose in these notes, we need to introduce another convenient decomposition. When one is given a split into a time direction and maximally-symmetric spatial slices, like we do in FLRW, by the introduction of fundamental observers, then one can decompose any tensor on the background into scalar, (divergenceless aka transverse) vector and (symmetric, transverse trace-free) tensor degree of freedom in the following way:

$$
\begin{aligned}
h_{00} &= -2\Phi && (4.65)\\
h_{0i} &= \partial_i B + \bar{B}_i \text{ with } \partial_i \bar{B}^i = 0 && (4.66)\\
h_{ij} &= -2\Psi\gamma_{ij} + 2\partial_{(i}\partial_{j)}E + 2\partial_{(i}\bar{E}_{j)} + 2\bar{E}_{ij} && (4.67)\\
&\quad \text{with } \partial_i \bar{E}^i = 0\,,\ \partial_i \bar{E}^i_j = 0\,,\ \bar{E}^i{}_i = 0\,,
\end{aligned}
$$

where $\partial_i = \frac{\partial}{\partial x^i}$ is the spatial partial derivative; $\bar{B}^i$ and $\bar{E}^i$ are transverse spatial vector fields, and $\bar{E}_{ij}$ is a transverse and traceless spatial tensor field. This is called a *scalar-vector-tensor decomposition*. We thus recover our ten functional degrees of freedom, called *metric potentials*:

1. 4 scalars: Φ, Ψ, B and E, corresponding to 4 degrees of freedom;

2. 2 transverse spatial vectors $\bar{B}^i$ and $\bar{E}^i$, corresponding to $2 \times (3-1) = 4$ degrees of freedom (transversality introduces one constraint for each vector);

3. 1 symmetric, transverse (divergenceless) and traceless spatial tensor $\bar{E}_{ij}$, corresponding to 10-4-3-1=2 degrees of freedom (symmetry leads to 10-4, transverse to -3 and traceless to -1).

The key reason to introduce this split, is that scalars, vectors and tensors decouple at linear order and all evolve independently (technically, this is because they are generated by the irreducible scalar, vector and tensor representations of the symmetry group of the symmetric background space). Thus, they can be studied separately, which greatly simplifies the study of perturbations.

The connection coefficients, Ricci tensor and Einstein tensor for the metric (4.64) are derived in details in appendix B.

4.2.3 Behaviour under gauge transformations

How are the metric potentials affected by a gauge transformation? Let us consider a generic vector field $\boldsymbol{\xi}$ that we decompose in a timelike and a spacelike part as follows:

$$\xi^\mu = T\delta^\mu{}_0 + L^i\delta^\mu{}_i \,, \tag{4.68}$$

with $L^i = \partial^i L + \bar{L}^i$ such that $\partial_i \bar{L}^i = 0$. Then, lowering and raising indices conformally, we write:

$$\xi_\mu = -a^2 T\delta_\mu{}^0 + a^2 L_i \delta^i{}_\mu \,. \tag{4.69}$$

Using the background connection coefficients given in appendix B:

$$\begin{cases} \nabla_{(0}\xi_{0)} = -\,a^2\left(T' + \mathcal{H}T\right) & (4.70) \\ \nabla_{(0}\xi_{i)} = \dfrac{1}{2}a^2\left(L_i' - \partial_i T\right) & (4.71) \\ \nabla_{(i}\xi_{j)} = a^2\left[\partial_{(i}L_{j)} + \mathcal{H}T\delta_{ij}\right] \,. & (4.72) \end{cases}$$

Thus, using a tilde to mark the metric potential in the new gauge, and using Eq.(4.62), we get:

Effect of a gauge transformation on metric potentials

$$\begin{cases} \tilde{\Phi} = \Phi + T' + \mathcal{H}T & (4.73) \\ \tilde{\Psi} = \Psi - \mathcal{H}T & (4.74) \\ \tilde{B} = B + L' - T & (4.75) \\ \tilde{E} = E + L & (4.76) \\ \tilde{\bar{B}}^i = \bar{B}^i + \partial_\eta \bar{L}^i & (4.77) \\ \tilde{\bar{E}}^i = \bar{E}^i + \bar{L}^i & (4.78) \\ \tilde{\bar{E}}_{ij} = \bar{E}_{ij} \,. & (4.79) \end{cases}$$

We see that the tensor perturbation $\bar{E}_{ij}$ is *gauge invariant*. However, the scalars and vectors are affected. We can construct some scalar and vector gauge invariant quantities that do not depend on the arbitrary choice we make to map background and perturbed spacetimes into each other. For

example, we have the *Bardeen potentials*:

$$\begin{cases} \Psi_{\rm B} = \Psi - \mathcal{H}(B - E') & (4.80) \\ \Phi_{\rm B} = \Phi + \mathcal{H}(B - E') + (B - E')' & (4.81) \\ \bar{U}^i = \partial_\eta \bar{E}^i - \bar{B}^i \ . & (4.82) \end{cases}$$

Analysing the dynamics in terms of these variables guarantees that one does not confuse spurious gauge modes with actual physical effects. However, one must note that gauge invariant quantities are not necessarily observable. An observable must relate to an observer and cosmologically relevant observers might not (and in general do not) correspond to gauges in which the Bardeen potentials or other gauge invariant quantities are easily relatable to the metric potentials.

4.2.4 Matter perturbations

In chapter 2 and chapter 3, we have seen that in the standard hot- Big-Bang model, the matter could be divided into two fluids, one relativistic and one non-relativistic. In chapter 5, we will come back to this particular situation but here, we are going to keep the discussion more generic. At the background level, we have used perfect fluids but in General Relativity, the energy-momentum tensor for a fluid takes the general form:

$$T_{\mu\nu} = (\rho + p)\, u_\mu u_\nu + p g_{\mu\nu} + 2q_{(\mu} u_{\nu)} + \pi_{\mu\nu} \ , \tag{4.83}$$

where:

- ρ and p are the energy density and (isotropic) pressure respectively;
- $\boldsymbol{u}$ is the 4-velocity of the fluid elements;
- $\boldsymbol{q}$ is the energy flux, such that $q_\mu u^\mu = 0$;
- $\boldsymbol{\pi}$ is the anisotropic stress, with $\pi_{\mu\nu} = \pi_{\nu\mu}$, $\pi^\mu{}_\mu = 0$, $\pi_{\mu\nu} u^\mu = 0$.

In this chapter and afterwards, when referring to 'the energy-momentum tensor', we will mean the *total energy-momentum tensor*, representing the cosmological fluid as a whole. In a perturbed

Universe, we decompose each of these quantities at first order:

$$\rho = \bar{\rho} + \delta\rho \ ; \ p = \bar{p} + \delta p \tag{4.84}$$

$$u^\mu = \bar{u}^\mu + \delta u^\mu \ ; \ q^\mu = \bar{q}^\mu + \delta q^\mu \tag{4.85}$$

$$\pi_{\mu\nu} = \bar{\pi}_{\mu\nu} + \delta\pi_{\mu\nu} \ , \tag{4.86}$$

where an overbar denotes a background quantity. Then, we have $T_{\mu\nu} = \bar{T}_{\mu\nu} + \delta T_{\mu\nu}$ with:

$$\bar{T}_{\mu\nu} = (\bar{\rho} + \bar{p})\, \bar{u}_\mu \bar{u}_\nu + \bar{p}\bar{g}_{\mu\nu} + 2\bar{q}_{(\mu}\bar{u}_{\nu)} + \bar{\pi}_{\mu\nu} \ , \tag{4.87}$$

and:

$$\begin{aligned} \delta T_{\mu\nu} =& 2(\bar{\rho} + \bar{p})\bar{u}_{(\mu}\delta u_{\nu)} + (\delta\rho + \delta p)\, \bar{u}_\mu \bar{u}_\nu \\ &+ \delta p \bar{g}_{\mu\nu} + \bar{p}\delta g_{\mu\nu} + 2\bar{q}_{(\mu}\delta u_{\nu)} + 2\delta q_{(\mu}\bar{u}_{\nu)} + \delta\pi_{\mu\nu} \ . \end{aligned} \tag{4.88}$$

In the background, $\bar{u}_\mu \bar{u}^\mu = -1$ gives:

$$a^2 \left(\bar{u}^0\right)^2 = 1 - a^2 \delta_{ij} \bar{u}^i \bar{u}^j \ . \tag{4.89}$$

Since homogeneity and isotropy implies that $u^\mu = u^\mu(\eta)$, the timelike geodesic equation for the fluid elements:

$$\bar{u}\nabla_\mu \bar{u}^\nu = 0 \tag{4.90}$$

implies that:

$$\bar{\boldsymbol{u}} = \frac{1}{a}\frac{\partial}{\partial\eta} \ , \tag{4.91}$$

i.e. $\bar{u}^0 = 1/a$ and $\bar{u}^i = 0$. Thus, we have:

$$\bar{q}^0 = 0 \ ; \ \bar{\pi}_{0\mu} = 0 \ . \tag{4.92}$$

Besides:

$$\bar{u}_\mu = -a\delta_{\mu 0} \ . \tag{4.93}$$

The background components of the Einstein tensor yield $\bar{G}_{0i} = 0$ and $\bar{G}_{ij} = 0$ for $i \neq j$ which implies, via the Einstein field equations that $\bar{q}^i = 0$ and $\bar{\pi}_{ij} = 0$. Thus, at the level of the background, the cosmological matter content is a perfect fluid with:

$$\bar{T}_{\mu\nu} = (\bar{\rho} + \bar{p})\, \bar{u}_\mu \bar{u}_\nu + \bar{p}\bar{g}_{\mu\nu} \ , \tag{4.94}$$

and we can write $\delta q^\mu = q^\mu$ and $\delta\pi_{\mu\nu} = \bar{p}\pi_{\mu\nu}$, keeping in mind that both energy flux and anisotropic stress are at most first order perturbations. As it turns out, one cannot distinguish a first order energy flux from a first order peculiar velocity, so we can, without loss of generality, set $q^i = 0$ and write:

$$\begin{aligned}\delta T_{\mu\nu} =& 2(\bar{\rho}+\bar{p})\bar{u}_{(\mu}\delta u_{\nu)} + (\delta\rho+\delta p)\,\bar{u}_\mu\bar{u}_\nu \\ &+ \delta p\bar{g}_{\mu\nu} + \bar{p}\delta g_{\mu\nu} + \bar{p}\pi_{\mu\nu}\ .\end{aligned} \tag{4.95}$$

Using $u_\mu u^\nu = -1$ and expanding at first order, we can get that:

$$u^\mu = \frac{1}{a}(1-\Phi)\delta^\mu{}_0 + \frac{1}{a}v^i\delta^\mu{}_i\ , \tag{4.96}$$

where we have defined the fluid (conformal) *peculiar velocity* $v^i = au^i$. In covariant form, we have:

$$u_\mu = -a(1+\Phi)\delta_\mu{}^0 + a\,(v_i + B_i)\,\delta^i{}_\mu\ . \tag{4.97}$$

Of course, like any 3-vector, we can decompose the peculiar velocity into a potential and a transverse part:

$$v^i = \partial^i V + \bar{V}^i \quad \text{with} \quad \partial_i\bar{V}^i = 0\ . \tag{4.98}$$

Similarly, $\pi_{00} = \pi_{0i} = 0$ and the anisotropic stress can be decomposed into scalar, vector and tensor parts:

$$\pi_{ij} = \left[\partial_i\partial_j - \frac{1}{3}\delta_{ij}\Delta\right]\bar{\pi} + \partial_{(i}\bar{\pi}_{j)} + \bar{\pi}_{ij}\ , \tag{4.99}$$

with $\partial_i\bar{\pi}^i = \partial_i\bar{\pi}^i{}_j = 0$. In components we have:

First order perturbations to the total energy-momentum tensor

$$\begin{cases}\delta T^0{}_0 = -\,\delta\rho & (4.100)\\ \delta T^0{}_i = (\bar{\rho}+\bar{p})\,(v_i + B_i) & (4.101)\\ \delta T^i{}_0 = -\,(\bar{\rho}+\bar{p})\,v^i & (4.102)\\ \delta T^i{}_j = \delta p\delta^i{}_j + \bar{p}\pi^i{}_j\ . & (4.103)\end{cases}$$

The quantity $Q_i = (\bar{\rho}+\bar{p})\,v_i$ is the *momentum density* of the fluid. Note that under a gauge transformation $\tilde{x}^\mu = x^\mu - \xi^\mu$, we have:

$$\tilde{T}^\mu{}_\nu(\tilde{x}) = \frac{\partial\tilde{x}^\mu}{\partial x^\rho}\frac{\partial x^\sigma}{\partial\tilde{x}^\nu}T^\mu{}_\sigma(x)\ , \tag{4.104}$$

which, at first order, gives:

$$\delta\tilde{T}^{\mu}{}_{\nu} = \delta T^{\mu}{}_{\nu} + \bar{T}^{\mu}{}_{\sigma}\frac{\partial\xi^{\sigma}}{\partial x^{\nu}} - \bar{T}^{\rho}{}_{\nu}\frac{\partial\xi^{\mu}}{\partial x^{\rho}} + T\frac{\mathrm{d}\bar{T}^{\mu}{}_{\nu}}{\mathrm{d}\eta} \ . \tag{4.105}$$

Therefore, under a gauge transformation, the fluid quantities change as:

Effect of gauge transformation on fluid quantities

$$\begin{cases} \widetilde{\delta\rho} = \delta\rho + \bar{\rho}'T & (4.106) \\ \widetilde{\delta p} = \delta p + \bar{p}'T & (4.107) \\ \tilde{Q}_i = Q_i - (\bar{\rho}+\bar{p})\,L_i' & (4.108) \\ \tilde{\pi}_{ij} = \pi_{ij} \ . & (4.109) \end{cases}$$

It is common to introduce the *density contrast* in a given gauge:

$$\delta = \frac{\delta\rho}{\bar{\rho}} \ . \tag{4.110}$$

A gauge invariant variable associated with the matter distribution that we will find particularly useful when studying large scale structure is the *comoving density contrast* Δ, defined as:

$$\bar{\rho}\Delta = \delta\rho + \bar{\rho}'(V+B) \ . \tag{4.111}$$

It owes its name to the fact that it matches the density contrast in the comoving gauge, defined as the gauge in which the coordinate system is comoving with the matter fluid, i.e. $\tilde{T}^{0}{}_{i} = \tilde{T}^{i}{}_{0} = 0$, which can be achieved by imposing $Q^{i} = B_i = 0$. Indeed, in that gauge, $V = B = 0$, and $\bar{\rho}\Delta = \widetilde{\delta\rho}$. Note that this gauge involves fixing more than 4 degrees of freedom so it is not properly defined if the flow has some vorticity. If the flow is purely potential, then, only the scalar (potential) parts of v^{i} and B_i need fixing, which is always possible. Therefore, we will only be able to use this gauge when the fluid vorticity can be neglected. On cosmological scales, this is always the case, as we will see.

Finally, we can introduce the *equation of state of the total fluid*:

$$w = \frac{\bar{p}}{\bar{\rho}} \ , \tag{4.112}$$

to characterise the link between pressure and energy density in the background (see chapter 2). To relate the energy density and pressure perturbations, we can notice that, apart from the anisotropic stress, there is only one gauge-invariant quantity that can be defined with the energy-momentum tensor alone:

$$\bar{p}\Gamma = \delta p - \frac{\bar{p}'}{\bar{\rho}'}\delta\rho \ . \tag{4.113}$$

Γ is called the *entropy perturbation* as it can be shown to be proportional to the entropy flux of the perturbations; see appendix 5 of [9] for a detailed proof. On the other hand:

$$\boxed{c_s^2 = \frac{\bar{p}'}{\bar{\rho}'} \ ,} \tag{4.114}$$

is known as the *adiabatic sound speed* of the fluid. We then have:

$$\boxed{\delta p = c_s^2 \delta\rho + \bar{p}\Gamma \ .} \tag{4.115}$$

4.3 Evolution equations for perturbations

We now have all the ingredients to write down and solve the equations for metric and matter perturbations in a cosmological background. Many textbooks use gauge invariant formulations at this stage but we are going to choose a different approach and rather fix a specific, convenient gauge in which to write down equations. We will see that vectors and tensors are damped in standard cosmology during the hot Big-Bang phase, so that they do not play any significant role in structure formation. Vectors are gauge dependent objects so this statement is in principle gauge dependent. But it turns out to be generic and therefore, we will neglect vectors and tensors in these notes (except in Chapter 8, in which tensors will make a come back).

4.3.1 Cosmological perturbations in the longitudinal gauge

The *longitudinal, or Newtonian, gauge* is defined by setting:

$$\begin{cases} E = B = 0 \text{ for scalars} & (4.116) \\ \bar{B}_i = 0 \text{ for vectors.} & (4.117) \end{cases}$$

The line element at first order in perturbations is then given by:

$$\mathrm{d}s^2 = a^2(\eta)\left\{-(1+2\Phi)\,\mathrm{d}\eta^2 + \left[(1-2\Psi)\delta_{ij} + 2\partial_{(i}\bar{E}_{j)} + 2\bar{E}_{ij}\right]\mathrm{d}x^i\mathrm{d}x^j\right\} . \tag{4.118}$$

This gauge is particularly pleasing for various reasons. First, let us note that in an arbitrary gauge, the hypersurfaces of constant (conformal) time have a Ricci curvature given by:

$${}^{(3)}R = \frac{4}{a^2}\Delta\Psi . \tag{4.119}$$

Therefore, the potential Ψ determines the curvature of spatial slices at constant η in the longitudinal gauge. Be careful that ${}^{(3)}R$ is not gauge invariant. More importantly for us, we will see that in this gauge, some of the Einstein equations look Newtonian, hence the name of the gauge. Let us now write the perturbed quantities in that gauge. Using the results of appendix B, the Einstein tensor reads:

$$\begin{cases}
\delta G_{00} = 2\Delta\Psi - 6\mathcal{H}\Psi' & (4.120)\\
\delta G_{0i} = \partial_i\left[2\Psi' + 2\mathcal{H}\Phi\right] + \frac{1}{2}\Delta\bar{E}_i' & (4.121)\\
\delta G_{ij} = \bar{E}_{ij}'' - \Delta\bar{E}_{ij} + 2\mathcal{H}\bar{E}_{ij}' - 2\left[2\mathcal{H}' + \mathcal{H}^2\right]\bar{E}_{ij} \\
\qquad + \partial_{(i}\left[\bar{E}_{|j)}'' + 2\mathcal{H}\bar{E}_{|j)}' - 2\left(2\mathcal{H}' + \mathcal{H}^2\right)\bar{E}_{|j)}\right] \\
\qquad + \partial_{(i}\partial_{j)}\left[\Psi - \Phi\right] \\
\qquad + \left[2\Psi'' + 4\mathcal{H}\Psi' + \Delta(\Phi - \Psi) + 2\left(2\mathcal{H}' + \mathcal{H}^2\right)(\Phi + \Psi) + 2\mathcal{H}\Phi'\right]\delta_{ij} . & (4.122)
\end{cases}$$

The energy momentum tensor becomes[2]:

$$\begin{cases}
\delta T_{00} = a^2(\delta\rho + 2\bar{\rho}\Phi) & (4.123)\\
\delta T_{0i} = -a^2(\bar{\rho} + \bar{p})\left[\partial_i V + \bar{V}_i\right] & (4.124)\\
\delta T_{ij} = a^2(\delta p - 2\bar{p}\Psi)\,\delta_{ij} + a^2\bar{p}\pi_{ij} + a^2\bar{p}h_{ij} . & (4.125)
\end{cases}$$

4.3.2 Perturbed Einstein field equations

First, we want to decompose the Einstein field equations:

$$G_{\mu\nu} + \Lambda g_{\mu\nu} = 8\pi G T_{\mu\nu} , \tag{4.126}$$

[2]Pay attention to the fact that $\delta T_{\mu\nu} = \bar{g}_{\mu\rho}\delta T^{\rho}{}_{\nu} + \delta g_{\mu\rho}\bar{T}^{\rho}{}_{\nu}$.

into a background part and a first order part. For what follows, it will be important to perform a slight trick and consider the cosmological constant as a perfectly homogeneous and isotropic (non clustering) fluid with energy momentum tensor:

$$T_{\mu\nu} = -\frac{\Lambda}{8\pi G} g_{\mu\nu} \,, \tag{4.127}$$

so that its energy density and pressure are simply given by $\bar{\rho}_\Lambda = -\bar{p}_\Lambda = \Lambda/8\pi G$. Then it can be re-absorbed into the total energy momentum tensor and the Einstein field equations simply read:

$$G_{\mu\nu} = 8\pi G T_{\mu\nu} \,, \tag{4.128}$$

We will always implicitly do that from now on. The background equations are then simply:

Background equations in conformal time

$$\mathcal{H}^2 = \frac{8\pi G}{3}\bar{\rho}a^2 \tag{4.129}$$

$$\mathcal{H}' = -\frac{4\pi G}{3}\left(\bar{\rho} + 3\bar{p}\right) a^2 = -\frac{1}{2}(1+3w)\mathcal{H}^2 \,. \tag{4.130}$$

and the energy-momentum conservation gives:

$$\bar{\rho}' + 3(1+w)\mathcal{H}\bar{\rho} = 0 \,. \tag{4.131}$$

The perturbation equations are then given by:

$$\delta G_{\mu\nu} = 8\pi G \delta T_{\mu\nu} \,, \tag{4.132}$$

which translates into a pure scalar equation ($\mu = \nu = 0$):

$$2\Delta\Psi - 6\mathcal{H}\Psi' = 8\pi G a^2 \left(\delta\rho + 2\bar{\rho}\Phi\right) \tag{4.133}$$

an equation mixing scalars and vectors ($\mu = 0$, $\nu = i$):

$$\partial_i \left[2\Psi' + 2\mathcal{H}\Phi\right] + \frac{1}{2}\Delta\bar{E}_i' = -8\pi G a^2 \left(\bar{\rho} + \bar{p}\right)\left[\partial_i V + \bar{V}_i\right] \tag{4.134}$$

and an equation mixing tensors, vectors and scalars ($\mu = i$, $\nu = j$):

$$\begin{aligned}
&\bar{E}''_{ij} - \Delta\bar{E}_{ij} + 2\mathcal{H}\bar{E}'_{ij} - 2\left[2\mathcal{H}' + \mathcal{H}^2\right]\bar{E}_{ij} + \partial_{(i}\left[\bar{E}''_{|j)} + 2\mathcal{H}\bar{E}'_{|j)} - 2\left(2\mathcal{H}' + \mathcal{H}^2\right)\bar{E}_{|j)}\right] \\
&+ \partial_{(i}\partial_{j)}\left[\Psi - \Phi\right] + \left[2\Psi'' + 4\mathcal{H}\Psi' + \Delta\left(\Phi - \Psi\right) + 2\left(2\mathcal{H}' + \mathcal{H}^2\right)\left(\Phi + \Psi\right) + 2\mathcal{H}\Phi'\right]\delta_{ij} \\
&= 8\pi G a^2\Big[\left(\delta p - 2\bar{p}\Psi\right)\delta_{ij} + \bar{p}\pi_{ij} + \bar{p}h_{ij}\Big] \,. \qquad (4.135)
\end{aligned}$$

The energy-momentum conservation reads:

$$\nabla_\mu T^\mu{}_\nu = 0 \;\Rightarrow\; \partial_\mu T^\mu{}_\nu + \Gamma^\mu{}_{\mu\rho}T^\rho{}_\nu - \Gamma^\rho{}_{\mu\nu}T^\mu{}_\rho = 0 \,, \qquad (4.136)$$

which, expanded at first order, gives:

$$\partial_\mu \delta T^\mu{}_\nu + \bar{\Gamma}^\mu{}_{\mu\rho}\delta T^\rho{}_\nu + \delta\Gamma^\mu{}_{\mu\rho}\bar{T}^\rho{}_\nu - \bar{\Gamma}^\rho{}_{\mu\nu}\delta T^\mu{}_\rho - \delta\Gamma^\rho{}_{\mu\nu}\bar{T}^\mu{}_\rho = 0 \,. \qquad (4.137)$$

All calculation done, this leads to ($\nu = 0$):

$$\delta\rho' + 3\mathcal{H}\left(\delta\rho + \delta p\right) = \left(\bar{\rho} + \bar{p}\right)\left(3\Psi' - \Delta V\right) \,, \qquad (4.138)$$

and ($\nu = i$):

$$\partial_\eta\left[(\bar{\rho} + \bar{p})v_i\right] + 4\mathcal{H}\left(\bar{\rho} + \bar{p}\right)v_i + \partial_i\left[\delta p + \frac{2}{3}\bar{p}\Delta\bar{\pi} + \bar{\rho}\Phi + \bar{p}\Psi\right] + \Delta\bar{\pi}_i = 0 \,. \qquad (4.139)$$

Isolating scalars, vectors and tensors

As mentioned previously, the scalar-vector-tensor decomposition is convenient because at linear order, their evolutions decouple. If one does not want to invoke subtle and complicated notions of differential geometry, this is most easily seen when performing a Fourier transform of the linear equations and the quantities that appear in there. Let us look a generic 3-vector with components U^i. This could be δG_{0i} or δT_{0i}, for example. Then, let us write it:

$$U^i = \partial^i U + \bar{U}^i \qquad (4.140)$$

with $\partial_i\bar{U}^i = 0$. We can write:

$$U\left(\eta, \vec{x}\right) = \int \hat{U}\left(\eta, \vec{k}\right)\mathrm{e}^{\mathrm{i}\vec{k}\cdot\vec{x}}\frac{\mathrm{d}^3k}{(2\pi)^3} \,, \qquad (4.141)$$

and:

$$\bar{U}^i\left(\eta,\vec{x}\right)=\int\hat{\bar{U}}^i\left(\eta,\vec{k}\right)\mathrm{e}^{\mathrm{i}\vec{k}\cdot\vec{x}}\frac{\mathrm{d}^3k}{(2\pi)^3}\,, \tag{4.142}$$

with hats denoting Fourier transforms. Thus:

$$\widehat{\partial^i U}\left(\eta,\vec{k}\right)=\mathrm{i}k^i\hat{U}\left(\eta,\vec{k}\right)\,, \tag{4.143}$$

and

$$k_i\hat{\bar{U}}^i\left(\eta,\vec{k}\right)=0\,. \tag{4.144}$$

Therefore, the vector $\hat{\bar{U}}^i\left(\eta,\vec{k}\right)$ is orthogonal to the wave vector $\vec{k}$. It lives in the two dimensional space orthogonal to the wave vector. We can thus define the projection operator:

$$P_{ij}=\delta_{ij}-\frac{k_ik_j}{\|\vec{k}\|^2}\,, \tag{4.145}$$

which obeys:

$$P^i{}_kP^k{}_j=P^i{}_j\quad\text{and}\quad P^i{}_jk_i=0\,. \tag{4.146}$$

Since:

$$\hat{U}_i=\mathrm{i}k_i\hat{U}+\hat{\bar{U}}_i\,, \tag{4.147}$$

we get:

$$\hat{\bar{U}}_i=P^j{}_i\hat{U}_j\,. \tag{4.148}$$

Taking the inverse Fourier transform, we then isolate the transverse part of U^i this way. For tensor modes, the projection operator is a bit more complicated and it reads:

$$\mathcal{P}_{ij}{}^{kl}=P_i{}^kP_j{}^l-\frac{1}{2}P_{ij}P^{kl}\,. \tag{4.149}$$

We can now apply these projection operators to Eqs (4.133)-(4.135) and (4.138)-(4.139) to separate the various modes and obtain our final equations.

Tensors

Only Eq. (4.135) contains any tensor modes. Applying $\mathcal{P}_{ij}{}^{kl}$ to it, we obtain:

$$\bar{E}_{ij}''-\Delta\bar{E}_{ij}+2\mathcal{H}\bar{E}_{ij}'-2\left[2\mathcal{H}'+\mathcal{H}^2\right]\bar{E}_{ij}=8\pi Ga^2\bar{p}\bar{\pi}_{ij}+16\pi G\bar{p}a^2\bar{E}_{ij}\,. \tag{4.150}$$

Using the background equations (4.129)-(4.130), we notice that:

$$-2\left[2\mathcal{H}' + \mathcal{H}^2\right] = 16\pi G\bar{p}a^2 \,, \tag{4.151}$$

so that we get:

$$\boxed{\bar{E}''_{ij} - \Delta\bar{E}_{ij} + 2\mathcal{H}\bar{E}'_{ij} = 8\pi G a^2\bar{p}\bar{\pi}_{ij} = 3\mathcal{H}^2 w\bar{\pi}_{ij} \,.} \tag{4.152}$$

In an expanding Universe, this is a simple damped oscillator with a driving term proportional to $\bar{\pi}_{ij}$.

Vectors

Eqs (4.134) and (4.135) both have vector parts. Isolating them, we get, from Eq. (4.135):

$$\partial_{(i}\left[\bar{E}''_{|j)} + 2\mathcal{H}\bar{E}'_{|j)} - 2\left(2\mathcal{H}' + \mathcal{H}^2\right)\bar{E}_{|j)}\right] = 8\pi G a^2\bar{p}\partial_{(i}\left[\bar{\pi}_{|j)} + 2\bar{E}_{|j)}\right] \,. \tag{4.153}$$

Therefore, up to an inessential pure function of time:

$$\bar{E}''_i + 2\mathcal{H}\bar{E}'_i - 2\left(2\mathcal{H}' + \mathcal{H}^2\right)\bar{E}_i = 8\pi G a^2\bar{p}\left[\bar{\pi}_i + 2\bar{E}_i\right] \,, \tag{4.154}$$

so that, once more we can simplify to get:

$$\boxed{\bar{E}''_i + 2\mathcal{H}\bar{E}'_i = 8\pi G a^2\bar{p}\bar{\pi}_i = 3\mathcal{H}^2\bar{\pi}_i \,.} \tag{4.155}$$

From Eq. (4.134):

$$\boxed{\Delta\bar{E}'_i = -16\pi G a^2\left(\bar{\rho} + \bar{p}\right)\bar{V}_i = -6\mathcal{H}^2(1+w)\bar{V}_i \,,} \tag{4.156}$$

where we used the background equation and introduced the equation of state $w = \bar{p}/\bar{\rho}$. The conservation equation (4.139) also has a vector part which reads:

$$\boxed{\partial_\eta\left[(\bar{\rho} + \bar{p})\bar{V}_i\right] + 4\mathcal{H}\left(\bar{\rho} + \bar{p}\right)\bar{V}_i + \bar{p}\Delta\bar{\pi}_i = 0 \,.} \tag{4.157}$$

Scalars

Scalars are a bit more involved as they appear in all the equations. Isolating them, we get, from the $(0,0)$ equation:

$$\Delta\Psi = 4\pi G a^2 \delta\rho + 3\mathcal{H}\left(\Psi' + \mathcal{H}\Phi\right) \ , \tag{4.158}$$

where we used the background equation to replace $8\pi G a^2 \bar{\rho} = 3\mathcal{H}^2$. The $(0,i)$ equation gives:

$$2\Psi' + 2\mathcal{H}\Phi = -8\pi G a^2 \bar{\rho}\left(1+w\right) V \ . \tag{4.159}$$

Finally, the (i,j) equation gives:

$$\begin{aligned}\partial_{(i}\partial_{j)}\left[\Psi - \Phi\right] + \Big[2\Psi'' + 4\mathcal{H}\Psi' + \Delta\left(\Phi - \Psi\right) + 2\left(2\mathcal{H}' + \mathcal{H}^2\right)\left(\Phi + \Psi\right) + 2\mathcal{H}\Phi'\Big]\delta_{ij} \\ = 8\pi G a^2 \Big[\left(\delta p - 2\bar{p}\Psi\right)\delta_{ij} + \bar{p}\partial_{(i}\partial_{j)}\bar{\pi}\Big] \ .\end{aligned} \tag{4.160}$$

This can be separated into two equations by taking the diagonal and off-diagonal elements separately. We get:

$$\begin{cases} \Psi - \Phi = 8\pi G a^2 \bar{p}\bar{\pi} = 3\mathcal{H}^2\bar{\pi} & (4.161) \\ 2\Psi'' + 4\mathcal{H}\Psi' + \Delta\left(\Phi - \Psi\right) + 2\left(2\mathcal{H}' + \mathcal{H}^2\right)\left(\Phi + \Psi\right) + 2\mathcal{H}\Phi' \\ \qquad = 8\pi G a^2\left(\delta p - 2\bar{p}\Psi\right) \ . & (4.162) \end{cases}$$

Most of the time, it is safe to assume that there is no anisotropic stress on large scales, so that Φ and Ψ are equal. A notable exception is when massive neutrinos are present. In general, we have:

$$\Psi = \Phi + 3\mathcal{H}^2\bar{\pi} \ . \tag{4.163}$$

This relation, simplifies a lot the other equations. Eq (4.158) becomes:

$$\Delta\Phi = 4\pi G a^2\delta\rho + 3\mathcal{H}\left(\Phi' + \mathcal{H}\Phi\right) - 3\mathcal{H}^2\left[\Delta\bar{\pi} - 2\mathcal{H}'\bar{\pi} - \mathcal{H}\bar{\pi}'\right] \ . \tag{4.164}$$

Eq. (4.159) leads to:

$$\Phi' + \mathcal{H}\Phi = -4\pi G a^2\bar{\rho}\left(1+w\right)V - 3\mathcal{H}\left(2\mathcal{H}'\bar{\pi} + \mathcal{H}\bar{\pi}'\right) \ . \tag{4.165}$$

This can be plugged back into Eq. (4.164) to get:

$$\Delta\Phi = 4\pi G a^2 \bar{\rho}\Delta - 3\mathcal{H}^2\left[\Delta\bar{\pi} + 4\mathcal{H}'\bar{\pi} + 2\mathcal{H}\bar{\pi}'\right] \tag{4.166}$$

$$= \frac{3}{2}\mathcal{H}^2\Delta - 3\mathcal{H}^2\left[\Delta\bar{\pi} + 4\mathcal{H}'\bar{\pi} + 2\mathcal{H}\bar{\pi}'\right] , \tag{4.167}$$

where we used the comoving density contrast Δ such that:

$$\bar{\rho}\Delta = \delta\rho + \bar{\rho}'V = \delta\rho - 3\mathcal{H}(1+w)\bar{\rho}V . \tag{4.168}$$

Finally, Eq. (4.162) gives:

$$\Psi'' + 3\mathcal{H}\left(1+c_s^2\right)\Psi' + \left[2\mathcal{H}' + \left(1+3c_s^2\right)\mathcal{H}^2\right]\Psi - c_s^2\Delta\Psi = \\ -9c_s^2\mathcal{H}^4\bar{\pi} - \left(\mathcal{H}^2 + 2\mathcal{H}'\right)\left[\frac{1}{2}\Gamma + \left(3\mathcal{H}^2 + 2\mathcal{H}'\right)\bar{\pi} + \mathcal{H}\bar{\pi}' + \frac{1}{3}\Delta\bar{\pi}\right] . \tag{4.169}$$

These have to be supplemented by the energy-momentum conservation equations (4.138) and (4.139):

$$\delta\rho' + 3\mathcal{H}\left(\delta\rho + \delta p\right) = \left(\bar{\rho} + \bar{p}\right)\left[3\Phi' - \Delta V\right] \tag{4.170}$$

$$\partial_\eta\left[\left(\bar{\rho} + \bar{p}\right)V\right] + \delta p = -\left(\bar{\rho} + \bar{p}\right)\left(\Phi + 4\mathcal{H}V\right) - \frac{2}{3}\Delta\bar{\pi} - 3\mathcal{H}^2\bar{p}\bar{\pi} . \tag{4.171}$$

Using the density contrast instead, these last two equations become:

$$\delta' + 3\left(c_s^2 - w\right)\mathcal{H}\delta = (1+w)\left(3\Phi' - \Delta V\right) - 3\left[(1+w)\bar{\pi}' + \mathcal{H}w\Gamma\right] \tag{4.172}$$

$$V' + \left(1 - 3c_s^2\right)\mathcal{H}V = -\Phi - \frac{c_s^2\delta}{1+w} - \frac{w\Gamma}{1+w} - \frac{w}{1+w}\left[\frac{2}{3}\Delta\bar{\pi} + \bar{\pi}\right] . \tag{4.173}$$

In the rest of these notes, we will always assume that the anisotropic stress is negligible, so that the scalar potentials are strictly equal:

$$\Psi = \Phi \quad \text{(No anisotropic stress).} \tag{4.174}$$

We will also usually assume that perturbations are purely adiabatic (with one notable exception in chapter 5, section 5.9). In that case: $\Gamma = 0$ and $\frac{\delta p}{\delta\rho} = \bar{p}'/\bar{\rho}' = c_s^2$ (see chapter 5 for details) and we can simplify our system further. Indeed, Eq. (4.166) simplifies greatly and the gravitational potential and the matter distribution are then related via the (generalised) Poisson equation[3]:

[3] Be careful: the Δ on the LHS is the Laplacian, and the one on the RHS is the comoving density perturbation, defined below! Sorry about this idiotic convention...

Poisson equation for purely adiabatic fluctuations in absence of anisotropic stress

$$\Delta\Phi = 4\pi G\bar{\rho}a^2\Delta\,. \tag{4.175}$$

The velocity potential is also uniquely determined by the potential Φ, since Eq. (4.165) becomes:

Velocity potential for purely adiabatic fluctuations in absence of anisotropic stress

$$V = -\frac{\Phi' + \mathcal{H}\Phi}{4\pi G a^2\bar{\rho}\,(1+w)}\,. \tag{4.176}$$

Finally, using $\mathcal{H}' = -(1+3w)\mathcal{H}^2/2$ and Eq. (4.166) to replace $\delta p = c_s^2\delta\rho$ in Eq. (4.169), we obtain the crucial:

Bardeen equation for purely adiabatic fluctuations in absence of anisotropic stress

$$\Phi'' + 3\left(1+c_s^2\right)\mathcal{H}\Phi' + 3\left(c_s^2 - w\right)\mathcal{H}^2\Phi = c_s^2\Delta\Phi\,. \tag{4.177}$$

We have decoupled the metric perturbation, Φ from the matter perturbations $\delta\rho$ and δp. For adiabatic perturbations, the Bardeen equation only depends on the background dynamics and allows one to determine the geometry of the universe at linear order. Once we have solved this equation for a given expansion history, we obtain a solution $\Phi\,(\eta, \vec{x})$ which then can be plugged in Eqs. (4.175)-(4.176) to obtain the matter perturbations from purely algebraic relations (without having to solve any further differential equations):

$$\delta = \frac{1}{4\pi G a^2\bar{\rho}}\left[\Delta\Phi - 3\mathcal{H}\left(\Phi' + \mathcal{H}\Phi\right)\right] \tag{4.178}$$

$$V = -\frac{1}{4\pi G a^2\bar{\rho}(1+w)}\left[\Phi' + \mathcal{H}\Phi\right]\,. \tag{4.179}$$

4.3.3 Road map to structure formation

These last remarks provide us with a clear (if not easy) road map to understanding structure formation *for adiabatic perturbations*:

1. First, we need to determine the evolution of Φ from the end of inflation, through the radiation, matter and Λ dominated phases, i.e. for a specific expansion history of the universe. This will be done by solving the Bardeen equation and will provide us with a **transfer function**.

2. Next, we need to fix some initial conditions for Φ on which the previously determined evolution will act. We will get that from generic arguments from inflation and we will see that in that context, $\Phi(\eta, \vec{x})$ is truly a random field, so that the standard model of cosmology only gives us access to statistical information on the formation of structure. That will lead us to introduce the notion of a **power spectrum**.

3. Once we know Φ (statistically) for the whole history of the universe, we will be able to determine the density contrast and peculiar velocity fields algebraically. But we will see that these are not observable quantities and that we need to introduce an observable density contrast of Dark Matter Δ_m, that we will link to Φ.

4. That will allow us to determine the power spectrum of this Dark Matter density contrast,

5. From the distribution of Dark Matter, we will reconstruct the distribution of galaxies in the late time universe. That will require the notion of **galaxy bias**.

6. Finally, we will relate the galaxy power spectrum to the observed galaxy power spectrum, that is to its projection on our past lightcone by introducing a **redshift-space distortion**. We will see that this distortion carries a very important piece of information regarding the way structure grow in the Universe and may be used to constrain the nature of Dark Energy.

4.4 Problems

Pb. 4.1 Derive Eqs. (4.28) (4.29).

Pb. 4.2 Consider the Newtonian growth of perturbations in a Universe filled with a perfect, non-relativistic, fluid, so that we can set $c_S^2 \sim 0$. We also set $\Lambda = 0$ and $K = 0$.

- Show that the general solution for the density contrast is given by:

$$\delta(t, \vec{x}) = \epsilon_+(\vec{x})\, t^{2/3} + \epsilon_-(\vec{x})\, t^{-1},$$

where $\epsilon_+(\vec{x})$ and $\epsilon_-(\vec{x})$ are arbitrary functions of space. Comment.

- In presence of Λ, or curvature, the equation usually needs to be solved numerically, but, by linearity, it obviously leads to solutions that are linear combinations of terms like:

$$\delta\left(t,\vec{x}\right) = D(t)\epsilon\left(\vec{x}\right).$$

Using Eq. (4.31) linearised at first order, show that the divergence of the velocity field is:

$$\theta\left(t,\vec{x}\right) \equiv \frac{1}{aH}\vec{\nabla}\cdot\vec{u} = -f(a)\delta\,, \tag{4.180}$$

where we have defined the growth function:

$$f(a) \equiv \frac{d\ln D}{d\ln a}.$$

What is $f(a)$ for the solutions found above in the pure matter case?

- We now look for a velocity potential α such that:

$$\vec{u} = \vec{\nabla}\alpha.$$

Show that a solution is:

$$\alpha = -\frac{2f(a)}{3aH}\Phi\,,$$

so that the velocity field can be written:

$$\vec{u} = -\frac{2f(a)}{3aH}\vec{\nabla}\Phi.$$

- Determine the velocity field for the solutions found above in the pure matter case and comment.

Pb. 4.3 Obtain Eqs (4.70)-(4.72) and deduce the transformation of metric potentials under a gauge transformation, Eqs. (4.73)-(4.79).

Pb. 4.4 Show that the Bardeen potentials (4.80)-(4.82) are gauge invariant.

Pb. 4.5 Obtain the transformation rules (4.106)-(4.109) of the matter quantities and show that the comoving density contrast Δ defined in Eq. (4.111) is gauge invariant.

Pb. 4.6 Show that the entropy perturbation defined in Eq. (4.113) is gauge invariant.

Pb. 4.7 Derive, *for scalars only and in the longitudinal gauge*, the results of appendix B, i.e. connection coefficients, Ricci tensor, Ricci scalar and Einstein tensor *up to first order in perturbations*.

Pb. 4.8 Starting from it definition, derive the energy momentum tensor at first order in perturbation, to obtain both its fully covariant components, $T_{\mu\nu}$ and its mixed ones, $T^{\mu}{}_{\nu}$.

5 Structure formation

Contents

This chapter will use the relativistic perturbative framework developed in Chapter 4 to explain how small initial fluctuations in the gravitational potential set at the beginning of the radiation dominated era by a process called inflation have grown via gravitational instability to give rise to large-scale structure we observe in the Universe today. There is more to structure formation than the linear perturbation theory presented in those notes. In particular, in the late time Universe, small scales below $\sim$ 10 Mpc, structures have entered the non-linear regime. Galaxy formation requires to deal with these non-linearity as well as complicated baryonic physics. We will not deal with this here. We rather focus on the formation of large scale, cosmological structure such as large voids and overdensities, which make the stage for the formation of smaller, non-linear objects.

5.1 Fourier decomposition

The Bardeen equation (4.177) is linear in the gravitational potential Φ by construction. As a result, decomposing $\Phi\left(t,\vec{x}\right)$ in Fourier modes will greatly simplify the resolution of the equation.[1] Let us recall that physical coordinates $\vec{x}_{\rm phys}$ and comoving coordinates $\vec{x}$ are related by the scale factor:

$$\vec{x}_{\rm phys} = a(\eta)\vec{x}\ . \tag{5.1}$$

We will decompose fields using the Fourier transform in terms of comoving coordinates; the comoving Fourier modes $\vec{k}$ are associated to the comoving coordinates $\vec{x}$ such that:

$$\Phi\left(\eta,\vec{x}\right) = \int \frac{\mathrm{d}^3\vec{k}}{(2\pi)^3}\hat{\Phi}\left(\eta,\vec{k}\right)\mathrm{e}^{\mathrm{i}\vec{k}\cdot\vec{x}}\ , \tag{5.2}$$

where $\hat{\Phi}\left(\eta,\vec{k}\right)$ is the Fourier transform of $\Phi\left(\eta,\vec{x}\right)$. Since comoving coordinates have dimensions of length, $[x] = L$, and since the metric potential Φ has no dimension, $[\Phi] = 1$, we see that the comoving wavenumber $k = \left\|\vec{k}\right\|$ has dimension $[k] = L^{-1}$ and that $\left[\hat{\Phi}\right] = L^3$. We can also define the physical wavelength, λ_{phys} and its comoving counterpart λ:

$$\lambda_{\rm phys} = a(\eta)\lambda = \frac{2\pi a(\eta)}{k}\ . \tag{5.3}$$

[1] Strictly speaking, the Fourier decomposition will only work for the curvature $K \leq 0$. For a positively curved Universe, the eigenfunctions of the Laplacian that must be used are generalisation of the spherical harmonics to S^3. For negatively curved spaces, a similar decomposition is also at hand. In every case, the decomposition is determined by the spectrum of the Laplace operator on the given space.

The inverse Fourier transform reads:

$$\hat{\Phi}\left(\eta, \vec{k}\right) = \int \mathrm{d}^3\vec{x}\Phi\left(\eta, \vec{x}\right) \mathrm{e}^{-\mathrm{i}\vec{k}\cdot\vec{x}} \ . \tag{5.4}$$

Properties of the Fourier transform

- Using these definitions, show that:

$$\int \mathrm{d}^3\vec{k}\mathrm{e}^{\mathrm{i}\vec{k}\cdot\left(\vec{x}-\vec{x}'\right)} = (2\pi)^3\delta_D\left(\vec{x}-\vec{x}'\right) \ , \tag{5.5}$$

  where $\delta_D\left(\vec{x}\right)$ is the Dirac delta distribution in three dimensions.

- Show that partial differential equations for Φ can be converted into ordinary differential equations for $\hat{\Phi}$ by replacing spatial gradients and Laplacian as follows:

$$\vec{\nabla}\Phi \ \mapsto \ \mathrm{i}\vec{k}\hat{\Phi} \tag{5.6}$$

$$\Delta\Phi \ \mapsto \ -k^2\hat{\Phi} \ . \tag{5.7}$$

Looking at the Bardeen equation, we see that we only have one lengthscale, the **comoving Hubble scale** $\mathcal{H}^{-1}$, associated to the comoving Hubble mode: $k_H = \mathcal{H}$; thus we expect the dynamics of a given scale k^{-1} to be governed by the relative size between that scale and the Hubble scale:

- *Sub-Hubble modes (scales):* $\lambda_{\mathrm{phys}} < H^{-1} \Leftrightarrow k > k_H = \mathcal{H}$;
- *Super-Hubble modes (scales):* $\lambda_{\mathrm{phys}} > H^{-1} \Leftrightarrow k < k_H = \mathcal{H}$.

As it turns out, the presence in the Universe of two types of fluids, relativistic and non-relativistic, gives rise to another critical scale, the *matter-radiation equality scale*: $k_{\mathrm{eq}} = \mathcal{H}_{\mathrm{eq}} \simeq 0.01\ \mathrm{Mpc}^{-1}$. Let us also mention that it is clear that the evolution of the modes $\hat{\Phi}$ only depends on the wave-vector $\vec{k}$ via its length k, as it should be from the assumption of isotropy.

5.2 The matter model

Once the geometry has been set, we need to describe the matter-energy content in the perturbed spacetime.

5.2.1 Matter content

For a perfect fluid in an arbitrary spacetime, we have the energy momentum tensor:

$$T_{\mu\nu} = (\rho + p)\, u_\mu u_\nu + p g_{\mu\nu}$$

where ρ and p are the energy density and pressure respectively, and:

$$u^\mu = \frac{1}{a}\left((1-\Phi)\delta^\mu_0 + v^i \delta^\mu_i\right) \tag{5.8}$$

are the components of the 4-velocity of the fluid. In the standard cosmological model that we are interested in, the matter-energy content receives 3 different contributions:

1. A relativistic fluid (photons; also neutrinos in the early Universe, but we neglect those here), characterised by a energy density ρ_r, a pressure p_r, such that $\bar{p}_r = w_r \bar{\rho}_r = \bar{\rho}_r/3$ and a 4-velocity:
$$u^\mu_{(r)} = \frac{1}{a}\left((1-\Phi)\delta^\mu_0 + v^i_{(r)} \delta^\mu_i\right) \tag{5.9}$$

2. a non relativistic fluid (dark matter and normal matter), with energy-density ρ_m, pressure $p_m \simeq 0$ and 4-velocity:
$$u^\mu_{(m)} = \frac{1}{a}\left((1-\Phi)\delta^\mu_0 + v^i_{(m)} \delta^\mu_i\right) \tag{5.10}$$

3. a cosmological constant Λ which can be identified with a homogeneous fluid with $\rho_\Lambda = -p_\Lambda = \Lambda/(8\pi G)$ and a 4-velocity equal to that of fundamental observers: $u^\mu_{(\Lambda)} = \delta^\mu_0/a(\eta)$.

For each of these fluids, we have a separate perfect fluid energy-momentum tensor:

$$T^{(i)}{}_{\mu\nu} = (\rho_i + p_i)\, u_{(i)\mu} u_{(i)\nu} + p_i g_{\mu\nu} \text{ for } i = r, m, \Lambda\,, \tag{5.11}$$

each satisfying the energy-momentum conservation equation:

$$\nabla_\mu T^{(i)\,\mu}{}_\nu = 0\,, \tag{5.12}$$

since we will assume that the fluid do not interact in any other way than gravitationally.

In what follows we define the:

Total matter-energy content

$$T_{\mu\nu} = (\rho + p)\, u_\mu u_\nu + p g_{\mu\nu} = \sum_i T^{(i)}_{\mu\nu} . \tag{5.13}$$

with:

$$\begin{cases} \rho = \rho_m + \rho_r + \rho_\Lambda = \underbrace{\bar\rho_m + \bar\rho_r + \bar\rho_\Lambda}_{=\bar\rho} + \underbrace{\delta\rho_m + \delta\rho_p}_{=\delta\rho} & (5.14) \\ p = p_r + p_\Lambda = \underbrace{\bar p_r + \bar p_\Lambda}_{=\bar p} + \underbrace{\delta p_r}_{=\delta p} & (5.15) \\ (\bar\rho + \bar p)\, v^i = \bar\rho_m v^i_{(m)} + (\bar\rho_r + \bar p_r)\, v^i_{(r)} & (5.16) \\ \quad = \bar\rho_m v^i_{(m)} + \dfrac{4}{3}\bar\rho_r v^i_{(r)} \ . & (5.17) \end{cases}$$

Strictly speaking, we should include some energy fluxes and anisotropic stresses in these energy-momentum tensors, at least at the level of perturbations and for the total energy momentum tensor. Anisotropic stresses and energy fluxes will be neglected throughout.

From these definitions, we find that the total equation of state is:

$$w = \frac{\bar p}{\bar\rho} = \frac{\bar p_r + \bar p_\lambda}{\bar\rho_m + \bar\rho_r + \bar\rho_\lambda} \tag{5.18}$$

$$= \frac{w_r \bar\rho_r - \bar\rho_\Lambda}{\bar\rho} \tag{5.19}$$

so that:

$$w = \frac{1}{3}\Omega_r - \Omega_\Lambda = \Omega_m + \frac{4}{3}\Omega_r - 1 \ . \tag{5.20}$$

Note that this equation of state depends on $z(\eta)$ with:

$$w(z) = \left[\Omega_{m,0}(1+z)^3 + \frac{4}{3}\Omega_{r,0}(1+z)^4 - 1\right]\left(\frac{H_0}{H(z)}\right)^2 \ . \tag{5.21}$$

The adiabatic sound speed reads:

$$c_s^2 = \frac{\bar p'}{\bar\rho'} = \frac{\bar p'_r}{\bar\rho'_m + \bar\rho'_r} \ . \tag{5.22}$$

Since:

$$\bar{\rho}'_m = -3\mathcal{H}\bar{\rho}_m \tag{5.23}$$

$$\bar{\rho}'_r = -4\mathcal{H}\bar{\rho}_r \ , \tag{5.24}$$

we can write:

$$\bar{\rho}'_m = \frac{3}{4}\frac{\rho_m}{\rho_r}\bar{\rho}'_r \ , \tag{5.25}$$

so that:

$$\boxed{c_s^2 = \frac{4\Omega_r}{9(1+w)} \ ,} \tag{5.26}$$

where we used that:

$$\Omega_m + \frac{4}{3}\Omega_r = 1 + \frac{1}{3}\Omega_r - \underbrace{[1 - \Omega_m - \Omega_r]}_{\Omega_\Lambda} = 1 + w \ , \tag{5.27}$$

and that for radiation:

$$c_{s,r}^2 = \frac{\bar{p}'_r}{\bar{\rho}'_r} = \frac{1}{3} \ . \tag{5.28}$$

This total equation of state and adiabatic sound speed are represented for our nominal cosmology on Fig 5.1, where we clearly see the three phases in the Universe expansion. The total density contrast and peculiar velocity simply read:

$$\boxed{\begin{cases} \delta = \Omega_m\delta_m + \Omega_r\delta_r & (5.29) \\ (1+w)v^i = \Omega_m v^i_{(m)} + \frac{4}{3}\Omega_r v^i_{(r)} \ , & (5.30) \end{cases}}$$

where we introduced the density contrasts for each species:

$$\delta_m = \frac{\delta\rho_m}{\bar{\rho}_m} \quad \text{and} \quad \delta_r = \frac{\delta\rho_r}{\bar{\rho}_r} \ . \tag{5.31}$$

Finally, the total entropy perturbation is obtained by writing δp in two ways. On the one hand:

$$\delta p = \delta p_r \tag{5.32}$$

$$= c_{s,r}^2\delta\rho_r + \bar{p}_r\Gamma_r \tag{5.33}$$

$$= \frac{1}{3}\delta\rho_r + \frac{1}{3}\bar{\rho}_r\Gamma_r \ . \tag{5.34}$$

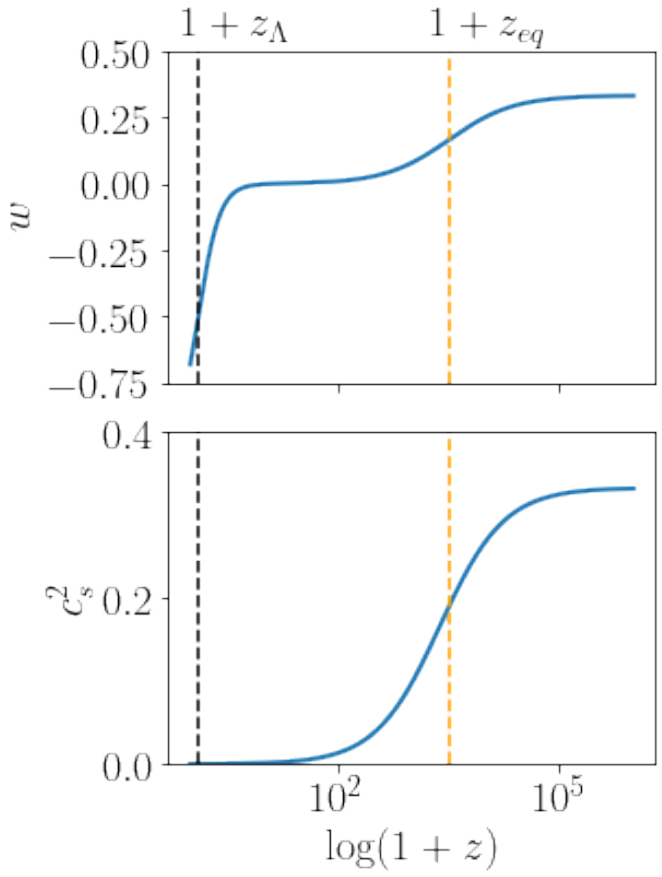

Figure 5.1: Total equation of state (upper panel) and adiabatic sound speed (lower panel) for our nominal cosmology. The orange vertical dashed line represent matter-radiation equality and the black one the transition from matter domination to Λ domination.

On the other hand:

$$\delta p = c_s^2 \left[\delta\rho_m + \delta\rho_r\right] + \bar{p}\Gamma \tag{5.35}$$

$$= \left(c_s^2 - c_{s,r}^2\right)\delta\rho_r + c_s^2\delta\rho_m + w\bar{\rho}\Gamma + c_{s,r}^2\delta\rho_r \tag{5.36}$$

$$= \left(c_s^2 - \frac{1}{3}\right)\delta\rho_r + c_s^2\delta\rho_m + w\bar{\rho}\Gamma + \frac{1}{3}\delta\rho_r \ . \tag{5.37}$$

Hence:

$$w\bar{\rho}\Gamma = \frac{1}{3}\bar{\rho}_r\Gamma_r + \left(\frac{1}{3} - c_s^2\right)\delta\rho_r - c_s^2\delta\rho_m \ . \tag{5.38}$$

Therefore:

$$w\Gamma = \frac{1}{3}\Omega_r\Gamma_r + \left(\frac{1}{3} - c_s^2\right)\Omega_r\delta_r - c_s^2\Omega_m\delta_m \ . \tag{5.39}$$

We see that, even if radiation perturbations are purely adiabatic ($\Gamma_r = 0$), the total entropy perturbation is non zero because the second term in Eq. (5.39) does not vanish *a priori*.

5.2.2 Adiabatic and isocurvature modes

To describe the evolution of the coupled system of relativistic and non-relativistic fluids, it is convenient to introduce the new quantities:

$$S_{mr} = \delta_m - \frac{3}{4}\delta_r = -S_{rm} = \frac{9(1+w)}{4\Omega_m\Omega_r}w\Gamma \ \text{ and } V_{mr} = V_m - V_r = -V_{rm} \ , \tag{5.40}$$

where V_m and V_r are the scalar velocity potentials for matter and radiation respectively, such that $v^i_{(m)} = \partial^i V_m$ and $v^i_{(r)} = \partial^i V_r$ if we focus on scalar modes only. Then, since we only consider fluids that interact purely via gravitation, we can write a conservation equation for each fluid individually:

$$\nabla_\mu T^\mu{}_{(i)\nu} = 0 \ \text{ for } i = m,\ r \ . \tag{5.41}$$

This results in equations like Eqs. (4.172)-(4.173) for each fluid, namely:

- for matter:

$$\begin{cases} \delta_m' = 3\Phi' - \Delta V_m & (5.42) \\ V_m' + \mathcal{H}V_m = -\Phi \ ; & (5.43) \end{cases}$$

- for radiation:

$$\begin{cases} \delta_r' = \dfrac{4}{3}\left(3\Phi' - \Delta V_r\right) & (5.44) \\ V_r' = -\Phi - \dfrac{1}{4}\delta_r \ , & (5.45) \end{cases}$$

  where we assumed $\Gamma_r = 0$ and no anisotropic stress.

Combining these equations, we obtain:

$$\begin{cases} S_{mr}' = -\Delta V_{mr} & (5.46) \\ V_{mr}' = -\mathcal{H} V_{mr} + \dfrac{1}{3(1+w)}\Delta - \dfrac{1}{3(1+w)}\Omega_m S_{mr} \ . & (5.47) \end{cases}$$

To obtain the complete evolution of the system we should thus solve Eqs. (5.46)-(5.47) at the same time as the Bardeen equation (4.162) with $\Psi = \Phi$ and an entropy perturbation given by Eq. (5.39) with $\Gamma_r = 0$. This will be done numerically in section 5.9. For now, we will use this approach to distinguish between two classes of initial conditions at the beginning of the radiation dominated era. Remember that the curvature of 3-space is given by Eq. (4.119). We can thus define the *comoving curvature perturbation* ζ such that the spatial curvature in the comoving gauge is given by ${}^{(3)}\delta R = 4\Delta\zeta/a^2$, requiring that ζ is gauge-invariant and corresponds to Ψ in the comoving gauge. We get:

$$\zeta = \Psi - \mathcal{H}\left(B + V\right) \ . \tag{5.48}$$

In the longitudinal gauge:

Comoving curvature perturbation in longitudinal gauge

$$\zeta = \Psi - \mathcal{H} V \ . \tag{5.49}$$

The reason why we use this quantity is because it is quite natural in the framework of inflation; see chapter 8. Using Eq. (4.165) and the fact that in absence of anisotropic stress, $\Psi = \Phi$, we get:

$$\zeta = \Phi + \frac{2}{3\mathcal{H}}\frac{\Phi' + \mathcal{H}\Phi}{1+w} \ . \tag{5.50}$$

Thus, using the Bardeen equation (4.162):

$$\zeta' = \frac{2\mathcal{H}}{3(1+w)}\left[\frac{3}{2}w\Gamma - \frac{c_s^2}{\mathcal{H}^2}\Delta\Phi\right] \ . \tag{5.51}$$

Using a Fourier transform, a long but straightforward calculation leads to:

$$\hat{\zeta}' = \frac{2\mathcal{H}}{3(1+w)}\left[\frac{3}{2}w\hat{\Gamma} + c_s^2\frac{k^2}{\mathcal{H}^2}\hat{\Phi}\right] . \tag{5.52}$$

The two terms on the RHS allow us to define two types of perturbations.

- *Adiabatic initial conditions*: we choose initially for the entropy perturbation to vanish: $S_{mr} = 0$, which results in:

  Adiabatic initial conditions

  $$\delta_m(\eta_i) = \frac{3}{4}\delta_r(\eta_i) . \tag{5.53}$$

  If the evolution is adiabatic, then on very large scales, for $k \ll \mathcal{H}$, and we have that $\zeta' \sim 0$: the comoving curvature perturbation remains constant on very large scales. We see that if perturbations remain adiabatic during the evolution, then the density contrasts are always close to each other, which means that:

  $$\bar{\rho}\delta\rho = \delta\rho = \bar{\rho}_m\delta_m + \bar{\rho}_r\delta_r \sim \begin{cases} \bar{\rho}_r\delta_r & \text{during radiation domination} \\ \bar{\rho}_m\delta_m & \text{during matter domination.} \end{cases} \tag{5.54}$$

  In other words, we can always approximate the total density contrast:

  $$\delta \sim \begin{cases} \delta_r & \text{deep in radiation domination} \\ \delta_m & \text{deep in matter domination.} \end{cases} \tag{5.55}$$

- *Isocurvature initial conditions*. Here, we suppose that the initial density contrasts are set so as to cancel the gravitational potential: $\Phi = 0$ on the RHS of Eq. (5.52). Then, we see that the comoving curvature perturbation evolves on any scale, large or small, because of the presence of entropy perturbations. $\Phi = 0$ implies that $\Delta = 0$. We then have:

Isocurvature initial conditions

$$\Omega_m(\eta_i)\left[\delta_m(\eta_i) - 3\mathcal{H}(\eta_i) V_m(\eta_i)\right] = -\Omega_r(\eta_i)\left[\delta_r(\eta_i) - 4\mathcal{H}(\eta_i) V_r(\eta_i)\right] \ . \tag{5.56}$$

Since the equations are linear by construction, any solution can be written as a linear combination of adiabatic and isocurvature initial conditions. As we will see in chapter 8, inflation predicts that initial conditions ought to be adiabatic so, in what follows, we will assume that they are so and neglect isocurvature initial conditions. Moreover, current observations of our Universe are perfectly compatible with fluctuations that are nearly adiabatic and we can thus assume, as a first approximation, that perturbations *remain adiabatic during the entire evolution of the Universe*. We will study deviation from adiabaticity in the evolution in section 5.9.

5.3 Tensor and Vector modes

Before we start studying the formation of structure in details, let us get rid quickly of tensor and vector modes. It turns out that, in the hot Big-Bang phase, neither of them are sourced, so that they decay naturally and do not contribute significantly to structure formation.

5.3.1 Tensor modes

Tensor modes obey Eq. (4.152) which, in absence of anisotropic stress, reads:

$$\bar{E}_{ij}'' - \Delta\bar{E}_{ij} + 2\mathcal{H}\bar{E}_{ij}' = 0 \ . \tag{5.57}$$

In Fourier space, this becomes (forgetting the hats to ease notations):

$$\bar{E}_{ij}'' + 2\mathcal{H}\bar{E}_{ij}' + k^2\bar{E}_{ij} = 0 \ . \tag{5.58}$$

Using:

$$a(\eta) \propto \eta^\nu = \begin{cases} \eta & \text{in RDE} \\ \eta^2 & \text{in MDE} \end{cases} \ , \tag{5.59}$$

we get:

$$\mathcal{H} = \frac{\nu}{\eta} \ , \tag{5.60}$$

so that, introducing $x = k\eta$:

$$\frac{\mathrm{d}^2\bar{E}_{ij}}{\mathrm{d}x^2} + \frac{2\nu}{x}\frac{\mathrm{d}\bar{E}_{ij}}{\mathrm{d}x} + \bar{E}_{ij} = 0 \,. \tag{5.61}$$

We can put this equation in the form of a Bessel equation by introducing:

$$F_{ij} = x^{\nu-1/2}\bar{E}_{ij} \,, \tag{5.62}$$

so that:

$$\frac{\mathrm{d}^2F_{ij}}{\mathrm{d}x^2} + \frac{1}{x}\frac{\mathrm{d}F_{ij}}{\mathrm{d}x} + \left(1 - \frac{(\nu-1/2)^2}{x^2}\right)F_{ij} = 0 \,, \tag{5.63}$$

whose general solution is:

$$F_{ij} = A_{ij}J_{\nu-1/2}(x) + B_{ij}N_{\nu-1/2}(x) \,, \tag{5.64}$$

for arbitrary integration constants A_{ij} and B_{ij}. $N_{\nu-1/2}$ is a decreasing function of its argument so it is singular at $x = 0$ and becomes negligible as expansion proceeds. It can thus be neglected:

$$\bar{E}_{ij}\left(\eta, \vec{k}\right) = A_{ij}\left(\vec{k}\right)(k\eta)^{1/2-\nu}\,J_{\nu-1/2}(k\eta) \,. \tag{5.65}$$

Introducing the spherical Bessel function:

$$j_\nu(x) = \sqrt{\frac{\pi}{2x}}J_{\nu+1/2}(x) \,, \tag{5.66}$$

we get:

$$\bar{E}_{ij} \propto \begin{cases} j_0(k\eta) & = \frac{\sin(k\eta)}{k\eta} \text{ for radiation domination} \\ \frac{3j_1(k\eta)}{k\eta} & = 3\left(\frac{\sin(k\eta)}{(k\eta)^2} - \frac{\cos(k\eta)}{k\eta}\right) \text{ for matter domination.} \end{cases} \tag{5.67}$$

These are depicted on Fig. 5.2. The tensor modes are frozen at long as $k\eta < 1$, i.e. as long as the mode remains larger than the Hubble radius. They decay afterwards.

5.3.2 Vector modes

The vector modes are even simpler. Eq. (4.155) reads:

$$\bar{E}_i'' + 2\mathcal{H}\bar{E}_i' = 0 \,. \tag{5.68}$$

Clearly:

$$\frac{\bar{E}_i'}{\bar{E}_i} = -2\frac{a'}{a} \,, \tag{5.69}$$

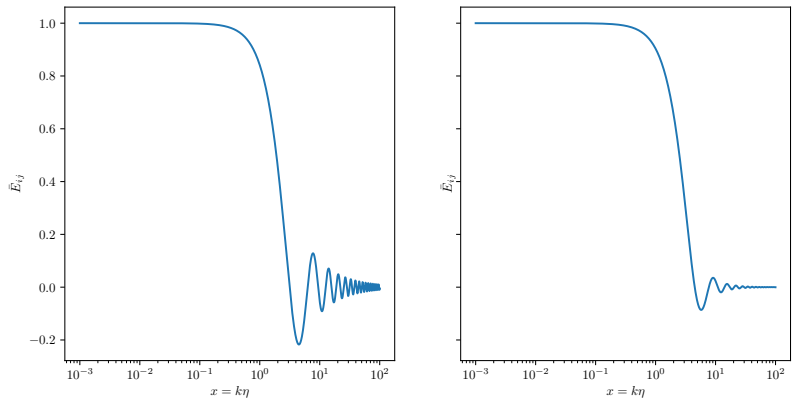

Figure 5.2: Tensor modes in the radiation dominated phase (left panel), and in the matter dominated phase (right panel).

which gives:

$$\bar{E}_i \propto a^{-2} \,, \tag{5.70}$$

so that, in absence of anisotropic stress, vector modes always decay, irrespective of the cosmological phase.

5.4 Evolution of the gravitational potential

We start our exploration of the growth of structure by focussing on the behaviour of the gravitational potential in the radiation and matter dominated eras, neglecting Dark Energy for the moment. According to what we have said, we also assume that the evolution is adiabatic. First, let us convert the Bardeen equation to Fourier space. We get:

$$\hat{\Phi}'' + 3(1 + c_s^2)\mathcal{H}\hat{\Phi}' + \left[3\left(c_s^2 - w\right)\mathcal{H}^2 + c_s^2 k^2\right]\hat{\Phi} = 0. \tag{5.71}$$

We recall that in a Universe containing a mixture of (non-relativistic) matter and radiation, the speed of sound and equation of state are functions of time, and obey:

$$c_s^2 = \frac{4}{3\left(4 + 3\frac{\Omega_{m,0}}{\Omega_{r,0}}a\right)} \tag{5.72}$$

$$w' = 3(1 + w)(w - c_s^2)\mathcal{H} \,. \tag{5.73}$$

The key feature here, due to the linearity of the equation, is that each Fourier mode k evolves independently from any other mode. So, these modes can be studied separately from each other.

5.4.1 Scale separation

Neglecting the cosmological constant (and curvature), we recall that the Friedmann equation reads:

$$\mathcal{H}^2 = \frac{8\pi G}{3}\bar{\rho}a^2 \ . \tag{5.74}$$

Thus, we see that the comoving Hubble scale is (of course) time-dependent and given by:

$$\lambda_H(\eta) = k_H^{-1}(\eta) = \begin{cases} \eta & \text{in the radiation dominated era} \\ \frac{1}{2}\eta & \text{in the matter dominated era.} \end{cases} \tag{5.75}$$

On figure 5.3, we represent comoving scales as functions of time, η. The Hubble scale is represented by the black line, with a change of slope at matter-radiation equality. Comoving scales are represented by horizontal lines (since they are comoving, thus constant by definition). At a given time η, super-Hubble modes are located above the black line representing the Hubble scale, while sub-Hubble modes are located below. Note the following important facts:

- *Early enough* in the history of the Universe ($\eta \to \eta_i$), *all modes are super-Hubble*, because the Hubble scale $\mathcal{H}^{-1}$ decreases and goes to zero as $\eta \to \eta_i \sim 0$.
- *A given mode k will change from being super-Hubble to sub-Hubble* while the Universe expands. If one waits long enough, all modes will become sub-Hubble.
- *Longer wavelengths become sub-Hubble later*.
- Modes on scales *smaller than the matter-radiation equality scale* $k_{\rm eq}^{-1}$ become *sub-Hubble during the radiation dominated era*.
- Modes on scales *larger than the matter-radiation equality scale* $k_{\rm eq}^{-1}$ become *sub-Hubble during the matter dominated era*.

Thus, we see that in order to follow the behaviour of a given mode throughout the expansion history of the Universe, we have four cases to consider separately:

1. Super-Hubble modes in Radiation Dominated Era;

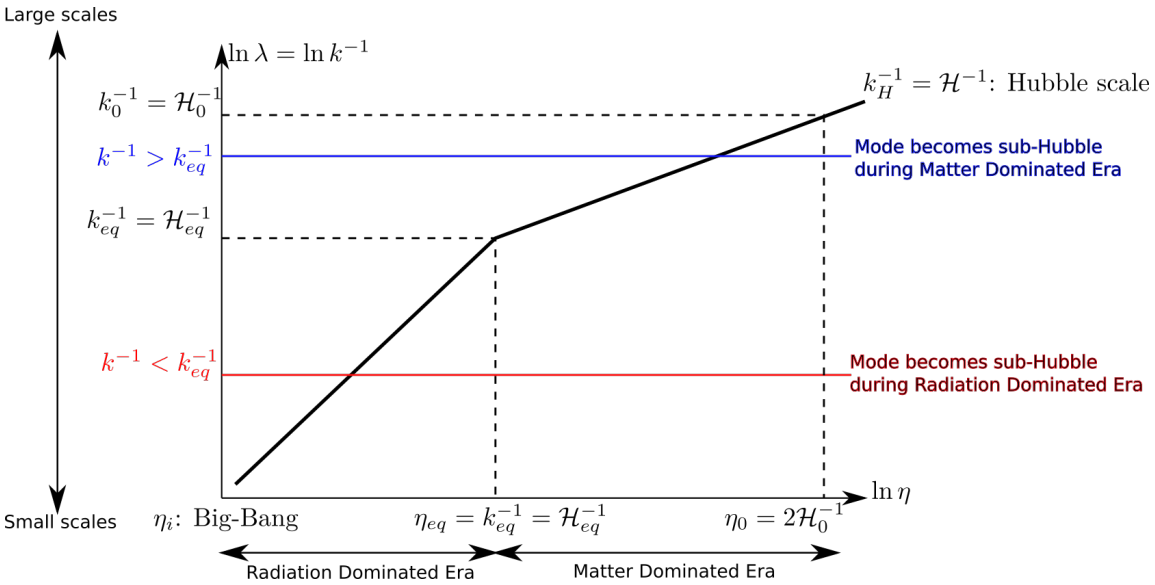

Figure 5.3: Comoving scales in terms of conformal time in a Universe with a mixture of radiation and non-relativistic matter.

2. Super-Hubble modes in Matter Dominated Era;

3. Sub-Hubble modes in Radiation Dominated Era;

4. Sub-Hubble modes in Matter Dominated Era;

5.4.2 Potential deep inside MDE

Let us start with the Matter Dominated Era, which is simpler to analyse. Deep in the Matter Dominated Era, for $\eta \gg \eta_{\rm eq}$, we have that $c_s^2 = w = 0$, thus the Bardeen equation simply reads:

$$\hat{\Phi}'' + 3\mathcal{H}\hat{\Phi}' = 0 \,. \tag{5.76}$$

We notice that this is independent of k, thus we see that during the Matter Dominated Era, all modes will behave in the same way, irrespective of the scale k. If one defines $x = \ln a(\eta)$, noting that $\mathcal{H}' = -\mathcal{H}^2/2$, the Bardeen equation becomes:

$$\frac{d^2\hat{\Phi}}{dx^2} + \frac{5}{2}\frac{d\hat{\Phi}}{dx} = 0 \,, \tag{5.77}$$

which is a simple linear equation whose solution is:

$$\hat{\Phi}\left(\eta, \vec{k}\right) = A\left(\vec{k}\right) + B\left(\vec{k}\right) e^{-5x/2} \,, \tag{5.78}$$

where $A\left(\vec{k}\right)$ and $B\left(\vec{k}\right)$ are arbitrary functions of $\vec{k}$ which must be set by initial conditions at the start of the Matter Dominated Era. In terms of the conformal times, we thus see that $\hat{\Phi}$ decomposes into two modes:

$$\hat{\Phi}\left(\eta, \vec{k}\right) = A\left(\vec{k}\right) + B\left(\vec{k}\right) a^{-5/2}(\eta) \,, \tag{5.79}$$

a constant mode, $A\left(\vec{k}\right)$ and a decaying mode $B\left(\vec{k}\right) a^{-5/2}(\eta)$ which decreases in an expanding Universe. In the following, we will neglect the decaying mode as it does not contribute to the formation of structure (you can try and show that). Thus, we will write the solution of the Bardeen equation in the Matter Dominated Era as:

Potential in the Matter Dominated Era

$$\hat{\Phi}_{\rm mat}\left(\eta, \vec{k}\right) = F\left(\vec{k}\right) = \text{cst for all } \vec{k} \,. \tag{5.80}$$

Thus, the gravitational potential does not change during the Matter Dominated Era.

5.4.3 Potential deep inside RDE

Deep inside the Radiation Dominated Era ($\eta \ll \eta_{eq}$), we have, on the other hand, $c_s^2 = w = 1/3$, so that the Bardeen equation becomes:

$$\hat{\Phi}'' + \frac{4}{\eta}\hat{\Phi}' + \frac{1}{3}k^2\hat{\Phi} = 0 \,, \tag{5.81}$$

which now depends on the wavenumber k. In order to solve this equation, we need to introduce a new adimensional "time" variable which "absorbs" the wavenumber:

$$x = \frac{1}{\sqrt{3}} k\eta = \frac{1}{\sqrt{3}} \frac{k}{k_H} \,,$$

since $k_H = \mathcal{H} = \eta^{-1}$. Hence, $x < 1/\sqrt{3}$ as long as the mode k is super-Hubble and $x > 1/\sqrt{3}$ when the mode k becomes sub-Hubble.

Then, by letting $\varphi = \eta\hat{\Phi}$, we get that:

$$\frac{d^2\varphi}{dx^2} + \frac{2}{x}\frac{d\varphi}{dx} + \left(1 - \frac{2}{x^2}\right)\varphi = 0 \,. \tag{5.82}$$

This is just the spherical Bessel equation:

$$\frac{d^2 f}{dx^2} + \frac{2}{x}\frac{df}{dx} + \left(1 - \frac{l(l+1)}{x^2}\right) f = 0 \,, \tag{5.83}$$

for the case $l = 1$. The general solution is then:

$$\varphi\left(x, \vec{k}\right) = C\left(\vec{k}\right) j_1(x) + D\left(\vec{k}\right) n_1(x) \,, \tag{5.84}$$

where we used the spherical Bessel and Neuman functions:

$$j_1(x) = \frac{\sin x}{x^2} - \frac{\cos x}{x} \tag{5.85}$$

$$n_1(x) = -\frac{\cos x}{x^2} - \frac{\sin x}{x} \,. \tag{5.86}$$

Notice that as $x \longrightarrow 0$, i.e. when one approaches the Big-Bang:

$$j_1(x) = \frac{x}{3} + O\left(x^2\right) \tag{5.87}$$

$$n_1(x) = -\frac{1}{x^2} + O\left(x^2\right) \,, \tag{5.88}$$

so that the Neuman function is divergent at the initial time. Therefore, we discard it from the solution as unphysical and we write the solution in the Radiation Dominated Era, $\hat{\Phi}_{\rm rad} = \varphi/\eta$:

Potential in the Radiation Dominated Era

$$\hat{\Phi}_{\rm rad}\left(\eta, \vec{k}\right) = 3\sqrt{3} G\left(\vec{k}\right) \frac{j_1\left(k\eta/\sqrt{3}\right)}{k\eta} \,, \tag{5.89}$$

for an arbitrary function $G\left(\vec{k}\right)$ which fixes the initial conditions. Indeed, as we saw previously, initially, all modes are super-Hubble, i.e. $k \ll \mathcal{H}$, so that $x \ll 1$ and:

$$\hat{\Phi}\left(\eta_i, \vec{k}\right) = G\left(\vec{k}\right) \,. \tag{5.90}$$

Similarly, because it is essentially the same limit, modes that remain super-Hubble during the entire Radiation Dominated Era , i.e. modes for which $k \ll \mathcal{H}$ for all times $\eta < \eta_{eq}$, we get a constant Bardeen potential:

$$\hat{\Phi}\left(\eta, \vec{k}\right)_{|k \ll \mathcal{H}} = G\left(\vec{k}\right) \text{ for all } \eta < \eta_{\rm eq} \,. \tag{5.91}$$

On the other hand, a mode becomes sub-Hubble, $k > \mathcal{H}$, at a time $\eta = k^{-1}$; it then starts to evolve. In the limit $k \gg \mathcal{H}$, $x \gg 1$ and $j_1(x) \sim -\frac{\cos x}{x^2}$, so that:

$$\hat{\Phi}_{\rm rad}\left(\eta, \vec{k}\right)_{|k>>\mathcal{H}} \sim -9\frac{\cos\left(k\eta/\sqrt{3}\right)}{k^2\eta^2} G\left(\vec{k}\right) \tag{5.92}$$

$$\sim -9\frac{\cos\left(k\eta/\sqrt{3}\right)}{k^2\eta^2} \hat{\Phi}\left(\eta, \vec{k}\right)_{|k\ll\mathcal{H}} . \tag{5.93}$$

Thus, one sees that *the potential* $\hat{\Phi}_{\rm rad}\left(\eta, \vec{k}\right)$ at a scale $k > k_{eq}$ *is suppressed during the Radiation Dominated Era* by a factor $1/k^2$ *with respect to the same potential on large scales*, $k < k_{\rm eq}$, as soon as it enters the Hubble radius. The suppression factor at the end of the Radiation Dominated Era, when $\eta = \eta_{\rm eq} = k_{\rm eq}^{-1}$ is actually simply proportional to $\left(k/k_{\rm eq}\right)^2$: *the shorter the mode, the more time it has spent inside the Hubble radius when matter starts dominating the dynamics of the Universe, and thus, the more the potential on that scale has had time to be damped during the Radiation Dominated Era*. Various modes are represented on figure 5.4 during the Radiation Dominated Era. All curves have been normalised by their initial value, so that the suppression of modes entering the Hubble radius with respect to those remaining super-Hubble is apparent: all curves start at 1; modes which never enter the Hubble radius ($k < k_{\rm eq}$) remain constant; modes which enter the Hubble radius ($k > k_{\rm eq}$) experience some decay with respect to their initial amplitude; this decay is more pronounced the smaller the scale of the mode, as modes with large k (small scale modes) spend more time within the Hubble radius that those with proportionally smaller k (larger scale modes). The overall decay of modes as a function of k is represented on figure 5.5. One clearly sees the $1/k^2$ decay for modes that entered the Hubble radius.

5.4.4 Connecting RDE and MDE

Once we have understood the behaviour of the Bardeen potential in each era, it remains to connect its value accross the radiation-matter transition. The most accurate way of doing that is of course to solve the Bardeen equation numerically for a mixture of radiation and matter. Here, we will try and understand what happens and to recover the main behaviour of the potential at the transition.
The way to proceed is to try and find some quantity that is conserved at the transition. As we have seen, for adiabatic fluctuations, one such quantity is the *comoving curvature perturbation*:

$$\zeta = \Phi - \mathcal{H}V . \tag{5.94}$$

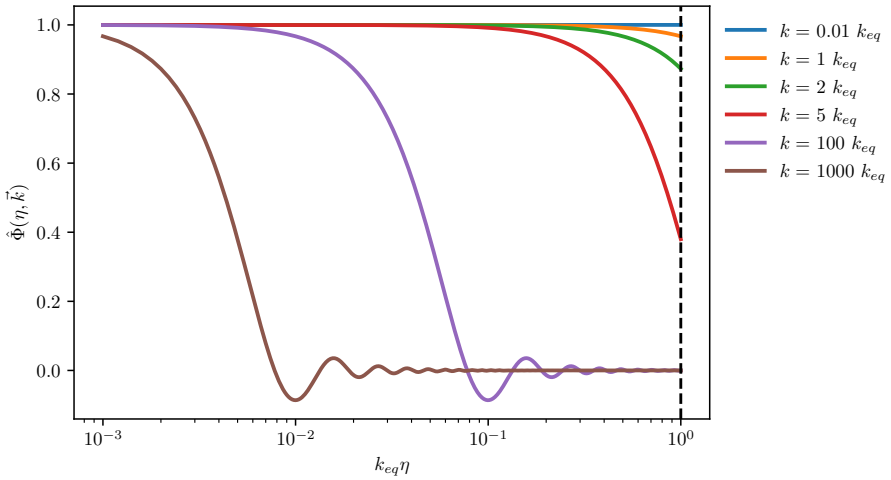

Figure 5.4: Evolution of the Bardeen potential for a fixed Fourier mode k, as a function of η in the adiabatic case.

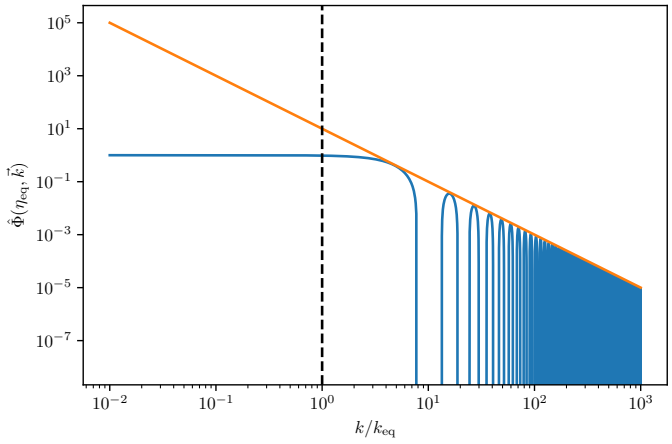

Figure 5.5: Blue curve: Bardeen potential at matter-radiation equality as a function of k/k_{eq}. The orange line has a slope $\left(k/k_{\mathrm{eq}}\right)^{-2}$.

Let us see how this happens. Using the momentum constraint:

$$V = -\frac{\Phi' + \mathcal{H}\Phi}{4\pi G\bar{\rho}a^2(1+w)} \ , \tag{5.95}$$

and the Friedmann equation, this can be rewritten:

$$\zeta = \Phi + \frac{2}{3(1+w)\mathcal{H}}\left(\Phi' + \mathcal{H}\Phi\right) \ . \tag{5.96}$$

Therefore, the variation of the comoving curvature perturbation obeys (show it):

$$\frac{3}{2}(1+w)\mathcal{H}\zeta' = c_s^2\Delta\Phi \ . \tag{5.97}$$

On super-Hubble scales, $|\Delta\Phi| \mapsto k^2\left|\hat{\Phi}\right| \ll \mathcal{H}^2\left|\hat{\Phi}\right|$, thus:

$$\frac{3(1+w)}{2\mathcal{H}}\hat{\zeta}' \ll 1 \ , \tag{5.98}$$

where we have used $\hat{\zeta}$ to represent the Fourier transform of ζ, a convention that we will use from now on for every field, when necessary. Thus, on super-Hubble scales, *the comoving curvature perturbation is constant*:

$$\hat{\zeta}\left(\eta, \vec{k}\right) = f\left(\vec{k}\right) \text{ for } k \ll \mathcal{H} \ . \tag{5.99}$$

In both the Radiation and Matter Dominated eras, on super-Hubble scales, we have that $\Phi' = 0$, and that $w = \text{cst}$, so that:

$$\hat{\zeta} = \frac{5+3w}{3(1+w)}\hat{\Phi} \text{ on super-Hubble scales.} \tag{5.100}$$

Thus, for $k \ll \mathcal{H}$:

$$\hat{\zeta} = \begin{cases} \frac{5}{3}\hat{\Phi}_{\text{mat}}\left(\eta, \vec{k}\right) = \frac{5}{3}F\left(\vec{k}\right) & \text{because } w = 0 \\ \frac{3}{2}\hat{\Phi}_{\text{rad}}\left(\eta, \vec{k}\right) = \frac{3}{2}G\left(\vec{k}\right) & \text{because } w = 1/\ . \end{cases} \tag{5.101}$$

Therefore, one finds that:

$$F\left(\vec{k}\right) = \frac{9}{10}G\left(\vec{k}\right) \text{ for } k \ll \mathcal{H} \ . \tag{5.102}$$

Hence, at matter-radiation equality, the modes that remained super-Hubble decay slightly, by a factor $9/10$. The other modes, those that already entered the Hubble radius during the Radiation dominated era, have already decayed by a factor $(k_{\text{eq}}/k)^2$ and freeze-out at the value of $\hat{\Phi}_{\text{rad}}$ they reach at $\eta = \eta_{\text{eq}}$.

All that remain to be fixed are the initial conditions for each mode, $G\left(\vec{k}\right)$. This is done by noticing

that all the modes of interest started super-Hubble at $\eta = \eta_i \ll \eta_{\rm eq}$. Therefore, we can use the relation (5.100) evaluated at the initial time to set:

$$\hat{\Phi}\left(\eta_i, \vec{k}\right) = G\left(\vec{k}\right) = \frac{2}{3}\zeta(\vec{k}) \text{ for all modes } \vec{k} \ . \tag{5.103}$$

$\zeta\left(\vec{k}\right)$ is the *initial comoving curvature perturbation*, which is the main ingredient generated by the inflationary phase that precedes the Hot Big-Bang expansion (see chapter 8). Putting all of this together, we can write the metric potential at the beginning of the Matter Dominated era as, $\hat{\Phi}_0\left(\vec{k}\right) \sim \hat{\Phi}_{\rm mat}\left(\eta \equiv \eta_{eq}, \vec{k}\right)$:

Potential at the beginning of the Matter Dominated Era

$$\hat{\Phi}_0\left(\vec{k}\right) \sim \begin{cases} \frac{3}{5}\zeta\left(\vec{k}\right) & \text{for } k \ll k_{eq} \\ -6\cos\left(k/k_{eq}\sqrt{3}\right)\left(\frac{k_{eq}}{k}\right)^2 \zeta\left(\vec{k}\right) & \text{for } k \gg k_{eq} \ . \end{cases} \tag{5.104}$$

All these analytic, approximate results can be checked by numerical integration. Solving the Bardeen equation numerically with the appropriate initial conditions, one finds the solutions depicted on figure 5.6, where one can clearly see the drop by a factor of $9/10$ on super-Hubble scales (orange curve), and the decay in $1/k^2$ for modes which enter the Hubble radius before matter-radiation equality.

5.4.5 The late-time Universe: the effect of Λ

So far, we have concentrated our discussion on the early Universe, i.e. on the Radiation and early Matter Dominated eras, neglecting the effect of the cosmological constant. In this section, we work in ΛCDM, i.e., in the late-time Universe, when we can neglect radiation: $\eta \gg \eta_{\rm eq}$. Let us call η_Λ the conformal time at which the cosmological constant and the matter energy densities coincide, which corresponds to a redshift:

$$1 + z_\Lambda\left(\eta_\Lambda\right) = \left(\frac{\Omega_{\Lambda,0}}{\Omega_{m,0}}\right)^{1/3} \sim 1.33. \tag{5.105}$$

In that framework, the Bardeen equation reads:

$$\hat{\Phi}'' + 3\mathcal{H}\hat{\Phi} = 0 \qquad \text{in CDM era} \tag{5.106}$$

$$\hat{\Phi}'' + 3\mathcal{H}\hat{\Phi}' + 3\mathcal{H}^2\hat{\Phi} = 0 \qquad \text{in } \Lambda \text{ era.} \tag{5.107}$$

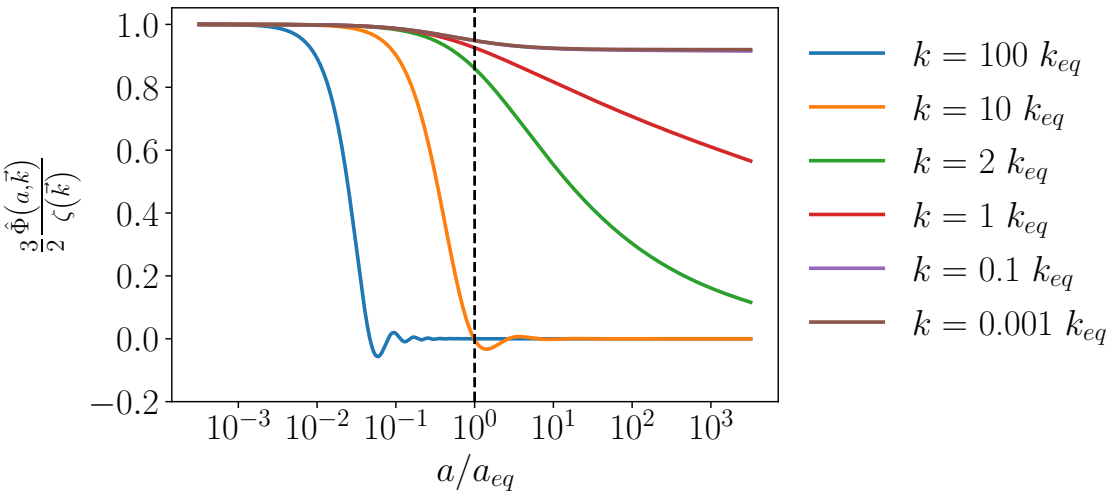

Figure 5.6: Evolution of the Bardeen potential through the radiation-matter transition.

In both phases, there is no dependence in the Fourier mode $\vec{k}$ in the coefficients of the equations. Therefore, $\vec{k}$ can only occur in the initial conditions, and we can seek a solution for $\hat{\Phi}$ using a separation of variables:

$$\hat{\Phi}\left(\eta, \vec{k}\right) = g(\eta)\hat{\Phi}_0\left(\vec{k}\right) , \tag{5.108}$$

where $\hat{\Phi}_0\left(\vec{k}\right)$ is the potential at the beginning of the Matter Dominated era, which is given by Eq. (5.104). We have already seen that, neglecting the decaying mode, the solution to Eq. (5.106) is given by $g(\eta) = 1$. In the Λ Dominated era, on the other hand, we can write:

$$\mathcal{H}^2 = \frac{\Lambda}{3}a^2 \text{ and } \mathcal{H}' = \mathcal{H}^2 . \tag{5.109}$$

Hence, by defining $x = \ln a$, Eq. (5.107) reads:

$$\frac{d^2\hat{\Phi}}{dx^2} + 4\frac{d\hat{\Phi}}{dx} + 3\hat{\Phi} = 0 . \tag{5.110}$$

The solution to this equation is trivial, and going back to the scale factor, we get:

$$\hat{\Phi}_\Lambda\left(\eta, \vec{k}\right) = \frac{A\left(\vec{k}\right)}{a(\eta)} + \frac{B\left(\vec{k}\right)}{a^3(\eta)} \tag{5.111}$$

$$\sim \frac{A\left(\vec{k}\right)}{a(\eta)} , \tag{5.112}$$

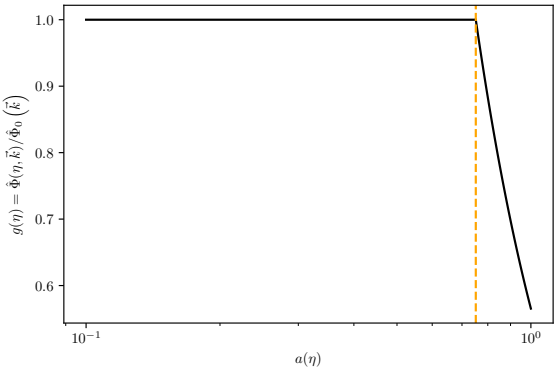

Figure 5.7: Function $g(\eta)$ showing the decay in the gravitational potential on all scales due to the presence of a cosmological constant. The orange vertical dashed line parks the transition between matter domination and Λ domination at $a_\Lambda = 1/(1+z_\lambda) \sim 0.75$.

where the second line was obtained by neglecting the fast decaying term in $1/a^3$ with respect to the term in $1/a$. Thus, we see that in the Λ Dominated era, $g(\eta) \sim 1/a(\eta)$: the cosmological constant leads to a decay in the gravitational potential. The function $g(\eta)$ is depicted in figure 5.7.

A numerical integration of the Bardeen equation for the nominal cosmology, with $\Omega_\Lambda = 0.68$ gives the results presented on Fig. 5.8. The scale invariant decrease is quite clearly shown.

5.5 Initial conditions: Inflation

We now have to determine the initial conditions for our previous analysis, i.e. we need to get an idea of what is the initial comoving curvature perturbation $\zeta\left(\vec{k}\right)$. In modern cosmology, this is calculated in the inflationary paradigm, for which you can find a somewhat detailed introduction in chapter 8. Here, we will simply list a few physical consequences of the model and explain roughly how it determines $\zeta\left(\vec{k}\right)$.

The background dynamics during inflation, described in section 2.4, is governed by a scalar field slowly rolling into its potential, and corresponds to an accelerated expansion with:

$$H(t) \simeq \text{cst}\ ,\ a(t) \sim e^{Ht}\ . \tag{5.113}$$

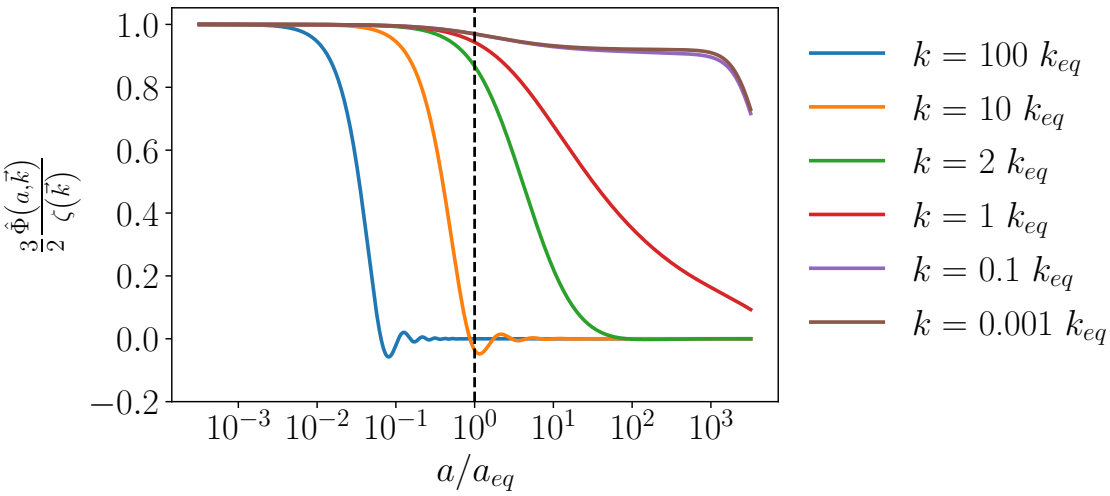

Figure 5.8: Evolution of the Bardeen potential through the radiation-matter transition.

Critically, this leads to a *decreasing comoving Hubble radius*:

$$\mathcal{H}^{-1} = (aH)^{-1} \propto \frac{1}{a} \,. \tag{5.114}$$

Moreover, the scalar field experiences quantum fluctuations on sub-Hubble scales:

$$\hat{\varphi}\left(\eta, \vec{k}\right) = \bar{\varphi}(\eta) + \delta\varphi\left(\eta, \vec{k}\right) \,, \tag{5.115}$$

for $k \gg \mathcal{H}$. These fluctuations are eventually expelled from the Hubble radius and, at this stage, freeze-out to become classical fluctuations which produce the comoving curvature perturbation $\zeta\left(\vec{k}\right)$, in a top-down process during which *larger scales are expelled before smaller scales*. Then, after the end of inflation, these scales re-enter the Hubble radius during the Radiation or the Matter Dominated eras, *the shorter scales entering before the larger scales*, hence the process, seen from the largest scales point of view is "first out last in". This is all summarised on figure 5.9.

A detailed study of the behaviour of quantum fluctuations during inflation shows that, in the simplest models:

$$\left|\hat{\zeta}\left(\vec{k}\right)\right| \propto k^{\frac{n_s-4}{2}} \,, \tag{5.116}$$

where n_s is called the *spectral index*. PLANCK measurements give $n_s \simeq 0.965$ and in what follows we will assume $n_s = 1$ for simplicity (this case is called scale-invariant). A key feature of this model is that, by design, since the curvature perturbations are generated by genuine quantum processes,

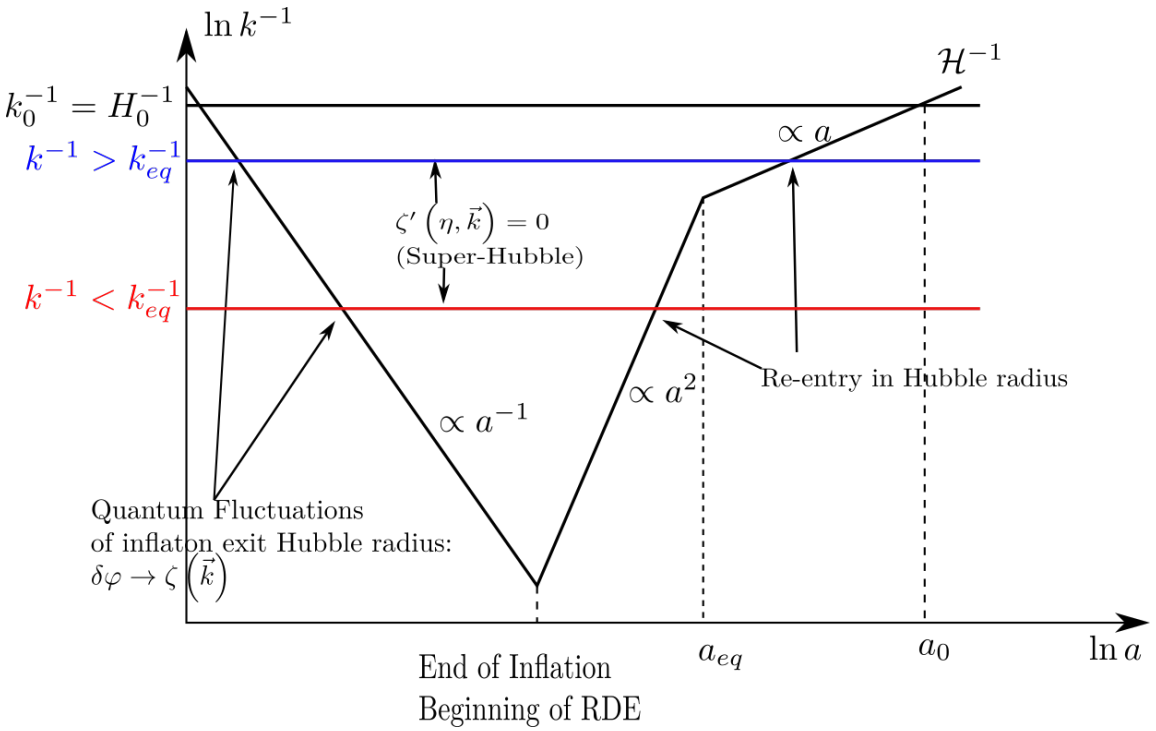

Figure 5.9: Behaviour of comoving scales in an inflationary universe.

inflation cannot predict the exact values of $\hat{\zeta}\left(\vec{k}\right)$ but rather gives some statistical distribution for each mode. As a result, all cosmological observables calculated in the standard model are actually random variables, as we will see further down.
In the simplest model of inflation, $\hat{\zeta}\left(\vec{k}\right)$ is a *Gaussian random field*, i.e. that for each mode $\vec{k}$, $\hat{\zeta}\left(\vec{k}\right)$ is a *Gaussian random variable*. It is normally distributed with mean 0 and covariance:

$$\left\langle \hat{\zeta}\left(\vec{k}\right)\hat{\zeta}\left(\vec{k}'\right)\right\rangle = (2\pi)^3\,\delta_D\left(\vec{k}+\vec{k}'\right)\mathcal{P}_\zeta\left(k\right)\ . \tag{5.117}$$

$\mathcal{P}_\zeta\left(k\right)$ is called the *power spectrum* of curvature perturbations. At fixed k, it is proportional to the variance of $\hat{\zeta}\left(\vec{k}\right)$; see appendix C. Note that modes on different scales are not correlated, as expected for a linear analysis. Inflation predicts:

$$\mathcal{P}_\zeta\left(k\right) \propto \left|\hat{\zeta}\left(\vec{k}\right)\right|^2 = \frac{A_s}{k^3}\left(\frac{k}{k_*}\right)^{n_s-1}\ , \tag{5.118}$$

where A_S is the scalar amplitude and k_* a pivot scale. PLANCK values for these parameters are:

$$A_s = 2.14\times10^{-9} \tag{5.119}$$

$$k_* = 0.05\ \mathrm{Mpc}^{-1}\ . \tag{5.120}$$

For simplicity, from now on, we will use $n_s = 1$, so that:

$$\mathcal{P}_\zeta\left(k\right) = \frac{A_s}{k^3}\ . \tag{5.121}$$

Hence, for scale-dependence, we can adopt:

$$\hat{\zeta}\left(\vec{k}\right) \propto \sqrt{\mathcal{P}_\zeta\left(k\right)} \propto k^{-3/2}\ . \tag{5.122}$$

Finally, inflation predicts that, at horizon exit, $\hat{\zeta}(\vec{k})$ is constant. According to Eq. (5.52), with $k \ll \mathcal{H}$, this means that $\Gamma = 0$: initial conditions set by inflation are *adiabatic*.

5.6 Transfer functions

We now have all the pieces of the puzzle and we can summarise everything we have learnt about the time behaviour of the metric potential Φ by introducing the notion of *transfer function*. This is

a function, $T_\Phi\left(\eta,\vec{k}\right)$, defined for $\eta > \eta_{eq}$ which relates the potential for a given mode $\vec{k}$, at η to the value of the curvature perturbation at $\vec{k}$ produced by inflation:

$$\hat{\Phi}\left(\eta,\vec{k}\right) = T_\Phi\left(\eta,\vec{k}\right)\hat{\zeta}\left(\vec{k}\right) \ . \tag{5.123}$$

Our previous studies have shown that:

$$T_\Phi\left(\eta,\vec{k}\right)\begin{cases} = \frac{3}{5} & \text{for } k \ll k_{eq} \\ \propto k^{-2} & \text{for } k \gg k_{eq} \end{cases} \tag{5.124}$$

Thus, if we define the power spectrum for the potential Φ at time η:

$$\left\langle \hat{\Phi}\left(\eta,\vec{k}\right)\hat{\Phi}\left(\eta,\vec{k}'\right)\right\rangle = (2\pi)^3\,\delta_D\left(\vec{k}+\vec{k}'\right)\mathcal{P}_\Phi\left(\eta,k\right) \ , \tag{5.125}$$

we get the relation:

$$\begin{aligned} \mathcal{P}_\Phi\left(\eta,k\right) &= T_\Phi^2\left(\eta,k\right)\mathcal{P}_\zeta\left(k\right) && (5.126)\\ &\propto T_\Phi^2\left(\eta,k\right)k^{n_s-4} && (5.127)\\ &\propto T_\Phi^2\left(\eta,k\right)k^{-3} \text{ for } n_s = 1 \ . && (5.128) \end{aligned}$$

Thus, the power spectrum of Φ at $\eta > \eta_{eq}$ behaves as:

$$\mathcal{P}_\Phi\left(\eta,k\right) \propto \begin{cases} k^{n_s-4} \simeq k^{-3} & \text{for } k \ll k_{eq} \\ k^{n_s-8} \simeq k^{-7} & \text{for } k \gg k_{eq} \ . \end{cases} \tag{5.129}$$

Note that here, we neglected Λ; its effect is to multiply the transfer function by the mode independent function $g(\eta)$ determined above. Therefore, this does not impact the scale dependence determined here, but only the overall amplitude of the power spectrum. Fig. 5.10 represents the power spectrum of Φ today ($\eta = \eta_0$) for $n_s = 0.965$, $A_s = 2.14 \times 10^{-9}$ and $k_* = 0.05\ \text{Mpc}^{-1}$ (PLANCK values) obtained by a full numerical integration of the system. This power spectrum is:

$$\mathcal{P}_\Phi\left(\eta_0,k\right) = g^2\left(\eta_0\right)T_\Phi^2\left(\eta_0,k\right)\mathcal{P}_\zeta(k)\,, \tag{5.130}$$

with $g\left(\eta_0\right) \simeq 0.75$. The transfer function is represented on Fig. 5.11 The asymptotic behaviour at large and small values of k agrees with the scalings we obtained.

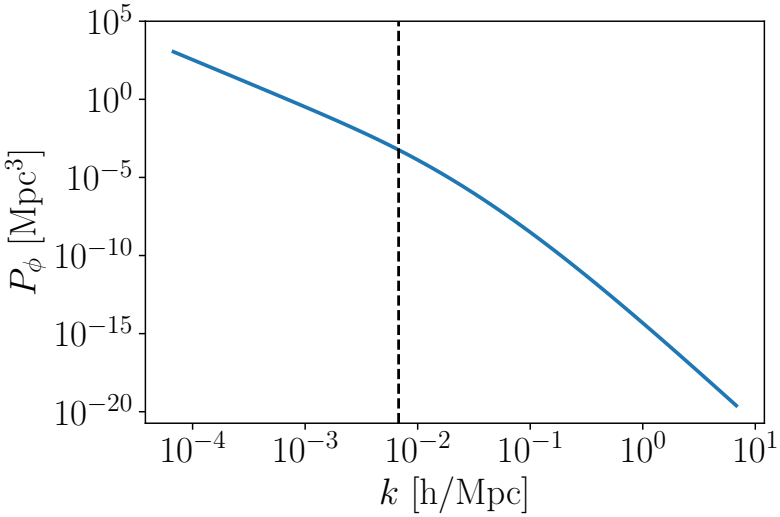

Figure 5.10: Power spectrum of Φ today. The vertical dashed line marks the matter-equality scale.

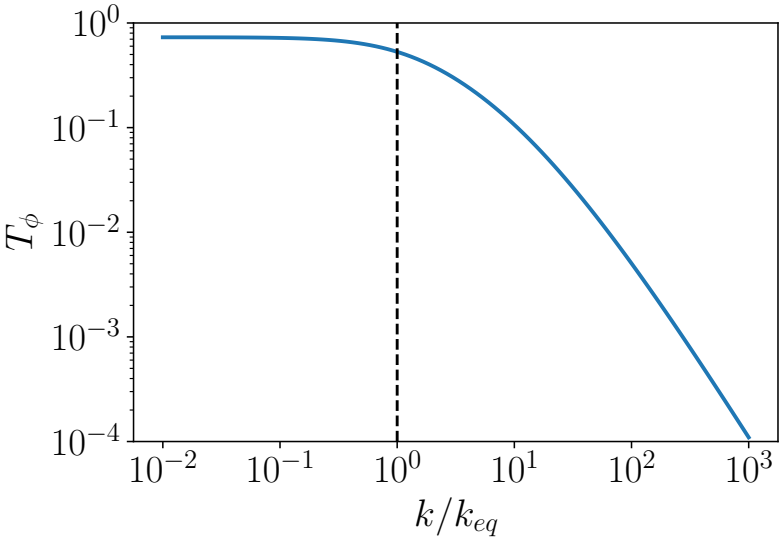

Figure 5.11: Transfer function of Φ today, $T_\Phi^2(\eta_0, k)$. The vertical dashed line marks the matter-equality scale.

5.7 Matter power spectrum in the late-time Universe

As explained in the roadmap at the end of chapter 4, now that we have characterised entirely the behaviour of the potential Φ (entirely, at least in the statistical sense, by the mean of the power spectrum, which is the best we can hope for in an inflationary Universe), we can determine the statistical properties of the matter variables, density contrast and velocity field. In this section, we will focus on the distribution of Dark Matter. Galaxies will be treated in the next chapter.

5.7.1 The comoving density contrast

The density contrast δ in the longitudinal gauge does not have a clear physical meaning. We will thus find it convenient to introduce a density perturbation with a well-defined physical meaning. We will use the density contrast measured by observers comoving with the non-relativistic, matter fluid, called the *comoving density contrast*, which we have already encountered. For the matter fluid, it reads:

$$\Delta_m = \delta_m + \frac{\bar{\rho}_m'}{\bar{\rho}_m} V_m \tag{5.131}$$

$$= \delta_m - 3\mathcal{H} V_m \ . \tag{5.132}$$

Since we are interested in the large-scale distribution of matter in the late-time Universe, when we can observe objects like galaxies, clusters etc., we will neglect the effects of radiation and work in a pure ΛCDM model. We have:

$$\delta = \frac{\delta\rho_m}{\bar{\rho}_m + \bar{\rho}_\Lambda} \tag{5.133}$$

$$\bar{\rho}\delta = \delta\rho_m = \bar{\rho}_m \delta_m \ . \tag{5.134}$$

Using that:

$$T^0{}_i = \delta T^0{}_i = (\bar{\rho} + \bar{p})\, \partial_i V \tag{5.135}$$

$$= \delta T^{(m)0}{}_i = \bar{\rho}_m \partial_i V_m \text{ because } T^{(\Lambda)0}{}_i = 0 \ , \tag{5.136}$$

we find that:

$$\bar{\rho}(1+w) V = \bar{\rho}_m V_m \ . \tag{5.137}$$

Using these relations, the momentum constraint and the Poisson equation become[2]:

$$\Phi' + \mathcal{H}\Phi = -4\pi G a^2 \bar{\rho}_m V_m \tag{5.138}$$

$$\Delta\Phi = 4\pi G a^2 \bar{\rho}_m \Delta_m \ . \tag{5.139}$$

We see that the comoving density contrast is particularly nice because it is the density contrast that truly sources the gravitational field. Furthermore, the Bardeen equation is given by:

$$\Phi'' + 3\mathcal{H}\Phi' + \Lambda a^2 \Phi = 0 \ , \tag{5.140}$$

after noticing that $c_s^2 = 0$ and:

$$w = \frac{-\bar{\rho}_\Lambda}{\bar{\rho}_m + \bar{\rho}_\Lambda} = -\frac{a^2\Lambda}{3\mathcal{H}^2} \ . \tag{5.141}$$

The energy-momentum conservation equations for matter:

$$\delta_m' = 3\Phi' - \Delta V_m \tag{5.142}$$

$$V_m' + \mathcal{H} V_m = -\Phi \, , \tag{5.143}$$

then also reduce to:

$$\Delta_m' = -\Delta V_m \tag{5.144}$$

$$V_m' + \mathcal{H} V_m = -\Phi \ . \tag{5.145}$$

Note that on small scales, velocity perturbations can be neglected as we have that $|\Phi| \ll |\Delta_m|$ (using the Poisson equation) and thus:

$$\Delta_m \simeq \delta_m \text{ on small scales} (k \gg k_{\rm eq}) \ . \tag{5.146}$$

This is not the case on large scales.

5.7.2 Matter power spectrum

As we have seen, in inflationary cosmology, Φ becomes a random field because its Fourier modes are produced by quantum mechanical processes in the early Universe. As a result, all other perturbative quantities are themselves random fields and thus, we will also characterise the matter distribution

[2]Remember that radiation is negligible both at the level of the background and fluctuations, for adiabatic perturbations.

by a power spectrum. Let us first introduce a matter transfer function $T_m\left(\eta,\vec{k}\right)$ linking the Fourier modes of Δ_m to the initial curvature perturbation:

$$\hat{\Delta}_m\left(\eta,\vec{k}\right) = T_m\left(\eta,\vec{k}\right)\hat{\zeta}\left(\vec{k}\right) \ . \tag{5.147}$$

Using the Poisson equation (5.139) in Fourier space, we have:

$$-k^2\hat{\Phi} = 4\pi G a^2\bar{\rho}_m\hat{\Delta}_m \ . \tag{5.148}$$

Thus:

$$T_m\left(\eta,\vec{k}\right) = -\frac{k^2}{4\pi G\bar{\rho}_m a^2}T_\Phi\left(\eta,\vec{k}\right) \ . \tag{5.149}$$

This can also be rewritten:

$$T_m\left(\eta,\vec{k}\right) = -\frac{2a(\eta)}{3\Omega_{m,0}H_0^2}k^2T_\Phi\left(\eta,\vec{k}\right) \ . \tag{5.150}$$

Plugging in the transfer function for Φ and focussing on the scale dependence (ignoring the time dependence for the moment) we then get:

Matter transfer function

$$T_m\left(\eta,\vec{k}\right) \propto \begin{cases} k^2 & \text{for } k \ll k_{\rm eq} \\ 1 & \text{for } k \gg k_{\rm eq} \ . \end{cases} \tag{5.151}$$

Besides, with $\hat{\zeta}\left(\vec{k}\right) \propto k^{(n_s-4)/2} \simeq k^{-3/2}$, we get:

$$\hat{\Delta}_m\left(\eta,\vec{k}\right) \propto \begin{cases} k^{n_s/2} \simeq k^{1/2} & \text{for } k \ll k_{\rm eq} \\ k^{(n_s-4)/2} \simeq k^{-3/2} & \text{for } k \gg k_{\rm eq} \ . \end{cases} \tag{5.152}$$

Finally, we can introduce the power spectrum for matter fluctuations:

$$\left\langle\hat{\Delta}_m\left(\eta,\vec{k}\right)\hat{\Delta}_m\left(\eta,\vec{k}'\right)\right\rangle = (2\pi)^3\,\delta_D\left(\vec{k}+\vec{k}'\right)\mathcal{P}_m\left(\eta,k\right) \ . \tag{5.153}$$

This leads to:

$$\mathcal{P}_m\left(\eta,k\right) = T_m^2\left(\eta,\vec{k}\right)\mathcal{P}_\zeta(k) \ , \tag{5.154}$$

so that:

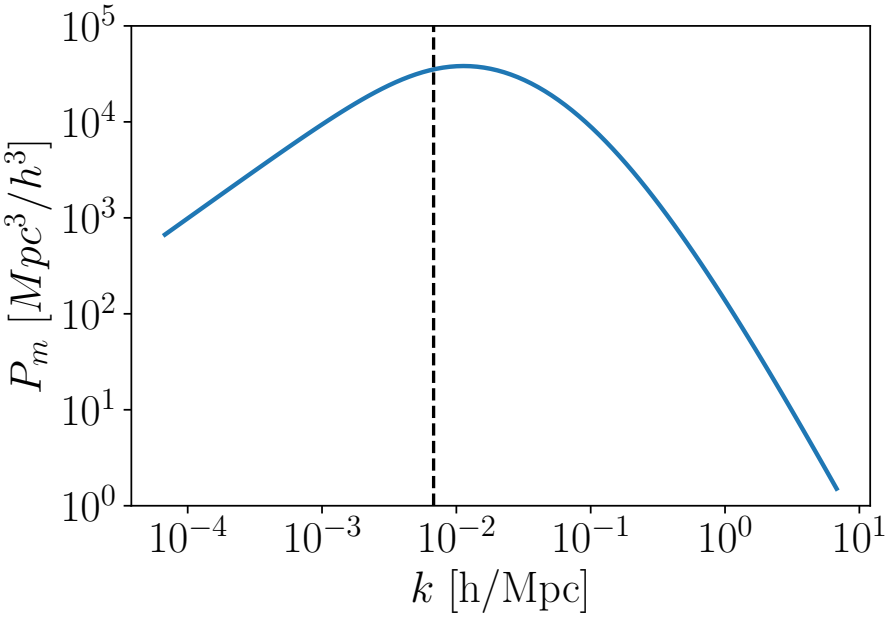

Figure 5.12: Linear matter power spectrum with the same parameters as the power spectrum for Φ on Fig. 5.10. The vertical dashed line indicates the matter-radiation equality scale.

Matter power spectrum

$$\mathcal{P}_m(\eta, k) \propto \begin{cases} k^{n_s} \simeq k & \text{for } k \ll k_{\text{eq}} \\ k^{n_s-4} \simeq k^{-3} & \text{for } k \gg k_{\text{eq}} \,. \end{cases} \tag{5.155}$$

This power spectrum is depicted on figure 5.12 for the potential's power spectrum shown on Fig. 5.10.

5.7.3 Effect of Λ

Let us now turn to the time dependence in the matter power spectrum. We saw that:

$$T_m\left(\eta, \vec{k}\right) = -\frac{2a(\eta)}{3\Omega_{m,0}H_0^2} k^2 T_\Phi\left(\eta, \vec{k}\right) \,, \tag{5.156}$$

so that, using our expression for the potential transfer function:

$$T_m\left(\eta,\vec{k}\right) = -\frac{2a(\eta)g(\eta)}{3\Omega_{m,0}H_0^2}T(k)\ , \tag{5.157}$$

where we defined:

$$T(k) = \begin{cases} k^2 & \text{for } k \ll k_{\rm eq} \\ 1 & \text{for } k \gg k_{\rm eq}\ . \end{cases} \tag{5.158}$$

Thus, the power spectrum depends on time via the factor $a^2(\eta)g^2(\eta)$ which grows like $a^2(\eta) \propto \eta$ during the Matter Dominated phase, until a_Λ and then becomes constant once Λ dominates. Thus, if we consider two cosmological models, one with $\Lambda = 0$ and one with $\Lambda \neq 0$ which start with the same power on all scales at the beginning of the Matter Dominated Era (same initial curvature perturbation spectrum), the model with $\Lambda \neq 0$ will have less power in its perturbations at present time than the one with $\Lambda = 0$. Indeed, for the model without Λ, the power spectrum continues to grow as a^2 all the way to today, while the one with $\Lambda \neq 0$ has a power spectrum that stops growing at $a_\Lambda \sim 0.75$ in concordance cosmology. Thus, the ratio of power at $\eta = \eta_0$, today should be $1/a_\Lambda^2 \sim 1.7$. But that is not what we see in figure 5.13. The previous estimate would be good if everything else was kept fixed, but changing the value of Λ also affects the equality scale. Indeed, that scale is given by:

$$k_{eq} = \Omega_{m,0}H_0\left(\frac{2}{\Omega_{r,0}}\right)^2\ . \tag{5.159}$$

The model $\Lambda = 0$ has $\Omega_{m,0} = 1$ while the model $\Lambda \neq 0$ has $\Omega_{m,0} \simeq 0.3 < 1$, therefore, the turn-over scale is displaced ($k_{eq}^{\Lambda\neq 0} \simeq 0.3 k_{eq}^{\Lambda=0}$) and since the transfer function T_Φ is proportional to k_{eq}^2, the ratio of the two powers spectra at a fixed k should be of the order $\left(k_{eq}^{\Lambda\neq 0}/k_{eq}^{\Lambda=0}\right)^4 \simeq 10^{-2}$ on sub-equality scales, which is exactly what we see on figure 5.13.

There is another important way to look at the growth of matter perturbations in the late Universe, via the *matter growth factor and growth rate*. First, le us rewrite Poisson equation:

$$\Delta\hat{\Phi} = \frac{3}{2}\Omega_{m,0}H_0^2\frac{\hat{\Delta}_m\left(\eta,\vec{k}\right)}{a}\ . \tag{5.160}$$

We then define the matter growth factor $D(\eta)$ via:

$$\hat{\Delta}_m\left(\eta,\vec{k}\right) = D(\eta)\hat{\Delta}_m\left(\eta_0,\vec{k}\right)\ . \tag{5.161}$$

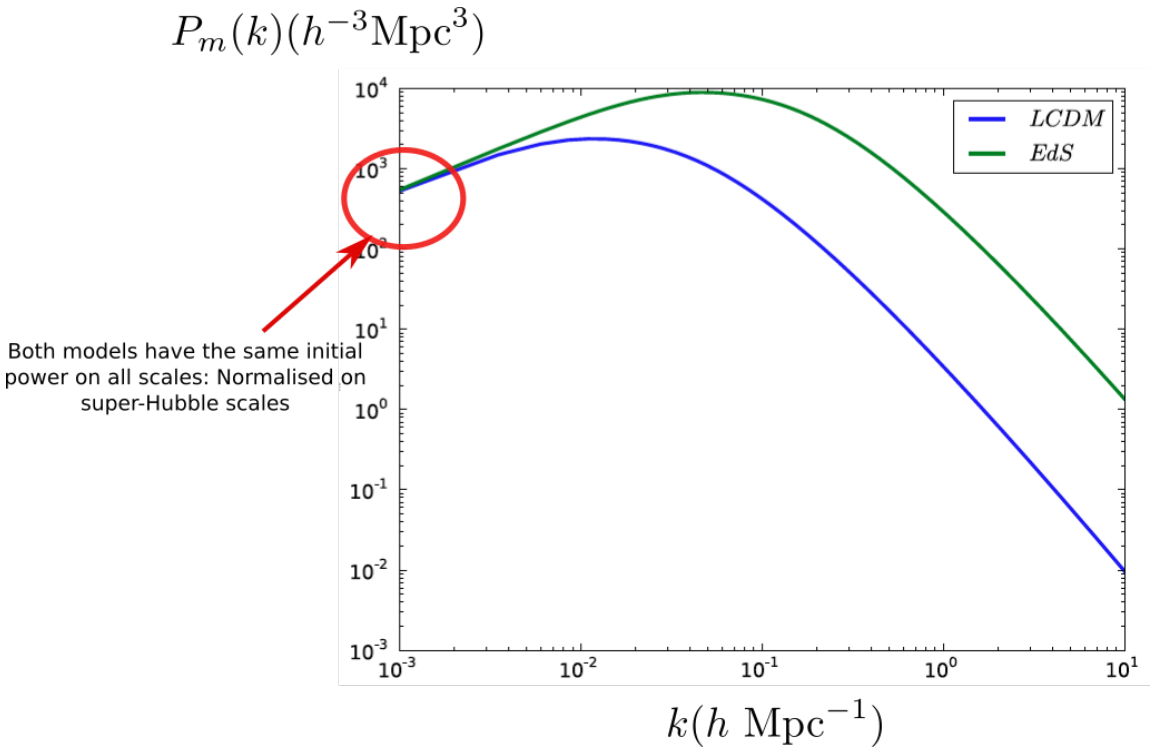

Figure 5.13: Matter Power spectra today for two models: LCDM with $\Lambda \neq 0$ and EdS (Einstein-de Sitter) with $\Lambda = 0$.

Note that this growth factor is normalised at present time: $D(\eta_0) = 0$. In the literature, one sometimes also encounter the potential growth function $G(\eta)$, such that:

$$\hat{\Phi}\left(\eta, \vec{k}\right) = G(\eta)\hat{\Phi}\left(\eta_0, \vec{k}\right) \ . \tag{5.162}$$

Functionally, this is the same function as $g(\eta)$ encountered earlier, but it is now normalised at the present time rather than at early times in the Matter dominated phase. We see that, trivially:

$$G(\eta) = \frac{D(\eta)}{a(\eta)} \ . \tag{5.163}$$

Using Eqs. (5.145)-(5.144) and the Poisson equation, we can decouple the system governing the behaviour of Δ_m to get to an autonomous equation:

$$\Delta_m'' + \mathcal{H}\Delta_m' - \frac{3}{2}\Omega_m(\eta)\mathcal{H}^2\Delta_m = 0 \ , \tag{5.164}$$

which, by separation of variables, leads to:

$$D'' + \mathcal{H}D' - \frac{3}{2}\Omega_m(\eta)\mathcal{H}^2 D = 0 \ . \tag{5.165}$$

In a pure Einstein-de Sitter Universe, with $\Lambda = 0$, we get $\Omega_m(\eta) = 1$, in which case it is easy to see that the growing solution to Eq. (5.165) is simply:

$$D_{EdS}(\eta) = a(\eta) \ . \tag{5.166}$$

In general however, this equation needs to be solved numerically. In that case, one finds it more natural to solve for a related quantity known as the *growth rate*, f:

$$f(\eta) \equiv \frac{d\ln D}{d\ln a} \ . \tag{5.167}$$

This function will appear in the next chapter as a measurable quantity that allows us to test the nature of Dark Energy. Writing:

$$\Delta_m' = f\mathcal{H}\Delta_m \ , \tag{5.168}$$

and after appropriate transformations, the evolution equation for the growth rate f is:

$$\frac{df}{dx} + \frac{1}{2}\left(4 - 3\Omega_m(x)\right) f + f^2 = \frac{3}{2}\Omega_m(x) \ , \tag{5.169}$$

where $x = \ln a$ and:

$$\Omega_m(x) = \frac{1}{1 + \frac{1-\Omega_{m,0}}{\Omega_{m,0}} e^{3x}} \ . \tag{5.170}$$

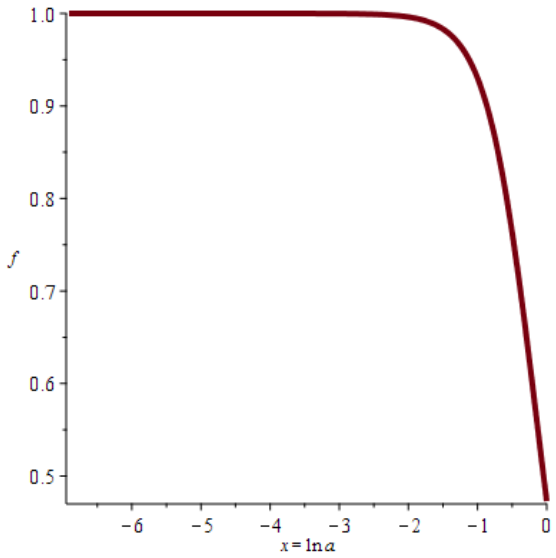

Figure 5.14: Growth rate f as a function of $x = \ln a$ in a ΛCDM Universe with $\Omega_{m,0} = 0.26$.

Note that this is a non-linear equation involving f^2; this does not contradict our assumption of linear perturbation theory. In an EdS Universe with $\Lambda = 0$ we recover that $f = 1$ is a solution, as expected. For $\Lambda \neq 0$, this equation needs to be solved numerically. The result is displayed on figure 5.14 for $\Omega_{m,0} = 0.26$.

As it turns out, a very good parametrisation for the growth rate is given by:

$$f(\eta) = (\Omega_m(\eta))^\gamma \text{ with } \gamma \simeq 0.55 \, . \tag{5.171}$$

This is still a very good approximation for a dynamical Dark Energy as long as its clustering can be neglected.

5.8 Photons and baryons

So far, we concentrated on the behaviour of the dark matter fluctuation in the late-time Universe as we wanted to construct the large-scale, linear matter power spectrum, but we have to say a few words about photons and baryons.

5.8.1 Photons

For adiabatic initial conditions, the density contrast during the radiation dominated phase is dominated by the one for radiation, so we can use the Poisson equation (4.175) to write:

$$4\pi G\bar{\rho}a^2\hat{\delta}_r = \frac{3}{2}\mathcal{H}^2\hat{\delta_r} = k^2\hat{\Phi}_{\rm rad} - 3\mathcal{H}\left(\hat{Phi}'_{\rm rad} + \mathcal{H}\hat{\Phi}_{\rm rad}\right) , \tag{5.172}$$

with $\mathcal{H} = 1/\eta$, so that:

$$\hat{\delta}_r = \frac{2}{3}\left((k\eta)^2 - 3\right)\hat{\Phi}_{\rm rad} - 2\eta\hat{\Phi}'_{\rm rad} \tag{5.173}$$

$$\hat{\Delta}_r = -\frac{2}{3}(k\eta)^2\,\hat{\Phi}_{\rm rad} . \tag{5.174}$$

On super-Hubble scales, i.e. for $k \ll 1/\eta$, $\hat{\Phi}_{\rm rad}$ is constant, so $\hat{\delta}_r$ is constant while $\hat{\Delta}_r \propto a^2$. On the other hand, for sub-Hubble scales, we have Eq. (5.92) for the potential, so that:

$$\hat{\delta}_r \simeq \hat{\Delta}_r = -\frac{2}{3}(k\eta)^2\,\hat{\Phi}_{\rm rad} \propto \cos\left(\frac{k\eta}{\sqrt{3}}\right) . \tag{5.175}$$

Therefore, on subhorizon scales, during the radiation dominated epoch, radiation perturbations oscillates around 0.

During the matter dominated epoch, radiation is negligible in the overall density perturbation and we must therefore use the conservation equations (5.44)-(5.45):

$$\hat{\delta}'_r = 4\hat{\Phi}' + \frac{4k^2}{3}\hat{V}_r \tag{5.176}$$

$$\hat{V}'_r = -\hat{\Phi} - \frac{1}{4}\hat{\delta}_r . \tag{5.177}$$

Since the potential is constant during that era, this simplifies to:

$$\hat{\delta}'_r = \frac{4k^2}{3}\hat{V}_r \tag{5.178}$$

$$\hat{V}'_r = -\hat{\Phi}_0 - \frac{1}{4}\hat{\delta}_r , \tag{5.179}$$

which gives:

$$\hat{\delta}''_r + \frac{k^2}{3}\hat{\delta}_r = -\frac{4k^2}{3}\hat{\Phi}_0(\vec{k}) . \tag{5.180}$$

This is the equation of a forced harmonic oscillator. The density contrast in radiation thus oscillates around the value $\left\langle\hat{\delta}_r(\eta,\vec{k})\right\rangle = -4\hat{\Phi}_{\rm mat}\left(\vec{k}\right)$ with a frequency $f_k = \frac{k}{\sqrt{3}}$:

$$\hat{\delta}_r\left(\eta,\vec{k}\right) = A(\vec{k})\cos\left(\frac{k\eta}{\sqrt{3}}\right) + B(\vec{k})\sin\left(\frac{k\eta}{\sqrt{3}}\right) - 4\hat{\Phi}_0(\vec{k}) . \tag{5.181}$$

For adiabatic initial conditions, we get[3] $\hat{\delta}_r(\eta_i) = -2\hat{\Phi}(\eta_i)$ and $\hat{V}_\gamma = 0$ deep in the radiation dominated phase. Then, as long as the mode remains super-Hubble, we have $\hat{\delta}_r' = 4\hat{\Phi}'$ and thus:

$$\hat{\delta}_r(\eta) = -2\hat{\Phi}(\eta_i) + 4\left[\hat{\Phi}(\eta) - \hat{\Phi}_i\right] \ . \tag{5.182}$$

Once the mode enters the Hubble radius during the radiation dominated phase, $\hat{\Phi}$ rapidly decreases to zero and we are left with:

$$\hat{\delta}_r \simeq -6\hat{\Phi}(\eta_i) \text{ before decoupling.} \tag{5.183}$$

This gives us the initial conditions at, say, matter radiation equality; we have $\hat{\delta}_r = -6\hat{\Phi}(\eta_i) \gg \hat{\Phi}_0$ and $\hat{\delta}_r' = 0$. With $\eta_{\rm eq} \ll \eta_{\rm dec}$, we get:

$$\hat{\delta}_r\left(\eta_{\rm dec}, \vec{k}\right) = -6\hat{\Phi}(\eta_i)\cos\left(\frac{k\eta_{\rm dec}}{\sqrt{3}}\right) - 4\hat{\Phi}_0\left(\boldsymbol{k}\right) \tag{5.184}$$

These oscillations leave an imprint on the CMB, in the form of the acoustic peaks observed in its anisotropy spectrum. Indeed, let us do some (very) crude estimates. Before decoupling, photons are tightly coupled to baryons and keep bouncing back and force. Their trajectories in spacetime are thus not geodesics, as they are not in free-fall. Rather, they follow null curves that are not geodesics. On the other hand, after decoupling, they propagate freely, they are free-falling and thus follow lightlike geodesics. On a given scale θ on the sky, we will observe a black-body, thermal spectrum with temperature $T_0(\theta) = \hat{T}\left(\eta_{\rm dec}, k\right)/(1 + z_{\rm dec})$, where the comoving mode k is given by:

$$k = \frac{2\pi\left(1 + z_{\rm dec}\right)}{\theta D_A\left(z_{\rm dec}\right)} \ . \tag{5.185}$$

Using that:

$$\hat{\rho}_r\left(\eta_{\rm dec}, k\right) = a_S\hat{T}^4\left(\eta_{\rm dec}, k\right) \ , \tag{5.186}$$

and expanding at first order, we get that:

$$\frac{\Delta\hat{T}}{\bar{T}}\left(\eta_{\rm dec}, k\right) = \frac{1}{4}\hat{\delta}_r\left(\eta_{\rm dec}, k\right) \ . \tag{5.187}$$

Varying the modes k, subtending given angles θ on the sky according to Eq. (5.185), an oscillatory pattern of temperature anisotropies gets imprinted on the distribution of light we receive today. with

[3] Under adiabiatic conditions, the dominant contribution to the source of the gravitational is the dominant species, here δ_r deep in the RDE. Then, Eq. (4.178) on large scales give the desired relationship

peaks and troughs at:

$$k_{\text{peaks}} = n\pi\sqrt{3}\mathcal{H}_{\text{dec}} \quad \text{for } n \in \mathbb{N} \tag{5.188}$$

$$k_{\text{troughs}} = \frac{n\pi\sqrt{3}}{2}\mathcal{H}_{\text{dec}} \quad \text{for } n \in \mathbb{N}\ . \tag{5.189}$$

These are the *anisotropies of the CMB*. As one can see, the positions of these peaks contain information about the size of the Hubble radius at decoupling. Actually, the full spectrum of fluctuations contain much more than that. This angular power spectrum of fluctuations in the CMB temperature across the sky is obtained by expanding the temperature anisotropies into into spherical harmonics, so that:

$$C(\theta) = \left\langle \frac{\Delta T\left(\theta_0\right)}{\bar{T}} \frac{\Delta T\left(\theta_0+\theta\right)}{\bar{T}} \right\rangle = \sum_{l=0}^{+\infty} \frac{2l+1}{4\pi} C_l P_l\left(\cos\theta\right)\ , \tag{5.190}$$

where $P_l(x)$ is the Legendre polynomial of order l. Then, all the correlations are encoded into the C_l, with the mode corresponding to l characterising correlations on angular scales $\theta \simeq \pi/l$. The spectrum is shown in Fig. 5.15. The series of peaks and troughs is clearly visible. These are the *acoustic peaks*.

Unfortunately, a proper treatment of the CMB in order to understand this spectrum in details requires much finer modelling of the baryons and photons, via the Boltzmann equation. A quick introduction to CMB anisotropies can be found in chapter 6.

5.8.2 Baryons

Fig. 5.16 shows the linear matter power spectrum computed with the code CAMB. Although our previous study reproduces nicely the power-law behaviours of the matter power spectrum for large and small scales, and the turn over at equality scale, there is an additional feature in this power spectrum that we missed.

Very visible above $0.1h$ Mpc^{-1} and actually extending over all sub-equality scales, are oscillations in the power spectrum. These come from the gravitational coupling between baryons and Dark Matter. In our previous analysis, we treated these two fluids as one and the same, but in the early Universe they are actually different because before recombination and decoupling, baryons are tightly coupled to photons via Thomson scattering and oscillating under the competition of plasma pressure and gravitational pull, whereas Dark Matter is already free to collapse under gravitational pull. This means that local overdensities of Dark Matter grow earlier and hence higher than those

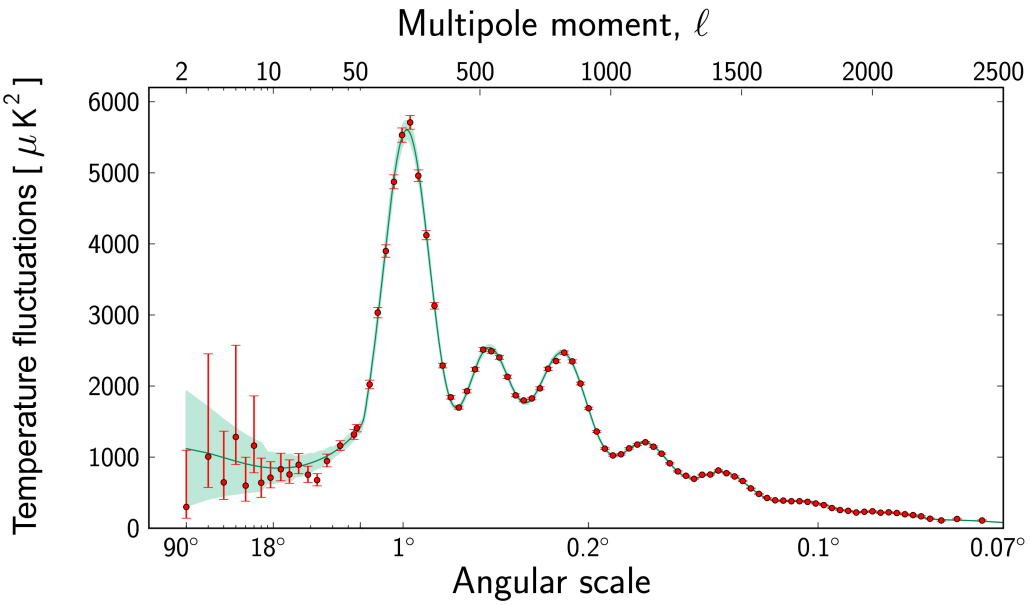

Figure 5.15: Angular power spectrum of temperature anisotropies, $\Delta T(\theta)/\bar{T}$ as measured by the Planck satellite (red dots). The blue curve represents the best ΛCDM fit to the data. Credits: ESA/-Planck

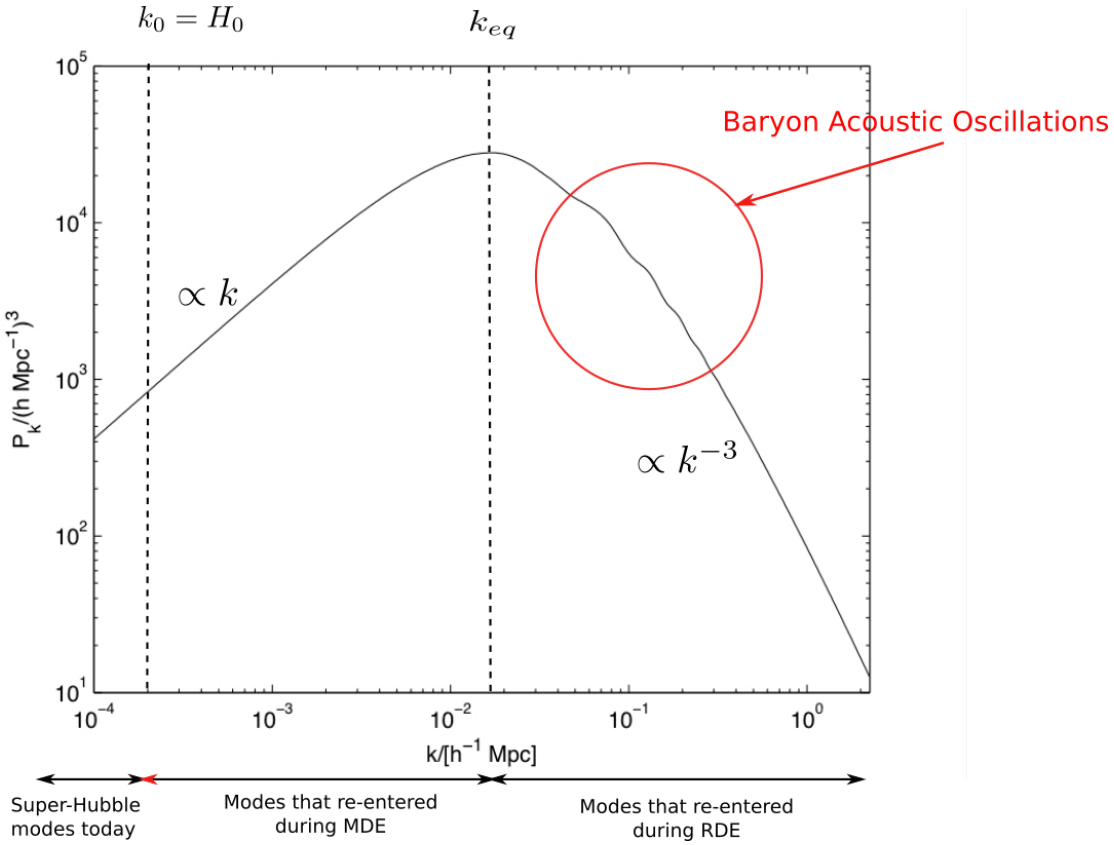

Figure 5.16: Matter power spectrum obtained with CAMB; the cosmological parameters used are those of PLANCK best fit.

of baryons. During that phase, the tight coupling between baryons and photons means that we can write: $V_r = V_b$. Besides, since, in a first approximation, baryons and photons can be treated as a single fluid, they have adiabatic perturbations, with $\delta_b = 3\delta_r/4$, which are thus frozen on super-Hubble scales and oscillate around a mean value of $-3\Phi_{\rm mat}\left(\vec{k}\right)$ on subhorizon scales, while Dark matter perturbations grow as a. Thus, at decoupling, we have $\delta_c \gg \delta_b$.

After decoupling, baryons are now neutral and start collapsing into structure. Neglecting radiation and interactions between baryons and Dark matter, we can write the evolution of both fluids as:

$$\delta'_{(i)} = -\Delta V_i \tag{5.191}$$

$$V'_i + \mathcal{H}V_i = -\Phi_{\rm mat}\ , \tag{5.192}$$

where we used that $\Phi_{\rm mat}$ was constant during the matter dominated phase. Thus, we obtain:

$$\delta''_b + \mathcal{H}\delta'_b = 4\pi G a^2\left(\bar{\rho}_b\delta_b + \bar{\rho}_c\delta_c\right) \tag{5.193}$$

$$\delta''_c + \mathcal{H}\delta'_c = 4\pi G a^2\left(\bar{\rho}_b\delta_b + \bar{\rho}_c\delta_c\right)\ . \tag{5.194}$$

The difference $D = \delta_b - \delta_c$ obeys:

$$D'' + \frac{2}{\eta}D' = 0\ . \tag{5.195}$$

The general solution is then:

$$D = C_1 + \frac{C_2}{\eta}\ , \tag{5.196}$$

where C_1 and C_2 are arbitrary constants (dependent on k) On the other hand, the total density contrast for non-relativistic matter obeys:

$$\delta''_m + \frac{2}{\eta}\delta'_m - \frac{6}{\eta^2}\delta_m = 0\ , \tag{5.197}$$

. whose genertal solution is:

$$\delta_m = D_1\eta^2 + D_2\eta^{-3}\ . \tag{5.198}$$

Clearly:

$$\frac{\delta_b}{\delta_c} = \frac{\bar{\rho}_m\delta_m + \bar{\rho}_c D}{\bar{\rho}_m\delta_m - \bar{\rho}_b D} \to \frac{\delta_m}{\delta_m} = 1\ , \tag{5.199}$$

when η increases. Therefore, the baryons density contrast gradually approaches the Dark Matter one on all scales[4].

But in the small initial values at decoupling of δ_b and δ_b', the acoustic oscillations visible in the CMB anisotropies, have been imprinted on the matter distribution. In particular, this is the case of the characteristic scale of the sound horizon at last scattering. Thus, as photons free-stream, baryons and Dark Matter interact gravitationally, and the characteristic scale of the sound horizon at last scattering present in the baryon distribution gets imprinted on the distribution of Dark Matter, leading to a bump in the correlation function of Dark Matter (see below for the notion of correlation function) that translates into the oscillations of the power spectrum on sub-equality scales. These are the so-called *Baryon Acoustic Oscillations*. This is most easily illustrated by considering a unique, simple spherical overdensity, as illustrated in figure 5.17.

5.9 Refinement: two fluid system and entropy generation

When studying the system composed of relativistic and non-relativistic fluids, we have assumed adiabaticity. But our discussion of photons above makes it clear that there is a problem with that approximation. Indeed, on sub-Hubble scales during the matter dominated epoch we found that δ_r was oscillating around a finite value, while our discussion of δ_m showed that it was growing as a. Thus, it is impossible for these two quantities to satisfy the adiabaticity condition:

$$\delta_m = \frac{3}{4}\delta_r \ , \tag{5.200}$$

at all times. Some entropy must be created. As we have seen in section 5.2.2, this is indeed the case, and this entropy must act on the Bardeen potential and change its evolution. Writing the Bardeen equation with some entropy production:

$$\delta p = c_s^2 \delta\rho + \bar{p}\Gamma \ , \tag{5.201}$$

with:

$$w\Gamma = \frac{4\Omega_m\Omega_r}{9(1+w)} S_{mr} \ , \tag{5.202}$$

we get:

$$\hat{\Phi}'' + 3\left(1+c_s^2\right)\mathcal{H}\hat{\Phi}' + 3\left(c_s^2 - w\right)\mathcal{H}^2\hat{\Phi} + c_s^2 k^2\hat{\Phi} = -\frac{2\Omega_m\Omega_r}{3(1+w)}\hat{S}_{mr} \ . \tag{5.203}$$

[4]But the density of baryons remain small compared to the Dark Matter one.

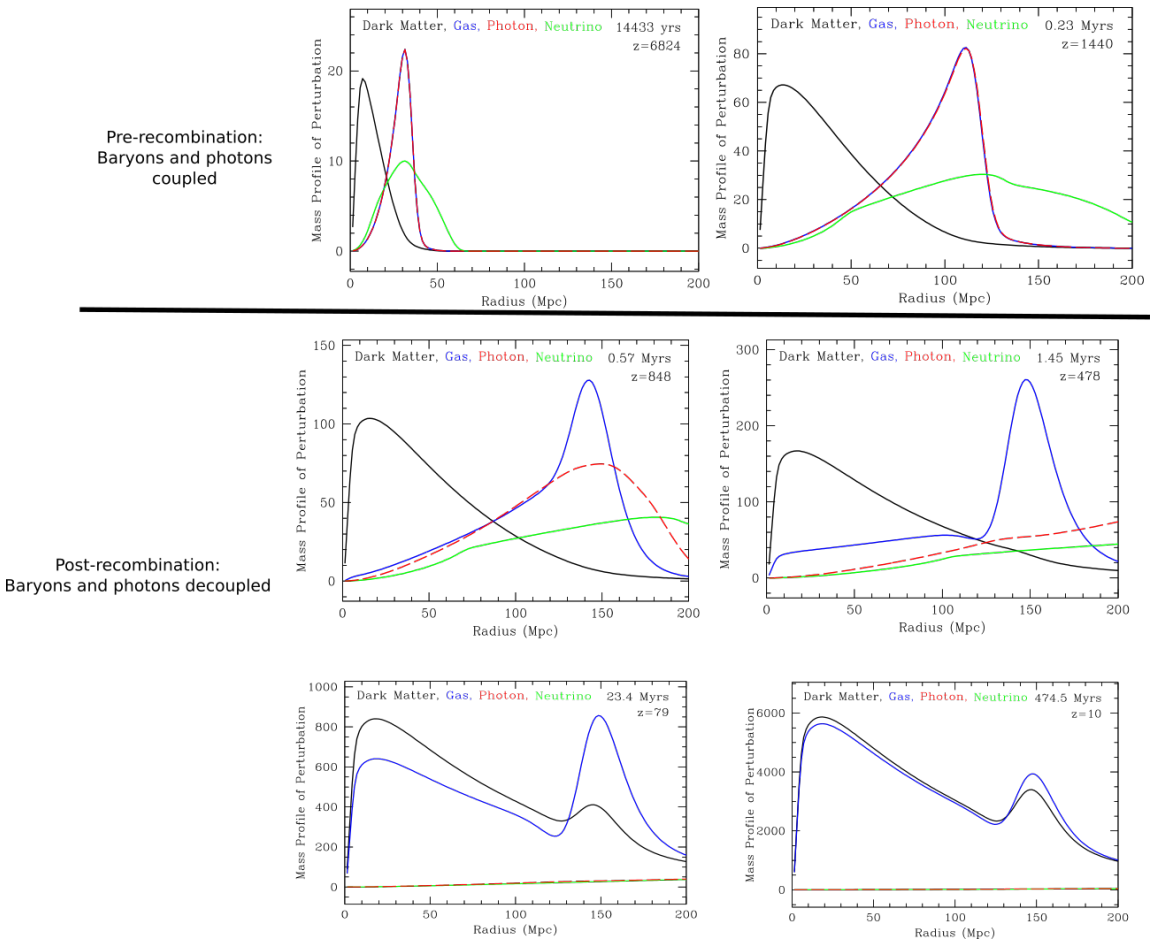

Figure 5.17: From [10]. Evolution of a unique spherical overdensity in a standard cosmology. The initial overdensity is located at $r = 0$. The plots represent $r^2\rho(\eta, r)$.

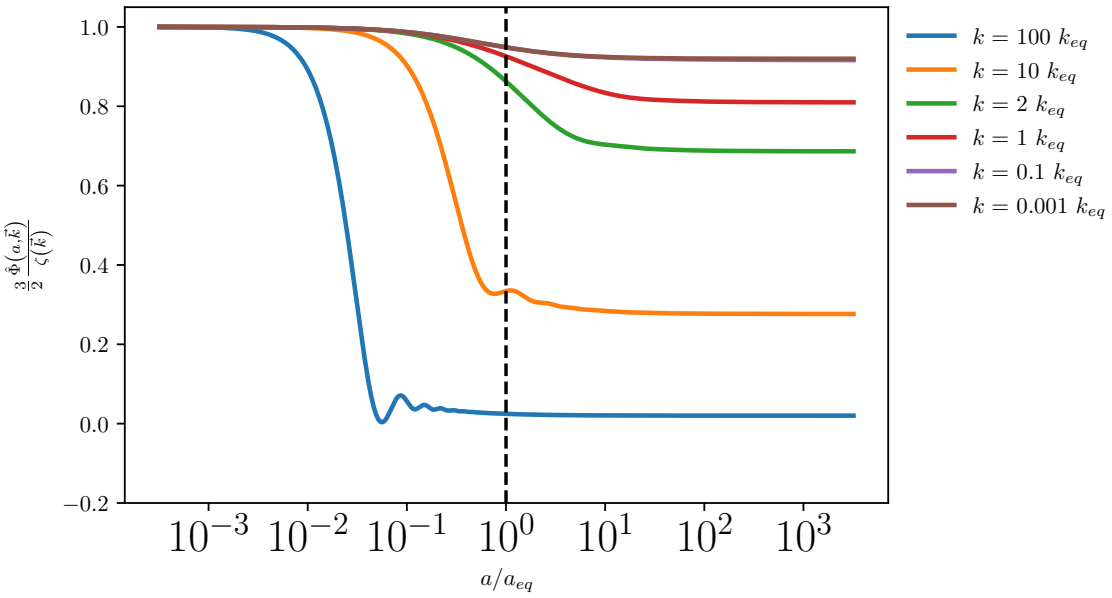

Figure 5.18: Evolution of the Bardeen potential through the radiation-matter transition when the entropy production is taken into account. The mode presented here are the same as the one of Fig. 5.6.

Combining Eqs (5.46) and (5.47), we get:

$$\hat{S}''_{mr} + \mathcal{H}\hat{S}'_{mr} - \frac{1}{3}\Omega_m k^2 \hat{S}_{mr} = -\frac{2}{\mathcal{H}^2}k^4\hat{\Phi}\ . \tag{5.204}$$

We can now solve numerically the coupled system (5.203)-(5.204) to get the more accurate behaviour of the potential $\hat{\Phi}$. The result of the numerical integration is presented on Fig. 5.18. The modes presented on this plot are the same as the ones of Fig. 5.6, which were obtained while neglecting the entropy production. We see that their behaviour is significantly altered for modes around the equality scale: these are not as damped after the matter-radiation transition as in the pure adiabatic case. Oscillations due to radiation that persisted deep into the matter epoch in the adiabatic case are also suppressed. For very large and very small modes, the adiabatic evolution is accurate, which explain why we were able to obtain the right asymptotic scaling.

The transfer function of Fig. 5.11 and the power spectra displayed on Figs. 5.10 and 5.12 all used the computations of the potential using entropy production to ensure that the transition between

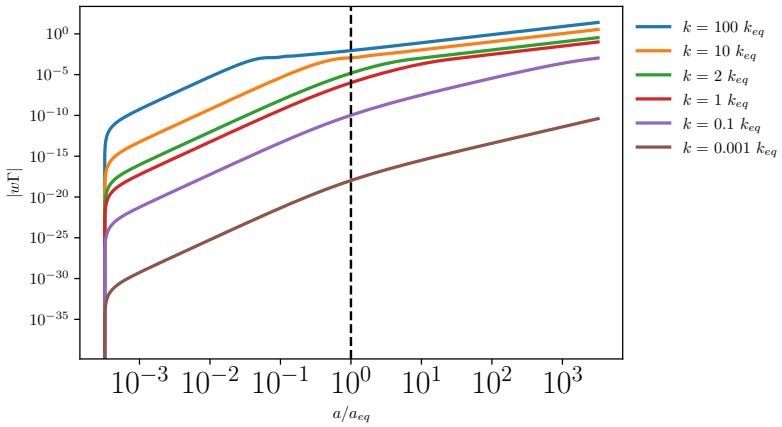

Figure 5.19: Evolution of the entropy produced, $w\Gamma$, for each mode presented on Fig. 5.18.

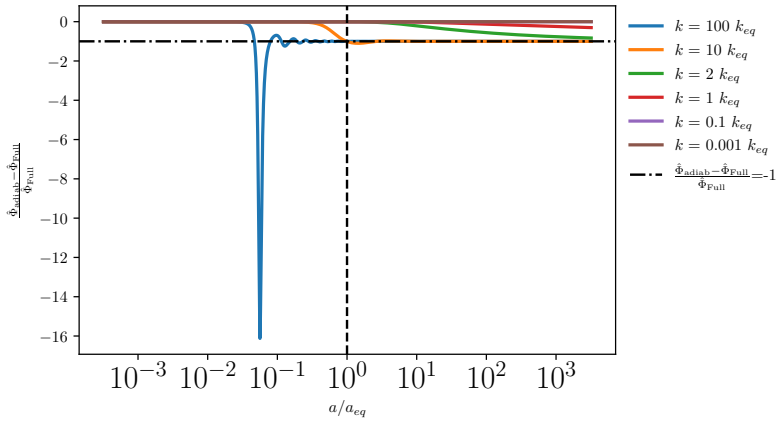

Figure 5.20: Relative differences in the value of the potential $\hat{\Phi}$ for adiabatic evolution and correct one taking into account entropy production .

super and sub-equality scales could be matched properly. Fig. 5.19 shows the evolution of the entropy $w\Gamma$ produced for each mode displayed on Fig. 5.18.

Clearly, entropy is produced more and more on small scales. However, modes that entered the Hubble radius very early in the radiation dominated phase are so damped by the time the entropy production kicks in, that they are not significantly affected in absolute terms, although they receive

corrections of order 100%; see Fig. 5.20. Note that entropy production systematically makes modes larger than in the pure adiabatic case.

5.10 Problems

Pb. 5.1 Show that the equation of state of the total fluid obeys:

$$w' = 3\mathcal{H}\left(w - c_s^2\right)(1+w) \ . \tag{5.205}$$

Pb. 5.2 Consider the evolution of the matter density contrast δ_m through the radiation and matter dominated phases (we neglect Λ).

- Using Eqs (5.42)-(5.43), show that:

$$\delta_m'' + \mathcal{H}\delta_m = \Delta\Phi + 3\left(\Phi'' + \mathcal{H}\Phi'\right) \ . \tag{5.206}$$

- Using what we have seen in the course, show that, when averaged over long enough periods of time, the gravitational potential Φ is only sourced by matter perturbations, so, if we are only interested in the long-time trends of δ_m, we have:

$$\delta_m'' + \mathcal{H}\delta_m - 4\pi G\bar{\rho}a^2\delta_m = 0 \ . \tag{5.207}$$

- By introducing the new variable $y = a/a_{\rm eq}$, show that:

$$\mathcal{H}^2 = \frac{H_0^2\Omega_{m,0}^2}{\Omega_{r,0}}\left[\frac{1}{y} + \frac{1}{y^2}\right] \ . \tag{5.208}$$

- Deduce that the density contrast obeys the *Mészáros equation*:

$$\frac{\mathrm{d}^2\delta_m}{\mathrm{d}y^2} + \frac{2+3y}{2y(1+y)}\frac{\mathrm{d}\delta_m}{\mathrm{d}y} - \frac{3}{2y(1+y)}\delta_m = 0 \ . \tag{5.209}$$

- First looking for an affine solution and then using a variation of parameters, show that the general solution to this equation is a linear combination of two independent solutions:

$$\begin{cases} D_+(y) = y + \dfrac{2}{3} & (5.210) \\ D_-(y) = D_+(y)\ln\left[\dfrac{\sqrt{1+y}+1}{\sqrt{1+y}-1}\right] - 2\sqrt{1+y} \ . & (5.211) \end{cases}$$

- Plot these solutions and comment.
- Study their asymptotic behaviours and show that we recover the results presented in the text.

6 The cosmic microwave background

Contents

In chapter 2, we described the emission of the homogeneous cosmic microwave background (CMB) when photons decouple from ordinary matter and start freely propagating in the universe. Of course, since the universe is not perfectly homogeneous and isotropic, we do not expect this decoupling itself to be homogeneous. In this chapter we propose a *preliminary* take on the emission of the CMB in a structured universe, focussing on the most basic approach to put forward the fundamental principles at hand. First, we restrict ourselves to a treatment of the scalar modes in the longitudinal gauge. Second, we will not treat the polarisation of the CMB radiation induced by Thomson scattering. A full theory of the CMB is beyond the scope of this course but can be found in [9].

In a first section, we introduce CMB temperature anisotropies and we derive the Sachs-Wolfe formula. Then, we define the CMB angular power spectrum and we use the Sachs-Wolfe formula to analyse some of teh features in that spectrum. In the second section, we introduce the proper, kinetic theory of the CMB, based on the Boltzmann equation

6.1 The Sach-Wolfe formula

We begin with a simplified derivation of the CMB temperature anisotropies based on the Sachs-Wolfe formula.

6.1.1 Derivation of the Sachs-Wolfe formula

For a given observer at $(\eta_0, vecx_0)$, the last scattering surface is a spacelike set of points of its past lightcone emitting photons when they last interact with electrons via Thomson scattering, before travelling freely in spacetime. That last scattering surface is thus defined by a constant free electron number density, $n_e = \text{cst}$. Since the matter density is not homogeneous, the electron number density at η constant fluctuates and the points of the last scattering surface are located at different values of the conformal time. We can label points on the last scattering surface of the observer by their coordinates:

$$\vec{x}_E = \vec{x}_0 + (\eta_0 - \eta_E)\,\vec{e} \tag{6.1}$$

$$\eta_E = \bar{\eta}_E + \delta\eta_E\ , \tag{6.2}$$

where $\vec{e}$ is the direction of observation on the observer's sky, $\bar{\eta}_E$ would be the time of emission in a perfectly homogeneous and isotropic universe, and $\delta\eta_E$ is the first order difference between the actual time of emission and $\bar{\eta}_E$. In what follows, we work in the Born approximation, evaluating all perturbed quantities along the unperturbed trajectory of photons. This justifies using Eq. (6.1) with $\eta_E = \bar{\eta}_E$.

A photon emitted on the last scattering surface follows a lightlike geodesics with tangent vector $\boldsymbol{k}$ obeying:

$$k^\mu k_\mu = 0 \text{ and } k^\nu \nabla_\nu k^\mu = 0 \,. \tag{6.3}$$

We can define a metric $\hat{\boldsymbol{g}}$ with[1] $g_{\mu\nu} = a^2 \hat{g}_{\mu\nu}$. In that case, the conformal structures of $\boldsymbol{g}$ and $\hat{\boldsymbol{g}}$ are identical: lightlike geodesics of one of the metric are mapped into lightlike geodesics of the other ones. Indeed, if the define the lightlike vector $\hat{\boldsymbol{k}} = a^2 \boldsymbol{k}$, we see that it is tangent to a lightlike geodesics of $\hat{\boldsymbol{g}}$:

$$\hat{k}^\mu \hat{k}_\mu = 0 \text{ and } \hat{k}^\nu \hat{\nabla}_\nu \hat{k}^\mu = 0 \,, \tag{6.4}$$

where $\hat{\nabla}_\mu$ denotes the components of the covariant derivative associated to $\hat{\boldsymbol{g}}$. We can thus study $\hat{k}^\mu$ to study geodesics of the full spacetime. This is particularly convenient since the spacetime with metric $\hat{g}_{\mu\nu}$ is simply a first order, perturbed Minkowski spacetime, so that its lightlikre geodesics are straightlines.

Therefore, let us introduce the following decomposition:

$$\hat{k}^\mu = \bar{E} \left(1 + \alpha\right) \delta^\mu{}_0 + \bar{E} \left(n^i + \delta n^i\right) \delta^\mu{}_i \,, \tag{6.5}$$

where $\bar{E}$ is a constant and $\vec{n}$ is a constant unit vector[2]. Using the fact that the geodesics in the perturbed Minkowski spacetime is lightlike, we arrive that:

$$\delta_{ij} n^i n^j = 1 \text{ and } \delta_{ij} n^i \delta n^j = \Phi + \Psi + \alpha \,. \tag{6.6}$$

Moreover, denoting $\hat{K}^\mu = \bar{E}\delta^\mu{}_0 + \bar{E} n^i \delta^\mu{}_i$ and $\delta\hat{k}^\mu = \hat{k}^\mu - \hat{K}^\mu$, and using λ to denote the affine parameter along the unperturbed geodesic, the geodesic equation gives, at first order:

$$\frac{\mathrm{d}\delta\hat{k}^\mu}{\mathrm{d}\lambda} = \hat{K}^\nu \partial_\nu \delta\hat{k}^\mu = -\delta\Gamma^\mu{}_{\nu\rho} \hat{K}^\nu \hat{K}^\mu \,. \tag{6.7}$$

[1] We work in (η, x, y, z) with x, y and z comoving Cartesian coordinates.

[2] They correspond respectively to the energy and direction of propagation of the photon in Minkowski spacetime, when perturbations are set to zero.

Isolating the time component of this equation, we get:

$$\frac{1}{\bar{E}}\frac{\mathrm{d}\alpha}{\mathrm{d}\lambda} = -\left(\Phi+\Psi\right)' - 2n^i\partial_i\Phi \ . \tag{6.8}$$

Given that, in the unperturbed, Minkowski spacetime, $\vec{n} = -\vec{e}$, we can relate the energy of the photon at observation, $E_0\left(\vec{e}\right)$ to its energy at emission, $E_E\left(\vec{x}_E, \eta_E\right)$, via:

$$\frac{E_0\left(\vec{e}\right)}{E_E\left(\vec{x}_E,\eta_E\right)} = \frac{\left(k^\mu u_\mu\right)_0}{\left(k^\mu u_\mu\right)_E} \ . \tag{6.9}$$

At first order, and using the baryon velocity potential, V_b, to describe the peculiar velocity of the observer, one gets:

$$\frac{E_0\left(\vec{e}\right)}{E_E\left(\vec{x}_E,\eta_E\right)} = \frac{a\left(\eta_E\right)}{a\left(\eta_0\right)}\left\{1+\left[\alpha+\Phi+n^i\partial_i V_b\right]_E^0\right\} \ . \tag{6.10}$$

For a radiation field in thermal equilibrium, this translates to a relationship between emitted and observed temperature of the thermal bath:

$$\frac{T_0\left(\vec{e}\right)}{T_E\left(\vec{x}_E,\eta_E\right)} = \frac{a\left(\eta_E\right)}{a\left(\eta_0\right)}\left\{1+\left[\alpha+\Phi+n^i\partial_i V_b\right]_E^0\right\} \ . \tag{6.11}$$

We can then define the temperature fluctuation at the emission time η_E via:

$$\Theta\left(\vec{x}_E,\eta_E\right) = \frac{T_E\left(\boldsymbol{x}_E,\eta_E\right) - \bar{T}_E\left(\eta_E\right)}{\bar{T}_E\left(\eta_E\right)} \ , \tag{6.12}$$

where $\bar{T}_E\left(\eta_E\right)$ is the spatial average of the temperature at time η_E. Similarly, we have the temperature fluctuation observed at η_0 in the direction $\vec{e}$:

$$\Theta_0\left(\vec{e}\right) = \frac{T_0\left(\vec{e}\right) - \bar{T}_0}{\bar{T}_0} \ , \tag{6.13}$$

with $\bar{T}_0$ the observed temperature averaged on the entire sky of the observer. We get a relationship between the temperature fluctuation at last scattering and its observed value :

$$\Theta_0\left(\vec{e}\right) = \Theta_E\left[\vec{x}_E,\eta_E\right] + \left[\alpha+\Phi+n^i\partial_i V_b\right]_E^0 \ , \tag{6.14}$$

together with the zeroth-order, expected relationship:

$$\frac{\bar{T}_0}{\bar{T}_E} = \frac{a\left(\bar{\eta}_E\right)}{a\left(\bar{\eta}_0\right)} \ . \tag{6.15}$$

Since the last scattering surface corresponds to $n_e = \text{cst}$ and since up to last scattering, photons and electrons are tightly coupled, we can also say that on the last scattering surface: $\rho_r = \text{cst}$. Hence, by the Stefan-Boltzmann law, we have that:

$$\delta_r\left(\vec{x}_E, \eta_E\right) = 4\Theta_E\left(\vec{x}_E, \eta_E\right) \ . \tag{6.16}$$

Further, noting that:

$$\frac{1}{\bar{E}}\frac{\mathrm{d}\cdot}{\mathrm{d}\lambda} = \frac{\partial\cdot}{\partial\eta} + n^i\frac{\partial\cdot}{\partial x^i} \ , \tag{6.17}$$

Eq. (6.8) gives, upon direct integration:

$$\alpha_0 - \alpha_E = -2\left(\Phi_0 - \Phi_E\right) + \int_{\bar{\eta}_E}^{\bar{\eta}_0}\frac{\partial}{\partial\eta}\left(\Phi + \Psi\right)\left[\vec{x}(\eta), \eta\right]\mathrm{d}\eta \ . \tag{6.18}$$

Finally, we get:

Sachs-Wolfe formula

$$\begin{aligned}\Theta\left[\vec{x}_0, \eta_0, \vec{e}\right] =& \frac{1}{4}\delta_r\left[\vec{x}_E, \bar{\eta}_E\right] + \Phi\left[\vec{x}_E, \bar{\eta}_E\right] - \Phi\left[\vec{x}_0, \bar{\eta}_0\right] - n^i\partial_i V_b\left[\vec{x}_E, \bar{\eta}_E\right] + n^i\partial_i V_b\left[\vec{x}_0, \bar{\eta}_0\right] \\ &+ \int_{\bar{\eta}_E}^{\bar{\eta}_0}\left(\Phi + \Psi\right)'\left[\vec{x}(\eta), \eta\right]\mathrm{d}\eta \ .\end{aligned} \tag{6.19}$$

In this formula, we can distinguish three terms:

- $\Theta^{\mathrm{SW}}\left[\vec{x}_E, \bar{\eta}_E\right] = \frac{1}{4}\delta_r\left[\vec{x}_E, \bar{\eta}_E\right] + \Phi\left[\vec{x}_E, \bar{\eta}_E\right] - \Phi\left[\vec{x}_0, \bar{\eta}_0\right]$ is the *Sachs-Wolfe term*. $\delta_r/4$ translates the fact that denser regions of the last scattering surface are hotter by virtue of the Stefan-Boltzmann law, while $\Phi_E - \Phi_0$ is here to take into account the additional redshift experienced by a photon trying to escape a local potential well on the last scattering surface and reaching the local potential well at the observer (Einstein effect).

- $\Theta^{\mathrm{Doppler}} = -n^i\partial_i V_b\left[\vec{x}_E, \bar{\eta}_E\right] + n^i\partial_i V_b\left[\vec{x}_0, \bar{\eta}_0\right]$ is a *Doppler term* taking into account the fact that emitter and receiver are moving with respect to the homogeneous and isotropic background.

- $\Theta^{\mathrm{ISW}} = \int_{\bar{\eta}_E}^{\bar{\eta}_0}\left(\Phi + \Psi\right)'\left[\vec{x}(\eta), \eta\right]\mathrm{d}\eta$ is the *Integrated Sachs-Wolfe term*. It depends on the entire photon history and receives contribution from two sources: locally forming non-linear

structures with an evolving potential well, and exotic energy content or a cosmological constant. Linear structures on large scales in the matter dominated phase do not contribute to this term as $\Phi = \Psi$ is constant in that case. Therefore, on large scales, this term is an unambiguous signature of dark energy.

6.1.2 The CMB angular power spectrum

In order to analyse the anisotropies of the CMB, it is convenient to expand the temperature fluctuation field on the sky. We start by relating the fields in real space to their counterparts in Fourier space:

$$\Theta\left[\vec{x}_0, \eta_0, \vec{e}\right] = \int \frac{\mathrm{d}^3 k}{(2\pi)^3} \mathrm{e}^{\mathrm{i}\vec{k}\cdot\vec{x}_0} \hat{\Theta}\left(\vec{k}, \eta_0, \vec{e}\right) \ . \tag{6.20}$$

Then, we expand the Fourier modes onto the sky using Legendre polynomials, $P_l(x)$:

$$\hat{\Theta}\left(\vec{k}, \eta_0, \vec{e}\right) = \sum_{l=0}^{+\infty} (-\mathrm{i})^l \hat{\Theta}_l\left(\eta_0, \vec{k}\right) P_l\left(\mu\right) \ , \tag{6.21}$$

where we introduced the variable $\mu = \frac{\vec{k}\cdot\vec{e}}{k}$, i.e. the cosine of the angle between $\vec{k}$ and $\vec{e}$. Then, we may want to introduce transfer functions $\hat{\Theta}_l(k)$ such that:

$$\hat{\Theta}_l\left(\eta_0, \vec{k}\right) = \hat{\Theta}_l(k)\zeta\left(\vec{k}\right) \ . \tag{6.22}$$

These transfer functions relate the moment of order l in the temperature fluctuations to the curvature fluctuations at the end of inflation. If we define the *angular two point correlation in the temperature fluctuations*:

$$C(\theta) = \left\langle \Theta\left(\vec{x}_0, \eta_0, \vec{e}_1\right) \Theta\left(\vec{x}_0, \eta_0, \vec{e}_2\right) \right\rangle \ , \tag{6.23}$$

where θ is the angle between the directions $\vec{e}_1$ and $\vec{e}_2$, we can also define its *angular power spectrum*, C_l such that:

$$C(\theta) = \sum_{l=0}^{+\infty} \frac{2l+1}{4\pi} C_l P_l\left(\cos\theta\right) \ . \tag{6.24}$$

Then, C_l measures the variance of $\Theta\left(\vec{x}_0, \eta_0, \vec{e}\right)$ on an angular scale π/l.
Plugging the relation (6.21) into the definition od $C(\theta)$, Eq. 6.23, we can get:

$$C\left(\theta\right) = \frac{1}{(2\pi)^3} \int k^2 \mathrm{d}k \mathcal{P}_\zeta(k) \sum_l \sum_{l'} (-i)^{l+l'} \hat{\Theta}_l(k) \hat{\Theta}_l(k') \int \mathrm{d}^2\hat{k} P_l\left(\hat{\vec{k}} \cdot \vec{e}_1\right) P_{l'}\left(\hat{\vec{k}} \cdot \vec{e}_2\right) \ , \tag{6.25}$$

where $\vec{\hat{k}} = \vec{k}/k$. Then, using that:

$$P_l(\vec{u}\cdot\vec{v}) = \frac{4\pi}{2l+1}\sum_{m=-l}^{l} Y_{lm}(\theta,\varphi)Y^*_{lm}(\theta',\varphi') \ , \tag{6.26}$$

where (θ,φ) are the spherical angles corresponding to the unit vector $\vec{u}$ and (θ',φ') those of the unit vector $\vec{v}$, the orthogonality relations between spherical harmonics lead to:

$$\int \mathrm{d}^2\hat{k} P_l\left(\vec{\hat{k}}\cdot\vec{e}_1\right) P_{l'}\left(\vec{\hat{k}}\cdot\vec{e}_2\right) = \frac{4\pi}{2l+1} P_l\left(\vec{e}_1\cdot\vec{e}_2\right)\delta_{ll'} \ . \tag{6.27}$$

Therefore, all calculations done, and comparing the result to Eq. (6.24) :

$$C_l = \frac{2}{(2l+1)^2\pi}\int k^2\mathrm{d}k\mathcal{P}_\zeta(k)\left|\Theta_l(k)\right|^2 \ . \tag{6.28}$$

Using some more algebra, and neglecting the terms evaluated purely at $(\vec{x}_0,\eta_0)$, which are not observable in the power spectrum of fluctuations, we can get, for each term:[3]

$$\hat{\Theta}_l^{\mathrm{SW}}\left(\eta_0,\vec{k}\right) = (2l+1)\left[\frac{1}{4}\hat{\delta}_r\left(\vec{k},\eta_E\right)+\hat{\Phi}\left(\vec{k},\eta_E\right)\right] j_l\left(k\Delta\eta\right) \tag{6.29}$$

$$\hat{\Theta}_l^{\mathrm{Doppler}}\left(\eta_0,\vec{k}\right) = -\left(2l+1\right)\frac{\hat{V}_b\left(\vec{k},\eta_E\right)}{k} j_l'(k\Delta\eta) \tag{6.30}$$

$$\hat{\Theta}_l^{\mathrm{ISW}}\left(\eta_0,\vec{k}\right) = (2l+1)\int_{\eta_E}^{\eta_0}\left(\hat{\Phi}\left(\vec{k},\eta\right)+\hat{\Psi}\left(\vec{k},\eta\right)\right)' j_l(k\Delta\eta)\mathrm{d}\eta \ , \tag{6.31}$$

where we set $\Delta\eta = \eta_0 - \eta_E$. Calculating C_l becomes then a matter of finding a way to connect the matter and metric variables $\hat{\delta}_r$, $\hat{V}_b$ and $\hat{\Phi}$ and $\hat{\Psi}$ to the initial fluctuations $\hat{\zeta}(k)$, after which one can plug these into Eq. (6.28). This is fairly involved but possible in principle. Just to illustrate some important points, let us look at a few physically important terms in that expression.

6.1.3 Properties of the CMB angular power spectrum

On large scales, the dominant term in the auto-correlation of the Sachs-Wolfe term:

$$C_l^{\mathrm{SW}} = \frac{2}{(2l+1)^2\pi}\int k^2\mathrm{d}k\mathcal{P}_\zeta(k)\left|\Theta_l^{\mathrm{SW}}(k)\right|^2 \ . \tag{6.32}$$

[3] The key is to realise that:

$$\mathrm{e}^{\mathrm{i}k\Delta\eta\mu} = \sum_{l=0}^{+\infty}(2l+1)(-i)^l j_l(k\Delta\eta)P_l(\mu) \ .$$

Since we restrict our discussion on large scales, which only enter the Hubble radius during the matter-dominated era, we have $k \ll k_{\rm eq}$. In that case, for adiabatic initial conditions, we get $\hat{\delta}_r = \frac{4}{3}\hat{\delta}_m = \frac{4}{3}\left(-2\hat{\Phi}\right) = -\frac{8}{3}\hat{\Phi}$, so that:

$$\hat{\Theta}_l^{\rm SW}\left(\vec{k},\eta_0\right) = \frac{2l+1}{3}\hat{\Phi}\left(\vec{k},\eta_E\right) j_l\left(k\Delta\eta\right) = -\frac{2l+1}{3}T_\Phi(k,\eta_E)\zeta(\vec{k}) j_l\left(k\Delta\eta\right) \ . \tag{6.33}$$

Thus, using that on scales larger than the equality scale, $T_\varphi(k,\eta_E) = 3/5$, we get, for a scale invariant primordial power spectrum[4]:

$$l(l+1)C_l^{\rm SW} = \frac{18A_S}{25\pi} \ . \tag{6.34}$$

The Sachs-Wolfe plateau, visible at small l on Fig. 6.1 is dominated by this term and its amplitude gives a direct access to the primordial amplitude of fluctuations, A_S.

On intermediate and small scales, one needs to follow the dynamics of the coupled baryon/photon fluid. This is done via a refined version of the model used in section 5.8. The continuity and Euler equations for baryons and photons can be obtained from the full Boltzmann equations (see below) and read:

- For radiation:

$$\hat{\delta}_r' = \frac{4}{3}k^2\hat{V}_r + 4\Phi' \tag{6.35}$$

$$\hat{V}_r' = -\frac{1}{4}\hat{\delta}_r - \Phi + \frac{1}{6}k^2\hat{\pi}_r + \tau'\left(\hat{V}_b - \hat{V}_r\right) \ , \tag{6.36}$$

  where $\hat{\pi}_r/6 = -16\hat{V}_r/45\tau'$ is the anisotropic stress and $\tau' = an_e\sigma_T$ is the differential optical depth associated with Thomson scattering (see next section on kinetic theory for details).

- For baryons:

$$\hat{\delta}_b' = k^2\hat{V}_b + 3\hat{\Phi}' \tag{6.37}$$

$$\hat{V}_b' = -\mathcal{H}\hat{V}_b - \hat{\Phi} + \frac{\tau'}{R}\left(\hat{V}_r - \hat{V}_b\right) \ , \tag{6.38}$$

  where

$$R(\eta) = \frac{3\bar{\rho}_b(\eta)}{4\bar{\rho}_r(\eta)} = \frac{3\Omega_{b,0}}{4\Omega_{r,0}(1+z)} \ . \tag{6.39}$$

[4] One needs to use that:

$$\int \frac{{\rm d}k}{k} j_l^2(k\Delta\eta) = \frac{1}{2l(l+1)} \ .$$

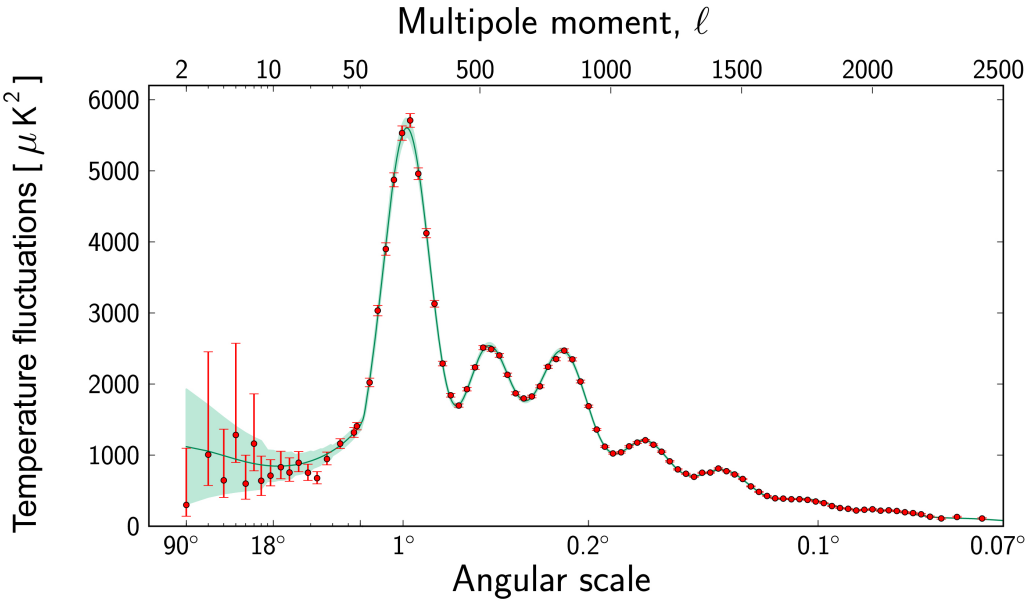

Figure 6.1: Angular power spectrum of temperature anisotropies, $\bar{T}_0^2 l(l+1)C_l/2\pi$ as measured by the Planck satellite (red dots). The blue curve represents the best ΛCDM fit to the data. Credits: ESA/Planck

At intermediate scales, we can assume that the typical length scale of the mode, k^{-1} is large compared to the characteristic scale $1/\tau'$. Then, we can look for a solution to the dynamics in terms of an expansion order by order in the small parameter k/τ'. At leading order, neglecting anisotropic pressure, we get:

$$\hat{V}_r = \hat{V}_b \quad \text{and} \quad \hat{\delta}'_r = \frac{4}{3}\hat{\delta}'_b \,, \tag{6.40}$$

the second equation implying that the mixing entropy of the coupled fluid remains constant during the evolution. This is known as the *tight coupling limit*. We can then combine the equations to arrive at:

$$\left[(1+R)\hat{V}_r\right]' = -\frac{1}{4}\hat{\delta}_r - (1+R)\Phi \,, \tag{6.41}$$

and:

$$\hat{\delta}''_r + \frac{R'}{1+R}\hat{\delta}'_r + kc_s^2\hat{\delta}_r = 4\left(\hat{\Phi}'' + \frac{R'}{1+R}\hat{\Phi} - \frac{1}{3}k^2\hat{\Phi}\right) \,, \tag{6.42}$$

where

$$c_s^2 = \frac{1}{3(1+R)} \tag{6.43}$$

is the square of the sound speed in the coupled fluid. This is the equation of a damped, forced oscillator. Pseudo-oscillations occur at a pulsation $\omega_s = kc_s$. A solution can be extracted using a WKB approach, in which we suppose that the amplitude of the solution varies slowly compared to its phase. In that case, at leading order, the general solution of Eq. (6.42) is given by[5]:

$$\begin{aligned}[1+R(\eta)]^{1/4}\,\hat{\delta}_r\left(\vec{k},\eta\right) =& \hat{\delta}_r\left(\vec{k},0\right)\cos\left[kr_s(\eta)\right] + \frac{\sqrt{3}}{k}\left[\hat{\delta}'_r\left(\vec{k},0\right) + \frac{R'(0)}{4}\hat{\delta}_r(\vec{k},0)\right]\sin\left[kr_s(\eta)\right] \\ &+ \frac{4\sqrt{3}}{k}\int_0^\eta [1+R(\eta')]^{3/4}\sin\left[kr_s(\eta) - kr_s(\eta')\right]F(\eta')\mathrm{d}\eta' \,,\end{aligned} \tag{6.44}$$

where we set:

$$F(\eta) = 4\left(\hat{\Phi}'' + \frac{R'}{1+R}\hat{\Phi} - \frac{1}{3}k^2\hat{\Phi}\right) \,. \tag{6.45}$$

The quantity:

$$r_S(\eta) = \int_0^\eta c_s(\eta')\mathrm{d}\eta' \tag{6.46}$$

is the radius of the acoustic horizon, i.e. the distance travelled by acoustic waves in the primordial plasma between the Big Bang and time η. If, for simplicity, we suppose that R = cst and $\hat{\Phi}$ = cst,

[5] One first needs to find the two independent general solutions without the forcing term and then use some variations of constants to find the particular solution with the forcing term.

we can get the Sachs-Wolfe term:

$$\hat{\Theta}^{\mathrm{SW}}\left(\vec{k},\eta_0,\vec{e}\right) = C_1\cos\left(kr_s(\eta)\right) + C_2\sin(kr_s(\eta)) - R\hat{\Phi}\ , \tag{6.47}$$

for some constants C_1 and C_2 fixed by initial conditions. This has the same formal form as the solution found without explicit baryon-photon coupling is section 5.8, the only differences being in the expression for r_s and the amplitude of the forcing. Qualitatively, though, the analysis we did of the positions of the peaks remain valid and will not be redone here. The Doppler term can be estimated similarly, and one finds an oscillatory behaviour, but in quadrature with respect to the Sachs-Wolfe term. For small R, i.e. at early times, the amplitude of both terms are comparable and oscillations are strongly suppressed. For large R however, the amplitude of the Doppler term is suppressed with respect to the amplitude of the Sachs-Wolfe term, thus, the spectrum exhibits some oscillations, albeit smaller ones that expected from the pure Sachs-Wolfe term. Finally, note that the hypothesis that R and $\hat{\Phi}$ are constant is not a good approximation. When taking that into account, the general solution ought to be used.

Finally, let us comment on what happens on small scales, where k/τ' is not longer infinitely small and we need to go beyond the tight-coupling limit. These scales entered the Hubble radius deep into the radiation dominated period, thus the gravitational potential on those scales has been significantly reduced compared to its primordial, large-scale value. Moreover, the characteristic time of acoustic oscillations is much shorter than the Hubble time. Therefore, for a rough, qualitative analysis, we can neglect potential terms as well as those proportional to $\mathcal{H}$ and the time dependence in R. The Euler equations then become simply:

$$\hat{V}_b' = \frac{\tau'}{R}\left(\hat{V}_r - \hat{V}b\right) \tag{6.48}$$

$$\hat{V}_r' = -\frac{1}{4}\hat{\delta}_r - \frac{16}{45}\frac{k^2}{\tau'}\hat{V}_r - \tau'\left(\hat{V}_r - \hat{V}_b\right)\ . \tag{6.49}$$

To go beyond the tight coupling limit, at leading order, we will retain terms proportional to $1/\tau'$ but neglect higher powers of $(1/\tau')$. First taking the difference between the two Euler equations, we get:

$$\hat{V}_r' - \hat{V}_b' = -\frac{1}{4}\hat{\delta}_r - \frac{16}{45}\frac{k^2}{\tau'}\hat{V}_r - \tau'\frac{1+R}{R}\left(\hat{V}_r - \hat{V}_b\right)\ . \tag{6.50}$$

Taking the formal limit $\tau' \to +\infty$, we recover the tight coupling limit so that $\hat{V}_r = \hat{V}_b$, and we learn that:

$$\frac{1}{4}\hat{\delta}_r = -\frac{1+R}{R}\tau'\left(\hat{V}_r - \hat{V}_b\right)\ . \tag{6.51}$$

Thus, we can write:

$$\hat{V}_r' + R\hat{V}_b' = (1+R)\hat{V}_r' + R\left(\hat{V}_b - \hat{V}_r\right)' \tag{6.52}$$

$$= -\frac{1}{4}\hat{\delta}_r - \frac{16}{45}\frac{k^2}{\tau'}\hat{V}_r \ , \tag{6.53}$$

so that, differentiating Eq. (6.51) and keeping only the leading order term to replace $\left(\hat{V}_b - \hat{V}_r\right)'$:

$$\hat{V}_r' = -\frac{1}{4(1+R)}\hat{\delta}_r - \frac{16k^2}{45(1+R)\tau'}\hat{V}_r - \frac{R^2}{4(1+R)^2\tau'}\hat{\delta}_r' \ . \tag{6.54}$$

Finally, using the continuity equation:

$$\hat{\delta}_r' = \frac{4k^2}{3}\hat{V}_r \ , \tag{6.55}$$

we get:

Evolution of the radiation density contrast

$$\hat{\delta}_r'' + \frac{k^2c_s^2}{\tau'}\left(\frac{16}{25} + \frac{R^2}{1+R}\right)\hat{\delta}_r' + k^2c_s^2\hat{\delta}_r = 0 \ . \tag{6.56}$$

This is the equation of a damped harmonic oscillator, whose WKB solutions go like:

$$\hat{\delta}_r \propto \exp\left[-\frac{k^2}{k_0^2}\right]\exp\left[\pm \mathrm{i}kr_s\right] \ , \tag{6.57}$$

with:

$$k_0^2 = \frac{1}{6}\int_0^\eta \left[\frac{1}{1+R}\left(\frac{16}{25} + \frac{R^2}{1+R}\right)\right]\frac{\mathrm{d}\eta'}{\tau'} \ . \tag{6.58}$$

The integrand varies very little over the history of the universe (between 16/25 and 1). Reasonable estimates of this damping scales show that this Silk damping starts being efficient for multipoles above $l \sim 140$, i.e. before the first peak. Peaks above $l = 2000$ are completely suppressed.

6.2 Kinetic theory

In practise, the rough work presented in the previous section cannot give us more than some semi-qualitative handle on some aspects of the CMB angular power spectrum, because in order to achieve analyticity, it requires a series of approximation to relate the temperature multipoles to initial conditions. In order to go further, one needs to employ the full strenght of the Boltzmann equation.

6.2.1 Boltzmann equation in a perturbed universe

The collective behaviour of photons is described by a distribution function $f\left(x^\mu, k_\mu\right)$ over phase-space, parametrised by the 4-position x^μ and the associated 4-momentum k_μ. We introduce the natural split of spacetime into spatial 3-hypersurfaces parametrised by the conformal time coordinate η, so that $x^\mu = \left(\eta, x^i\right)$. These hypersurfaces of constant η are fully characterised by their normal vector field:

$$N^\mu = \frac{1}{a}\left(1-\Phi\right)\delta^\mu{}_0 \,, \tag{6.59}$$

which is nothing but the 4-velocity of observers at constant x^i with clocks ticking at the rate $(1+\Phi)\mathrm{d}t$. The position of photons being marked by $x^\mu = \left(\eta, x^i\right)$, there is a natural associated split for the 4-momentum:

$$k^\mu = \frac{E}{a}\left[(1-\Phi)\delta^\mu{}_0 + (1+\Psi)n^i\delta^\mu{}_i\right] \,, \tag{6.60}$$

where $E = -g_{\mu\nu}k^\mu N^\nu$ is the energy of the photons measured by observers with 4-velocity N^μ and $\vec{n}$ is the instantaneous direction of propagation of photons, obeying $\delta_{ij}n^i n^j = 1$. The momentum of photons is thus entirely characterised by teh functions of spacetime E and n^i. Then, it is natural to write:

$$f\left(x^\mu, k_\mu\right) = f\left(\eta, x^i, E, n^j\right) \tag{6.61}$$

$$= \bar{f}\left(\eta, E\right) + \delta f\left(\eta, x^i, E, n^j\right) \,, \tag{6.62}$$

where $\bar{f}\left(\eta, E\right)$ is the homogeneous and isotropic distribution function in FLRW (which cannot depend on position or direction of propagation by symmetries) and $\delta f\left(\eta, x^i, E, n^j\right)$ is the first order correction coming from inhomogeneities. Then, the Boltzmann equation along photon trajectories read:

$$\frac{\mathrm{d}}{\mathrm{d}\eta} f\left(\eta, x^i(\eta), E(\eta), n^i(\eta)\right) = C\left[f\right] \,. \tag{6.63}$$

On the RHS, $C\left[f\right]$ is called the collision term and it encodes interactions of photons with other particles. Here, it will take into account Thomson scattering off the electrons and will be described later. First, let us concentrate on the LHS. Clearly, the variables x^i, E and n^i depend on η in the sense that a given conformal time η, a given photon occupies a spatial position x^i, with a given energy E and direction of propagation n^i. Thus, we have that:

$$\frac{\mathrm{d}f}{\mathrm{d}\eta} = \frac{\partial f}{\partial \eta} + \frac{\mathrm{d}x^i}{\mathrm{d}\eta}\frac{\partial f}{\partial x^i} + \frac{\mathrm{d}E}{\mathrm{d}\eta}\frac{\partial f}{\partial E} + \frac{\mathrm{d}n^i}{\mathrm{d}\eta}\frac{\partial f}{\partial n^i} \,. \tag{6.64}$$

Next, we need to use the geodesic equation for photons:

$$\frac{\mathrm{d}k^\mu}{\mathrm{d}\lambda} = -\Gamma^\mu{}_{\nu\rho} k^\nu k^\rho \ . \tag{6.65}$$

At order 0, this leads to:

$$\bar{E}' + \mathcal{H}\bar{E} = 0 \tag{6.66}$$

$$\frac{\mathrm{d}\bar{n}^i}{\mathrm{d}\eta} = 0 \ , \tag{6.67}$$

where we used that $\mathrm{d}\eta = \bar{k}^0 \mathrm{d}\lambda$ along the photon path. Note that since $\frac{\partial f}{\partial n^i}$ is at most of order 1 by symmetries, this implies that we only need to know $\frac{\mathrm{d}n^i}{\mathrm{d}\eta}$ at order 0. Since it is zero at that order, we have:

$$\frac{\mathrm{d}f}{\mathrm{d}\eta} = \frac{\partial f}{\partial \eta} + \frac{\mathrm{d}x^i}{\mathrm{d}\eta}\frac{\partial f}{\partial x^i} + E'\frac{\partial f}{\partial E} \ . \tag{6.68}$$

With the same reasoning, we now need to evaluate $\frac{\mathrm{d}x^i}{\mathrm{d}\eta}$ at order 0 and E' at order 1. Clearly:

$$\frac{\mathrm{d}\bar{x}^i}{\mathrm{d}\eta} = \frac{\bar{k}^i}{\bar{k}^0} = n^i \ , \tag{6.69}$$

so that:

$$\frac{\mathrm{d}f}{\mathrm{d}\eta} = \frac{\partial f}{\partial \eta} + n^i\frac{\partial f}{\partial x^i} + E'\frac{\partial f}{\partial E} \ . \tag{6.70}$$

To find E' at order 1 we need to write the geodesic equation at that order. Some simple algebra shows that:

$$E' = E\left[-\mathcal{H} - n^i\partial_i\Phi + \Psi'\right] \ . \tag{6.71}$$

Therefore, the Boltzmann equation at first order is:

Boltzmann equation at first order

$$\frac{\partial f}{\partial \eta} + n^i\frac{\partial f}{\partial x^i} - E\left[\mathcal{H} + n^i\partial_i\Phi - \Psi'\right]\frac{\partial f}{\partial E} = C\left[f\right] \ . \tag{6.72}$$

By decomposing the distribution function, we get:

$$\frac{\partial \bar{f}}{\partial \eta} - \mathcal{H}E\frac{\partial \bar{f}}{\partial E} = 0 \tag{6.73}$$

$$\frac{\partial \delta f}{\partial \eta} + n^i\frac{\partial \delta f}{\partial x^i} - \mathcal{H}E\frac{\partial \delta f}{\partial E} - \left[n^i\partial_i\Phi - \Psi'\right]\frac{\partial \bar{f}}{\partial E} = C\left[\delta f\right] \ , \tag{6.74}$$

where we wrote that photons were free particles at order 0. In the background, photons follows Bose-Einstein distribution with:

$$\bar{f}(\eta, E) = \frac{1}{\mathrm{e}^{E/k_B T(\eta)} - 1} , \tag{6.75}$$

Therefore, Eq. (6.73) leads to:

$$\frac{T'}{T} = -\mathcal{H} \implies T \propto a^{-1} , \tag{6.76}$$

as expected. At first order, we can always assume that:

$$f\left(\eta, x^i, E, n^j\right) = \frac{1}{\mathrm{e}^{E/k_B T\left(\eta, x^i, n^j\right)} - 1} . \tag{6.77}$$

Then, we define the temperature fluctuations $\Theta\left(\eta, x^i, n^j\right)$ via:

$$T\left(\eta, x^i, n^j\right) = \bar{T}(\eta)\left[1 + \Theta\left(\eta, x^i, n^j\right)\right] . \tag{6.78}$$

Then:

$$f\left(\eta, x^i, E, n^j\right) = \bar{f}(\eta, E) - E\frac{\partial \bar{f}}{\partial E}\Theta\left(\eta, x^i, n^j\right) . \tag{6.79}$$

Note that we assumed without proof that Θ did not explicitly depend on E. This can be justified once $C[f]$ has been introduced, and corresponds to assuming that spectral distortions are negligible.

6.2.2 Macroscopic quantities

Using the distribution function, one can define a set of macroscopic quantities describing the gas of photons. We shall start with fluid quantities coming from the energy-momentum tensor of the photon gas:

$$T^{\mu\nu}(x^\alpha) = \int k^\mu k^\nu f\left(x^\alpha, k^\beta\right) E\frac{\mathrm{d}E\mathrm{d}^2 n}{(2\pi)^3} . \tag{6.80}$$

Details of this construction can be found in [19]. With this expression and the usual definitions we can find the expressions for the energy density, pressure and anisotropic stress measured by observers comoving with the photon gas, with 4-velocity u^μ:

$$\begin{cases} \rho_r = \int \left(k^\mu u_\mu\right)^2 f\dfrac{E\mathrm{d}E\mathrm{d}^2 n}{(2\pi)^3} & (6.81) \\ P_r = \dfrac{1}{3}\displaystyle\int k^\mu k^\nu h_{\mu\nu} f\frac{E\mathrm{d}E\mathrm{d}^2 n}{(2\pi)^3} = \frac{1}{3}\rho_r & (6.82) \\ \Pi^{\mu\nu} = \displaystyle\int k^\alpha k^\beta \left[h^\mu{}_\alpha h^\nu_\beta - \frac{1}{3}h_{\alpha\beta}h^{\mu\nu}\right] f\frac{E\mathrm{d}E\mathrm{d}^2 n}{(2\pi)^3} , & (6.83) \end{cases}$$

where we introduced the projector onto the observer's restframe: $h_{\mu\nu} = g_{\mu\nu} + u_\mu u_\nu$. Using $u^\mu = a\,(-1-\Phi)\,\delta^\mu{}_0 + a v_r^i \delta^\mu{}_i$, we get:

$$\int \bar{f} n^i \mathrm{d}^2 n = 0 \;\text{ by isotropy of the background.} \tag{6.84}$$

Besides:

$$\begin{cases} \delta\rho_r = \displaystyle\int \delta f E^3 \frac{\mathrm{d}E\mathrm{d}^2 n}{(2\pi)^3} & (6.85) \\ (\rho_r + P_r)\, v_r^i = \displaystyle\int n^i \delta f E^3 \frac{\mathrm{d}E\mathrm{d}^2 n}{(2\pi)^3} & (6.86) \\ \Pi_r^{ij} = P_r \pi_r^{ij} = \displaystyle\int n^{ij} \delta f E^3 \frac{\mathrm{d}E\mathrm{d}^2 n}{(2\pi)^3}\,, & (6.87) \end{cases}$$

with $n^{ij} = n^i n^j - \frac{1}{3}\delta^{ij}$. The next macroscopic quantity we introduce is called brightness, or luminous intensity:

$$I\left(\eta, x^i, n^j\right) = \int E^3 f\left(\eta, x^i, E, n^j\right) \frac{\mathrm{d}E}{2\pi^2}\,. \tag{6.88}$$

It is the energy density of the fluid, per unit solid angle travelling along the direction n^j at a point (η, x^i). Clearly, we have that the energy density at a given point is the monopole of the brightness:

$$\rho_r\left(\eta, x^i\right) = \int \frac{\mathrm{d}^2 n}{4\pi} I\left(\eta, x^i, n^j\right)\,. \tag{6.89}$$

Then, decomposing as usual in background and perturbation: $I = \bar{I} + \delta I$, we get:

$$\begin{cases} \bar{I} = \displaystyle\int E^3 \bar{f}\left(\eta, E\right) \frac{\mathrm{d}E}{2\pi^2} & (6.90) \\ \delta I = 4\pi \displaystyle\int E^3 \delta f\left(\eta, x^i, E, n^j\right) \mathrm{d}E\,. & (6.91) \end{cases}$$

Using Eq. (6.73), we get immediately that:

$$\bar{I}' + 4\mathcal{H}\bar{I} = 0\,, \tag{6.92}$$

so that:

$$\bar{I} = \bar{\rho}_r\,. \tag{6.93}$$

We can also write:

$$C[\delta I] = \int C\left[\delta f\right] E^3 \frac{\mathrm{d}E}{2\pi^2}\,, \tag{6.94}$$

so that integrating Eq. (6.74), we get:

$$\delta I' + n^i \partial_i \delta I + 4\mathcal{H}\delta^i + 4\left[n^i \partial_i \Phi - \Psi'\right] \bar{I} = C\left[\delta I\right] \ . \tag{6.95}$$

Moreover:

$$\delta f = -E \frac{\partial \bar{f}}{\partial E} \Theta \ , \tag{6.96}$$

so that:

$$\delta I = -\int E^4 \frac{\partial \bar{f}}{\partial E} \Theta \frac{\mathrm{d}E}{2\pi^2} \tag{6.97}$$

$$= -\Theta \int E^4 \frac{\partial \bar{f}}{\partial E} \frac{\mathrm{d}E}{2\pi^2} \quad \text{since } \Theta \text{ is independent of } E \tag{6.98}$$

$$= 4\Theta \bar{I} \quad \text{(Integration by part)} \ . \tag{6.99}$$

Thus, we find that:

$$\Theta = \frac{1}{4} \frac{\delta I}{\bar{I}} \ . \tag{6.100}$$

Thus, taking the monopole:

$$\Theta_0\left(\eta, x^i\right) = \int \Theta\left(\eta, x^i, n^j\right) \frac{\mathrm{d}^2 n}{4\pi} = \frac{1}{4} \delta_r\left(\eta, x^i\right) \ . \tag{6.101}$$

Finally, the Bolztmann equation gives us the equation obeyed by the temperature fluctuations:

Evolution of temperature fluctuations

$$\Theta' + n^i \partial_i \Theta + n^i \partial_i \Phi - \Psi' = C\left[\Theta\right] \ , \tag{6.102}$$

with:

$$C\left[\Theta\right] = \frac{C[\delta I]}{4\bar{I}} \ . \tag{6.103}$$

6.2.3 Collision term

Before recombination, photons are coupled to electrons via Thomson scattering. Let us consider a beam of photons travelling in a gas of free electrons with number density n_e. Then, along a little distance $\mathrm{d}l$, the flux of photons vary as:

$$\mathrm{d}\phi = -n_e \sigma_T \phi \mathrm{d}l = -a(\eta) n_e \sigma_T \phi \mathrm{d}\chi \ , \tag{6.104}$$

where σ_T is the cross section of Thomson scattering (dimension sof L^2). The optical depth of the plasma τ is defined by:

$$\tau = \ln\left(\frac{\phi_{\text{received}}}{\phi_{\text{transmitted}}}\right) , \tag{6.105}$$

where ϕ_{received} is the flux received by a layer of plasma and $\phi_{\text{transmitted}}$ is the one exiting the layer. Clearly:

$$\mathrm{d}\tau = -\frac{\mathrm{d}\phi}{\phi} , \tag{6.106}$$

so that we defined the *differential optical depth* (dimensions of T^{-1}):

$$\tau' = \frac{\mathrm{d}\tau}{\mathrm{d}\eta} = c\frac{\mathrm{d}\tau}{\mathrm{d}\chi} = can_e\sigma_T = can_bX_e\sigma_T . \tag{6.107}$$

Then, one can show (see [16] for details) that:

$$C\left[\Theta\right] = \tau'\left[\Theta_0 - \Theta + n_iV_b^i + \frac{1}{16}\Pi_{ij}^r n^i n^j\right] , \tag{6.108}$$

where V_b is the velocity potential of baryons.

6.2.4 Legendre expansion and hierarchy

Going to Fourier space:

$$\Theta\left(\eta, x^i, n^j\right) = \frac{1}{(2\pi)^3}\int \hat{\Theta}(\eta, k^i, n^j)\mathrm{e}^{\mathrm{i}\vec{k}\cdot\vec{x}}\mathrm{d}^3k , \tag{6.109}$$

we can rewrite Eq. (6.102) as:

$$\hat{\Theta}' + \mathrm{i}k\mu\left[\hat{\Theta} + \hat{\Phi}\right] = \hat{\Psi}' + \tau'\left[\hat{\Theta}_0 - \hat{\Theta} + \mathrm{i}k\mu\hat{V}_b + \frac{1}{16}\hat{\Pi}_{ij}^r n^i n^j\right] . \tag{6.110}$$

where $\mu = \frac{\vec{k}\cdot\vec{n}}{k}$. Then, we define the transfer functions of each mode, as before:

$$\hat{\Theta}\left(\eta, k^i, n^i\right) = \hat{\Theta}\left(\eta, k, \mu\right)\zeta\left(\vec{k}\right) , \tag{6.111}$$

and we proceed to decompose the Fourier modes into Legendre polynomials:

$$\hat{\Theta}\left(\eta, k, \mu\right) = \sum_{i=0}^{+\infty}(-i)^l\Theta_l\left(\eta, k\right)P_l(\mu) . \tag{6.112}$$

Noting the identy:

$$(l+1)P_{l+1}(\mu) = (2l+1)\mu P_l(\mu) - lP_{l-1}(\mu) , \tag{6.113}$$

we get that:

$$\mathrm{i}k\mu\hat{\Theta} = k\zeta\left(\vec{k}\right)\sum_{l=0}^{+\infty}(-i)^l\left[\frac{l+1}{2l+3}\Theta_{l+1} - \frac{l}{2l-1}\Theta_{l-1}\right]P_l \ . \tag{6.114}$$

We also notice that ($P_0(\mu) = 1$):

$$\hat{\Psi}' + \tau'\Theta_0 = \left(\hat{\Psi}' + \tau'\Theta_0\right)P_0(\mu) \ , \tag{6.115}$$

and that:

$$\mathrm{i}\ k\mu\tau'\hat{V}_b = -(-\mathrm{i})^1 k\hat{V}_b P_1(\mu) \ . \tag{6.116}$$

Finally some careful algebra leads to:

$$\frac{1}{16}\hat{\Pi}^r_{ij}n^i n^j = (-\mathrm{i})^2\frac{\Theta_2\zeta}{10}P_2(\mu) \ . \tag{6.117}$$

With these relations at hand, we can now write:

Boltzmann hierarchy for the temperature fluctuation multipoles

$$\begin{cases} \Theta_0' = -\dfrac{k}{3}\Theta_1 + \hat{\Psi}' & (6.118) \\ \Theta_1' = k\left(\Theta_0 - \dfrac{2}{5}\Theta_2 + \hat{\Phi}\right) - \tau'\left(k\hat{V}_b + \Theta_1\right) & (6.119) \\ \Theta_2' = k\left(\dfrac{2}{3}\Theta_1 - \dfrac{3}{7}\Theta_3\right) - \dfrac{9}{10}\tau'\Theta_2 & (6.120) \\ \Theta_l' = k\left(\dfrac{l}{2l-1}\Theta_{l-1} - \dfrac{l+1}{2l+3}\Theta_{l+1}\right) - \tau'\Theta_l \quad \text{for } l \geq 3 \ . & (6.121) \end{cases}$$

Note the slight abuse of notations here, where we used the metric and velocity potentials instead of their transfer functions, to keep expressions simple and on par with the literature. As expected, the metric potential only contribute to the monopole and dipole evolutions, and baryons appear only in the dipole equation. Finally, the collision term is always the same for $l > 2$. We have the remarkable identities (still keeping quantities rather than their transfer functions on the RHS):

$$\begin{cases} \Theta_0 = \dfrac{1}{4}\hat{\delta}_r & (6.122) \\ \Theta_1 = -kV_b & (6.123) \\ \Theta_2 = \dfrac{5}{12}k^2\pi_r \ . & (6.124) \end{cases}$$

This shows that the first two equations of the hierarchy are nothing but the continuity and Euler equations of the fluid description. This hierarchy is solved numerically in Boltzmann codes that are used to study the CMB in details [1, 2].

7

Probing the Universe with galaxy surveys

Contents

Although the dynamics of structures on large scales is dominated by Dark Matter, we can only observe ordinary matter, and thus, we only have access to the distribution of gas and galaxies through telescopes, not to the actual distribution of Dark Matter[1]. In this chapter, we would like to touch on some of the many subtleties involved in linking the observed distribution of galaxies on large-scales to the theoretical predictions we have presented in the previous chapters. This includes:

1. The *biasing* between the distribution of galaxies and Dark Matter. This comes from the fact that galaxies do not form in arbitrary regions of the Dark Matter+baryons distribution but rather at peaks of the density contrast, where the overdensity in the field is high. To put it simply: if a galaxy forms at a place where $\Delta_m \sim \Delta_{m,\mathrm{crit}}$ one cannot form half a galaxy in a place where $\Delta_m \sim \Delta_{m,\mathrm{crit}}/2$. Therefore, the distribution of galaxies does not completely faithfully trace the underlying distribution of Dark Matter. Since our model only predicts the distribution of Dark Matter, this is a problem that needs to be addressed.

2. The *projection effects*. We only see a slice of the Universe which is not spatial: our past lightcone is a null surface that cuts through the large-scale structure of the Universe. Thus, we do not observe directly the spatial distribution of galaxies, but a certain projection of it on our past lightcone. This introduces projection effects which distort the observed distribution of galaxies compared to its theoretical, spatial prediction. The most important of these distortions in the local Universe is the *redshift space distortion* that we will describe here. We will see that this distortion is actually a blessing: since it breaks statistical isotropy by selecting a specific line of sight, it offers a way to measure at the same time the bias and the growth rate of perturbations, thus allowing to test the nature of Dark Energy and/or of gravitation on large scales. There are many more projection effects which start playing important roles on large scales. Incorporating them in observables is an important challenge of modern observational cosmology if we want to be able to make use of the wealth of data that galaxy surveys will provide in the near future.

In this chapter, we concentrate on galaxy number counts as a fundamental probe of the matter power spectrum, but there are, of course, other probes, such as, for example, *cosmological weak lensing*, i.e. the statistical deformation of the shapes of background galaxies by the large-scale distribution of matter along the line of sight. As usual in cosmology, it is the interplay between these probes

[1]Except in the very interesting case of gravitational lensing measurements, which will not be discussed here.

that will allow us to extract as much information about the Universe as possible.

7.1 The matter correlation function and power spectrum

Let us start by defining what is observed in a galaxy survey.

7.1.1 Two-point correlation function: definition

Consider a collection of small objects, for example galaxies, distributed in space. If the distribution is completely "random", i.e. that it follows a Poisson distribution, the probability of finding two objects in small volumes $\mathrm{d}V_1$ and $\mathrm{d}V_2$ separated by a direction vector $\vec{r}_{12}$ is given by:

$$\mathrm{d}P_{12}^{\mathrm{Poisson}} = \bar{n}\mathrm{d}V_1\bar{n}\mathrm{d}V_2 \ , \tag{7.1}$$

where $\bar{n}$ is the average number density of galaxies, i.e. the average number of galaxies per unit of volume. Of course, because they form dynamically in the inhomogeneous Dark Matter density field, galaxies are not distributed completely randomly: they exhibit correlations in their spatial distribution. Fig. 7.1 shows the slices of our past lightcone observed by the eBOSS survey.

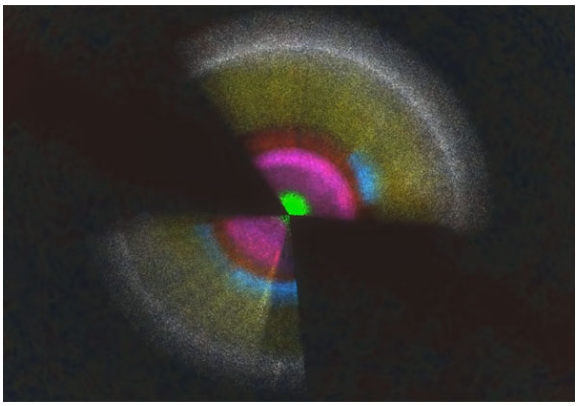

Figure 7.1: Distribution of galaxies and quasars observed by the eBOSS survey. Credits: SDSS collaboration.

These correlations are encapsulated in the *2-point correlation function* for the distribution of

galaxies: $\xi_g\left(\vec{r}_{12}\right)$. It is the excess of probability relative to the Poisson noise:

$$\mathrm{d}P_{12} = \bar{n}^2\left[1+\xi_g\left(\vec{r}_{12}\right)\right]\mathrm{d}V_1\mathrm{d}V_2\ . \tag{7.2}$$

As long as the distribution is Gaussian, this correlation function contains all the statistical information on the distribution. For a continuous random field, like Δ_m, one can also define a matter 2-point correlation function:

$$\xi_m\left(\eta,\vec{r}_1,\vec{r}_2\right) = \left\langle\Delta_m\left(\eta,\vec{r}_1\right)\Delta_m\left(\eta,\vec{r}_2\right)\right\rangle\ . \tag{7.3}$$

The two definitions coincide in the continuous limit of the definition for a discrete distribution. In real life, there is some shot noise introduced by the discreteness of the distribution of galaxies; we will not consider that here. In the next section we will relate the galaxy 2-point correlation function to the matter 2-point correlation function, but let us first study the latter.

7.1.2 Two-point correlation function: properties

First, let us rewrite Eq. (7.3) in a convenient way. We single out a position $\vec{r}_1 = \vec{x}$ and we consider all the points on the sphere centred on $\vec{r}_1 = \vec{x}$ of radius r; these points are at $\vec{r}_2 = \vec{x}+\vec{r}$ with $|\vec{r}| = r$. The 2-point correlation function in these new variables then gives the correlation between the field at $\vec{x}$ and the field at $\vec{x}+\vec{r}$. It reads:

$$\xi_m\left(\eta,\vec{x},\vec{r}\right) = \left\langle\Delta_m\left(\eta,\vec{x}\right)\Delta_m\left(\eta,\vec{x}+\vec{r}\right)\right\rangle\ . \tag{7.4}$$

Statistical homogeneity implies that this 2-point correlation function cannot depend explicitly on the base point $\vec{x}$. Moreover, statistical isotropy means that, around a given point, the 2-point correlation function cannot depend on the direction considered, but only on the distance to the base point, thus it cannot depend on $\vec{r}/r$, but only on r. Therefore:

$$\xi_m\left(\eta,\vec{x},\vec{r}\right) = \xi_m(\eta,r)\ . \tag{7.5}$$

Replacing the density field by its Fourier expansion and integrating once, one can show that (do it):

$$\xi_m\left(\eta,r\right) = \int\frac{d^3k}{\left(2\pi\right)^3}P_m\left(\eta,k\right)e^{-i\vec{k}\cdot\vec{r}}\ . \tag{7.6}$$

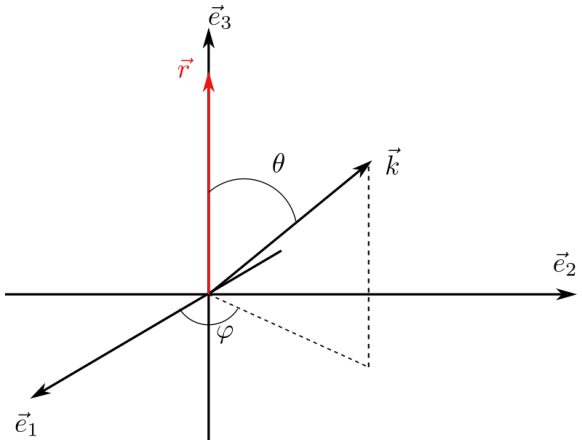

Figure 7.2: Spherical coordinates to calculate the 2-point correlation function.

i.e. that the *power spectrum* $P_m(k)$ is *the Fourier transform of the 2-point correlation function*. This integral can be further simplified by using spherical coordinates in Fourier space: fix $\vec{r}$ and define a Cartesian basis in Fourier space $\{\vec{e}_1, \vec{e}_2, \vec{e}_3\}$, such that $\vec{k} = k_1\vec{e}_1 + k_2\vec{e}_2 + k_3\vec{e}_3$ with $\vec{e}_3$ aligned along $\vec{r}$. Then define spherical coordinates with respect to this Cartesian basis with $\theta \in [0, \pi]$ the angle between $\vec{r}$ and $\vec{k}$ and $\varphi \in [0, 2\pi]$ the angle between $\vec{e}_1$ and $k_1\vec{e}_1 + k_2\vec{e}_2$. This configuration is depicted on figure 7.2. Then:

$$\mathrm{d}^3k = k^2\mathrm{d}k\sin\theta\mathrm{d}\theta\mathrm{d}\varphi \tag{7.7}$$

$$\vec{k}\cdot\vec{r} = kr\cos\theta\ . \tag{7.8}$$

Further, let $\mu = \cos\theta$. Then the angular part of the integral can be performed and one gets:

$$\xi_m(\eta, r) = \frac{1}{2\pi^2}\int_0^{+\infty} dk k^2 P_m(\eta, k)\frac{\sin kr}{kr} = \frac{1}{2\pi^2}\int_0^{+\infty} dk k^2 P_m(k) j_0(kr)\ . \tag{7.9}$$

This function is plotted on Fig. 7.3 with and without baryons, using CAMB to obtain the power spectrum. Note that, for numerical purposes, we used a cut-off in Fourier space: $H_0 < k < 1\ \mathrm{hMpc}^{-1}$, although the integral converges as the integrand behaves like k^2 at 0 and k^{-2} at infinity. One can clearly see the bump at the characteristic scale $\sim 100 - 120$ Mpc coming from Baryon Acoustic Oscillations. One should also note that on large enough scales, typically above 150 Mpc, the correlation function goes to zero, which means that the matter field becomes completely uncorrelated.

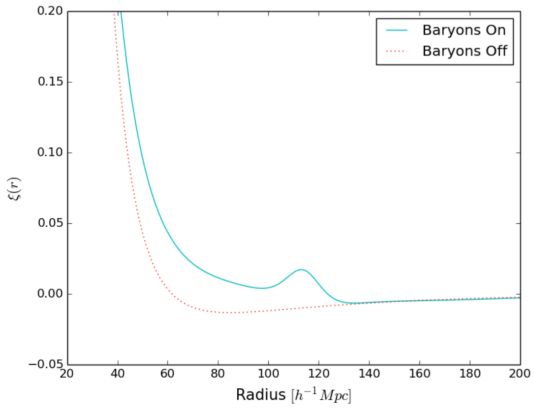

Figure 7.3: 2-point correlation function of matter with and without baryons obtained using CAMB.

This is a signature of large-scale statistical homogeneity: seen on large enough scales, the Universe is well-described by its average properties only.

7.1.3 The galaxy two-point correlation function and power spectrum

After forming, galaxies separate from the overall large-scale dynamics of the cosmological non-relativistic fluid. Then, they become some bound objects with a characteristic size much smaller than the ones involved when describing the large scale structure. Thus, on large enough scales, the large number of small galaxies, only interacting with each other via gravity, effectively behave collectively as a non-relativistic perfect fluid, distinct from the matter fluid studied so far that is mostly composed of Dark Matter (and baryonic matter which has not yet clustered in galaxies), with its own density contrast and velocity field, δ_g and V_g. But, because as we mentioned previously, galaxies form in Cold Dark Matter halos that correspond to peaks in the distribution of matter on large scales, we expect the density contrast of galaxies and of matter to differ:

$$\hat{\delta}_g\left(\eta, \vec{k}\right) \neq \hat{\delta}_m\left(\eta, \vec{k}\right) \ . \tag{7.10}$$

On the other hand, the ”fluid of galaxies” and the cosmological matter fluid have to have the same velocity field on linear scales. Indeed, they have the same equation of state ($w_{(i)} = 0$), thus applying

the Euler equation (5.43) to each fluid separately gives the same equation for both peculiar velocities:

$$V_m' + \mathcal{H} V_m = -\Phi \tag{7.11}$$

$$V_g' + \mathcal{H} V_g = -\Phi \, . \tag{7.12}$$

Assuming they start with the same initial conditions deep in the matter dominated phase, we thus get:

$$V_g = V_m \, . \tag{7.13}$$

Thus, we should have:

$$\hat{\Delta}_g \left(\eta, \vec{k}\right) \neq \hat{\Delta}_m \left(\eta, \vec{k}\right) . \tag{7.14}$$

This difference is called the galaxy *bias*. On linear scales, when Fourier modes are decoupled, this can be captured accurately by a scale-independent bias model:

$$\hat{\Delta}_g \left(\eta, \vec{k}\right) = b(\eta) \hat{\Delta}_m \left(\eta, \vec{k}\right) , \tag{7.15}$$

where $b(\eta)$ is the *linear bias* and we usually denote $b = b(\eta_0)$. This formula simply expresses that, on linear scales, the formation of galaxy is a linear response to the overall matter overdensity. Thus the power spectrum of galaxies today is related to the power spectrum of matter today through:

$$P_g(k) = b^2 P_m(k). \tag{7.16}$$

For $b^2 > 1$, there is more power at fixed k in the galaxies distribution that in the overall matter distribution; this simply expresses the fact that, in that case, galaxies are more clustered than the large scale structure.

7.2 The Observed power spectrum and redshift space distortion

Large-scale structures contain information about many properties of the Universe on large scales:

1. k_{eq}: The *turn-over scale* in $P_m(k)$ fixes the scale of *matter-radiation equality*, i.e. the ratio of energy density between non-relativistic and relativistic matter in the Universe. This is important to determine the length of the various eras in the history of the Universe.

2. λ_{BAO}, the *scale of Baryon Acoustic Oscillations* in the correlation function is directly related to the comoving size of the sound horizon at baryon-photon decoupling. This depends on the *ratio of energy density between baryons and photons*, a very important quantity related to the entropy of the early Universe.

3. The power spectrum on scales $k < k_{eq}$, which is very well described by the linear theory and not contaminated by non-linear physics on small scales offers a *direct probe into the initial conditions for the formation of structure*, i.e. on the spectrum of curvature perturbations generated by inflation. It also offers the prospect of testing the *Gaussianity of the initial conditions*, which is very important to our understanding of the very early Universe.

4. The growth factor f depends on *the theory of gravity and the nature of Dark Energy*. Measuring it would then be very interesting.

7.2.1 Lightcone projection effects

Despite all these appealing features, the power spectrum is not observable, even if we make abstraction of the galaxy biasing. Indeed, we calculated $P_g(k)$ in real space. But we only observe the Universe on our past lightcone, so that we know about galaxies lying on a null slice of our Universe, rather than a spatial slice. Linking the two, i.e. the theoretical description, available in real space with the actual observable is a very delicate business. Here we will focus on one special aspect of it, which dominates all the other lightcone effects on small enough scales, i.e. as long as *we only probe a small fraction of our visible Universe*, in which case the difference between our past lightcone and a spatial slice is very small. Roughly speaking, what we need to understand here is that what we know about an observed galaxy is not its triplet of spatial coordinates, but rather:

- its redshift: z;
- its angular position on the sky around us: (θ, ϕ).

Redshift

Note that the background redshift due to the Hubble expansion must be corrected by a Doppler effect coming from the peculiar velocities of galaxies. Let us see how it works. Let us consider a galaxy S emitting light received here and now at O. The light ray has a null tangent vector field

k^μ. Let us denote $\vec{n}(\theta, \phi)$ the vector pointing from the observer towards its sky in the direction of observation, (θ, ϕ). Then, the null vector can be decomposed as:

$$k^\mu = \bar{k}^\mu + \delta k^\mu = \frac{E}{a}(1, -\vec{n}) + \delta k^\mu \ . \tag{7.17}$$

Note the minus sign in front of $\vec{n}$ compared to previous calculations in these notes; this comes from the fact that $\vec{n}$ point from observer to source instead of source to observer when we were using the instantaneous direction of propagation of the photons. Since we recall that:

$$u_\mu = a\,(-1 - \Phi, \vec{v}) \ , \tag{7.18}$$

we get:

$$u_\mu k^\mu = -E\,(1 + \Phi + \vec{v} \cdot \vec{n}) - \delta k^0. \tag{7.19}$$

In what follows we will neglect the following terms, which are subdominant on small enough scales (be careful: here k on RHS is a scale, not a null vector field!):

- $\delta k^0 = -2a^{-2} \int_S^O \mathrm{d}\lambda \vec{n} \cdot \vec{\nabla}\Phi \sim 0$ assuming that $\Phi \sim$ cst on small enough scales;
- Φ with respect to $\vec{v}.\vec{n}$ because on small scales $|\vec{v}| \sim k\,|\Phi| \gg |\Phi|$.

Since, by definition:

$$1 + z = \frac{\left(u_\mu k^\mu\right)_S}{\left(u_\mu k^\mu\right)_0} \ , \tag{7.20}$$

evaluating the previous expression at source and observer and using the approximations:

$$1 + z = \frac{E_S\,(1 + \vec{v}_S \cdot n)}{E_0\,(1 + \vec{v}_0 \cdot n)} \tag{7.21}$$

$$= (1 + \bar{z})\,[1 + (\vec{v}_S - \vec{v}_0) \cdot n] \tag{7.22}$$

$$= (1 + \bar{z})\,(1 + \vec{v}_S \cdot n) \ , \tag{7.23}$$

where we worked in the observer's rest frame, setting $\vec{v}_0 = \vec{0}$, since we are the observer. We also denoted:

$$1 + \bar{z}(\eta) = \frac{1}{a(\eta)} \ . \tag{7.24}$$

There is thus a redshift perturbation (we drop the subscript S from now on):

$$\boxed{\delta z = (1 + \bar{z})\,\vec{v} \cdot \vec{n} \ ,} \tag{7.25}$$

which is exactly a non-relativistic Doppler term coming from the proper motion of the source.

Volume effect

Next, we need to understand how the infinitesimal volume of a fixed, small observed region is affected when going from real to redshift space. Using the comoving radial distance $\chi(z)$, consider the real (in the sense of actual: it is where the source is actually located) comoving position of the source:

$$\vec{x} = \chi\left(\bar{z}\right)\vec{n}\ , \tag{7.26}$$

where $\vec{n}$ is still the direction of observation on the sky. On the other hand, its observed position is given by:

$$\vec{x}_{\rm obs} = \chi_{\rm obs}(z)\vec{n}\ , \tag{7.27}$$

where:

$$\chi_{\rm obs}(z) = \chi\left(\bar{z} + \delta z\right) = \chi\left(\bar{z}\right) + \frac{d\chi}{d\bar{z}}_{|\bar{z}}\delta z\ . \tag{7.28}$$

We have assumed that $\vec{n}$ was not affected by perturbations; indeed corrections to the light-of-sight due to the light deviation introduced by structure situated between the source and observer do exist but are sub-dominant on small scales; as these are integrated effects, they do become important on large scales, though. Since we have that:

$$\frac{d\chi}{d\bar{z}} = \frac{1}{\left(1+\bar{z}\right)\mathcal{H}\left(\bar{z}\right)}\ , \tag{7.29}$$

we find that:

$$\chi_{\rm obs}(z) = \chi\left(\bar{z}\right) + \frac{\delta z}{\left(1+\bar{z}\right)\mathcal{H}\left(\bar{z}\right)}\ . \tag{7.30}$$

If we observe a small cylindrical region seen with an infinitesimal volume $\mathrm{d}V_{obs} = \rho\mathrm{d}\rho\mathrm{d}\theta\mathrm{d}\chi_{obs}$ around the redshift $\bar{z}$, keeping only the deformation along the line-of-sight, so that the actual real space volume of the region is given by: $\mathrm{d}V = \rho\mathrm{d}\rho\mathrm{d}\theta\mathrm{d}\chi$, we get that our coordinates in both spaces:

$$\begin{cases} \vec{x}_{obs} = (\chi_{\rm obs}, \rho, \theta) & (7.31) \\ \quad \vec{x} = (\chi, \rho, \theta)\ , & (7.32) \end{cases}$$

are related by the Jacobian matrix:

$$\frac{\partial\vec{x}_{\rm obs}}{\partial\vec{x}} = \begin{pmatrix} \frac{\partial\chi_{\rm obs}}{\partial\chi} & 0 & 0 \\ 0 & 1 & 0 \\ 0 & 0 & 1 \end{pmatrix}, \tag{7.33}$$

whose determinant is:

$$\left|\frac{\partial \vec{x}_{\rm obs}}{\partial \vec{x}}\right| = \frac{\partial \chi_{\rm obs}}{\partial \chi} = 1 + \frac{\partial}{\partial \chi}\left(\frac{\delta z}{(1+\bar{z})\,\mathcal{H}\,(\bar{z})}\right) \tag{7.34}$$

$$= 1 + \frac{1}{(1+\bar{z})\,\mathcal{H}\,(\bar{z})}\frac{\partial \delta z}{\partial \chi}\,. \tag{7.35}$$

Hence, the change in volume between real space and redshift (observed) space is given by:

$$\mathrm{d}V_{\rm obs} = \left[1 + \frac{1}{(1+\bar{z})\,\mathcal{H}\,(\bar{z})}\frac{\partial \delta z}{\partial \chi}\right]\mathrm{d}V\,. \tag{7.36}$$

Kaiser Formula

Moreover, the transformation from real to observational coordinates concerns the same region of space, so this transformation does not affect the number of galaxies seen in the region. If we call $n_{g,\rm obs} = \bar{n}_g\left(1+\delta_{g,\rm obs}\right)$ the observed galaxy number density, and $n_g = \bar{n}_g\left(1+\delta_g\right)$ the actual one, we get a number of galaxies in the small region[2]:

$$\mathrm{d}N = \bar{n}_g\left(1+\delta_{g,\rm obs}\right)\mathrm{d}V_{obs} = \bar{n}_g\left(1+\delta_g\right)\mathrm{d}V. \tag{7.37}$$

Thus, we obtain the *Kaiser formula* for redshift space distortions:

Kaiser formula

$$\delta_{g,\rm obs} = \delta_g - \frac{1}{\mathcal{H}}\frac{\partial}{\partial \chi}\left(\vec{v}\cdot\vec{n}\right)\,. \tag{7.38}$$

A physical illustration of the effect can be seen on Fig. 7.4. Along the line of sight, the variation of $\vec{v}\cdot\vec{n}$ induces a tidal deformation of the apparent structure. A local overdensity tends to attract the matter around it, thus, $\vec{v}\cdot\vec{n}$ goes from positive to negative as we follow the line of sight, thus, $\partial_\chi\left(\vec{v}\cdot\vec{n}\right) < 0$ and $\mathrm{d}V_{\rm obs} < \mathrm{d}V$, so we expect overdensities to appear denser than they are in real space. Besides, in redshift space, matter infalling onto the local overdensity appear further from us than in the background if it is between us and the overdense region, and closer to us than in the background if it is behind the overdensity. Therefore, overdense regions appear oblate to us in redshift space. For underdense regions, the converse of these phenomena occur: underdense regions appear less dense than in real space, and they take prolate shapes in redshift space.

[2]Note that since we are on small scales, we approximated $\Delta_i \simeq \delta_i$.

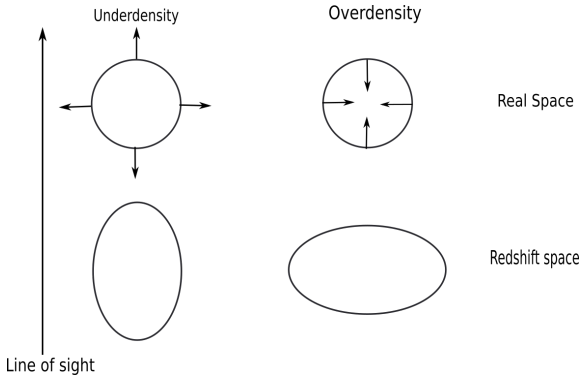

Figure 7.4: Pictorial principle of the redshift space distortion effect on linear structures.

7.2.2 Redshift space distortions and measurements of the growth rate of matter

These distortions offer a unique way to measure the peculiar velocity of distant galaxies. In order to access this extra information, we need to relate the Doppler term to the local value of the density contrast. Let us recall the bias $\delta_g = b\delta$, the continuity equation: $\hat{\delta}'_m = k^2 \hat{V}_m$ and the relation to the growth rate:

$$\Delta'_m = f\mathcal{H}\Delta_m \ . \tag{7.39}$$

Then, using $\partial_\chi = n^i \partial_i$, we find that, going to Fourier space:

$$\partial_\chi \left(\vec{n} \cdot \vec{v}\right) \mapsto - \left(\vec{n} \cdot \vec{k}\right)^2 \hat{V}_m \ , \tag{7.40}$$

where we used that $V_g = V_m$. Thus:

$$\hat{\delta}_{g,\mathrm{obs}} = b\hat{\delta}_m + \frac{1}{\mathcal{H}} \left(\vec{n} \cdot \frac{\vec{k}}{k}\right)^2 f\mathcal{H}\hat{\delta}_m \ . \tag{7.41}$$

Finally:

$$\boxed{\hat{\delta}_{g,\mathrm{obs}} = \left(b + f\mu^2\right) \hat{\delta}_m \ ,} \tag{7.42}$$

with:

$$\mu = \vec{n} \cdot \frac{\vec{k}}{k} = \frac{k_{||}}{k} = \cos\alpha \ , \tag{7.43}$$

where α is the angle between the mode $\vec{k}$ and the line of sight, in Fourier space. The power spectrum becomes:

Observed power spectrum of galaxies

$$\mathcal{P}_{g,\mathrm{obs}}(\eta, k, \mu) = \left(b(\eta) + f\mu^2\right)^2 \mathcal{P}_m(\eta, k) \ . \tag{7.44}$$

This shows that the *observed power spectrum depends on the direction of the Fourier mode* $\vec{k}$ and not just on its length any longer: that the actual *observation breaks the isotropy* because of the selection of a line of sight.

The next, natural question is whether one can separate the effects of the linear bias b and of the redshift space distortion, $f\mu^2$, and thus measure the growth function. The key is to exploit the anisotropic nature of the observed power spectrum and to decompose the power spectrum into spherical harmonics. Using the standard spherical angles $\theta \in [0, \pi]$ and $\phi \in [0, 2\pi)$, we define spherical harmonics as:

$$Y_{lm}(\theta, \phi) = (-1)^m \sqrt{\frac{(2l+1)(l-m)!}{4\pi(l+m)!}} P_{lm}(\cos\theta)\, e^{im\phi} \ , \ l \in \mathbb{N} \text{ and } m \in \mathbb{Z} \text{ with } -l \leq m \leq l \ , \tag{7.45}$$

where $P_{lm}(x)$ are the associated Legendre polynomials. Here we will only need:

$$P_{00}(x) = 1 \text{ and } P_{20}(x) = \frac{3x^2 - 1}{2} \ . \tag{7.46}$$

Then, any function on the sphere, $f(\theta, \phi)$ can be decomposed into spherical harmonics:

$$f(\theta, \phi) = \sum_{l,m} a_{lm} Y_{lm}(\theta, \phi) \ , \tag{7.47}$$

where the coefficients $a_{lm} \in \mathbb{C}$ characterise the function and are given by:

$$a_{lm} = \int_0^{\pi} \int_0^{2\pi} f(\theta, \phi)\, Y^*_{lm}(\theta, \phi) \sin\theta \mathrm{d}\theta \mathrm{d}\phi \ . \tag{7.48}$$

For a function f with axial symmetry, i.e. independent of ϕ, one can easily show that $a_{lm} = 0$ for any l and for $m \neq 0$. Then, the only surviving coefficients are the multipoles:

$$A_l = a_{l0} = \sqrt{(2l+1)\pi} \int_0^{\pi} \sin\theta f(\theta) P_{l0}(\cos\theta) \mathrm{d}\theta \ . \tag{7.49}$$

For the power spectrum, we have such an axial symmetry, and it is convenient to align the mode $\vec{k}$ with the z-axis, in order to have $\alpha = \theta$. Then, the multipoles of the power spectrum read:

$$A_l = \sqrt{(2l+1)\pi} \int_{-1}^{1} \left(b + f\mu^2\right)^2 P_{l0}(\mu) \mathcal{P}_m(\eta, k) \ . \tag{7.50}$$

Thus, we notice that the only non-zero multipoles are those with l even, because for l odd, the associated Legendre polynomials are odd and thus the integrals vanish. We can then compute the first two non-zero multipoles, the monopole A_0 and the quadrupole A_2:

$$A_0(\eta, k) = 2\left(b^2 + \frac{2}{3}fb + \frac{1}{5}f^2\right)\mathcal{P}_m(\eta, k) \tag{7.51}$$

$$A_2(\eta, k) = \frac{4}{5}\sqrt{\frac{2}{\pi}}\left(\frac{2}{3}bf + \frac{2}{7}f^2\right)\mathcal{P}_m(\eta, k)\ . \tag{7.52}$$

Therefore, by measuring both the monopole and the quadrupole of the observed power spectrum one can determine b and f. Note that the quadrupole vanishes in absence of redshift space distortion as it is proportional to f. Also, for $b \sim 1$ and $f \sim 1/2$, $\frac{2}{3}fb + \frac{1}{5}f^2 \sim 10^{-1}$, so that the monopole is mostly sensitive to the bias b. On the other hand, $\frac{2}{3}bf + \frac{2}{7}f^2 \sim 10^{-1}$, so the quadrupole is approximately one order of magnitude smaller than the monopole. See Fig. 7.5 for actual measurements. Measuring the growth rate f is key to constraining the theory of gravity on large scale, as it depends strongly on potential deviations from General Relativity. One uses the following parametrisation, also allowing for some scale dependence that appears in some extensions of General Relativity:

$$f\left(\eta, \vec{k}\right) = [\Omega(\eta)]^{\gamma\left(\eta, \vec{k}\right)}\ . \tag{7.53}$$

In General Relativity with a cosmological constant, $\gamma \simeq 0.55$ is constant. Recent constraints on a constant γ are represented in Fig. 7.6.

7.3 Problems

Pb. 7.1 Derive Eq. (7.6).

Pb. 7.2 Derive Eq. (7.9).

Pb. 7.3 Derive the results of subsection 7.2.2.

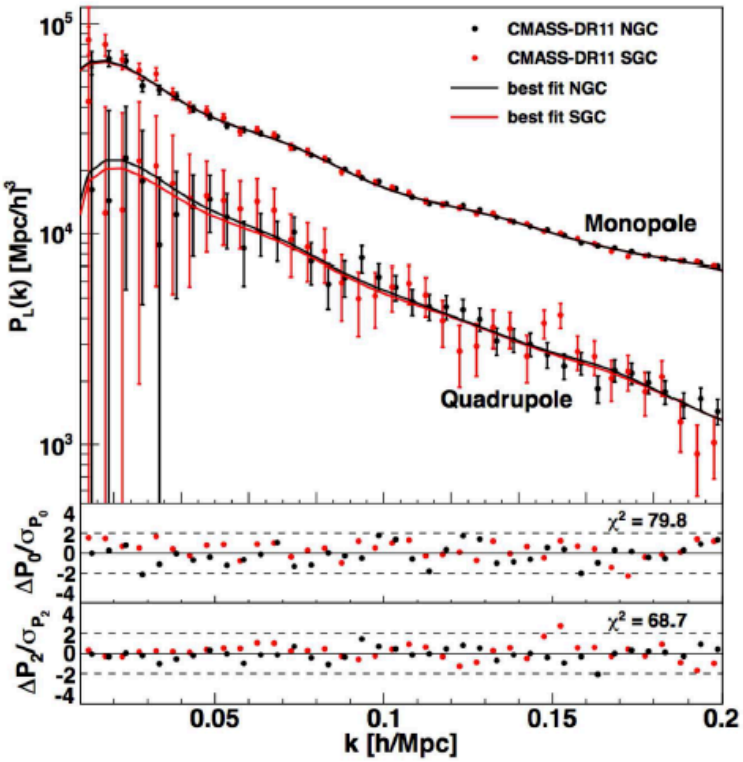

Figure 7.5: Measurements of the monopole and quadrupole of the galaxy power spectrum from the BOSS survey. From [7].

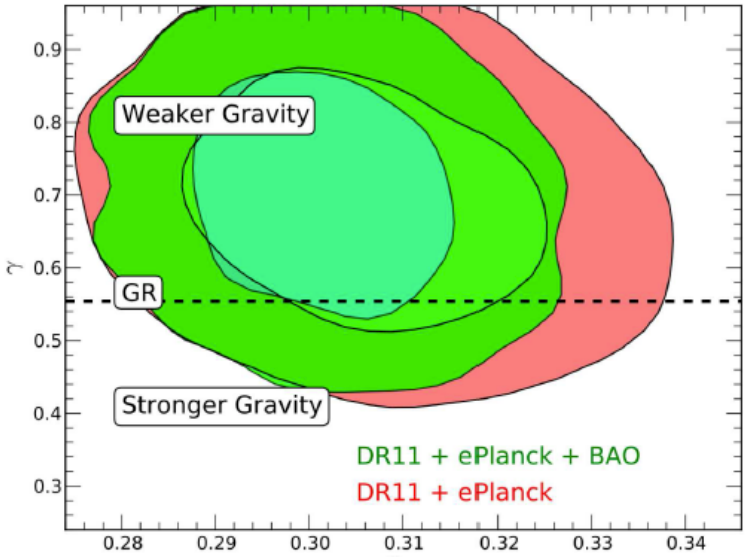

Figure 7.6: Constraints on γ and $\Omega_{m,0}$ from the BOSS survey. From [18].

8

An introduction to inflation

Contents

In section 2.4 we explained how a general mechanism, called inflation, could be used to sort out some problems in the hot Big-Bang model. We also invoked inflation in section 5.5 to explain how to set up the initial conditions for structure formation, via the initial comoving curvature perturbation $\hat{\xi}\left(\vec{k}\right)$. In this chapter we would like to explain how these two tasks are actually realised in a specific class of simple inflationary models, giving rise to inflationary cosmology, which is today the standard model of cosmology, namely *single (scalar) field inflation*. We do not focus on some particular model in the sense that we will not spend time trying to design a potential for the scalar field and test the properties of that field. Inflation is not yet properly connected to fundamental physics and since our interest in this course lies with the formation of structure, it is better for us to see inflation as a *mechanism* responsible for setting initial conditions. Most of the lessons learnt this way can be translated in more complex models of inflation without altering too much the part of the picture important for the hot Big-Bang Universe, while preserving the presentation from getting into too many subtle details too early. Readers wanting to go further can read [16] or [12].

8.1 Inflation: definition

8.1.1 First slow-roll parameter

In section 2.4, we saw that inflation was characterised by an early phase in the expansion of the Universe during which the comoving Hubble scale decreases:

$$\frac{d}{dt}\left(aH\right)^{-1} < 0 \, . \tag{8.1}$$

This implies in particular that the expansion is accelerating: $\ddot{a} > 0$. We may also write:

$$\frac{d}{dt}\left(aH\right)^{-1} = -\frac{\dot{a}H + a\dot{H}}{a^2H^2} = -\frac{1}{a}\left(1-\epsilon\right) \, , \tag{8.2}$$

where we defined the *first slow-roll parameter*:

$$\boxed{\epsilon = -\frac{\dot{H}}{H^2} \, .} \tag{8.3}$$

Inflation is then equivalent to $\epsilon < 1$. Note that in the limit of perfect inflation, with $\epsilon = 0$, $H = \text{cst}$ and the scale factor becomes:

$$a(t) \propto e^{Ht} \, . \tag{8.4}$$

This corresponds to a de Sitter spacetime. This is usually a very good approximation to the dynamics of the background during inflation. Of course, inflation eventually has to stop, so ϵ cannot be exactly 0. Therefore, usually, one builds inflationary models such that $\epsilon \ll 1$ but $\epsilon \neq 0$. Then, the slow-roll parameter becomes dynamical; it remains small for a certain period of inflation, and then increases rapidly so that inflation ends when it reaches 1. This is known as quasi-de Sitter inflation.

8.2 Energy-momentum during inflation

What form of stress-energy source can drive such a phase of inflation? Let us assume that it comes in the form of a perfect fluid with energy density ρ and pressure p. Then[1]:

$$H^2 = \frac{8\pi G\rho}{3} \tag{8.5}$$

$$\dot{\rho} = -3H(\rho + p) \ . \tag{8.6}$$

Thus:

$$\dot{H} = -4\pi G(\rho + p) \ , \tag{8.7}$$

and:

$$\epsilon = \frac{3}{2}\left(1 + \frac{p}{\rho}\right) = \frac{3}{2}(1 + w) \ . \tag{8.8}$$

Hence, inflation requires:

$$w < -\frac{1}{3} \ . \tag{8.9}$$

Using the energy-conservation equation, this leads to:

$$\left|\frac{d\ln\rho}{d\ln a}\right| = 2\epsilon < 2 \ . \tag{8.10}$$

For $\epsilon \ll 1$, this corresponds to $\rho \simeq$ cst, thus this cannot be achieved with normal matter. Inflation needs to be generated by some exotic source for the gravitational field. In the simplest models, which serve to set the paradigm, this is achieved with a single, minimally coupled, scalar field. This is what we will study in the rest of this chapter.

[1]For now, since we concentrate only on the FLRW dynamics, we drop the bar on top of densities and pressures for ease of notation.

8.3 Scalar field inflation

8.3.1 Scalar field action

At the moment, no fundamental theory predicts what the true degrees of freedom are in the very early Universe, when inflation is supposed to take place. The usual approach is then to model this early phase by using a simple, effective approach. We bundle all possible fundamental degrees of freedom into a single scalar field φ called the *inflaton*. It is an effective description, and we remain agnostic as to whether or not this field is a fundamental degree of freedom (actually, it is very unlikely that it is). The field is characterised by its potential $V(\varphi)$, through the action:

$$S_\varphi = -\int \sqrt{-g}\left[\frac{1}{2}g^{\mu\nu}\partial_\mu\varphi\partial_\nu\varphi + V(\varphi)\right]\mathrm{d}^4x \ , \tag{8.11}$$

where $g = \det(\boldsymbol{g})$. Varying the action with respect to $g^{\mu\nu}$, gives an energy-momentum tensor, source of the Einstein field equation:

$$T_{\mu\nu} = \frac{2}{\sqrt{-g}}\frac{\delta S_\varphi}{\delta g^{\mu\nu}} \ , \tag{8.12}$$

which for the scalar field, takes the form:

$$T_{\mu\nu} = \partial_\mu\varphi\partial_\nu\varphi - \left(\frac{1}{2}g^{\alpha\beta}\partial_\alpha\varphi\partial_\beta\varphi + V(\varphi)\right)g_{\mu\nu} \ . \tag{8.13}$$

In the FLRW background, we can write $\varphi = \bar{\varphi}(t)$, thus getting a perfect fluid with energy-density and pressure:

$$\rho_\varphi = \frac{1}{2a^2}\varphi'^2 + V(\varphi) = \frac{1}{2}\dot{\varphi}^2 + V(\varphi) \tag{8.14}$$

$$p_\varphi = \frac{1}{2a^2}\varphi'^2 - V(\varphi) = \frac{1}{2}\dot{\varphi}^2 - V(\varphi) \ . \tag{8.15}$$

8.3.2 The inflaton

Since inflation is possible when $p_\varphi < -\rho_\varphi/3$, this leads to the necessary condition to get scalar field inflation:

$$\boxed{\dot{\varphi}^2 < V(\varphi) \ .} \tag{8.16}$$

In other words, *the potential energy in the field must dominate over its kinetic energy*.

Next, let us look at the dynamics of the background. In cosmic time:

$$H^2 = \frac{8\pi G}{3}\left(\frac{1}{2}\dot{\varphi}^2 + V(\varphi)\right) - \frac{K}{a^2} \tag{8.17}$$

$$\frac{\ddot{a}}{a} = \frac{8\pi G}{3}\left(V(\varphi) - \dot{\varphi}^2\right) \tag{8.18}$$

$$\ddot{\varphi} = -3H\dot{\varphi} - \frac{dV}{d\varphi} \text{ (Klein-Gordon equation).} \tag{8.19}$$

This leads to:

$$\dot{H} = \frac{\ddot{a}}{a} - H^2 = -4\pi G\dot{\varphi}^2 + \frac{K}{a^2}\ . \tag{8.20}$$

In what follows we will neglect curvature, as it is wiped out very quickly if inflation is allowed to start. The first slow-roll parameter is then given by:

$$\boxed{\epsilon = \frac{4\pi G\dot{\varphi}^2}{H^2}\ .} \tag{8.21}$$

This means that inflation proceeds when $4\pi G\dot{\varphi}^2 < H^2$. In other words, $\dot{\varphi}^2/2$ must make a small contribution to the energy density ρ_φ, which means that the field must evolve slowly into its potential. This is *slow-roll inflation*. For this slow-roll condition to persist for a finite amount of time, $\ddot{\varphi}$ must also remain small. Thus, we define the *second slow-roll parameter*:

$$\boxed{\delta = -\frac{\ddot{\varphi}}{H\dot{\varphi}}\ .} \tag{8.22}$$

Slow-roll inflation will persist for as long as $\delta \ll 1$. Note that we can write:

$$\dot{\epsilon} = \frac{8\pi G\dot{\varphi}\ddot{\varphi}}{H^2} - \frac{8\pi G\dot{H}\dot{\varphi}^2}{H^3}\ , \tag{8.23}$$

so that, if we define the *third slow-roll parameter*:

$$\boxed{\tilde{\eta} = \frac{\dot{\epsilon}}{H\epsilon}\ ,} \tag{8.24}$$

we get the relation:

$$\tilde{\eta} = 2\left(\epsilon - \delta\right)\ . \tag{8.25}$$

Be careful that this is not related to conformal time! The tilde is here to remind you of that. Hence if any two of the three slow-roll parameters are small, so is the third and we can define slow-roll inflation as:

$$\epsilon \ll 1 \text{ and } \delta \ll 1 \ . \tag{8.26}$$

Using the first of these conditions, we get that:

$$\frac{1}{2}\dot{\varphi}^2 \ll V(\varphi) \ , \tag{8.27}$$

so that:

$$H^2 \simeq \frac{8\pi G}{3} V(\varphi) \ . \tag{8.28}$$

Moreover, $\delta \ll 1$ gives, using the Klein-Gordon equation:

$$3H\dot{\varphi} \simeq -\frac{dV}{d\varphi} \ . \tag{8.29}$$

We can then re-express ϵ is terms of the potential only:

$$\epsilon \simeq \frac{1}{16\pi G}\left(\frac{V_{,\varphi}}{V}\right)^2 \text{ during slow-roll inflation.} \tag{8.30}$$

Then deriving the Klein-Gordon equation:

$$\delta + \epsilon \simeq \frac{1}{8\pi G}\frac{V_{,\varphi\varphi}}{V} \text{ during slow-roll inflation.} \tag{8.31}$$

During slow-roll, all the slow-roll parameters are related to the shape of the potential of the inflaton. Thus, in order to assess if a potential $V(\varphi)$ can lead to slow-roll inflation, we can compute the *potential slow-roll parameters*:

$$\begin{cases} \epsilon_V = \dfrac{1}{16\pi G}\left(\dfrac{V_{,\varphi}}{V}\right)^2 & (8.32) \\ \eta_V = \dfrac{1}{8\pi G}\dfrac{V_{,\varphi\varphi}}{V} \ . & (8.33) \end{cases}$$

During slow-roll inflation, one then has that $\epsilon \simeq \epsilon_V \ll 1$ and $\epsilon + \delta = \eta_V \ll 1$. Typically, this means that the potential must have a 'flat' region in which the field can evolve slowly to ensure slow-roll, and steeper regions in which the field falls to end inflation. That end of inflation occurs

when $\max\{\epsilon, |\delta|\} \simeq 1$.

We can now conclude this subsection by calculating the number of e-folds of inflation. Remember that it is defined as:

$$N(t_I, t_E) = \int_{t_I}^{t_E} H(t)\mathrm{d}t = \ln\frac{a_E}{a_I} , \tag{8.34}$$

where t_I and t_E denote the beginning and end of inflation, respectively. They are typically defined by $\epsilon(t_I) \simeq \epsilon(t_E) \simeq 1$. Since we have that:

$$H\mathrm{d}t = \frac{H}{\dot{\varphi}}\mathrm{d}\varphi , \tag{8.35}$$

we can use the scalar field as a clock and write:

$$N(\varphi_I, \varphi_E) = -\sqrt{4\pi G}\int_{\varphi_I}^{\varphi_E} \frac{\mathrm{d}\varphi}{\sqrt{\epsilon(\varphi)}} . \tag{8.36}$$

We can also use the value of the mode $k = a(t)H(t)$ exiting the Hubble radius at time t, equivalent to the value of the field $\varphi(t)$ as an evolution variable:

$$k(\varphi) = a_E H(\varphi)\, e^{-N(\varphi)} . \tag{8.37}$$

8.4 Quantum fluctuations of a test scalar field during inflation

The inflaton, like any other field, will be subjected to fluctuations around its FLRW background value. Besides, because of the scales involved, these fluctuations will have to be treated as quantum[2]. The purpose of this chapter is to arrive at a full treatment of these fluctuations in the slow-roll approximation, and to show that these give rise to the nearly scale-invariant power spectrum of comoving perturbations on super-Hubble scales, which we used to set the initial conditions of our study of structure formation.

This is a subtle problem and we will approach it step by step. Before we do so, let us see how it works. During inflation, the evolution of the inflaton governs the expansion of the Universe. Essentially, as we saw, $\varphi(t)$ plays the role of a clock reading the amount of inflation still to occur. But quantum mechanical clocks are subjected to fluctuations, by virtue of the uncertainty principle, $\Delta E \Delta t \geq \hbar$. Thus we need to replace:

$$\varphi(t, \vec{x}) = \bar{\varphi}(t) + \delta\varphi(t, \vec{x}) \ . \tag{8.38}$$

[2]Namely, this comes from the fact that while modes remain sub-Hubble, the inflaton is in its vacuum state, so that its fluctuations are indeed quantum fluctuations around this vacuum; see [12] for details.

These fluctuations introduce local differences in the cosmic time at which inflation ends, $\delta t\,(\vec{x})$, so that different regions of space inflate by different amounts. This means that at t_E, different $\delta\rho\,(\vec{x})$ have been generated. These fluctuations are the source of primordial inhomogeneities we are looking for.

8.4.1 Quantisation of the 1D harmonic oscillator

Let us start by quickly reviewing the standard quantisation of the harmonic oscillator in quantum mechanics. It is one degree of freedom $q(t)$ with the action:

$$S\left[q,\dot{q}\right] = \frac{1}{2}\int \mathrm{d}t\left(\dot{q}^2 - \omega^2 q^2\right) \ . \tag{8.39}$$

The Euler-Lagrange equation is that of the harmonic oscillator:

$$\ddot{q} + \omega^2 q = 0 \ . \tag{8.40}$$

The momentum conjugate to q is:

$$p = \frac{\delta\mathcal{L}}{\delta\dot{q}} = \dot{q} \ . \tag{8.41}$$

Standard quantisation consists in promoting q and p to linear operators $\hat{q}$ and $\hat{p}$ obeying:

$$[\hat{q},\hat{p}] = i \ , \tag{8.42}$$

where we work in units with $\hbar = 1$ to simplify notations. Since the equation of motion (8.40) is second order and linear, its general solution is characterised by initial conditions $q(0)$ and $\dot{q}(0) = p(0)$ as the linear combination of two linearly independent solutions. Therefore, in the Heisenberg representation:

$$\hat{q}(t) = A(t)\hat{q}(0) + B(t)\hat{p}(0) \ . \tag{8.43}$$

Since $\hat{q}(0)$ and $\hat{p}(0)$ are Hermitian (they must have real eigenvalues), $A(t)$ and $B(t)$ are real and we can define a new operator $\hat{a}$ as:

$$\hat{a} = \frac{\beta^*\hat{q}(0) - \alpha^*\hat{p}(0)}{\beta^*\alpha - \beta\alpha^*} \ , \tag{8.44}$$

for any complex numbers α and β such that the denominator does not cancel. Then, we can write the solution:

$$\hat{q}(t) = q(t)\hat{a} + q^*(t)\hat{a}^\dagger \ , \tag{8.45}$$

for $q(t)$ a complex function. A $\dagger$ denotes Hermitian conjugation and a star complex conjugation. It is easy to see that $q(t)$ is a solution to the Euler-Lagrange equation (8.40). The canonical momentum is then:

$$\hat{p}(t) = \dot{q}(t)\hat{a} + \dot{q}^*(t)\hat{a}^\dagger \ . \tag{8.46}$$

Therefore, the commutation relation (8.42) imposes that:

$$2\,\mathrm{Im}(q\dot{q}^*)\left[\hat{a}, \hat{a}^\dagger\right] = 1 \ . \tag{8.47}$$

We can always normalise our operator $\hat{a}$ to make the pre-factor equal to 1:

$$2\,\mathrm{Im}(q\dot{q}^*) = 1 \ , \tag{8.48}$$

so that:

$$\left[\hat{a}, \hat{a}^\dagger\right] = 1 \ . \tag{8.49}$$

Now, we can require that $\hat{a}^\dagger$ and $\hat{a}$ be respectively the creation and annihilation operators associated with the Hamiltonian:

$$\hat{H} = \frac{1}{2}\hat{p}^2 + \frac{1}{2}\omega^2\hat{q}^2 \ , \tag{8.50}$$

i.e. that we impose that, for the ground state of the Hamiltonian, $|0\rangle$:

$$\hat{a}\,|0\rangle = 0 \ , \tag{8.51}$$

and any eigenstate $|n\rangle$ of $\hat{H}$ can be generated by repeated application of the creation operator:

$$|n\rangle = \frac{1}{\sqrt{n!}}\left(\hat{a}^\dagger\right)^n |0\rangle \ . \tag{8.52}$$

Note that this amounts to selecting a vacuum, ground state $|0\rangle$. This is unambiguous in our case but will be relevant in curved spacetime. Then, the number operator $\hat{N}$ which counts the number of quanta in each energy eigenstate becomes:

$$\hat{N} = \hat{a}^\dagger\hat{a} \ \text{ with } \ \hat{N}\,|n\rangle = n\,|n\rangle \ . \tag{8.53}$$

Requiring that $|0\rangle$ is annihilated by $\hat{a}$ but that $\hat{a}^\dagger\,|0\rangle = |1\rangle$ imposes that:

$$\dot{q}^2 + \omega^2 q^2 = 0 \implies \dot{q} = \pm i\omega q \ . \tag{8.54}$$

But then, $2\,\mathrm{Im}(q\dot{q}^*) = \mp 2\omega\,|q|^2 = 1$ leads to $\dot{q} = -i\omega q$, so that:

$$q(t) = \frac{1}{\sqrt{2\omega}} e^{-i\omega t} \ . \tag{8.55}$$

One can then check that in the vacuum:

$$\langle \hat{q} \rangle = \langle 0|\, \hat{q}\, |0\rangle = 0 \ , \tag{8.56}$$

but:

$$\left\langle |\hat{q}|^2 \right\rangle = \langle 0|\, \hat{q}^\dagger \hat{q}\, |0\rangle = |q(t)|^2 \ . \tag{8.57}$$

Restoring $\hbar$, we find the amplitude of the quantum fluctuations in the vacuum:

$$\left\langle |\hat{q}|^2 \right\rangle = \frac{\hbar}{2\omega} \ . \tag{8.58}$$

8.4.2 Quantum fluctuations of a scalar field in de Sitter spacetime

We are now going to repeat the procedure followed for the harmonic oscillator, but in the case of a test scalar field $\chi\,(\eta, \vec{x})$ in a de Sitter background geometry. We will suppose that the field is free and massless, for simplicity. This means that we have to quantise a field relativistically, and that because we assume that this field is a test field, the metric remains de Sitter and is not affected by the fluctuations in the field. The classical evolution equation for χ in an arbitrary FLRW background is given by:

$$\ddot{\chi} + 3H\dot{\chi} - a^{-2}\Delta\chi = 0 \ . \tag{8.59}$$

Let us define a new, re-scaled field $f\,(\eta, \vec{x}) = a(\eta)\chi\,(\eta, \vec{x})$ that we further expand in Fourier modes $f_{\vec{k}}(\eta)$. These Fourier modes obey the *Mukhanov-Sasaki equation*:

$$f''_{\vec{k}} + \left(k^2 - \frac{a''}{a}\right) f_{\vec{k}} = 0 \ . \tag{8.60}$$

This equation is valid in any FLRW background. In a de Sitter background, we have moreover that:

$$\frac{a''}{a} = 2H^2a^2 = 2\mathcal{H}^2 = \frac{2}{\eta^2} \ . \tag{8.61}$$

Note that on sub-Hubble scales, $k \gg \mathcal{H}^2$ and the Mukhanov-Sasaki equation reduces to that of an harmonic oscillator with frequency k in a flat background. This justifies the fact that f, rather than χ is the right degree of freedom to quantise. Its canonical momentum is:

$$\pi\,(\eta, \vec{x}) = f' \ . \tag{8.62}$$

We quantise by promoting f and π to linear operators $\hat{f}$ and $\hat{\pi}$ which obey equal time commutation relations:

$$\left[\hat{f}\left(\eta,\vec{x}\right),\hat{\pi}\left(\eta,\vec{x}'\right)\right]=i\delta_D\left(\vec{x}-\vec{x}'\right)\ . \tag{8.63}$$

By introducing the Fourier decomposition of the operators:

$$\hat{f}_{\vec{k}}\left(\eta\right)=\int\frac{\mathrm{d}^3x}{(2\pi)^{3/2}}\hat{f}\left(\eta,\vec{x}\right)e^{-i\vec{k}\cdot\vec{x}}\ , \tag{8.64}$$

and similarly for $\hat{\pi}$, we get the equal time commutation relations in Fourier space:

$$\left[\hat{f}_{\vec{k}}(\eta),\hat{\pi}_{\vec{k}'}(\eta)\right]=i\delta_D\left(\vec{k}-\vec{k}'\right)\ . \tag{8.65}$$

Inspired by the similarity of the Mukhanov-Sasaki equation with the equation for an harmonic oscillator, we further decompose $\hat{f}_k$ in terms of an operator $a_{\vec{k}}$ and its Hermitian conjugate:

$$\hat{f}_{\vec{k}}(\eta)=f_k(\eta)\hat{a}_{\vec{k}}+f_k^*(\eta)\hat{a}_{\vec{k}}^\dagger\ , \tag{8.66}$$

where f_k satisfies the Mukhanov-Sasaki equation:

$$f_k''+\omega_k^2(\eta)f_k=0\text{ with }\omega_k^2(\eta)=k^2-\frac{a''}{a}\ . \tag{8.67}$$

Similarly to the case of the harmonic oscillator above, we can impose that:

$$-i\left(f_k\left(f_k'\right)^*-f_k^*f_k'\right)=1\ , \tag{8.68}$$

and then:

$$\left[\hat{a}_k,\hat{a}_k^\dagger\right]=\delta_D\left(\vec{k}-\vec{k}'\right)\ . \tag{8.69}$$

As previously, in order to interpret $\hat{a}_{\vec{k}}$ and its conjugate as annihilation and creation operators of a mode with wavevector $\vec{k}$, we need to fix the vacuum, i.e. the vector $|0\rangle$ such that $\hat{a}_{\vec{k}}\left|0\right\rangle$. Moreover, we also want $\hat{a}_{\vec{k}}^\dagger$ to create one mode with wavevector $\vec{k}$ after each application. In particular, that means that $\hat{a}_{\vec{k}}^\dagger\neq0$. To choose this mode, as we have seen, amounts to finding a solution for the modes $f_k(\eta)$. Let us remember that during inflation $\mathcal{H}$ decreases, therefore, all the modes k, if we go far enough into the past, will be deep inside the Hubble radius. This means that for $\eta\to-\infty$, $k\gg\mathcal{H}$. Thus, early enough the Mukhanov-Sasaki equation reads like the equation for an harmonic oscillator with frequency k, whose solution is:

$$f_k(\eta)\propto e^{\pm ik\eta}\ . \tag{8.70}$$

The normalisation chosen above selects the negative sign again, and we find that our modes have the initial condition:

$$f_k(\eta) \sim \frac{1}{\sqrt{2k}} e^{-ik\eta} \text{ for } \eta \to -\infty \,. \tag{8.71}$$

In practise, this means that at early times, deep inside the Hubble radius, modes evolve as in Minkowski: they do not feel the curvature that is only present on much larger scales. If we further assume that the background is de Sitter, the Mukhanov-Sasaki equation has the general solution:

$$f_k\left(\eta\right) = \alpha \frac{e^{-ik\eta}}{\sqrt{2k}} \left(1 - \frac{i}{k\eta}\right) + \beta \frac{e^{ik\eta}}{\sqrt{2k}} \left(1 + \frac{i}{k\eta}\right) \,, \tag{8.72}$$

for numbers α and β. Our initial condition as $-\infty$ then forces $\alpha = 1$ and $\beta = 0$. Thus:

$$\boxed{f_k(\eta) = \frac{e^{-ik\eta}}{\sqrt{2k}} \left(1 - \frac{i}{k\eta}\right) \,.} \tag{8.73}$$

Note that $\hat{N}_{\vec{k}} = \hat{a}^\dagger_{\vec{k}} \hat{a}_{\vec{k}}$ corresponds to the occupation number of the mode $\vec{k}$ at initial time, $\eta \to -\infty$. Therefore, the occupation number of the mode $\vec{k}$ at an ulterior time η is:

$$\hat{N}_{\vec{k}}(\eta) = |f_k(\eta)|^2 \, \hat{N}_{\vec{k}} \,. \tag{8.74}$$

Since, re-establishing $\hbar$:

$$|f_k(\eta)|^2 = \frac{\hbar}{2k} \left(1 + \frac{1}{(k\eta)^2}\right) \,, \tag{8.75}$$

as soon as $k\eta \ll 1$, i.e. as soon as the mode exits the Hubble radius, his number becomes very large and the mode becomes classical; see [12] for another argument. They can then be treated as standard Gaussian random fields (Gaussianity is also a consequence of their quantum mechanical origin), and the vacuum expectation values can be replaced with regular ensemble averages. This explains how the inflationary era transforms quantum fluctuations into classical ones.

The spectrum of fluctuations is related to the expectation value of the fluctuations in the vacuum:

$$\left\langle \left|\hat{f}\right|^2 \right\rangle = \langle 0| \, \hat{f}\left(\eta, \vec{x}\right) \hat{f}^\dagger\left(\eta, \vec{x}\right) |0\rangle \tag{8.76}$$

$$= \int \frac{\mathrm{d}^3 k}{(2\pi)^3} \, |f_k(\eta)|^2 \tag{8.77}$$

$$= \int \mathrm{d}\ln k \frac{k^3}{2\pi^2} \, |f_k(\eta)|^2 = \int \mathrm{d}\ln k \Delta^2_f\left(\eta, \vec{k}\right) \,, \tag{8.78}$$

where we used the *dimensionless power spectrum*:

$$\Delta_f^2\left(\eta,\vec{k}\right) = k^3\mathcal{P}_f\left(\eta,\vec{k}\right) = \frac{k^3}{2\pi^2}\left|f_k(\eta)\right|^2 = \frac{\mathcal{H}^2}{(2\pi)^2}\left(1+\left(\frac{k}{\mathcal{H}}\right)^2\right) . \tag{8.79}$$

The dimensionless power spectrum of the actual scalar field $\chi = f/a$ is then:

$$\Delta_\chi^2\left(\eta,\vec{k}\right) = a^{-2}k^3\Delta_f^2\left(\eta,\vec{k}\right) = \left(\frac{H}{2\pi}\right)^2\left(1+\left(\frac{k}{aH}\right)^2\right) . \tag{8.80}$$

When the modes exit the Hubble scale and become classical, this leads to a scale invariant power spectrum (this is a direct consequence of the symmetries of de Sitter):

Scale-invariant dimensionless power spectrum

$$\Delta_\chi^2\left(\vec{k}\right) = \left(\frac{H}{2\pi}\right)^2 . \tag{8.81}$$

This is the power that is going to generate comoving curvature perturbations. Indeed, in our approximation of a test field, we have $\Phi \simeq 0$, so, because for a scalar field $\delta T^0{}_i = -\bar{\chi}'\partial_i\chi$, the comoving curvature perturbation simply reads:

$$\zeta = \frac{\mathcal{H}}{\bar{\chi}'}\chi . \tag{8.82}$$

Fluctuations in the field are thus fluctuations in the comoving curvature perturbations. Strictly speaking it should be small since we neglected the backreaction of the field on the metric (and did not even consider a background dynamics for our field...) but this calculation will essentially carry forward in the general case so let us pursue it in this simplest, neat framework. We see that the power spectrum for the curvature perturbation is then:

$$\Delta_\zeta^2\left(\vec{k}\right) = \frac{GH^2}{\pi\epsilon} , \tag{8.83}$$

where $\epsilon = 4\pi G\bar{\chi}'^2/\mathcal{H}^2$ is the "slow-roll parameter" of our fiducial field.

This is related to the dimensionful power spectrum we used before by a factor of k^{-3}, so this is exactly what we denoted $A_s\left(k/k_*\right)^{n_s-1}$ with $n_s = 1$.

Of course, you see that if our field is the inflaton, as we want it to be, these fluctuations become large during slow-roll, so they are going to influence the geometry, and we need a full relativistic calculation with an almost de Sitter background and perturbations to get the full picture. Then, the spectral index will depend on the slow-roll parameters and the spectrum will be nearly but not exactly scale-invariant.

8.5 Quantum fluctuations of the inflation

In this section, we attack the central issue of this chapter: we are going to perturb the inflaton itself, while taking into account metric perturbations. We work in conformal time throughout.

8.5.1 Perturbed scalar field

We write the inflaton:

$$\varphi(t,\vec{x}) = \bar{\varphi}(t) + \delta\varphi(t,\vec{x}) \ . \tag{8.84}$$

Writing the energy-momentum tensor at first order in the scalar field and metric fluctuations, we get:

$$\begin{aligned}\delta T_{\mu\nu} =& 2\partial_{(\nu}\bar{\varphi}\partial_{\mu)}\delta\varphi - \left(\frac{1}{2}\bar{g}^{\alpha\beta}\partial_\alpha\bar{\varphi}\partial_\beta\bar{\varphi} + \bar{V}\right)\delta g_{\mu\nu} \\ & - \bar{g}_{\mu\nu}\left(\frac{1}{2}\delta g_{\mu\nu}\partial_\alpha\bar{\varphi}\partial_\beta\bar{\varphi} + \bar{g}^{\alpha\beta}\partial_\alpha\delta\varphi\partial_\beta\bar{\varphi} + \bar{V}_{,\varphi}\delta\varphi\right) \ ,\end{aligned} \tag{8.85}$$

where we used the notations $\bar{V} = V(\bar{\varphi})$ and $\bar{V}_{,\varphi} = \frac{\mathrm{d}V}{\mathrm{d}\varphi}(\bar{\varphi})$. In an arbitrary gauge:

$$\begin{cases} \delta T_{00} = \bar{\varphi}'\delta\varphi' - 2a^2\bar{V}\Phi + a^2\dfrac{\mathrm{d}\bar{V}}{\mathrm{d}\varphi}\delta\varphi & (8.86) \\ \delta_{0i} = \bar{\varphi}'\partial_i\delta\varphi + \left(\dfrac{1}{2}\left(\bar{\varphi}'\right)^2 - a^2\bar{V}\right)B_i & (8.87) \\ \delta T_{ij} = \left[\bar{\varphi}'\delta\varphi' - \left(\bar{\varphi}'\right)^2(\Phi+\Psi) + 2a^2\bar{V}\Psi - a^2\dfrac{\mathrm{d}\bar{V}}{\mathrm{d}\varphi}\delta\varphi\right]\delta_{ij} \\ \qquad + \left[\left(\bar{\varphi}'\right)^2 - 2a^2\bar{V}\right]\left[\partial_i\partial_j E + \partial_{(i}\bar{E}_{j)} + \bar{E}_{ij}\right] \ . & (8.88) \end{cases}$$

In mixed form, this gives:

$$\begin{cases} a^2\delta T^0{}_0 = -\bar{\varphi}'\delta\varphi' - a^2\dfrac{\mathrm{d}\bar{V}}{\mathrm{d}\varphi}\delta\varphi + \left(\bar{\varphi}'\right)^2\Phi & (8.89) \\ a^2\delta T^0{}_i = -\bar{\varphi}'\partial_i\delta\varphi & (8.90) \\ a^2\delta T^i{}_0 = \partial^i\left[\bar{\varphi}'\delta\varphi + + \left(\bar{\varphi}'\right)^2 B\right] + + \left(\bar{\varphi}'\right)^2\bar{B}^i & (8.91) \\ a^2\delta T^i{}_j = \left[\bar{\varphi}'\delta\varphi' - + \left(\bar{\varphi}'\right)^2\Phi - a^2\dfrac{\mathrm{d}\bar{V}}{\mathrm{d}\varphi}\delta\varphi\right]\delta^i{}_j \ . & (8.92) \end{cases}$$

Since $\delta\varphi$ is a scalar, under a gauge transformation generated by $\boldsymbol{\xi} = T\frac{\partial}{\partial\eta} + L^i\frac{\partial}{\partial x^i}$, it transforms as:

$$\widetilde{\delta\varphi} = \delta\varphi + \bar{\varphi}'T \ . \tag{8.93}$$

We can introduce two gauge invariant scalars associated to the inflaton:

$$\chi = \delta\varphi + \bar{\varphi}'\left(B - E'\right) \ , \tag{8.94}$$

which corresponds to the *inflaton fluctuations in the Newtonian gauge*, and:

$$Q = \delta\varphi + \frac{\bar{\varphi}'}{\mathcal{H}}\Psi \ . \tag{8.95}$$

Q is called the *Mukhanov-Sasaki* variable. It matches the inflaton fluctuations in the *flat-slicing gauge*, defined as the gauge in which the scalar part of the curvature perturbation of spatial section completely vanishes ${}^{(3)}R = 0$, which, according to Eq. (4.119), means $\Psi = 0$. The extra gauge degrees of freedom are then fixed by imposing $E = 0$ and $\bar{E}^i = 0$. Note that in this gauge, the comoving curvature perturbation ζ simply reads:

$$\zeta = -\mathcal{H}\left[B + V\right] \ , \tag{8.96}$$

where V is the velocity potential of the matter content. To find V for our scalar field, we must remember that for scalar modes only:

$$\delta T^0{}_i = \left(\bar{\rho} + \bar{p}\right)\partial_i\left(V + B\right) = -\frac{1}{a^2}\bar{\varphi}'\partial_i\delta\varphi \ . \tag{8.97}$$

Since, for the scalar field:

$$\bar{\rho} = \frac{1}{2a^2}\bar{\varphi}'^2 + \bar{V} \tag{8.98}$$

$$\bar{p} = \frac{1}{2a^2}\bar{\varphi}'^2 - \bar{V} \ , \tag{8.99}$$

this leads to:

$$V + B = -\frac{\delta\varphi}{\bar{\varphi}'} \ . \tag{8.100}$$

Hence, in the flat slicing gauge:

$$\zeta = \frac{\mathcal{H}}{\bar{\varphi}'}\delta\varphi = \frac{\mathcal{H}}{\bar{\varphi}'}Q \ . \tag{8.101}$$

This is why the flat slicing gauge is ideal for inflation. Making calculations in that gauge gives immediately the fluctuations in ζ in terms of those in the inflaton. In what follows, we will do everything in that gauge.

8.5.2 Perturbed equations

We can now write the Einstein Field equations with $\Lambda = 0$, supplemented with the dynamical equation for φ coming from the conservation of the energy-momentum tensor. Note that, since φ is a scalar, its evolution equation, $\nabla_\mu T^\mu{}_\nu = 0$, does not contribute to vector and tensor equations. In the background:

$$\begin{cases} \mathcal{H}^2 = \dfrac{8\pi G}{3}\left[\dfrac{1}{2}\left(\bar{\varphi}'\right)^2 + a^2\bar{V}\right] & (8.102) \\ \mathcal{H}^2 + 2\mathcal{H}' = -8\pi G\left[\dfrac{1}{2}\left(\bar{\varphi}'\right)^2 - a^2\bar{V}\right] & (8.103) \\ \bar{\varphi}'' + 2\mathcal{H}\bar{\varphi}' + a^2\dfrac{\mathrm{d}V}{\mathrm{d}\varphi}(\bar{\varphi}) = 0\ . & (8.104) \end{cases}$$

And at first order:

$$\delta G^\mu{}_\nu = 8\pi G \delta T^\mu{}_\nu\ , \tag{8.105}$$

In the flat slicing gauge we get:

- For *tensor modes*:

  We get one equation:

  $$\bar{E}_{ij}'' - \Delta\bar{E}_{ij} + 2\mathcal{H}\bar{E}_{ij}' = 0\ . \tag{8.106}$$

  This is the same that we had during the hot Big-Bang phase but the story will be a bit different. As is well known, tensor modes can be decomposed into two independent polarisation modes, $\times$ and +, rotated by $\pi/4$ with respect to each other. Then, a generic solution in Fourier space (we are not using hats for Fourier modes here to avoid confusion with quantised fields) reads:

  $$\begin{aligned} \bar{E}_{ij}\left(\eta, \vec{k}\right) &= \bar{E}_+(\eta, \vec{k})\varepsilon_{ij}^+\left(\vec{k}\right) + \bar{E}_\times(\eta, \vec{k})\varepsilon_{ij}^\times\left(\vec{k}\right) & (8.107) \\ &= \sum_{\lambda=+,\times} \bar{E}_\lambda(\eta, \vec{k})\varepsilon_{ij}^\lambda\left(\vec{k}\right)\ , & (8.108) \end{aligned}$$

  where the polarisation tensors satisfy:

  $$\begin{cases} \delta^{ij}\varepsilon_{ij}^\lambda\left(\vec{k}\right) = k^i\varepsilon_{ij}^\lambda\left(\vec{k}\right) = 0 & (8.109) \\ \varepsilon_{ij}^\lambda\left(\vec{k}\right)\varepsilon_{\lambda'}^{ij}\left(\vec{k}\right) = \delta^\lambda{}_{\lambda'} & (8.110) \\ \varepsilon_{ij}^\lambda\left(-\vec{k}\right) = \left[\varepsilon_{ij}^\lambda\left(\vec{k}\right)\right]^*\ . & (8.111) \end{cases}$$

Then, the modes separately obey:

$$\bar{E}_\lambda'' + k^2 \bar{E}_\lambda + 2\mathcal{H}\bar{E}_\lambda' = 0 \,. \tag{8.112}$$

As in the case of the scalar field in de Sitter spacetime, the correct degree of freedom to quantise turns out to be $\mu_\lambda = a\bar{E}_\lambda$, which obeys the equation:

$$\boxed{\mu_\lambda'' + \left(k^2 - \frac{a''}{a}\right)\mu_\lambda = 0 \,.} \tag{8.113}$$

This is exactly the Mukhanov-Sasaki equation (8.60) that was governing the evolution of modes for a scalar field in de Sitter spacetime, except that now, a''/a is not quite as simple.

- For *vector modes*:
  We obtain two equations, from the $(0, i)$ and the (i, j) Einstein field equations:

$$\begin{cases} \Delta\bar{B}_i = 0 & (8.114) \\ \bar{B}_i' + 2\mathcal{H}\bar{B}_i = 0 \,. & (8.115) \end{cases}$$

  The second equation implies that:

$$\bar{B}_i \propto a^{-2} \,, \tag{8.116}$$

  so that any amount of initial vector modes present at the beginning of inflation gets completely washed out. We will not concern ourselves with vectors any longer.

- For *scalar modes*:

  We obtain four equations from the Einstein field equations:

$$\begin{cases} -2\mathcal{H}\Delta B = 8\pi G\left[\bar{\phi}'Q' + a^2\dfrac{\mathrm{d}\bar{V}}{\mathrm{d}\phi}Q + 2a^2\bar{V}\Phi\right] & (8.117) \\ 2\mathcal{H}\Phi - \left(2\mathcal{H}' + \mathcal{H}^2\right)B = 8\pi G\left[\bar{\varphi}'Q + \left(\dfrac{1}{2}\varphi'^2 - a^2V\right)B\right] & (8.118) \\ -\left(B' + 2\mathcal{H}B\right) - \Phi = 0 & (8.119) \\ 2\left(2\mathcal{H}' + \mathcal{H}^2\right)\Phi + 2\mathcal{H}\Phi' + 8\pi G\bar{\varphi}'^2\Phi = 8\pi G\left[\bar{\varphi}'Q' - a^2\dfrac{\mathrm{d}\bar{V}}{\mathrm{d}\varphi}Q\right] \,, & (8.120) \end{cases}$$

as well as an evolution equation for Q from the conservation of the energy-momentum tensor:

$$Q'' + 2\mathcal{H}Q' - \Delta Q + a^2 \frac{\mathrm{d}^2 \bar{V}}{\mathrm{d}\phi^2} Q = \bar{\varphi}' \left[\Phi' + \Delta B\right] \ . \tag{8.121}$$

Combining Eqs (8.119) and (8.118), we get:

$$\Phi = \frac{4\pi G \bar{\varphi}'}{\mathcal{H}} Q \ . \tag{8.122}$$

In turn, we can substitute that in Eq. (8.117) to obtain ΔB in terms of Q and Q'. Therefore, the source term in Eq. (8.121) can be expressed in terms of the scalar field Q only, and we can obtain a decoupled equations for that field. It turns out that for quantisation, as usual, the right degree of freedom is not Q, but $v = aQ$, which then can be shown (after some tedious calculations) to obey, in Fourier space:

$$\boxed{v'' + \left(k^2 - \frac{z''}{z}\right) v = 0 \ ,} \tag{8.123}$$

with:

$$z = \frac{a\bar{\varphi}'}{\mathcal{H}} \ . \tag{8.124}$$

Once again, we find something akin to the Mukhanov-Sasaki equation (8.60), albeit with a different time dependent term in the effective mass.

8.5.3 Quantum fluctuations

To quantise the fields, we proceed as in subsection 8.4.2.

Scalars

For scalar, our canonical variable is $v = aQ$. Its canonical momentum is $\pi = v'$. Then, for each mode $\vec{k}$, we promote v and π to operators, $\hat{v}$ and $\hat{\pi}$ satisfying canonical commutation relations on constant time hypersurfaces:

$$\left[\hat{v}\left(\eta, \vec{k}\right), \hat{v}\left(\eta, \vec{k}'\right)\right] = \left[\hat{\pi}\left(\eta, \vec{k}\right), \hat{\pi}\left(\eta, \vec{k}'\right)\right] = 0 \tag{8.125}$$

$$\left[\hat{v}\left(\eta, \vec{k}\right), \hat{\pi}\left(\eta, \vec{k}'\right)\right] = \mathrm{i}\delta_D\left(\vec{k} - \vec{k}'\right) \ . \tag{8.126}$$

Next, we look for solutions decomposed according to the basis of creation and annihilation parameters:

$$\hat{v} = v_k(\eta)\,\hat{a}_{\vec{k}} + v_k^*(\eta)\,\hat{a}_{\vec{k}}^\dagger\,, \tag{8.127}$$

where the amplitude satisfies the classical equation:

$$v_k'' + \left(k^2 - \frac{z''}{z}\right) v_k = 0\,, \tag{8.128}$$

with:

$$z = \frac{a\bar{\varphi}'}{\mathcal{H}}\,. \tag{8.129}$$

The subtlety, as always, lies in the definition of the vacuum state, and that is where the use of v as a canonical variable becomes handy. As in the de Sitter case, requiring that the sub-Hubble modes behave as in flat spacetime imposes:

$$v_k(\eta) \sim \frac{1}{\sqrt{2k}} \mathrm{e}^{-\mathrm{i}k\eta}, \quad \text{when} \quad k\eta \to -\infty\,. \tag{8.130}$$

Given a background dynamics, we can estimate $z(\eta)$ and solve Eq. (8.128) to get the the evolution of the quantised field. We will do that in slow-roll inflation is subsection 8.5.4 below. Once we have the solution for v_k, as in the de Sitter case above, we construct the dimensionless power spectrum of f such that:

$$\Delta_v^2\left(\eta, \vec{k}\right) = \frac{k^3}{2\pi^2}\left|v_k(\eta)\right|^2\,. \tag{8.131}$$

Finally, remembering that:

$$v = aQ = a\frac{\bar{\varphi}'}{\mathcal{H}}\zeta = z\zeta\,, \tag{8.132}$$

we get the dimensionless power spectrum for the comoving curvature perturbation, ζ, as:

$$\Delta_\zeta^2\left(\eta, \vec{k}\right) = \frac{1}{z^2}\Delta_v^2\left(\eta, \vec{k}\right) = \frac{k^3}{2\pi^2 z^2}\left|v_k(\eta)\right|^2\,. \tag{8.133}$$

And finally, the power spectrum, which is relevant to connect to the hot Big-Bang phase, is:

$$\mathcal{P}_\zeta\left(\eta, \vec{k}\right) = \frac{1}{2\pi^2 z^2}\left|v_k(\eta)\right|^2\,. \tag{8.134}$$

Tensors

For tensors, we proceed exactly the same way, but the variables to quantise are the μ_λ 's and their canonical momenta. Then we write:

$$\hat{\mu}_\lambda = \mu_{k,\lambda}(\eta)\,\hat{a}_{\vec{k}} + \mu^*_{k,\lambda}(\eta)\,\hat{a}^\dagger_{\vec{k}}\,, \tag{8.135}$$

with:

$$\boxed{\mu''_{k,\lambda} + \left(k^2 - \frac{a''}{a}\right)\mu_{k,\lambda} = 0\,.} \tag{8.136}$$

Since we have to sum over all possible states of polarisations, the dimensionless power spectrum of tensor modes is eight times the one for one polarisation state:

$$\Delta^2_T\left(\eta,\vec{k}\right) = 8\Delta^2_{E_\lambda}\left(\eta,\vec{k}\right) = 8\frac{k^3}{2\pi^2a^2}\left|\mu_{k,\lambda}\right|^2\,. \tag{8.137}$$

Thus:

$$\boxed{\Delta^2_T\left(\eta,\vec{k}\right) = k^3\mathcal{P}_T\left(\eta,\vec{k}\right) = \frac{4k^3}{\pi^2a^2}\left|\mu_{k,\lambda}\right|^2\,.} \tag{8.138}$$

The existence of a background of primordial gravitational waves corresponding to these tensor modes is a generic prediction of inflation and can be considered a calculation in perturbative, semi-classical, quantum gravity, since the metric potential $\bar{E}_{ij}$ has been treated as a quantum field on a classical background spacetime.

8.5.4 Slow-roll inflation

To make some definite prediction, we need to determine $a(\eta)$ and $z(\eta)$, in order to solve Eqs (8.128) and (8.136). The solutions can then be plugged into Eqs (8.133) and (8.138). After taking the limit $k\eta \to +\infty$, which corresponds to the end of inflation, once all modes of interests have been stretched out of the Hubble, we will have our primordial, initial power spectra, which are the initial conditions for the Hot Big-Bang phase that follows inflation. Here, we will look at carrying on this plan for slow-roll inflation. The first thing to notice is that, in slow-roll:

$$z = a\bar{\varphi}'\mathcal{H} = \frac{a\dot{\varphi}}{H} = a\sqrt{\frac{\varepsilon}{4\pi G}}\,. \tag{8.139}$$

Besides, we will limit our discussion to simple models, called power law inflation. In such models, the scalar field potential is constructed so that the background dynamics during slow-roll reduces to:

$$a(\eta) \propto |\eta|^{1+\beta} \ , \tag{8.140}$$

for some constant $\beta < -2$. This can be achieved with potentials:

$$V(\varphi) = V_i \exp\left[4\sqrt{\frac{\pi}{p}}\frac{\varphi - \varphi_i}{M_{\rm Pl}}\right] \ , \tag{8.141}$$

with $p = (1+\beta)/(2+\beta)$. Then, the scalar field dynamics is given by:

$$\bar{\varphi}(\eta) = \varphi_i + \frac{M_{\rm Pl}}{2\sqrt{p}}(1+\beta)\ln|\eta| \ . \tag{8.142}$$

The slow-roll parameters of this model are constant:

$$\varepsilon = \delta = \frac{1}{p} \ , \tag{8.143}$$

so that $\tilde{\eta} = 0$ and slow-roll never ends. Since we have the exact expansion, we can obtain:

$$z = \sqrt{\pi p}\,|\eta|^{1+\beta} \ , \tag{8.144}$$

and the conformal Hubble rate:

$$\mathcal{H} = -\frac{1}{1-\varepsilon}\frac{1}{\eta} \ . \tag{8.145}$$

We see that $\eta \in \mathbb{R}_-$. The equation for the scalar modes thus reads:

$$v_k'' + \left[k^2 - \frac{\nu^2 - 1/4}{\eta^2}\right] v_k = 0 \ , \tag{8.146}$$

for $\nu = -\beta - 1/2$. The solution must satisfy the initial condition (8.130). It is given in terms of a Hankel function:

$$v_k\,(\eta) = \frac{\sqrt{\pi}}{2}\mathrm{e}^{\mathrm{i}(\nu-1/2)\pi/2}\sqrt{-\eta}H_\nu^{(1)}\,(-k\eta) \ . \tag{8.147}$$

Since we are interested in the solution once the modes have exited the Hubble scale, at the end of inflation, we estimate as $-k\eta \ll 1$:

$$v_k(\eta) \sim 2^{\nu-3/2}\frac{\Gamma(\nu)}{\Gamma(3/2)}\mathrm{e}^{\mathrm{i}(\nu-1/2)\pi/2}\frac{1}{\sqrt{2k}}\,(-k\eta)^{-\nu+1/2} \ . \tag{8.148}$$

Note that $\zeta = v_k/z \sim \eta^{-1-\beta}(-k\eta)^{-\nu+1/2} \sim \eta^{-1/2-(\beta+\nu)} \sim$ constant. Thus we see that, as announced, inflation predicts that comoving curvature perturbations freeze when they become super-Hubble. Inflation *predicts* adiabatic initial conditions for the hot Big-Bang phase. Finally, we get:

$$\mathcal{P}_\zeta(\eta,k) = \frac{k^{-3}H^2}{\pi M_{\rm Pl}^2\varepsilon}\left[2^{\nu-3/2}\frac{\Gamma(\nu)}{\Gamma(3/2)}\right]^2\left(\nu-\frac{1}{2}\right)^{1-2\nu}\left(\frac{k}{aH}\right)^{-2\nu+3} . \tag{8.149}$$

Since modes are practically frozen when they exit the Hubble radius, we can evaluate that power spectrum at the time η such that $k = \mathcal{H}(\eta) = aH$. Thus, the primordial power spectrum is:

$$\boxed{\mathcal{P}_\zeta(k) = \frac{k^{-3}}{\pi M_{\rm Pl}^2}\left[2^{\nu-3/2}\frac{\Gamma(\nu)}{\Gamma(3/2)}\right]^2\left(\nu-\frac{1}{2}\right)^{1-2\nu}\left(\frac{H^2}{\varepsilon}\right)_{k=aH}} \tag{8.150}$$

Because at $k = aH$, $k \propto 1/\eta$, and $H^2 \propto \eta^{4+2\beta}$, we see that the power spectrum goes like $k^{-3-(4+2\beta)}$. In slow roll, $\varepsilon \ll 1$, and thus $\beta \sim -2$, so that we recover a primordial power spectrum in k^{-3}, as announced in section 5.5. At linear order in the slow-roll parameters:

$$\nu = \frac{3}{2} + O(\varepsilon^2) , \tag{8.151}$$

so that we have the easier to remember leading results:

$$\boxed{\mathcal{P}_\zeta(k) = \frac{k^{-3}}{\pi M_{\rm Pl}^2}\left(\frac{H^2}{\varepsilon}\right)_{k=aH}} \tag{8.152}$$

Finally, in this class of models, the study of gravitational waves follows closely that of scalars since $z \propto a$. The solution to Eq. (8.136) is thus given by (8.147). Therefore:

$$\boxed{\mathcal{P}_T = 16\varepsilon\mathcal{P}_\zeta} . \tag{8.153}$$

This relation, as well as the form (8.152) are actually features of slow-roll inflation and persist in a more general setting. Checking this relation between the amplitude of scalar and tensor primordial fluctuations is thus a very important aspect of modern cosmology. To date, primordial gravitational waves still elude us and the relation remains untested. We can define the spectral indices for both spectra as the logarithmic running of the dimensionless power spectra:

$$n_S - 1 = \frac{{\rm d}\ln\Delta_\zeta^2}{{\rm d}\ln k} \quad \text{and} \quad n_T = \frac{{\rm d}\ln\Delta_T^2}{{\rm d}\ln k} . \tag{8.154}$$

Then:

$$n_S = 2\beta + 5 = 2\frac{\varepsilon - 2}{1-\varepsilon} = \frac{1-3\varepsilon}{1-\varepsilon} \simeq 1 - 2\varepsilon \text{ in slow-roll} \tag{8.155}$$

$$n_T = 2\beta + 4 = \frac{-2\varepsilon}{1-\varepsilon} \simeq -2\varepsilon \text{ in slow-roll .} \tag{8.156}$$

This, we have the *consistency relation*:

$$\boxed{\mathcal{P}_T = -8 n_T \mathcal{P}_\zeta \ .} \tag{8.157}$$

The key simplifying assumptions here is that slow-roll parameters were assumed constant. when this is no longer the case, things become much more complicated. One needs to use an expansion scheme to calculate corrections to the spectral indices which, generically, receive scale-dependent corrections. However, the physics remain the same as the one explored previously.

8.6 Problems

Pb. 8.1 Recover the form of the energy-momentum tensor for a scalar field, Eq. (8.13).

Pb. 8.2 Recover the Klein-Gordon equation (8.19) for the conservation of the energy momentum tensor of the scalar field.

Pb. 8.3 The Higgs field as inflaton

As it is the only fundamental scalar field we know in nature, it is tempting to ask if the Higgs field could have been responsible for inflation.

- Let the Higgs potential be:

$$V(\varphi) = \lambda \left(\varphi^2 - v^2\right)^2 \ , \tag{8.158}$$

  with $v = 246$ GeV. Sketch this potential and identify the regions in which slow-roll inflation light occur.
- Give the slow-roll parameters ε_V and η_V.
- Show that the hilltop region $0 < \varphi < v$ cannot accommodate slow-roll inflation.
- Show that slow-roll inflation is possible if $\varphi \gg v$. Determine the final value φ_E of φ at the end of inflation, and its value 60 e-folds before the end, φ_I, assuming $\varphi_I \gg \varphi_E$.

- Estimate the amplitude of the scalar power spectrum generated by an Higgs inflation and compare it to observations. Conclude.

Appendices

A

Formulæ from General Relativity

Contents

This is not a course in General Relativity so we urge the readers to familiarise themselves with the basics of this theory in standard textbooks or in the notes for the M1 course. Here we will simply list some useful conventions and formulæ that we will be using.

A.1 Metric and convariant derivatives

Greek letters will denote spacetime indices and run in $\{0, 1, 2, 3\}$ and Latin, second-half of the alphabet, letters will denote spatial indices and run in $\{1, 2, 3\}$. We will adopt Einstein summation convention for repeated indices.

We will always work on 4-dimensional spacetimes with a pseudo-Riemannian metric g with signature $(-, +, +, +)$. This means that locally, in a coordinate system $\left(x^0, x^i\right)$, x^0 will be timelike, x^i's spacelike and:

$$\boldsymbol{g} = g_{\mu\nu}\,(x)\,\mathrm{d}x^\mu \otimes \mathrm{d}x^\nu\ . \tag{A.1}$$

A vector field $\boldsymbol{u}$ is timelike (resp. spacelike) if and only if $\boldsymbol{g}(\boldsymbol{u}, \boldsymbol{u}) < 0$ (resp. $\boldsymbol{g}(\boldsymbol{u}, \boldsymbol{u}) > 0$). It is null or lightlike if and only if $\boldsymbol{g}(\boldsymbol{u}, \boldsymbol{u}) = 0$. Each vector field defines a covector (one-form field, field of linear functions on the vectors) $\boldsymbol{g}(\boldsymbol{u}, \cdot)$. In physics, we replace these tensorial notations with component notations. For example, we introduce the convenient line element:

$$\mathrm{d}s^2 = g_{\mu\nu}\,(x)\,\mathrm{d}x^\mu \mathrm{d}x^\nu\ . \tag{A.2}$$

Vectors and covectors are decomposed in local coordinate bases:

$$\boldsymbol{u} = u^\mu \frac{\partial}{\partial x^\mu} \text{ and } \boldsymbol{\omega} = \omega_\mu \mathrm{d}x^\mu\,, \tag{A.3}$$

with, as usual: $\mathrm{d}x^\nu \left(\frac{\partial}{\partial x^\mu}\right) = \delta^\nu{}_\mu$. We pass from vector to covectors and conversely by 'raising and lowering the indices with the metric tensor':

$$u_\mu = g_{\mu\nu} u^\nu \tag{A.4}$$

$$\omega^\mu = g^{\mu\nu} \omega_\nu\,, \tag{A.5}$$

where $g^{\mu\nu}$ is the 'inverse' of $g_{\mu\nu}$:

$$g^{\mu\rho} g_{\rho\nu} = \delta^\mu{}_\nu\ . \tag{A.6}$$

Associated to a metric structure, is an affine connection which allows one to define a notion of parallel transport of vectors, covectors and tensors that is compatible with the metric and torsionless.

We denote that connection by $\boldsymbol{\nabla}$. If we write vector fields in a local coordinate basis: $\boldsymbol{u} = u^\mu \frac{\partial}{\partial x^\mu}$ and $\boldsymbol{v} = v^\mu \frac{\partial}{\partial x^\mu}$, the covariant derivative of $\boldsymbol{u}$ along $\boldsymbol{v}$ is a vector field denoted $\boldsymbol{\nabla_v u}$, with components:

$$(\nabla_v u)^\mu = v^\nu \partial_\nu u^\mu + \Gamma^\mu{}_{\rho\nu} u^\rho v^\nu \,, \tag{A.7}$$

where the functions $\Gamma^\mu{}_{\rho\nu}$ are not the components of a tensor, but are the Christoffel symbols, given by:

$$\Gamma^\mu{}_{\rho\nu} = \frac{1}{2} g^{\mu\lambda} \left[\partial_\rho g_{\lambda\nu} + \partial_\nu g_{\rho\lambda} - \partial_\lambda g_{\rho\nu} \right] \,. \tag{A.8}$$

By choosing the basis vectors for our coordinate basis for $\boldsymbol{v}$, we usually define the covariant derivatives of the components of $\boldsymbol{u}$:

$$\nabla_\mu u^\nu = (\nabla_{\partial/\partial x^\mu} u)^\nu = \partial_\mu u^\nu + \Gamma^\nu{}_{\rho\mu} u^\rho \,. \tag{A.9}$$

The action of the covariant derivative on covectors is given similarly by:

$$\nabla_\mu u_\nu = (\nabla_{\partial/\partial x^\mu} u)_\nu = \partial_\mu u_\nu - \Gamma^\rho{}_{\mu\nu} u_\rho \,, \tag{A.10}$$

and the action on the components of a generic tensor follows, each index being treated as a vector or covector index appropriately.
A geodesic of the connection is a curve whose tangent vector field is parallel propagated along the curve itself:

$$\boldsymbol{\nabla_u u} = 0 \,. \tag{A.11}$$

In components, this gives the geodesic equation:

$$u^\mu \nabla_\mu u^\nu = u^\mu \partial_\mu u^\nu + \Gamma^\mu{}_{\rho\nu} u^\rho u^\nu = 0 \,. \tag{A.12}$$

In GR, geodesics are timelike, spacelike or lightlike (null) depending on whether their tangent vector field is everywhere timelike, spacelike or null. Timelike geodesics corresponds to the worldlines of free-falling massive particles while lightlike ones are the worldlines of free-falling photons and other massless particles.

A.2 Curvature and Einstein field equations

From the affine connection, we can then define a Riemann tensor, which, in components reads:

$$R^\mu{}_{\nu\alpha\beta} = \partial_\alpha \Gamma^\mu{}_{\nu\beta} - \partial_\beta \Gamma^\mu{}_{\nu\alpha} + \Gamma^\mu{}_{\sigma\alpha} \Gamma^\sigma{}_{\nu\beta} - \Gamma^\mu{}_{\sigma\beta} \Gamma^\sigma{}_{\nu\alpha} \,. \tag{A.13}$$

From this, we can form the Ricci tensor and its trace, the Ricci scalar:

$$R_{\mu\nu} = R^{\alpha}{}_{\mu\alpha\nu} \tag{A.14}$$

$$R = g^{\mu\nu}R_{\mu\nu} \, . \tag{A.15}$$

Finally, the Einstein tensor has components:

$$G_{\mu\nu} = R_{\mu\nu} - \frac{R}{2}g_{\mu\nu} \, , \tag{A.16}$$

and the Einstein Field equations, linking geometry and mater sources, are given by:

$$G_{\mu\nu} + \Lambda g_{\mu\nu} = \frac{8\pi G}{c^4}T_{\mu\nu} \, , \tag{A.17}$$

where Λ is a number called the cosmological constant, and $T_{\mu\nu}$ are the components of the energy-momentum tensor of the matter present in spacetime. It is conserved as a consequence of the Bianchi identities which are purely geometric:

$$\nabla_{\mu}T^{\mu}{}_{\nu} = \partial_{\mu}T^{\mu}{}_{\nu} + \Gamma^{\mu}{}_{\rho\mu}T^{\rho}{}_{\nu} - \Gamma^{\rho}{}_{\nu\mu}T^{\mu}{}_{\rho} = 0 \, . \tag{A.18}$$

This is the conservation of energy-momentum.

B

Geometric objects for the perturbed, flat FLRW spacetime

Contents

In this appendix, we will derive in (some) details, the quantities associated to the metric of a perturbed flat FLRW Universe given in Eq. (4.64). Let us start with the metric:

$$\begin{aligned} \mathrm{d}s^2 &= a^2(\eta)\left(\bar{g}_{\mu\nu} + h_{\mu\nu}\right)\mathrm{d}x^\mu \mathrm{d}x^\nu & \text{(B.1)} \\ &= a^2(\eta)\left[(-1+h_{00})\,\mathrm{d}\eta^2 + 2h_{0i}\mathrm{d}\eta\mathrm{d}x^i + \left(\delta_{ij} + h_{ij}\mathrm{d}x^i\mathrm{d}x^j\right)\right]\,, & \text{(B.2)} \end{aligned}$$

in which we define the metric potentials:

$$\begin{aligned} h_{00} &= -2\Phi & \text{(B.3)} \\ h_{0i} &= \partial_i B + \bar{B}_i \text{ with } \partial_i \bar{B}^i = 0 & \text{(B.4)} \\ h_{ij} &= -2\Psi\gamma_{ij} + 2\partial_{(i}\partial_{j)}E + 2\partial_{(i}\bar{E}_{j)} + 2\bar{E}_{ij} & \text{(B.5)} \\ &\quad \text{with } \partial_i \bar{E}^i = 0\,,\ \partial_i \bar{E}^i_j = 0\,,\ \bar{E}^i{}_i\,. \end{aligned}$$

Note that we can write:

$$g_{\mu\nu} = a^2\left[\eta_{\mu\nu} + h_{\mu\nu}\right]\,, \tag{B.6}$$

so that the inverse metric at first order reads:

$$g^{\mu\nu} = a^{-2}\left[\eta^{\mu\nu} - h^{\mu\nu}\right]\,. \tag{B.7}$$

Indices on the perturbations are lowered and raised using the Minkowski metric since we defined conformal perturbations:

$$h^\mu{}_\nu = \eta^{\mu\rho}h_{\rho\nu} \text{ and } h^{\mu\nu} = \eta^{\mu\rho}\eta^{\nu\sigma}h_{\rho\sigma}\,. \tag{B.8}$$

B.1 Connection coefficients

The connection coefficients read:

$$\Gamma^\mu{}_{\nu\rho} = \frac{1}{2a^2}\left[\eta^{\mu\lambda} - h^{\mu\lambda}\right]\left\{\partial_\nu\left[a^2\left(\eta_{\rho\lambda} + h_{\rho\lambda}\right)\right] + \partial_\rho\left[a^2\left(\eta_{\nu\lambda} + h_{\nu\lambda}\right)\right] - \partial_\lambda\left[a^2\left(\eta_{\rho\nu} + h_{\rho\nu}\right)\right]\right\} \tag{B.9}$$

$$= \bar{\Gamma}^\mu{}_{\nu\rho} + \delta\Gamma^\mu{}_{\nu\rho}\,, \tag{B.10}$$

where the background connection coefficients are:

$$\bar{\Gamma}^{\mu}{}_{\nu\rho} = \frac{1}{2a^2}\eta^{\mu\lambda}\left[\partial_\nu a^2\eta_{\rho\lambda} + \partial_\rho a^2\eta_{\nu\lambda} - \partial_\lambda a^2\eta_{\rho\nu}\right] \tag{B.11}$$

$$= \frac{2aa'}{a^2}\eta^{\mu\lambda}\left[\delta_{\nu 0}\eta_{\rho\lambda} + \delta_{\rho 0}\eta_{\nu\lambda} - \delta_{\lambda 0}\eta_{\rho\nu}\right] \tag{B.12}$$

$$= \mathcal{H}\left[\delta_{\nu 0}\delta^{\mu}{}_{\rho} + \delta_{\rho 0}\delta^{\mu}{}_{\nu} - \eta^{\mu 0}\eta_{\nu\rho}\right] \; .. \tag{B.13}$$

Thus, using $\eta^{\mu 0} = -\delta^{\mu 0}$:

$$\bar{\Gamma}^{\mu}{}_{\nu\rho} = \mathcal{H}\left[\delta_{\nu 0}\delta^{\mu}{}_{\rho} + \delta_{\rho 0}\delta^{\mu}{}_{\nu} + \delta^{\mu 0}\eta_{\nu\rho}\right] \; . \tag{B.14}$$

We can expand this expression to write the only non-zero connection coefficients in the background:

Background connection coefficients

$$\begin{cases} \bar{\Gamma}^{0}{}_{\mu\nu} = \mathcal{H}\delta_{\mu\nu} & \text{(B.15)} \\ \bar{\Gamma}^{i}{}_{0j} = \bar{\Gamma}^{i}{}_{j0} = \mathcal{H}\delta^{i}{}_{j} \; . & \text{(B.16)} \end{cases}$$

For the perturbed part, on the other hand:

$$\delta\Gamma^{\mu}{}_{\nu\rho} = \frac{1}{2a^2}\eta^{\mu\lambda}\left[\partial_\nu\left(a^2 h_{\rho\lambda}\right) + \partial_\rho\left(a^2 h_{\lambda\nu}\right) - \partial_\lambda\left(a^2 h_{\rho\nu}\right)\right]$$
$$- \frac{1}{2a^2}h^{\mu\lambda}\left[\partial_\nu\left(a^2\right)\eta_{\rho\lambda} + \partial_\rho\left(a^2\right)\eta_{\lambda\nu} - \partial_\lambda\left(a^2\right)\eta_{\rho\nu}\right] \tag{B.17}$$

$$= \frac{1}{2}\eta^{\mu\lambda}\left[\partial_\nu h_{\rho\lambda} + \partial_\rho h_{\lambda\nu} - \partial_\lambda h_{\rho\nu}\right] + \mathcal{H}\eta^{\mu\lambda}\left[h_{\rho\lambda}\delta_{\nu 0} + h_{\nu\lambda}\delta_{\rho 0} - h_{\nu\rho}\delta_{\lambda 0}\right]$$
$$- \mathcal{H}h^{\mu\lambda}\left[\eta_{\rho\lambda}\delta_{\nu 0} + \eta_{\nu\lambda}\delta_{\rho 0} - \eta_{\nu\rho}\delta_{\lambda 0}\right] \tag{B.18}$$

$$= \frac{1}{2}\eta^{\mu\lambda}\left[\partial_\nu h_{\rho\lambda} + \partial_\rho h_{\lambda\nu} - \partial_\lambda h_{\rho\nu}\right]$$
$$+ \mathcal{H}\left[h_{\rho}{}^{\mu}\delta_{\nu 0} + h_{\nu}{}^{\mu}\delta_{\rho 0} - h_{\nu\rho}\eta^{\mu 0} - h^{\mu}{}_{\rho}\delta_{\nu 0} - h^{\mu}{}_{\nu}\delta_{\rho 0} + \eta_{\nu\rho}h^{\mu 0}\right] \; , \tag{B.19}$$

so that:

$$\delta\Gamma^{\mu}{}_{\nu\rho} = \frac{1}{2}\eta^{\mu\lambda}\left[\partial_\nu h_{\rho\lambda} + \partial_\rho h_{\lambda\nu} - \partial_\lambda h_{\rho\nu}\right] - \mathcal{H}\left[\eta^{\mu\sigma}h_{\sigma 0}\eta_{\nu\rho} - h_{\nu\rho}\delta^{\mu 0}\right] \; , \tag{B.20}$$

where we used that: $h_{\rho}{}^{\mu} = h^{\mu}{}_{\rho}$. We can now list the non-zero ones:

Non-zero perturbations to the connection coefficients in flat FLRW

$$
\begin{cases}
\delta\Gamma^0{}_{00} = \Phi' & \text{(B.21)} \\
\delta\Gamma^0{}_{0i} = \delta\Gamma^0{}_{i0} = \partial_i\Phi + \mathcal{H}\left[\partial_i B + \bar{B}_i\right] & \text{(B.22)} \\
\delta\Gamma^0{}_{ij} = -\left[\partial_{(i}\partial_{j)}\left(B - E'\right) + \partial_{(i}\left(\bar{B}_{|j)} - \bar{E}'_{|j)}\right) + \Psi'\delta_{ij} - \bar{E}'_{ij}\right] & \\
\qquad\qquad - \mathcal{H}\left[2\left(\Phi - \Psi\right)\delta_{ij} + 2\partial_{(i}\partial_{j)}E + 2\partial_{(i}\bar{E}_{j)} + 2\bar{E}_{ij}\right] & \text{(B.23)} \\
\delta\Gamma^i{}_{00} = \partial_i\left(B' - \Phi\right) + \bar{B}'_i + \mathcal{H}\left[\partial_i B + \bar{B}_i\right] & \text{(B.24)} \\
\delta\Gamma^i{}_{0j} = \delta\Gamma^i{}_{j0} = -\Psi'\delta^i{}_j + \partial_{(i}\partial_{j)}E' + \partial_{(i}\bar{E}'_{j)} + \bar{E}'_{ij} + \partial_{[i}\bar{B}_{i]} & \text{(B.25)} \\
\delta\Gamma^i{}_{jk} = 2\partial_{[i}\Psi\delta_{j]k} - \partial_k\Psi\delta^i{}_j - \mathcal{H}\left(\partial_i B + \bar{B}_i\right)\delta_{jk} & \\
\qquad\qquad + \partial_i\partial_{(j}\partial_{k)}E + \partial_{(j}\partial_{k)}\bar{E}_i + 2\partial_{(j}\bar{E}_{k)i} - \partial_i\bar{E}_{jk}\ . & \text{(B.26)}
\end{cases}
$$

B.2 Ricci tensor

Using the expression for the Ricci tensor (A.14) and the components of the Riemman tensor (A.13):

$$R_{\mu\nu} = \partial_\rho\Gamma^\rho{}_{\mu\nu} - \partial_\nu\Gamma^\rho{}_{\mu\rho} + \Gamma^\rho{}_{\lambda\rho}\Gamma^\lambda{}_{\mu\nu} - \Gamma^\rho{}_{\lambda\nu}\Gamma^\lambda{}_{\mu\rho}\ . \tag{B.27}$$

Expanding the connection coefficients, we can write:

$$R_{\mu\nu} = \bar{R}_{\mu\nu} + \delta R_{\mu\nu}\ , \tag{B.28}$$

with the background Ricci tensor:

$$\bar{R}_{\mu\nu} = \partial_\rho\bar{\Gamma}^\rho{}_{\mu\nu} - \partial_\nu\bar{\Gamma}^\rho{}_{\mu\rho} + \bar{\Gamma}^\rho{}_{\lambda\rho}\bar{\Gamma}^\lambda{}_{\mu\nu} - \bar{\Gamma}^\rho{}_{\lambda\nu}\bar{\Gamma}^\lambda{}_{\mu\rho}\ , \tag{B.29}$$

and the perturbation:

$$\delta R_{\mu\nu} = \partial_\rho\delta\Gamma^\rho{}_{\mu\nu} - \partial_\nu\delta\Gamma^\rho{}_{\mu\rho} + \bar{\Gamma}^\rho{}_{\lambda\rho}\delta\Gamma^\lambda{}_{\mu\nu} + \delta\Gamma^\rho{}_{\lambda\rho}\bar{\Gamma}^\lambda{}_{\mu\nu} - \left\{\bar{\Gamma}^\rho{}_{\lambda\nu}\delta\Gamma^\lambda{}_{\mu\rho} + \delta\Gamma^\rho{}_{\lambda\nu}\bar{\Gamma}^\lambda{}_{\mu\rho}\right\}\ . \tag{B.30}$$

Using the generic form of connection coefficients (B.14) we get[1], after some lengthy calcula-

[1]Do not use the expressions expanded in terms of metric potential at this stage, that would be pure folly! It is better to replace once the final results are obtained

tions:

$$\begin{cases} \partial_\rho \bar{\Gamma}^\rho{}_{\mu\nu} = \mathcal{H}' \delta_{\mu\nu} & \text{(B.31)} \\ \partial_\nu \delta\Gamma^\rho{}_{\mu\rho} = 4\mathcal{H}' \delta_{\mu 0}\delta_{\nu 0} & \text{(B.32)} \\ \bar{\Gamma}^\rho{}_{\lambda\rho}\bar{\Gamma}^\lambda{}_{\mu\nu} = 4\mathcal{H}^2 \delta_{\mu\nu} & \text{(B.33)} \\ \bar{\Gamma}^\rho{}_{\lambda\nu}\bar{\Gamma}^\lambda{}_{\mu\rho} = 2\mathcal{H}^2 \left[\delta_{\mu\nu} + \delta_{\mu 0}\delta_{\nu 0}\right] , & \text{(B.34)} \end{cases}$$

and, after even scarier ones:

$$\begin{cases} \partial_\rho \delta\Gamma^\rho{}_{\mu\nu} = \frac{1}{2}\left(\partial_\mu \partial^\lambda h_{\lambda\nu} + \partial_\nu \partial^\lambda h_{\mu\lambda} - \Box h_{\mu\nu}\right) - \mathcal{H}\left[\partial^\sigma h_{\sigma 0}\eta_{\mu\nu} - \partial_0 h_{\mu\nu}\right] \\ \qquad\qquad + \mathcal{H}'\left[h_{\mu\nu} + h_{00}\eta_{\mu\nu}\right] & \text{(B.35)} \\ \partial_\nu \delta\Gamma^\rho{}_{\mu\rho} = \frac{1}{2}\partial_\nu \partial_\mu h^\alpha{}_\alpha & \text{(B.36)} \\ \bar{\Gamma}^\rho{}_{\lambda\rho}\delta\Gamma^\lambda{}_{\mu\nu} + \delta\Gamma^\rho{}_{\lambda\rho}\bar{\Gamma}^\lambda{}_{\mu\nu} = \mathcal{H}\left[\delta_{0(\mu}\partial_{\nu)} h^\alpha{}_\alpha + \frac{1}{2}\partial_0 h^\alpha{}_\alpha \eta_{\mu\nu} - 4\partial_{(\mu}h_{\nu)0} + 2\partial_0 h_{\mu\nu}\right] \\ \qquad\qquad + 4\mathcal{H}^2\left[h_{\mu\nu} + h_{00}\eta_{\mu\nu}\right] & \text{(B.37)} \\ \bar{\Gamma}^\rho{}_{\lambda\nu}\delta\Gamma^\lambda{}_{\mu\rho} + \delta\Gamma^\rho{}_{\lambda\nu}\bar{\Gamma}^\lambda{}_{\mu\rho} = \mathcal{H}\left[\delta_{0(\mu}\partial_{\nu} h^\alpha{}_\alpha - 2\partial_{(\mu}h_{\nu)0} + 2\partial_0 h_{\mu\nu}\right] \\ \qquad\qquad + 2\mathcal{H}^2\left[h_{\mu\nu} + h_{00}\eta_{\mu\nu}\right] . & \text{(B.38)} \end{cases}$$

Putting everything together at last, we get:

$$\bar{R}_{\mu\nu} = \left[\mathcal{H}' + 2\mathcal{H}^2\right]\delta_{\mu\nu} - \left[4\mathcal{H}' + 2\mathcal{H}^2\right]\delta_{\mu 0}\delta_{\nu 0} , \tag{B.39}$$

and:

$$\begin{aligned} \delta R_{\mu\nu} = &-\frac{1}{2}\Box h_{\mu\nu} + \partial_{(\mu}\partial^\lambda h_{\nu)\lambda} - \partial_{(\mu}\partial_{\nu)} h^\alpha{}_\alpha + \left[\mathcal{H}' + 2\mathcal{H}^2\right]\left[h_{\mu\nu} + h_{00}\eta_{\mu\nu}\right] \\ &+ \mathcal{H}\left[\partial_0 h_{\mu\nu} - \left(\partial^\sigma h_{\sigma 0} - \frac{1}{2}\partial_0 h^\alpha{}_\alpha\right)\eta_{\mu\nu} - 2\partial_{(\mu}h_{\nu)0}\right] . \end{aligned} \tag{B.40}$$

We can now substitute the expressions for $h_{\mu\nu}$ in terms of the metric potentials. to simplify the notations, we define the spatial trace:

$$h = h^i{}_i = -6\Psi + 2\Delta E , \tag{B.41}$$

so that:

$$h^\alpha{}_\alpha = h^0{}_0 + h = -h_{00} + h = 2\Phi + h . \tag{B.42}$$

We get:

Non-zero components of the Ricci tensor for flat perturbed FLRW

$$
\begin{cases}
\delta R_{00} = \Delta\Phi + 3\mathcal{H}\Phi' + \Delta\left[B' + \mathcal{H}B\right] - \frac{1}{2}\left[h'' + \mathcal{H}h'\right] & \text{(B.43)} \\
\delta R_{0i} = -\frac{1}{2}\Delta\bar{B}_i + \left[\mathcal{H}' + 2\mathcal{H}^2\right]B_i + 2\mathcal{H}\partial_i\Phi + \frac{1}{2}\partial^j h'_{ij} - \frac{1}{2}\partial_i h' & \text{(B.44)} \\
\delta R_{ij} = \frac{1}{2}h''_{ij} + \mathcal{H}h'_{ij} - \frac{1}{2}\Delta h_{ij} + \partial^k\partial_{(i}h_{j)k} + \left(\mathcal{H}' + 2\mathcal{H}^2\right)h_{ij} \\
\qquad - \frac{1}{2}\partial_i\partial_j h - \partial_{(i}B'_{j)} - 2\mathcal{H}\partial_{(i}B_{j)} - \partial_i\partial_j\Phi \\
\qquad + \left[\frac{1}{2}\mathcal{H}h' - \mathcal{H}\Delta B - \mathcal{H}\Phi' - 2\left(\mathcal{H}' + 2\mathcal{H}^2\right)\Phi\right]\delta_{ij}\ . & \text{(B.45)}
\end{cases}
$$

Contracting with the metric to take the trace, we get the Ricci scalar:

$$
\begin{aligned}
R &= g^{\mu\nu}R_{\mu\nu} && \text{(B.46)} \\
&= \underbrace{a^{-2}\eta^{\mu\nu}\bar{R}_{\mu\nu}}_{=\bar{R}} + \underbrace{a^{-2}\eta^{\mu\nu}\delta R_{\mu\nu} - a^{-2}h^{\mu\nu}\bar{R}_{\mu\nu}}_{=\delta R}\ , && \text{(B.47)}
\end{aligned}
$$

with:

$$
a^2\bar{R} = 6\left[\mathcal{H}' + \mathcal{H}^2\right]\ , \tag{B.48}
$$

and:

$$
a^2\delta R = h'' + 3\mathcal{H}h' - 2\Delta\Phi - 6\mathcal{H}\Phi' - 12\left[\mathcal{H}^2 + \mathcal{H}'\right]\Phi + 4\Delta\Psi - 2\Delta\left[B' + 3\mathcal{H}B\right]\ . \tag{B.49}
$$

Finally, we can form the Einstein tensor:

$$
G_{\mu\nu} = \bar{G}_{\mu\nu} + \delta G_{\mu\nu}\ , \tag{B.50}
$$

with:

$$
\bar{G}_{\mu\nu} = \bar{R}_{\mu\nu} - \frac{a^2}{2}\bar{R}\eta_{\mu\nu}\ , \tag{B.51}
$$

and:

$$
\delta G_{\mu\nu} = \delta R_{\mu\nu} - \frac{a^2\bar{R}}{2}h_{\mu\nu} - \frac{a^2\delta R}{2}\eta_{\mu\nu}\ . \tag{B.52}
$$

Expanding in terms of metric potentials, we get:

Non-zero components of the Einstein tensor for flat perturbed FLRW

$$\begin{cases} \bar{G}_{00} = 3\mathcal{H}^2 & \text{(B.53)} \\ \bar{G}_{ij} = -\left[2\mathcal{H}' + \mathcal{H}^2\right]\delta_{ij}\,, & \text{(B.54)} \end{cases}$$

and:

$$\begin{cases} \delta G_{00} = 2\mathcal{H}\Delta\left(E' - B\right) + 2\Delta\Psi - 6\mathcal{H}\Psi' & \text{(B.55)} \\ \delta G_{0i} = \partial_i\left[2\Psi' + 2\mathcal{H}\Phi - \left(2\mathcal{H}' + \mathcal{H}^2\right)B\right] \\ \qquad + \frac{1}{2}\Delta\left[\bar{E}_i' - \bar{B}_i\right] - \left[2\mathcal{H}' + \mathcal{H}^2\right]\bar{B}_i & \text{(B.56)} \\ \delta G_{ij} = \bar{E}_{ij}'' - \Delta\bar{E}_{ij} + 2\mathcal{H}\bar{E}_{ij}' - 2\left[2\mathcal{H}' + \mathcal{H}^2\right]\bar{E}_{ij} \\ \qquad + \partial_{(i}\left[\left(\bar{E}_{|j)}' - \bar{B}_{|j)}\right)' + 2\mathcal{H}\left(\bar{E}_{|j)}' - \bar{B}_{|j)}\right) - 2\left(2\mathcal{H}' + \mathcal{H}^2\right)\bar{E}_{|j)}\right] \\ \qquad + \partial_{(i}\partial_{j)}\left[(E' - B)' + 2\mathcal{H}(E' - B) - 2\left(2\mathcal{H}' + \mathcal{H}^2\right)E + \Psi - \Phi\right] \\ \qquad + \Big[2\Psi'' + 4\mathcal{H}\Psi' + \Delta\left(\Phi - \Psi\right) + 2\left(2\mathcal{H}' + \mathcal{H}^2\right)\left(\Phi + \Psi\right) + 2\mathcal{H}\Phi' \\ \qquad - \Delta\left((E' - B)' + 2\mathcal{H}(E' - B)\right)\Big]\delta_{ij}\,. & \text{(B.57)} \end{cases}$$

C

Random fields

In this appendix, we would like to summarise the basic properties of Gaussian random fields we need in these notes. As we explain in chapter 8, inflation predicts that the Fourier transform of the metric perturbation Φ, $\hat{\Phi}\left(\eta, \vec{k}\right)$, is a *Gaussian random field*. This means that at fixed $\vec{k}$, $g_{\vec{k}}(\eta) = \hat{\Phi}\left(\eta, \vec{k}\right)$ is a random variable (time dependent) following the normal law. In addition, these random variables are all independent of each other: the modes $\vec{k}_1$ and $\vec{k}_2$ have independent distributions as long as $\vec{k}_1 \neq \vec{k}_2$.

However, $g_{\vec{k}}$ is complex in general, so it being Gaussian means that its real and imaginary parts each follow normal laws. Let us write $g_{\vec{k}} = R_{\vec{k}} + iI_{\vec{k}}$ for the decomposition in real and imaginary parts. Then, R_n and I_n both follow a normal law of mean 0 and of variance:

$$\sigma_{\vec{k}}^2 = \frac{1}{2}\left\langle \left|g_{\vec{k}}\right|^2 \right\rangle = \left\langle R_{\vec{k}}^2 \right\rangle = \left\langle I_{\vec{k}}^2 \right\rangle \ , \tag{C.1}$$

which is often written:

$$g_{\vec{k}} \sim \mathcal{N}\left(0, \sigma_{\vec{k}}\right) \ , \tag{C.2}$$

and which means that the probability of finding the random variable $R_{\vec{k}}$ (and $I_{\vec{k}}$) in an interval of size dR is given by:

$$\mathrm{d}P = f(R)\mathrm{d}R = \frac{1}{\sqrt{2\pi}\sigma_{\vec{k}}} \exp\left(-\frac{R^2}{2\sigma_{\vec{k}}^2}\right)\mathrm{d}R \ . \tag{C.3}$$

Independence of the various modes and the random (uniformly distributed) phase then lead to:

$$\left\langle g_{\vec{k}_1}^* g_{\vec{k}_2} \right\rangle = 2\delta_D(\vec{k}_1 - \vec{k}_2)\sigma_{\vec{k}_1}^2 \ . \tag{C.4}$$

Here and everywhere else in the text, $\langle\cdot\rangle$ denotes an ensemble average for the Gaussian distribution. Namely, for example, for any function F of the random variable R:

$$\langle F \rangle = \int_{-\infty}^{+\infty} F(R) f(R) \mathrm{d}R \ . \tag{C.5}$$

Going back to our random process in real space, we can calculate the variance of $\Phi\left(\vec{x}\right)$ at a given position in space $\vec{x}$ (and a given time η); we suppress time dependence from now on for the ease of notation. Using Fourier transforms, we get:

$$\left\langle \Phi^2\left(\vec{x}\right) \right\rangle = \frac{1}{4\pi^3} \int \mathrm{d}^3k \sigma_{\vec{k}}^2 \, , \tag{C.6}$$

which is independent on $\vec{x}$, as it should be by invariance by translation and rotation (statistical homogeneity and isotropy). We can then obtain:

$$\sigma_\Phi^2 = \left\langle \Phi^2\left(\vec{x}\right)\right\rangle = 4\pi \int_0^{+\infty} \frac{\mathrm{d}k}{k} \Delta_\Phi^2(k) \ , \tag{C.7}$$

where we have defined the *dimensionless power spectrum* of Φ, $\Delta_\Phi^2(k)$ by:

$$\left\langle \hat{\Phi}\left(\vec{k}\right)\hat{\Phi}\left(\vec{k'}\right)\right\rangle = \left(\frac{2\pi}{k}\right)^3 \Delta_\Phi^2(k)\delta_D\left(\vec{k}+\vec{k'}\right) \ . \tag{C.8}$$

Note that this can be rewritten:

$$\Delta_\Phi^2(k) = \left(\frac{k}{2\pi}\right)^3 \left\langle \hat{\Phi}\left(\vec{k}\right)\hat{\Phi}\left(-\vec{k}\right)\right\rangle \tag{C.9}$$

$$= \left(\frac{k}{2\pi}\right)^3 \left\langle \left|\hat{\Phi}\left(\vec{k}\right)\right|^2\right\rangle = \frac{k^3}{4\pi^3}\sigma_{\vec{k}}^2 \ , \tag{C.10}$$

because, since $\Phi\left(\vec{x}\right)$ is real, we have for any mode $\vec{k}$:

$$\hat{\Phi}\left(-\vec{k}\right) = \hat{\Phi}^*\left(\vec{k}\right) \ . \tag{C.11}$$

Then, by the central limit theorem[1], $\Phi\left(\vec{x}\right)$ is a Gaussian random variable at each point in space $\vec{x}$, with mean 0 and variance σ_Φ^2 given above. Finally, we define the *power spectrum* of Φ:

$$\mathcal{P}_\Phi(k) = k^{-3}\Delta_\Phi^2(k) \ , \tag{C.12}$$

which is just the variance (up to a $4\pi^3$ term).

[1]One actually needs to discretise the Fourier integrals and turn them into Fourier series by working into a box of large but finite size, in order to be able to sum a finite but large number of independent, Gaussian modes. Then, one takes a limit sending to boundaries of the box to infinity. As always in physics, everything is assumed to work fine with swapping limits etc.

Bibliography

[1] CAMB code homepage. https://camb.readthedocs.io/en/latest/. 184

[2] CLASS code homepage. https://lesgourg.github.io/class_public/class.html. 184

[3] Elcio Abdalla et al. Cosmology intertwined: A review of the particle physics, astrophysics, and cosmology associated with the cosmological tensions and anomalies. *JHEAp*, 34:49–211, 2022. 46

[4] Daniel Baumann. *Cosmology*. Cambridge University Press, 7 2022. iv, 59

[5] K. G. Begeman, A. H. Broeils, and R. H. Sanders. Extended rotation curves of spiral galaxies: Dark haloes and modified dynamics. *Mon. Not. Roy. Astron. Soc.*, 249:523, 1991. 33

[6] M. Betoule et al. Improved cosmological constraints from a joint analysis of the SDSS-II and SNLS supernova samples. *Astron. Astrophys.*, 568:A22, 2014. 35

[7] Florian Beutler et al. The clustering of galaxies in the SDSS-III Baryon Oscillation Spectroscopic Survey: Testing gravity with redshift-space distortions using the power spectrum multipoles. *Mon. Not. Roy. Astron. Soc.*, 443(2):1065–1089, 2014. 199

[8] C. Clarkson. Establishing homogeneity of the universe in the shadow of dark energy. *Comptes Rendus Physique*, 13:682–718, 2012. 8

[9] Ruth Durrer. *The Cosmic Microwave Background*. Cambridge University Press, Cambridge, 2008. 105, 166

[10] Daniel J. Eisenstein, Hee-jong Seo, and Martin J. White. On the Robustness of the Acoustic Scale in the Low-Redshift Clustering of Matter. *Astrophys. J.*, 664:660–674, 2007. 160

[11] W. L. Freedman et al. Final results from the Hubble Space Telescope key project to measure the Hubble constant. *Astrophys. J.*, 553:47–72, 2001. 4

[12] Andrew R. Liddle and D. H. Lyth. *Cosmological inflation and large scale structure*. Cambridge University Press, 2000. 202, 207, 212

[13] V. Mukhanov. *Physical Foundations of Cosmology*. Cambridge University Press, Oxford, 2005. iii

[14] P. J. E. Peebles. *Physical cosmology*. Princeton University Press, 1971. iii

[15] P. J. E. Peebles. *Principles of physical cosmology*. Princeton University Press, 1994. iv

[16] Patrick Peter and Jean-Philippe Uzan. *Primordial Cosmology*. Oxford Graduate Texts. Oxford University Press, 2013. iii, 182, 202

[17] Cyril Pitrou, Alain Coc, Jean-Philippe Uzan, and Elisabeth Vangioni. Precision big bang nucleosynthesis with improved Helium-4 predictions. *Phys. Rept.*, 754:1–66, 2018. 78, 79

[18] Lado Samushia et al. The clustering of galaxies in the SDSS-III Baryon Oscillation Spectroscopic Survey: measuring growth rate and geometry with anisotropic clustering. *Mon. Not. Roy. Astron. Soc.*, 439(4):3504–3519, 2014. 200

[19] Jean-Philippe Uzan. Dynamics of relativistic interacting gases: From a kinetic to a fluid description. *Class. Quant. Grav.*, 15:1063–1088, 1998. 179